



Dipl.-Ing. Silvia Wallner

Flavoproteins
with bicovalent flavin tethering

DISSERTATION

zur Erlangung des akademischen Grades einer
Doktorin der technischen Wissenschaften (Dr. *techn.*)

erreicht an der
Technischen Universität Graz

Betreuer: Univ.-Prof. Mag. *rer. nat.* Dr. *rer. nat.* Peter Macheroux
Institut für Biochemie
Technische Universität Graz

Graz, 2012

Acknowledgements

First of all, I would like to thank all people who have helped and inspired me during the time of my PhD project and who contributed to a pleasant atmosphere and enjoyable working hours in the lab. Therefore, I am grateful to all my colleagues, present and former members of my working group, for their support, for all valuable and motivating discussions, and for many friendships formed in the last years.

I want to express my gratitude to my supervisor Prof. Peter Macheroux for giving me the opportunity to work on such an interesting research project. Besides, I want to thank him for his constant support and encouragement throughout the whole project.

My special thanks go to Rosemarie Trenker, Steve Stipsits, and Martin Puhl for their excellent support in matters of practical lab work and, certainly, for helping me pushing on my research project. In particular, I want to thank Steve for assisting me at any times and for accompanying me even during long night shifts.

During the last years I also had the pleasure to supervise several talented and highly motivated students through their bachelor or diploma projects. Thanks to Birgit Luef, Hannah Jaritz, Philipp Markolin, Stefanie Horvath, and Sabrina Tatzl, essential contributions to the STOX-project were made. Moreover, Corinna Dully and Altijana Hromic helped me getting deeper insights in the field of bicovalent flavin tethering. With their optimism all students provided a great source of motivation for me and made me enjoy the subprojects which we performed together.

I also want to thank Bastian Daniel, who continues my work on bicovalently linked flavoproteins, for all valuable discussions on this topic.

My thesis committee members Prof. Anton Glieder, Prof. Karl Gruber, and Prof. Kurt Faber deserve special thanks for dedicating time and knowledge to advise and support me during the time of my PhD project.

I am also grateful to all cooperation partners for making my work diversified. Special thanks go to Katharina Durchschein, Jörg Schrittwieser, Verena Resch and Prof. Wolfgang Kroutil for sharing their success with me.

Last but not least, I want to express my gratitude to my dear parents for their love, their constant support and for always believing in me. Moreover, special thanks go to my sister and my brother for encouraging and helping me in difficult situations, and to Stefan for his endless patience and for motivating me to accomplishing this thesis.

Abstract

Flavoproteins are a large and diverse group of proteins that possess a non-, mono- or bicovalently bound FMN or FAD cofactor for catalysis. Covalent attachment of the cofactor occurs when either the 8 α - or 6-position of the isoalloxazine forms a covalent bond to the amino acid side chain of a cysteine, histidine or tyrosine residue, respectively. Flavoproteins with bicovalent cofactor linkage are a novel class of proteins which are present in both prokaryotic and eukaryotic organisms. These enzymes have extraordinary properties, such as unusually high redox potentials that enable catalysis of challenging chemical reactions in plants, fungi and bacteria as was shown by redox potential determinations. Moreover, bicovalent linkage appears to be crucial for structural integrity of the protein and correct positioning of the flavin in the active site. Many bicovalently-linked flavoenzymes can be exploited as capable biocatalysts; hence, a detailed understanding of these enzymes is of utmost importance. This work is intended to get a deeper insight in the role of bicovalent flavin tethering and to identify and characterize new members of this class of proteins. (*S*)-Tetrahydroprotoberberine oxidase (STOX) was identified as a new bicovalent flavoprotein in poppy and berberis species and was found to be involved in benzyloquinoline alkaloid biosynthesis by catalyzing the stereoselective oxidation of various (*S*)-tetrahydroprotoberberines. In the course of this thesis project a system for heterologous protein expression was established using *Pichia pastoris* as host organism, which resulted in the formation of low quantities of STOX and in the identification of (*S*)-tetrahydropalmatine as preferred substrate of STOX from *Argemone mexicana*.

A further objective was to perform in-depth studies on berberine bridge enzyme (BBE), a paradigm for bicovalent flavoproteins which is used for the biocatalytic production of (*S*)-berbines and (*R*)-benzyloquinolines. We created BBE variants, which should accept non-natural substrates leading to the formation of new pharmacologically active compounds. Moreover, biochemical studies on BBE showed that His174 seems to stabilize the uptake of negative charge into the isoalloxazine ring system during catalysis. The respective variant protein features a reduced midpoint potential of the cofactor and significantly decreased overall enzyme efficiency and hence provides further insights in the catalytic properties of BBE.

Kurzfassung

Flavoproteine sind eine große und vielfältige Enzymklasse, deren FAD- oder FMN-Kofaktor nicht-kovalent, mono- oder bivalent an das jeweilige Protein gebunden vorkommen kann. Der erste Vertreter der bivalent verknüpften Flavoproteine war Glucosylglycosaminidase (GOOX), bei der im Jahr 2005 sowohl Histidinylierung als auch eine Cysteinylierung des Flavins entdeckt wurden. Bivalent verknüpfte Flavoproteine kommen in prokaryotischen wie auch in eukaryotischen Organismen vor und zeigen außergewöhnliche Eigenschaften. Durch die kovalente Kofaktorbindung besitzen sie außerordentlich hohe Redoxpotentiale, die es ihnen ermöglichen schwierige Oxidationsreaktionen zu katalysieren. Der Einfluss von kovalenten Verknüpfungen auf das Redoxpotential konnte im Rahmen dieser Arbeit anhand von Redoxpotentialbestimmungen an Dbv29, einem bivalenten Flavoprotein aus *Nonomurea* sp., gezeigt werden.

Das Hauptziel dieser Arbeit ist es tiefere Einblicke in die Funktion der kovalenten Flavinylierung zu erzielen und auch neue Vertreter dieser interessanten Enzymklasse zu identifizieren und zu charakterisieren. (*S*)-Tetrahydroprotoberberine oxidase (STOX) ist ein neuer Vertreter der Gruppe der bivalent verknüpften Flavoproteine und kommt in verschiedenen Mohn und Berberitzen-Spezies, wie etwa in *Argemone mexicana* und *Berberis wilsoniae*, vor. Das Enzym scheint für die stereospezifische Oxidation von (*S*)-Tetrahydroprotoberberinen verantwortlich zu sein, die als Intermediate in der Alkaloid-Biosynthese vorkommen. Im Rahmen dieser Arbeit wurde ein System zur heterologen Expression von STOX in *Pichia pastoris* entwickelt, welches jedoch nur zu einer sehr geringen Proteinausbeute führte. Die Mengen waren dennoch ausreichend um (*S*)-Tetrahydropalmitine als das bevorzugte Substrat für STOX von *Argemone mexicana* zu identifizieren.

Ein weiteres Ziel der Arbeit war es zusätzliche Studien zum Berberine Bridge Enzyme (BBE) durchzuführen. BBE gilt als Paradigma für bivalent verknüpfte Flavoproteine, da dieses Protein sehr gut biochemisch und strukturell charakterisiert wurde. Im Rahmen dieser Arbeit wurden neue BBE-Mutanten hergestellt, die ein breiteres Substratspektrum besitzen und daher die Bildung von neuen pharmakologisch aktiven Substanzen ermöglichen sollen. Außerdem wurde His174 als wichtige Active Site Aminosäure identifiziert, die die Aufnahme einer negativen Ladung während der Katalyse stabilisiert und so die Substratoxidation erleichtert.

EIDESSTATTLICHE ERKLÄRUNG

Ich erkläre an Eides statt, dass ich die vorliegende Arbeit selbstständig verfasst, andere als die angegebenen Quellen/Hilfsmittel nicht benutzt, und die den benutzten Quellen wörtlich und inhaltlich entnommene Stellen als solche kenntlich gemacht habe.

STATUTORY DECLARATION

I declare that I have authored this thesis independently, that I have not used other than the declared sources / resources, and that I have explicitly marked all material which has been quoted either literally or by content from the used sources.

Graz, am 22. 03. 2012

Silvia Wallner

Table of Contents

ACKNOWLEDGEMENTS.....	II
ABSTRACT	III
KURZFASSUNG	IV
1 ALKALOIDS - A DIVERSE CLASS OF PHARMACOLOGICAL ACTIVE COMPOUNDS	9
1.1 General aspects	2
1.2 Benzylisoquinoline alkaloids	3
1.2.1 Biosynthesis of benzylisoquinoline alkaloids.....	3
1.2.2 Pharmacology of benzylisoquinoline alkaloids	6
1.2.3 Biotechnological production of benzylisoquinoline alkaloids.....	8
1.3 References.....	10
2 BERBERINE BRIDGE ENZYME AND THE FAMILY OF BICOVALENT FLAVOENZYMES	14
3 AIMS OF THE PROJECT	50
3.1 References.....	53
4 (S)-TETRAHYDROPROTOBERBERINE OXIDASE (STOX) - A MYSTERIOUS ENZYME IN ALKALOID BIOSYNTHESIS	54
4.1 STOX - the early beginnings	56
4.2 Materials and Methods.....	60
4.2.1 Reagents.....	60
4.2.2 Expression strains.....	60
4.2.3 DNA constructs	61
4.2.4 Cloning and expression in <i>Escherichia coli</i>	63
4.2.5 Refolding of inclusion bodies.....	64
4.2.6 Assembling and transformation of expression cassettes for <i>P. pastoris</i>	65
4.2.7 Small scale expression in <i>P. pastoris</i>	67
4.2.8 Large scale expression and purification.....	69
4.2.9 Design of a fluorescence-based screening system for heterologous protein expression in <i>P. pastoris</i>	70

4.2.10	<i>Isolation of periplasmic proteins</i>	75
4.2.11	<i>Protein purification</i>	75
4.2.12	<i>Activity assays</i>	76
4.2.13	<i>Immunoblotting</i>	77
4.3	Results.....	78
4.3.1	<i>Computational analysis</i>	78
4.3.2	<i>E. coli expression experiments</i>	80
4.3.3	<i>Expression of Am and Bw STOX in P. pastoris</i>	82
4.3.4	<i>Design of a fluorescence-based screening system</i>	86
4.4	Discussion	95
4.4.1	<i>General aspects</i>	95
4.4.2	<i>Substrate specificity of Am and Bw STOX</i>	97
4.4.3	<i>Heterologous expression of STOX - a mystery</i>	99
4.4.4	<i>Fluorescence-based screening system</i>	105
4.5	References.....	106
5	CATALYTIC AND STRUCTURAL ROLE OF A CONSERVED ACTIVE SITE HISTIDINE IN BERBERINE BRIDGE ENZYME	112
6	TUNING BBE FOR NEW BIOCATALYTIC APPLICATIONS - ACTIVE SITE REDESIGN OF BERBERINE BRIDGE ENZYME	127
6.1	Biocatalytic synthesis of berbine and benzyloquinoline alkaloids.....	129
6.2	Objectives	130
6.3	Materials and Methods.....	133
6.3.1	<i>Reagents</i>	133
6.3.2	<i>Site-directed mutagenesis</i>	133
6.3.3	<i>Transformation, expression, and purification</i>	134
6.4	Results and discussion	135
6.5	References.....	137
7	REDOX POTENTIAL DETERMINATIONS FOR DBV29 - A BICOVALENTLY FLAVINYLATED OXIDASE.....	138
7.1	Dbv29 - oxidative power for A40926 maturation.....	140
7.1.1	<i>A40926 and the dbv gene cluster for A40926 biosynthesis</i>	140
7.1.2	<i>What is known about Dbv29?</i>	142

7.2	Materials and Methods.....	146
7.2.1	<i>Reagents</i>	146
7.2.2	<i>Dbv29 wild type and muteins</i>	146
7.2.3	<i>Redox potential determination</i>	147
7.3	Results.....	148
7.3.1	<i>Spectral characteristics of Dbv29 wild type and muteins</i>	148
7.3.2	<i>Redox potentials of Dbv29 wild type and muteins</i>	149
7.4	Discussion.....	153
7.5	References.....	157
8	APPENDIX.....	160
	List of Abbreviations.....	161
	List of Publications.....	163
	Curriculum vitae.....	165

CHAPTER 1

- 1 Alkaloids - a diverse class of pharmacological active compounds
-

1.1 General aspects

Alkaloids are a large and diverse group of nitrogen-containing low-molecular-weight compounds that are common secondary metabolites in about 20% of all plant species [1, 2]. In plants, alkaloids play a major role in defence against herbivores and pathogens [1, 3, 4].

The historical use of these substances traces back almost to the start of civilization, and alkaloids were commonly used as poisons and as active agents in traditional medicine ever since [5]. Famous examples for the early application of alkaloids are the execution of Socrates with coniine-containing hemlock [6] or the use of atropine-containing extracts of Egyptian henbane in the age of Cleopatra. At that time women dilated their pupils as a sign of beauty and also today synthetic derivatives of atropine are routinely used as mydriatics for eye examinations [5].

Research on plant alkaloids started with the identification and isolation of morphine from the opium poppy *Papaver somniferum* 200 years ago [7]. Today more than 12,000 alkaloids are known and many of them are exploited as pharmaceuticals, stimulants, narcotics, or poisons [1, 8]. About 25% of all pharmaceuticals in use are derived from plants in form of extracts, teas, or as purified substances with biological activity. [9]. Taxol, a common anticancer agent [10], is derived from the western yew *Taxus brevifolia*, and the antimalarial drug quinine is extracted from bark of *Cinchona officinalis* [5, 11]. Moreover, many other alkaloids such as the analgesics morphine and codeine from *P. somniferum*, the muscle relaxants (+)-tubocurarine from *Chondodendron tomentosum*, the anti-arrhythmic ajmaline from *Rauwolfia serpentina*, or the sedative scopolamine from *Atropa belladonna* are important drugs in modern medicine [1, 5].

Most alkaloids are derived from amino acids, such as histidine, lysine, ornithine, tryptophan and tyrosine, in complex biosynthetic pathways [12]. According to their structural properties, alkaloids are divided into several classes with (benzyl)isoquinoline, indole, tropane, purine, pyrrolizidine, and quinolizidine type alkaloids as well-investigated representatives [1].

Due to their complexity and chirality, total organic synthesis is not feasible for many alkaloids and the extraction from natural sources very often results in low yields of purified biological active substances [4, 13]. Great efforts are being made to

understand the biosynthetic routes leading to the formation of different types of alkaloids in order to find cost-effective ways of drug production. Today several new strategies exist such as the use of transgenic plants for improved accumulation of pathway intermediates or metabolic engineering of microbial host organisms to create platforms for fermentative production of plant alkaloids [12-16].

1.2 Benzyloisoquinoline alkaloids

Benzyloisoquinoline alkaloids are a large group of alkaloids comprising more than 2500 defined structures [4]. They are derived from tyrosine in a series of decarboxylation, intramolecular coupling, reduction, methylation, hydroxylation, and further modification reactions [8] and they share the benzyloisoquinoline heterocycle as common structural feature.

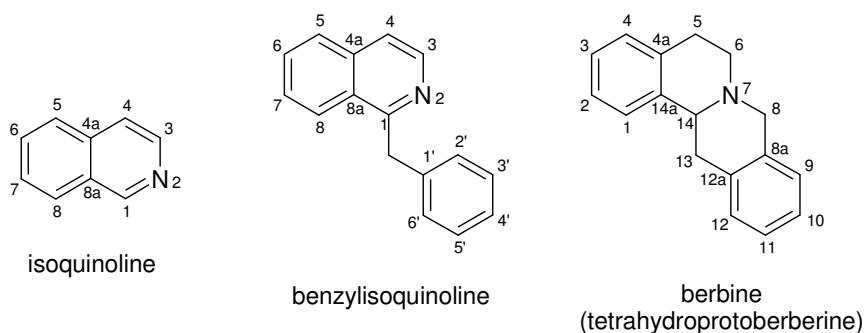


Figure 1: Structure and numbering conventions of benzyloisoquinoline alkaloids.

Benzyloisoquinoline alkaloids are mainly produced by members of the order of Ranunculales, such as *Berberidaceae*, *Papaveraceae*, and *Ranunculaceae* [17]. California poppy (*Eschscholzia californica*), opium poppy (*P. somniferum*), Japanese goldthread (*Coptis japonica*), and yellow meadow rue (*Thalictrum flavum*) were used as model systems for investigating sanguinarine and berberine biosynthesis [8, 18-35].

1.2.1 Biosynthesis of benzyloisoquinoline alkaloids

Biosynthesis of benzyloisoquinoline alkaloids starts with the condensation of dopamine and 4-hydroxyphenylacetaldehyde, which both are ultimately derived from L-tyrosine (see Figure 2) [8, 36]. This first committed step leading to the formation

of (*S*)-norcoclaurine is catalyzed by norcoclaurine synthase (NCS) [37-40]. (*S*)-Norcoclaurine is further transformed to (*S*)-reticuline in a series of methylation and oxidation reactions catalyzed by norcoclaurine 6-*O*-methyltransferase (6OMT), coclaurine *N*-methyltransferase (CNMT), *N*-methylcoclaurine 3'-hydroxylase (NMCH), and 3'-hydroxy-*N*-methylcoclaurine 4'-*O*-methyltransferase (4'OMT) [1, 8, 37]. (*S*)-Reticuline is an important branch point intermediate in benzyloisoquinoline alkaloid biosynthesis, which can undergo diverse enzymatic reactions leading to the formation of morphinan, benzophenanthridine, protoberberine, and aporphine alkaloids [1, 8]. Moreover, (*S*)-reticuline can be derivatized e.g. by methylation resulting in the formation of laudanosine [37].

For entering the morphinan biosynthetic route, (*S*)-reticuline has to be isomerized to (*R*)-reticuline via 1,2-dehydroreticuline synthase (DRS) and 1,2-dehydroreticuline reductase (DRR) [1, 4, 8, 37]. (*R*)-Reticuline is further converted to salutaridine, which is hydroxylated and acetylated leading to the formation of salutaridinol 7-*O*-acetate [30, 41]. From this intermediate thebaine is formed by thebaine synthase (THS) [42]. Thebaine can either be oxidized to codeinone via neopinone, and is subsequently reduced to codeine by codeinone reductase (COR) [43]. Alternatively, thebaine can be demethylated and oxidized yielding morphinone. Both morphinone and codeine can be converted into morphine, the final alkaloid of this branch of benzyloisoquinoline alkaloids [1, 8, 37].

In another branch of benzyloisoquinoline alkaloid biosynthesis (*S*)-reticuline is converted to (*S*)-scoulerine through the action of berberine bridge enzyme (BBE), which catalyzes the oxidative intramolecular C-C bond formation thereby creating the so called "berberine bridge" [44, 45]. The latter reaction is the committed step in the biosynthetic routes leading to the formation of protoberberine, protopine, and benzophenanthridine alkaloids [8].

In the benzophenanthridine branch (*S*)-scoulerine is converted to (*S*)-stylophine via the formation of two methylenedioxy bridges by cheilanthifoline synthase (CHS) and stylophine synthase (STS) [46, 47]. (*S*)-Stylophine is then converted to (*S*)-*cis*-*N*-methylstylophine by (*S*)-tetrahydroprotoberberine *cis*-*N*-methyltransferase (TNMT) [48], which is subsequently hydroxylated by *N*-methyl-stylophine 14-hydroxylase (MSH) [8, 37]. The latter reaction product tautomerizes to protobine which is further hydroxylated yielding dihydrosanguinarine. In a last step sanguinarine can be produced by oxidation with dihydrobenzophenanthridine oxidase (DBOX) [8, 49].

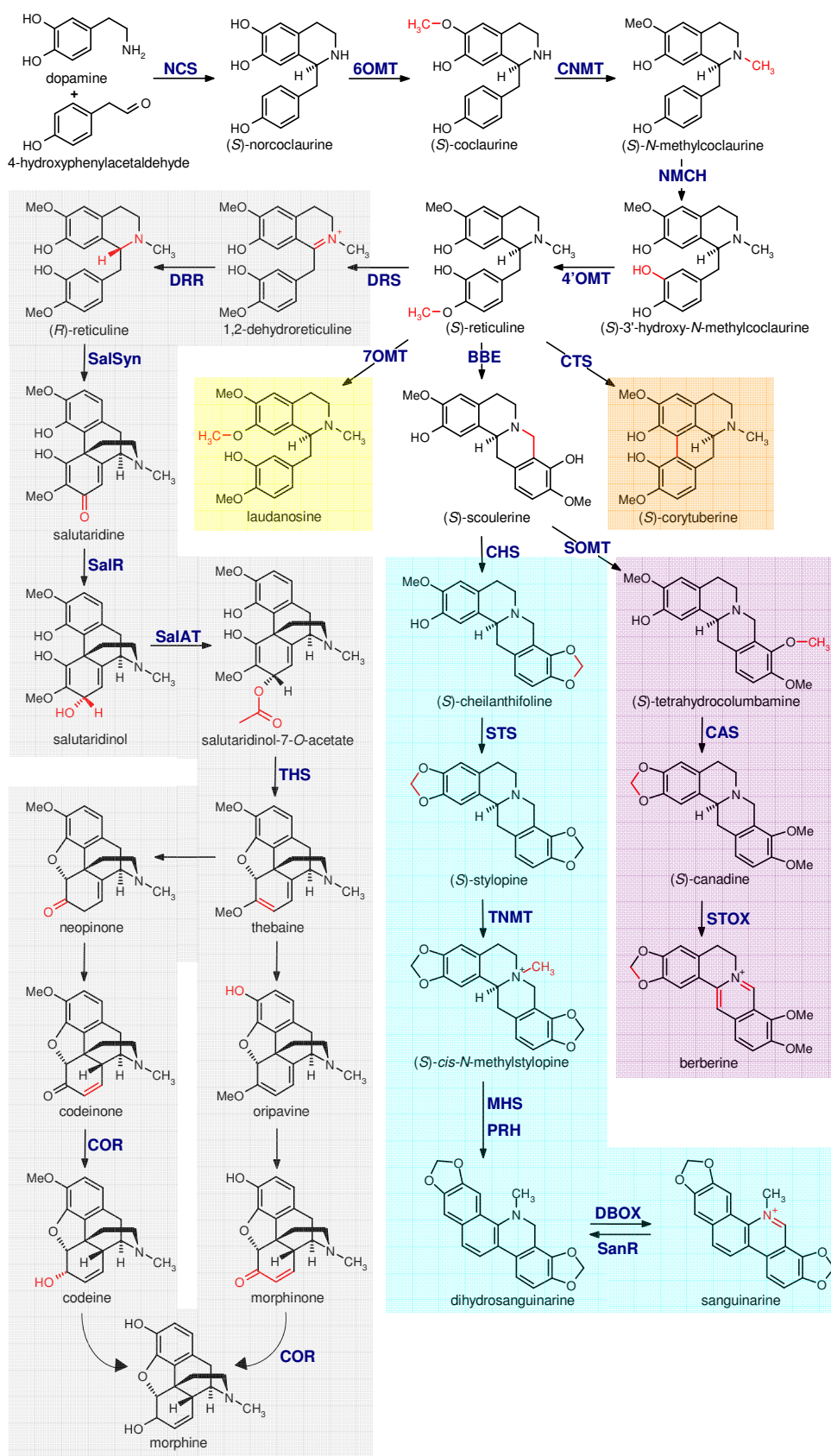


Figure 2: Biosynthesis of benzyloquinoline alkaloids.

Scheme of benzyloquinoline biosynthesis adapted from [8]. Branches of benzyloquinoline biosynthesis are colour-coded: grey, morphinan alkaloids; yellow, laudanosine; cyan, benzo-phenanthridine alkaloids; purple, protoberberine alkaloids; orange, aporphine alkaloids. Abbreviations: NCS, norcoclaurine synthase; 6OMT, norcoclaurine 6-*O*-methyltransferase; CNMT, coclaurine *N*-methyltransferase; NMCH, *N*-methylcoclaurine 3'-hydroxylase; 4'OMT, 3'-hydroxy-*N*-methylcoclaurine 4'-*O*-methyltransferase;

DRS, 1,2-dehydroreticuline synthase; DRR, 1,2-dehydroreticuline reductase; SalSyn, salutaridine synthase; SalR, salutaridine:NADPH 7-oxidoreductase; SalAT, salutaridinol-7-*O*-acetyltransferase; THS, thebaine synthase; COR, codeinone reductase; 7OMT, reticuline 7-*O*-methyltransferase; BBE, berberine bridge enzyme; CHS, cheilanthifoline synthase; STS, stylophine synthase; TNMT, tetrahydroprotoberberine *cis-N*-methyltransferase; MSH, *N*-methylstylophine 14-hydroxylase; PRH, protopine 6-hydroxylase; DBOX, dihydrobenzophenanthridine oxidase; SanR, sanguinarine reductase; SOMT, scoulerine-9-*O*-methyltransferase; CAS, canadine synthase; STOX, (*S*)-tetrahydroprotoberberine oxidase; CTS, corytuberine synthase

Additionally, (*S*)-scoulerine can be channeled towards berberine biosynthesis by methylation with scoulerine 9-*O*-methyltransferase (SOMT) leading to the formation of (*S*)-tetrahydrocolumbamine [50]. This intermediate is converted to (*S*)-canadine by methylenedioxy bridge formation catalyzed by canadine synthase (CAS) [51]. In a final step of berberine biosynthesis (*S*)-canadine is oxidized to berberine by the flavin dependent (*S*)-tetrahydroprotoberberine oxidase (STOX) [52].

1.2.2 Pharmacology of benzyloquinoline alkaloids

Benzyloquinoline alkaloids are a very interesting class of alkaloids since these compounds show a wide range of pharmacological activities [4]. For example, they are applied as analgesics, sedatives, hypnotics, antineoplastics, tranquilizing, muscle relaxant or depressant drugs [53-57]. Pharmacological properties of many benzyloquinoline alkaloids were recognized very early leading to an extensive use of alkaloid containing plants and plant extracts in folk- and alternative medicine. In Brazil various species of the *Ocotea* genus are used for the treatment of pain and neuralgia. The major alkaloid accumulated in these plants is (*S*)-reticuline, which was shown to have major effects on the central nervous system [58]. Oriental medicine uses all parts of *Nelumbo nucifera*, a perennial aquatic crop containing (*R*)-coclaurine and (*S*)-norcoclaurine, to treat fever, sweating, and strangury [59]. Different *Mahonia* species contain a high content of protoberberine alkaloids and are used as folk medicinal plants as antipyretic, anti-inflammatory and analgesic drugs [60]. Pseudocoptisine, a quaternary alkaloid with benzyloquinoline skeleton, is a major active compound in *Corydalis* species and shows anti-amnesic properties [61]. Moreover, plant constituents are frequently used as models for the design of modern synthetic drugs and active plant extract screening programs continuously result in the identification of novel active compounds [5].

A general pharmacological property of many benzyloquinolines is their antispasmodic activity, which is caused by inhibition of Ca^{2+} transport [62, 63]. MARTIN *et al.* demonstrated a muscle-relaxing effect of reticuline, noramepavine, coclaurine, and papaverine [55] *in vitro*. Muscle-relaxing properties were also found for laudanosine which acts as a selective α_1 -adrenoceptor blocker [56, 64]. Additionally, reticuline was demonstrated to cause sedation and decreased locomotor activity [58], and it was suggested to accelerate hair growth [65]. Recently, benzyloquinoline alkaloids were tested for potential application in the treatment of HIV-patients [59]. (*R*)-coclaurine, (*S*)-norcoclaurine, and several synthetic benzyloquinolines exhibited low toxicity and considerable anti-HIV activity making these compounds interesting for the development of new antiretroviral drugs. Armepavine oxalate was shown to be a potent anticancer drug by inducing cell death in leukemia cell lines [66].

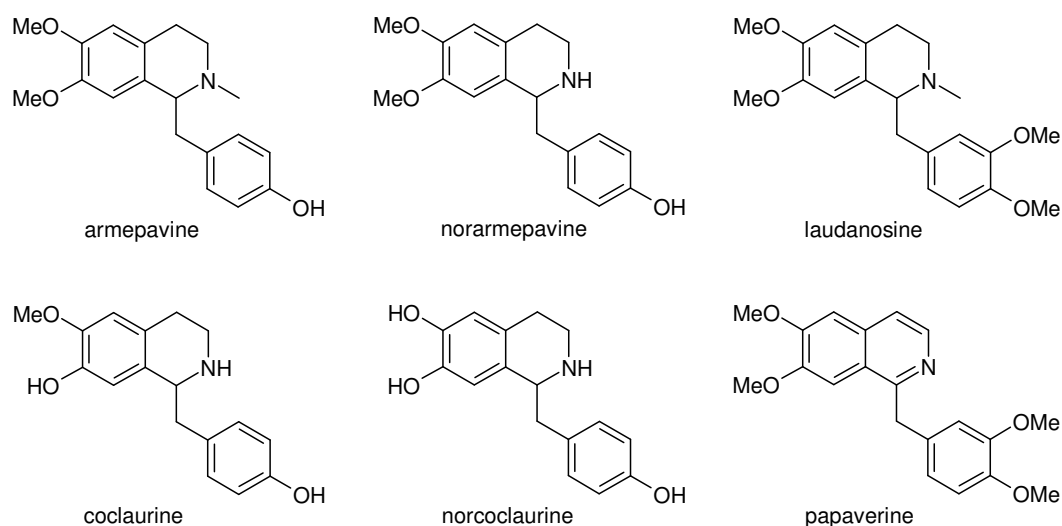


Figure 3: Structures of biological active benzyloquinolines

A common pharmacological activity of most berbine alkaloids is their depressant activity on the central nervous system. Studies on rats and mice revealed that tetrahydroberberine, tetrahydrocoptisine, and tetrahydropalmatine are potent sedative drugs [57]. Further studies showed analgesic and anti-inflammatory effects of berberine, palmatine, and jatrorrhizine, which are the active components of many extracts from medicinal plants [60]. Additionally, different protoberberines, such as berberine, palmatine, jatrorrhizine and coptisine and the aporphine alkaloid magnoflorine possess antioxidant and neuroprotective activity and have a strong potential of prevention of Alzheimer's disease [67]. Antioxidant and thus

chemopreventive properties of berberine and 1-benzylisoquinolines were also suggested by CUI *et al.*, who investigated the ability of these compounds to scavenge free radicals [68]. Recently, (*S*)-stepholidine and (*S*)-chloroscoulerine were shown to effect the dopaminergic system, thus making these compounds potent drugs for the treatment of schizophrenia and symptoms related to Parkinson's disease [69-78].

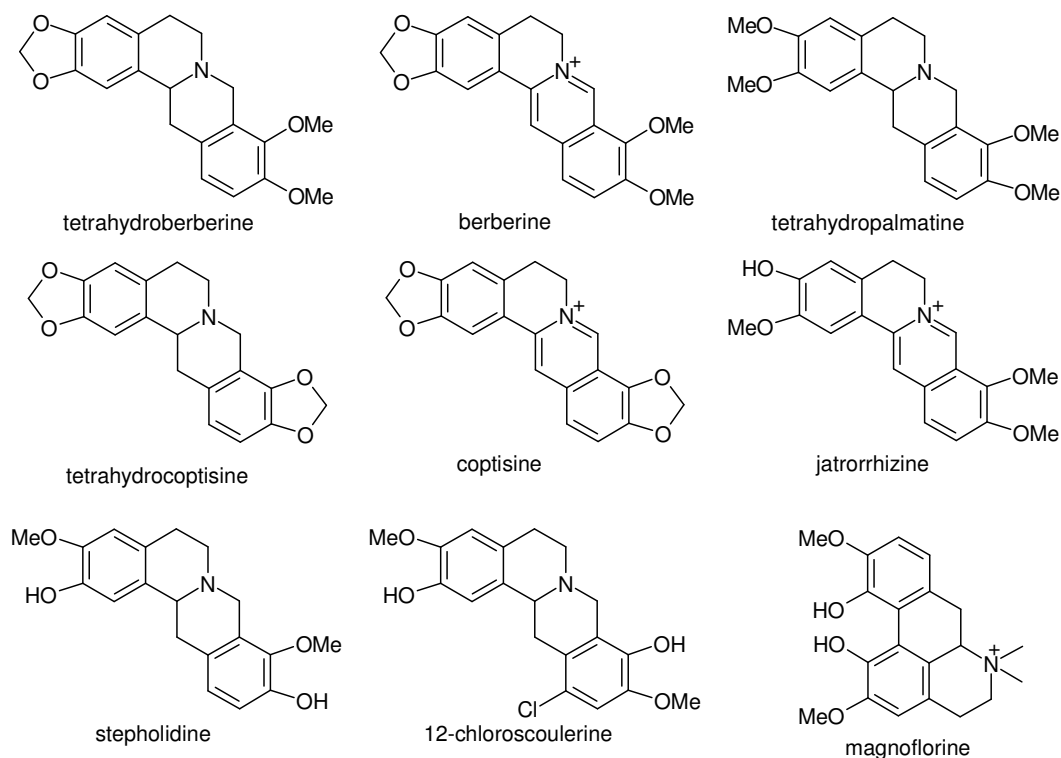


Figure 4: Structures of biological active berbines and aporphines

1.2.3 Biotechnological production of benzyloisoquinoline alkaloids

Since benzyloisoquinoline alkaloids possess a variety of pharmacological activities, cost-efficient production of these compounds for medicinal application is a major challenge in today's research [13]. Extraction from natural sources often results in low yields since benzyloisoquinoline and berbine alkaloids are intermediates rather than final products in the respective biosynthetic routes and hence accumulate only in marginal amounts [79]. Moreover, organic synthesis of such complex substances is difficult or even not feasible in an economic manner [13]. Today new biotechnological approaches are available for the production of some important

benzylisoquinoline alkaloids. MINAMI *et al.* found an efficient way for the synthesis of (*S*)-reticuline, (*S*)-scoulerine, and magnoflorine using a combination of transgenic *E. coli* and *Saccharomyces cerevisiae* cells. (*S*)-Reticuline was produced from dopamine using norcoclaurine synthase, norcoclaurine 6-*O*-methyltransferase, coclaurine-*N*-methyltransferase, and 3'-hydroxy-*N*-methylcoclaurine 4'-*O*-methyltransferase from *C. japonica* [12]. Besides, the production of (*R*)- and (*S*)-reticuline from laudanosine was performed using a combination of recombinant enzymes for *T. flavum*, *P. somniferum*, and a human cytochrome P450 enzyme [15]. Today, a bacterial platform is available for the production of various plant alkaloids from simple carbon sources [13, 14]. The biotechnological processes employ artificial biosynthetic pathways, which comprise heterologously expressed enzymes from different microbial, plant, and mammalian sources [16]. These first examples clearly show the applicability of biotechnological processes for the production of complex alkaloids. Additionally, further metabolic and protein engineering strategies might open up pathways for novel benzylisoquinoline alkaloids, which can be tested as new pharmaceuticals [12].

1.3 References

- [1] Facchini, P.J., and St-Pierre, B. *Curr Opin Plant Biol* **2005**, *8*, 657-666.
- [2] Hashimoto, T., and Yamada, Y. *Annu Rev Plant Physiol Plant Mol Biol* **1994**, *45*, 257-285.
- [3] Schmeller, T., Latz-Brüning, B., and Wink, M. *Phytochemistry* **1997**, *44*, 257-266.
- [4] Facchini, P.J. *Annu Rev Plant Physiol Plant Mol Biol* **2001**, *52*, 29-66.
- [5] Kutchan, T. M. *Plant Cell* **1995**, *7*, 1059-1070.
- [6] Reynolds, T. *Phytochemistry* **2005**, *66*, 1399-1406.
- [7] Klockgether-Radke, A.P. *Anesthesiol Intensivmed Notfallmed Schmerzther* **2002**, *37*, 244-249.
- [8] Liscombe, D.K., and Facchini, P.J. *Curr Opin Biotechnol* **2008**, *19*, 173-180.
- [9] Tyler, V.E. *Herbs of Choice: The Therapeutic use of Phytomedicinals*. **1994** Haworth Press, New York.
- [10] Martin, M., Pienkowski, T., Mackey, J., Pawlicki, M., Guastalla, J.P., Weaver, C., *et al.* *N Engl J Med* **2005**, *352*, 2302-2313.
- [11] Kutchan, T.M. *Gene* **1996**, *179*, 73-81.
- [12] Minami, H., Kim, J.S., Ikezawa, N., Takemura, T., Katayama, T., Kumagai, H., and Sato, F. *Proc Natl Acad Sci USA* **2008**, *105*, 7393-7398.
- [13] Nakagawa, A., Minami, H., Kim, J.S., Koyanagi, T., Katayama, T., Sato, F., and Kumagai, H. *Nat Commun* **2011**, *2*, 326.
- [14] Nakagawa, A., Minami, H., Kim, J.S., Koyanagi, T., Katayama, T., Sato, F., and Kumagai, H. *Bioeng Bugs* **2012**, *3*.
- [15] Hawkins, K.M., and Smolke, C.D. *Nat Chem Biol* **2008**, *4*, 564-573.
- [16] Lee, S.Y., Kim, H.U., Park, J.H., Park, J.M., and Kim, T.Y. *Drug Discov Today* **2009**, *14*, 78-88.
- [17] Liscombe, D.K., Macleod, B.P., Loukanina, N., Nandi, O.I., and Facchini, P.J. *Phytochemistry* **2005**, *66*, 1374-1393.
- [18] Kleinschmidt, G., and Mothes, K. *Z Naturforsch* **1959**, *14*, 52-56.
- [19] Gear, J.R., and Spenser, I.D. *Nature* **1961**, *191*, 1393-1395.
- [20] Barton, D.H., Hesse, R.H., and Kirby, G.W. *J Chem Soc Perkin Trans 1* **1965**, 6379-6389.
- [21] Barton, D.H., Kirby, G.W., Steglich, W., Thomas, G.M., Battersby, A.R., Dobsan, T.A., and Ramuz, H. *J Chem Soc* **1965**, *65*, 2423-2438.
- [22] Zenk, M.H., Rueffer, M., Amann, M., Deus-Neumann, B., and Nagakura, N. *J Nat Prod* **1985**, *48*, 725-738.
- [23] Stadler, R., Kutchan, T.M., and Zenk, M.H. *Phytochemistry* **1989**, *28*, 1083-1086.

- [24] Muller, M.J., and Zenk, M.H. *Planta Med* **1992**, *58*, 524-527.
- [25] Facchini, P.J., Johnson, A.G., Poupart, J., and de Luca, V. *Plant Physiol* **1996**, *111*, 687-697.
- [26] Park, S.U., Johnson, A.G., Penzes-Yost, C., and Facchini, P.J. *Plant Mol Biol* **1999**, *40*, 121-131.
- [27] Bock, A., Wanner, G., and Zenk, M.H. *Planta* **2002**, *216*, 57-63.
- [28] Bird, D.A., Franceschi, V.R., and Facchini, P.J. *Plant Cell* **2003**, *15*, 2626-2635.
- [29] Alcantara, J., Bird, D.A., Franceschi, V.R., and Facchini, P.J. *Plant Physiol* **2005**, *138*, 173-183.
- [30] Ziegler, J., Voigtlander, S., Schmidt, J., Kramell, R., Miersch, O., Ammer, C., Gesell, A., and Kutchan, T.M. *Plant J* **2006**, *48*, 177-192.
- [31] Ziegler, J., Facchini, P.J., Geissler, R., Schmidt, J., Ammer, C., Kramell, R., Voigtlander, S., Gesell, A., Pienkny, S., and Brandt, W. *Phytochemistry* **2009**, *70*, 1696-1707.
- [32] Pienkny, S., Brandt, W., Schmidt, J., Kramell, R., and Ziegler, J. *Plant J* **2009**, *60*, 56-67.
- [33] Samanani, N., Park, S.U., and Facchini, P.J. *Plant Cell* **2005**, *17*, 915-926.
- [34] Zulak, K.G., Cornish, A., Daskalchuk, T.E., Deyholos, M.K., Goodenowe, D.B., Gordon, P.M., Klassen, D., Pelcher, L.E., Sensen, C.W., and Facchini, P.J. *Planta* **2007**, *225*, 1085-1106.
- [35] Hagel, J.M., Weljie, A.M., Vogel, H.J., and Facchini, P.J. *Plant Physiol* **2008**, *147*, 1805-1821.
- [36] Samanani, N., Liscombe, D.K., and Facchini, P.J. *Plant J* **2004**, *40*, 302-313.
- [37] Facchini, P., Hagel, J., Liscombe, D., Loukanina, N., MacLeod, B., Samanani, M., and Zulak, K. *Phytochem Rev* **2007**, *6*, 97-124.
- [38] Minami, H., Dubouzet, E., Iwasa, K., and Sato, F. *J Biol Chem* **2007**, *282*, 6274-6282.
- [39] Luk, L.Y., Bunn, S., Liscombe, D.K., Facchini, P.J., and Tanner, M.E. *Biochemistry* **2007**, *46*, 10153-10161.
- [40] Berkner, H., Engelhorn, J., Liscombe, D.K., Schweimer, K., Wohrl, B.M., Facchini, P.J., Rosch, P., and Matecko, I. *Protein Expr Purif* **2007**, *56*, 197-204.
- [41] Grothe, T., Lenz, R., and Kutchan, T.M. *J Biol Chem* **2001**, *276*, 30717-30723.
- [42] Fisinger, U., Grobe, N., and Zenk, M.H. *Nat Prod Commun* **2007**, *2*, 249-253.
- [43] Unterlinner, B., Lenz, R., and Kutchan, T.M. *Plant J* **1999**, *18*, 465-475.
- [44] Rink, E., and Bohm, H. *FEBS Lett* **1975**, *49*, 396-399.
- [45] Steffens, P., Nagakura, N., and Zenk, M.H. *Tetrahedron Lett* **1984**, *25*, 951-952.
- [46] Ikezawa, N., Iwasa, K., and Sato, F. *Plant Cell Rep* **2009**, *28*, 123-133.
- [47] Ikezawa, N., Iwasa, K., and Sato, F. *FEBS J* **2007**, *274*, 1019-1035.
- [48] Liscombe, D.K., and Facchini, P.J. *J Biol Chem* **2007**, *282*, 14741-14751.

- [49] Ignatov, A., Clark, W.G., Cline, S.D., Psenak, M., Krueger, J., and Coscia, C.J. *Phytochemistry* **1996**, *43*, 1141-1144.
- [50] Takeshita, N., Fujiwara, H., Mimura, H., Fitchen, J.H., Yamada, Y., and Sato, F. *Plant Cell Physiol* **1995**, *36*, 29-36.
- [51] Ikezawa, N., Tanaka, M., Nagayoshi, M., Shinkyō, R., Sakaki, T., Inouye, K., and Sato, F. *J Biol Chem* **2003**, *278*, 38557-38565.
- [52] Amann, M., Nagakura, N., and Zenk, M.H. *Eur J Biochem* **1988**, *175*, 17-25.
- [53] Eisenreich, W.J., Hofner, G., and Bracher, F. *Nat Prod Res* **2003**, *17*, 437-440.
- [54] Gao, J.M., Liu, W.T., Li, M.L., Liu, H.W., Zhang, X.C., and Li, Z.X. *J Mol Struct* **2008**, *892*, 466-469.
- [55] Martin, M.L., Diaz, M.T., Montero, M.J., Prieto, P., San Roman, L., and Cortes, D. *Planta Med* **1993**, *59*, 63-67.
- [56] Chulia, S., Ivorra, M.D., Lugnier, C., Vila, E., Noguera, M.A., and D'Ocon, P. *Br J Pharmacol* **1994**, *113*, 1377-1385.
- [57] Yamahara, J., Konoshima, T., Sakakibara, Y., Ishiguro, M., and Sawada, T. *Chem Pharm Bull* **1976**, *24*, 1909-1912.
- [58] Morais, L.C., Barbosa-Filho, J.M., and Almeida, R.N. *J Ethnopharmacol* **1998**, *62*, 57-61.
- [59] Kashiwada, Y., Aoshima, A., Ikeshiro, Y., Chen, Y.P., Furukawa, H., Itoigawa, M., *et al.* *Bioorg Med Chem* **2005**, *13*, 443-448.
- [60] Chao, J., Lu, T.C., Liao, J.W., Huang, T.H., Lee, M.S., Cheng, H.Y., Ho, L.K., Kuo, C. L., and Peng, W. H. *J Ethnopharmacol* **2009**, *125*, 297-303.
- [61] Hung, T.M., Ngoc, T.M., Youn, U.J., Min, B.S., Na, M., Thuong, P.T., and Bae, K. *Biol Pharm Bull* **2008**, *31*, 159-162.
- [62] King, J.F., Grant, A., Keirse, M.J., and Chalmers, I. *Br J Obstet Gynaecol* **1988**, *95*, 211-222.
- [63] Anselmi, E., Fayos, G., Blasco, R., Candenias, L., Cortes, D., and D'Ocon, P. *J Pharm Pharmacol* **1992**, *44*, 337-343.
- [64] Chulia, S., Ivorra, M.D., Martinez, S., Elorriaga, M., Valiente, M., Noguera, M.A., Lugnier, C., Advenier, C., and D'Ocon, P. *Br J Pharmacol* **1997**, *122*, 409-416.
- [65] Nakaoji, K., Nayeshiro, H., and Tanahashi, T. *Biol Pharm Bull* **1997**, *20*, 586-588.
- [66] Jow, G.M., Wu, Y.C., Guh, J.H., and Teng, C.M. *Life Sci* **2004**, *75*, 549-557.
- [67] Jung, H.A., Min, B.S., Yokozawa, T., Lee, J.H., Kim, Y.S., and Choi, J.S. *Biol Pharm Bull* **2009**, *32*, 1433-1438.
- [68] Cui, W., Iwasa, K., Tokuda, H., Kashihara, A., Mitani, Y., Hasegawa, T., *et al.* *Phytochemistry* **2006**, *67*, 70-79.
- [69] Mo, J., Guo, Y., Yang, Y.S., Shen, J.S., Jin, G.Z., and Zhen, X. *Curr Med Chem* **2007**, *14*, 2996-3002.
- [70] Jin, G.Z., and Sun, B.C. *Adv Exp Med Biol* **1995**, *363*, 27-28.

- [71] Sun, B.C., Zhang, X.X., and Jin, G.Z. *Life Sci* **1996**, *59*, 299-306.
- [72] Dong, Z.J., Guo, X., Chen, L.J., Han, Y.F., and Jin, G.Z. *Life Sci* **1997**, *61*, 465-472.
- [73] Jin, G.Z., Zhu, Z.T., and Fu, Y. *Trends Pharmacol Sci* **2002**, *23*, 4-7.
- [74] Fu, W., Shen, J., Luo, X., Zhu, W., Cheng, J., Yu, K., Briggs, J. M., Jin, G., Chen, K., and Jiang, H. *Biophys J* **2007**, *93*, 1431-1441.
- [75] Natesan, S., Reckless, G.E., Barlow, K.B. L., Odontiadis, J., Nobrega, J.N., Baker, G.B., George, S.R., Mamo, D., and Kapur, S. *Psychopharmacology* **2008**, *199*, 275-289.
- [76] Guo, Y., Zhang, H., Chen, X., Cai, W., Cheng, J., Yang, Y., Jin, G., and Zhen, X. *Schizophr Res* **2009**, *115*, 41-49.
- [77] Sun, Y., Dai, J., Hu, Z., Du, F., Niu, W., Wang, F., Liu, F., Jin, G., and Li, C. *Br J Pharmacol* **2009**, *158*, 1302-1312.
- [78] Gao, M., Chu, H.Y., Jin, G.Z., Zhang, Z.J., Wu, J., and Zhen, X.C. *Synapse* **2011**, *65*, 379-387.
- [79] Oger, J. M., Fardeau, A., Richomme, P., Guinaudeau, H., and Fournet, A. *Can J Chem* **1993**, *71*, 1128-1135.

CHAPTER 2

2 Berberine bridge enzyme and the family of bicovalent flavoenzymes

Author contributions

My contribution to this review was to search for literature and to plan the chapters on BBE, and on bicovalent flavoenzymes in plants and fungi. I performed most of the Blast-searches and bioinformatical analyses and I wrote the above mentioned parts of the manuscript. CORINNA DULLY helped me with analyzing homology models of all BBE-like enzymes in *Arabidopsis thaliana*. BASTIAN DANIEL wrote the part on BBE in biocatalysis and helped to draw the required figures. PETER MACHEROUX wrote the introduction and the chapter on BBE-like enzymes in the bacterial kingdom and corrected the whole manuscript.

Berberine bridge enzyme and the family of bicovalent flavoenzymes

Silvia Wallner, Corinna Dully, Bastian Daniel and Peter Macheroux*

*From the Graz University of Technology, Institute of Biochemistry, Petersgasse 12,
A-8010 Graz, Austria; Tel.: +43-316-873 6450, Fax: +43-316-873 6952,
Email: peter.macheroux@tugraz.at

Table of Contents

1	INTRODUCTION	18
2	THE PARADIGM OF BICOVALENT FLAVOENZYMES: BERBERINE BRIDGE ENZYME (BBE) FROM <i>ESCHSCHOLZIA CALIFORNICA</i>	22
3	THE FAMILY OF BBE-LIKE ENZYMES IN THE PLANT KINGDOM: HOW MANY AND WHAT FOR?	27
4	THE OCCURRENCE OF BBE-LIKE ENZYMES IN FUNGI.....	37
5	BBE-LIKE ENZYMES IN BACTERIA: OXIDATIVE POWER FOR THE BIOSYNTHESIS OF ANTIBIOTICS.....	41
6	CONCLUSIONS.....	43

Abstract

Flavoproteins are a large and diverse group of proteins that employ either FMN or FAD for catalysis. In the majority of flavoproteins (~90%) the flavin coenzyme is tightly but noncovalently bound in the active site of the enzyme. In the 1950s the first example of a covalently attached flavocoenzyme was discovered in succinate dehydrogenase followed by several more cases where either the 8 α - or 6-position of the isoalloxazine forms a covalent bond to the amino acid side chain of a cysteine, histidine or tyrosine. Very recently, in 2005, the first representative of a bicovalently linked flavocoenzyme was discovered in glucoooligosaccharide oxidase. Since then, the number of bicovalently linked flavoproteins has risen rapidly and appears to be more common than any of the monocovalent attachment modes. These enzymes have extraordinary properties, such as unusually high redox potentials that enable catalysis of challenging chemical reactions in plants, fungi and bacteria. Moreover, bicovalent linkage appears to be crucial for structural integrity of the protein and correct positioning of the flavin in the active site. As a starting point, we review the wealth of information available for berberine bridge enzyme from *Eschscholzia californica* which can be considered a paradigm for the family of bicovalent flavoproteins. Moreover, we discuss the scope of reactions catalyzed by these enzymes in plants, fungi and bacteria. Finally, genomic information is explored to predict the number of bicovalent flavoenzymes present in nature. This analysis suggests that some genera are rich in bicovalent flavoproteins while others appear to have only a few members of this family of enzymes.

Introduction

The majority of flavoproteins (approximately 90%) contain noncovalently bound (dissociable) FMN or FAD as cofactor [1]. The first example of a covalently bound flavin was discovered in the 1950ies by SINGER and coworkers. SINGER's group demonstrated that succinate dehydrogenase, a central enzyme of the tricarboxylic acid cycle and entry point of electrons into the mitochondrial electron transport chain („complex II“), contains a covalently attached FAD [2]. Further studies demonstrated a linkage of the 8 α -methyl group of the isoalloxazine ring to N-3 of a histidine residue of the protein [3]. In the following years several other covalent linkages in flavoenzymes emerged such as tyrosinylation and cysteinylolation at the 8 α -methyl group and cysteinylolation of C-6 [4, 5]. At the end of the last century, MEWIES *et al.* listed 24 flavoenzymes with a known linkage to either the 8 α - or 6-position of the flavin [4, 6]. A few years later, in 2005, the elucidation of the crystal structure of glucooligosaccharide oxidase (GOOX) provided the first example of a bicovalently linked FAD cofactor [7]. In this fungal enzyme the FAD is linked to a histidine and cysteine residue at the 8 α -methyl and C-6 position of the flavin, respectively. In other words, in this flavoenzyme the already known monocovalent attachments are combined to give a bicovalently linked flavin. At the time, this finding may have been regarded as a peculiarity of an enzyme that catalyzes the oxidation of a variety of mono- and oligosaccharides in a pathogenic fungus (for structures, see later). However, in the meantime it appears that bicovalent attachment occurs in many bacterial, fungal and plant enzymes and may eventually outnumber monocovalent attachment. From the current list of 43 flavoproteins bearing a covalent flavin cofactor, eleven are reported or predicted to feature bicovalent flavin attachment (Tab.1). Interestingly, bicovalent flavin attachment is confined to bacteria, fungi and plants and is absent from archaea and the animal kingdom as is evident from BlastP searches. It is also notable that all bicovalently attached flavins are found in proteins adopting a fold first observed in *p*-cresolmethylhydroxylase (PCMH) in the clan FAD_binding_4 of the PCMH protein family. With only a few exceptions this structural environment appears to prefer covalent binding of the flavin cofactor either mono- (as in PCMH) or in a bicovalent fashion [1]. On the other hand, monocovalent attachment occurs in at least three different protein topologies: NADP_Rossman and

GMC_oxred_C for FAD-containing and TIM_barrel for FMN-containing enzymes (Tab.1).

Recent research offers several explanations for the role of bicovalent flavin tethering in flavoenzymes [8]. It increases the midpoint potential of the flavin cofactor to unprecedented high values and thus enables challenging substrate oxidations [9-11]. Furthermore, it appears that these enzymes have very bulky substrates and hence the binding cavity near the flavin cofactor is very large potentially leading to high mobility of the isoalloxazine ring. This mobility is severely restricted by bicovalent linkage and freezes out translational modes that could compromise catalytic efficiency [8]. Indeed, these two factors play a role in chitoooligosaccharide oxidase (ChitO) from *Fusarium graminearum* where bicovalent flavinylation modulates the redox potential and is required for correct positioning of cofactor and substrate in the active site and hence is a prerequisite for the formation of a catalytically competent Michaelis-Menten-complex [10]. Moreover, bicovalent linkage appears to be crucial for structural integrity as is evident from the low yields of protein variants, which lack one or both flavinylated sites [12]. Thus it appears that several factors must be considered to rationalize bicovalent linkage of the flavin and their relative contribution may also vary depending on the enzyme.

Tab.1: Covalent attachment of FMN and FAD; bicovalent attachment is marked by an asterisk.

No.	E.C.	Enzyme	Cofactor	Structure Clan (Family)	Genus
1*	1.1.3.5	hexose oxidase	8 α -(His, 6-Cys)-FAD	-----	<i>Chondrus</i>
2	1.1.3.6	cholesterol oxidase	8 α -(N1-His)-FAD	FAD_PCMH (FAD_binding_4)	<i>Brevibacterium</i>
3	1.1.3.8	L-gulonolactone oxidase	8 α -(N1-His)-FAD	-----	ubiquitous
4	1.1.3.10	pyranose 2-oxidase	8 α -(N3-His)-FAD	GMC_oxred_C	<i>Trametes,</i> <i>Peniophora</i>
5	1.1.3.17	choline oxidase	8 α -(N3-His)-FAD	NADP_Rossmann (GMC_oxred_N)	<i>Arthrobacter</i>
6	1.1.3.23	thiamine oxidase	8 α -(N1-His)-FAD	-----	soil bacteria
7	1.1.3.37	D-arabino-1,4-lactone oxidase	8 α -(N1-His)-FAD	-----	<i>Candida,</i> <i>Saccharomyces</i>
8	1.1.3.38	vanillyl-alcohol oxidase	8 α -(N3-His)-FAD	FAD_PCMH (FAD_binding_4)	<i>Penicillium</i>
9	1.1.3.39	nucleoside oxidase (H ₂ O ₂ -forming)	FAD (covalent)	-----	<i>Elizabethkingia</i>
10	1.1.3.41	alditol oxidase	8 α -(N1-His)-FAD	FAD_PCMH (FAD_binding_4)	<i>Streptomyces</i>
11*	1.1.3.-	aclacinomycin oxidoreductase	8 α -(N1-His, 6-Cys)-FAD	FAD_PCMH (FAD_binding_4)	<i>Streptomyces</i>
12*	1.1.3.-	chitooligosaccharide oxidase	8 α -(N1-His, 6-Cys)-FAD	predicted ^a	<i>Fusarium</i>
13	1.1.3.-	eugenol oxidase	8 α -(N3-His)-FAD	predicted ^a	<i>Rhodococcus</i>
14	1.1.3.-	D-gluconolactone oxidase	8 α -(N3-His)-FAD	predicted ^a	<i>Penicillium</i>
15*	1.1.3.-	glucooligosaccharide oxidase	8 α -(N1-His, 6-Cys)-FAD	FAD_PCMH (FAD_binding_4)	<i>Acremonium</i>
16*	1.1.3.-	glycopeptide hexose oxidase (Dbv29)	8 α -(N1-His, 6-Cys)-FAD	FAD_PCMH (FAD_binding_4)	<i>Actinomadura</i>
17*	1.1.3.-	10-hydroxy-dehydrogenase in tirandamycin biosynthesis (TrdL, TamL)	8 α -(N1-His, 6-Cys)-FAD	FAD_PCMH (FAD_binding_4)	<i>Streptomyces</i>
18	1.1.3.-	nectarin V (putative sugar oxidase)	FAD (covalent)?	-----	<i>Nicotiana</i>
19*	1.1.3.-	pregilvocarcin V dehydrogenase, GilR	8 α -(N1-His, 6-Cys)-FAD	FAD_PCMH (FAD_binding_4)	<i>Streptomyces</i>
20	1.1.99.3	gluconate 2-dehydrogenase (acceptor)	8 α -(N3-His)-FAD	-----	bacteria
21	1.1.99.4	dehydrogluconate dehydrogenase	8 α -(N3-His)-FAD	-----	bacteria
22*	1.3.3.8	(S)-tetrahydroprotoberberine oxidase	8 α -(N1-His, 6-Cys)-FAD	predicted from homology modelling ^b	<i>Argemone</i>

23	1.3.5.1	succinate dehydrogenase (ubiquinone)	8 α -(N3-His)-FAD	NAPH_Rossmann (FAD_binding_2)	ubiquitous
24	1.3.99.1	succinate dehydrogenase / fumarate reductase	8 α -(N3-His)-FAD	NADP_Rossmann (FAD_binding_2)	<i>Shewanella</i> , <i>Wolinella</i>
25	1.4.3.4	monoamine oxidase	8 α -(Cys)-FAD	NADP_Rossmann (Amino_oxidase)	mammals
26	1.4.3.-	amino acid oxidase, NikD	8 α -(Cys)-FAD	NADP_Rossmann (DAO)	<i>Streptomyces</i>
27	1.5.3.1	sarcosine oxidase (monomeric) sarcosine oxidase (heterotetrameric)	8 α -(Cys)-FAD 8 α -(N3-His)-FMN	NADP_Rossmann (DAO) α and β interface	<i>Bacillus</i> <i>Corynebacterium</i>
28	1.5.3.6	(<i>R</i>)-6-hydroxynicotine oxidase	8 α -(N1-His)-FAD	FAD_PCMH (FAD_binding_4)	<i>Arthrobacter</i>
29	1.5.3.7	L-pipecolate oxidase	8 α -(Cys)-FAD ?	-----	<i>Pseudomonas</i>
30	1.5.3.10	dimethylglycine oxidase	8 α -(N3-His)-FAD	NADP_Rossmann (DAO)	<i>Arthrobacter</i>
31	1.5.3.-	γ - <i>N</i> -methylaminobutyrate oxidase	8 α -(His)-FAD	-----	<i>Arthrobacter</i>
32	1.5.8.1	dimethylamine dehydrogenase	6-(Cys)-FMN	-----	<i>Hyphomicrobium</i>
33	1.5.8.2	trimethylamine dehydrogenase	6-(Cys)-FMN	TIM_barrel (Oxidored_FMN)	<i>Hyphomicrobium</i>
34	1.5.99.1	sarcosine dehydrogenase	8 α -(N3-His)-FAD	-----	ubiquitous
35	1.5.99.2	dimethylglycine dehydrogenase	8 α -(N3-His)-FAD	-----	ubiquitous
36	1.5.99.12	cytokinin dehydrogenase	8 α -(N1-His)-FAD	FAD_PCMH (FAD_binding_4)	plants
37	1.14.14.-	halogenase in chloramphenicol biosynthesis (CmlS)	8 α -(Asp)-FAD	NADP_Rossmann (Trp_halogenase)	<i>Streptomyces</i>
38	1.17.99.1	4-cresol dehydrogenase (hydroxylating)	8 α -(<i>O</i> -Tyr)-FAD	FAD_PCMH (FAD_binding_4)	<i>Pseudomonas</i>
39*	1.21.3.3	reticuline oxidase (berberine bridge enzyme)	8 α -(N1-His, 6-Cys)-FAD	FAD_PCMH (FAD_binding_4)	<i>Eschscholzia</i>
40	1.21.99.1	β -cyclopiazonate dehydrogenase	8 α -(N1-His)-FAD	-----	<i>Aspergillus</i>
41*	1.-.-.-	Δ^1 -tetrahydrocannabinolic acid synthase	8 α -(N1-His, 6-Cys)-FAD	FAD_PCMH (FAD_binding_4)	<i>Cannabis</i>
42	-----	redox driven ion pumps, RnfG and RnfD	ribitylphosphate- (<i>O</i> -Thr)-FMN	-----	<i>Vibrio</i>
43*	-----	pollen allergens (BBE-like proteins)	8 α -(N1-His, 6-Cys)-FAD	FAD_PCMH (FAD_binding_4)	grasses

^apredicted (Leferink, N.G.H., Heuts, D.P.H.M., Fraaije, M.W., van Berkel, W.J.H.: The growing VAO flavoprotein family, Arch. Biochem. Biophys. 474:292-301, 2008)

^bpredicted from homology modeling (Gesell, A., Diaz Chavez, M. L., Kramell, R., Piotrowski, M., Macheroux, P., Kutchan, T.: Heterologous expression of two FAD-dependent oxidases with (*S*)-tetrahydroprotoberberine oxidase activity from *A. mexicana* and *B. wilsoniae*, Planta, 233:1185-1197, 2011)

The paradigm of bivalent flavoenzymes: Berberine bridge enzyme (BBE) from *Eschscholzia californica*

BBE is a branch point enzyme in benzyloisoquinoline alkaloid biosynthesis [13]. It catalyzes the oxidative cyclization of (*S*)-reticuline to (*S*)-scoulerine and hence opens the way towards formation of protoberberine, protobine and benzophenanthridine alkaloids (Fig.5) [14, 15].

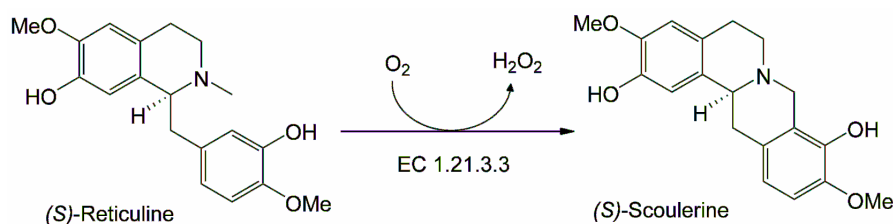


Fig.5: Overall reaction catalyzed by BBE.

The first isolation of the enzyme dates back to 1975, when RINK and BÖHM reported the partial purification of BBE from *Macleaya microcarpa* cell cultures [16]. Subsequently STEFFENS *et al.* found BBE activity in 66 differentiated plants and cell suspension cultures, mainly from the families *Papaveraceae* and *Fumariaceae* [17]. Later the enzyme was successfully expressed in small amounts in insect cell culture and it was demonstrated that the FAD cofactor is covalently linked to a histidine residue via its 8 α -position [18]. During our studies with BBE, expressed in the methylotrophic host *Pichia pastoris*, we noticed that photoreduction of the enzyme yields 6-thio-FAD, a product known to form during photoreduction of 6-cysteinyl-flavins [19]. This observation prompted us to isolate the flavin-containing tryptic fragment and analyze its composition by amino acid sequencing and mass spectrometry [20]. This analysis clearly revealed that the FAD bears two peptides and we proposed that His104 and Cys166 forms a linkage to position 8 α and 6 of the flavin isoalloxazine ring system, respectively [20]. Later, the elucidation of the crystal structure confirmed our model of bivalent cofactor attachment [14].

Not surprisingly, the structural topology turned out to be very similar to GOOX, which is also a member of the PCMH superfamily (clan FAD_binding_4). The structure is composed of a FAD and a substrate binding domain, which is formed by a seven-stranded antiparallel β -sheet in an α/β domain [14] (Fig.6). It provided the ultimate proof for the bivalent tethering of the flavin cofactor to

His104 and Cys166 of the protein. The substrate (*S*)-reticuline is found in a relatively open substrate binding site sandwiched between the flavin cofactor and active site amino acid residues extending from the central β -sheet.

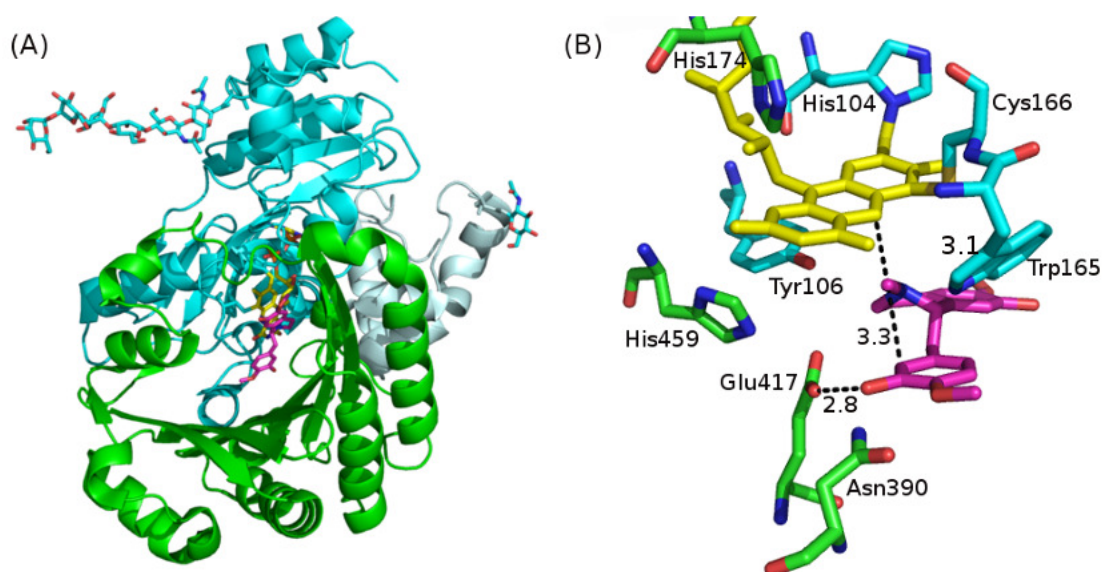


Fig.6: Schematic representation of the protein structure.

(A) Overall topology of BBE. The N-terminal FAD-binding subdomains are shown in cyan including the C-terminal α -helical stretch in pale blue. The central substrate binding domain is shown in green. N-linked sugar residues (blue), the FAD cofactor (yellow), and the substrate (*S*)-reticuline are represented as stick models.

(B) Active site of BBE in complex with (*S*)-reticuline. The flavin cofactor is shown in yellow with its bicovalent linkage to His104 and Cys166. Important active site amino acid residues are drawn in stick representation. The substrate (*S*)-reticuline is shown in magenta. Distances are indicated in Å.

The structure of BBE enabled a comprehensive mutagenesis program geared towards a better understanding of the mechanism for C-C bond formation. This program comprised the replacement of active site residues Glu417, Tyr106, and His459 with Gln, Phe, and Ala, respectively, and determination of kinetic parameters for all variant proteins (see Fig.6 for an active site representation of BBE) [14]. Eventually, these studies culminated in the formulation of a concerted reaction mechanism for the formation of the “berberine” bridge in the product (*S*)-scoulerine. In this mechanism, Glu417 acts as catalytic base by deprotonating the C3' hydroxy group of (*S*)-reticuline and thereby increases the nucleophilicity of the C2' atom, which further performs a S_N2 - nucleophilic attack on the *N*-methyl group of the substrate. Thus the methylene bridge of (*S*)-scoulerine is formed and a hydride is transferred to the flavin cofactor (Fig.7) [14].

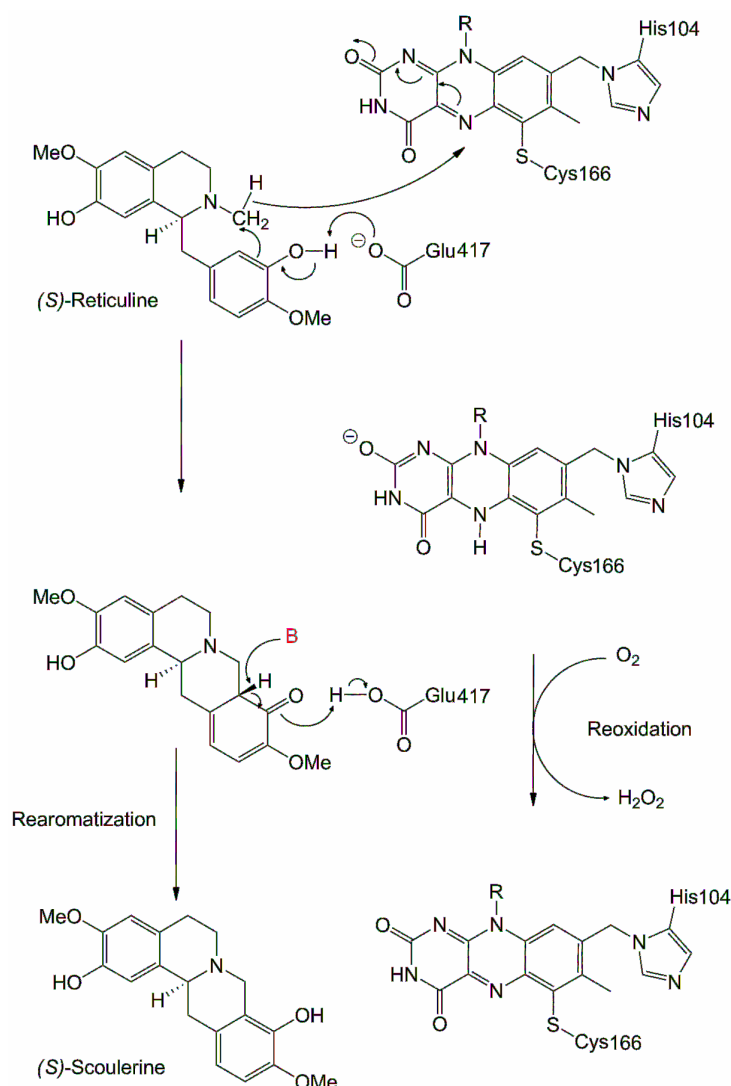


Fig.7: Concerted mechanism for BBE.

Single variant proteins with either His104 or Cys166 replaced by alanine were expressed and resulted in a decrease in midpoint potentials and k_{cat} -values compared to wild type BBE [12]. Thus bicovalent linkage in BBE increases the redox potential of the flavin cofactor and is crucial for enzyme activity. Unfortunately, attempts to obtain the H104A/C166A double-variant failed presumably because covalent cofactor linkage is required for protein folding and/or stability [12].

Even before the first crystal structures of flavoproteins became available, the presence of a positive charge in vicinity to the N(1)-C(2)=O locus was suggested as a common feature of flavin-dependent oxidases [21-24]. Upon electron uptake the resulting negative charge at the N(1)-C(2)=O locus of the isoalloxazine ring system is stabilized by a positive environment [8, 25]. This property of flavin oxidases also leads to the stabilization of anionic flavin semiquinones, N(5)-sulfite adducts as well

as the deprotonated forms of artificial flavins bearing an ionizable group at positions 6 or 8 (e.g. 6- or 8-mercaptoflavin) [21-23, 26-34, 34]. So far, investigations on different flavoproteins suggest that this charge can be supplied by either a positively charged amino acid residue, such as a histidine [35-37], lysine [27, 38-41], or arginine [42], or by the positive end of a helix dipole [8, 43-45]. BBE exhibits characteristic properties of flavoprotein oxidases, such as stabilization of the anionic semiquinone, or the ability to form N(5)-sulfite adducts, albeit with a dissociation constant that is notably higher than for other characterized flavin-dependent oxidases [46]. His174 was identified to be the respective amino acid in BBE supplying stabilization of negative charges. Interestingly, this residue does not directly interact with the N(1)-C(2)=O locus of the flavin, but forms a hydrogen bonding network via the C2' hydroxyl group of the ribityl side chain of the flavin. Exchange of His174 to Ala had a pronounced effect on the catalytic activity by decreasing k_{cat} 120-fold (WALLNER *et al.* 2012, submitted).

Today, BBE is considered a paradigm of the entire family of enzymes as it is arguably one of the best characterized members. Our detailed understanding of the *E. californica* BBE has also led to the exploitation of the enzyme for the production of enantiomerically pure alkaloids with different pharmacological activities [47].

Recently SCHRITTWIESER *et al.* applied BBE for the production of various (*S*)-berbines and (*R*)-benzylisoquinolines [48]. Berbines and benzylisoquinoline alkaloids are a related class of natural compounds [49] that share the isoquinoline heterocycle as a common structural feature (Fig.8).

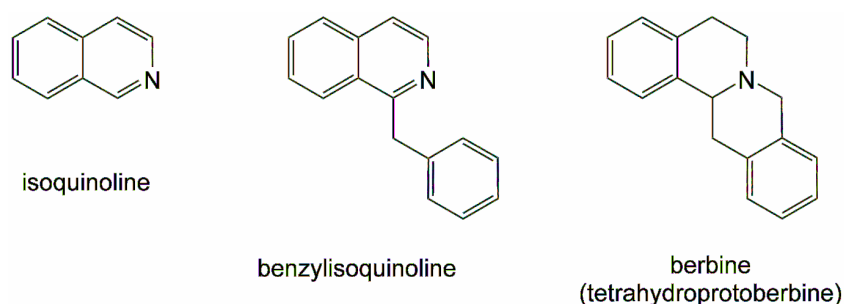


Fig.8: Structure of benzylisoquinoline and berbine alkaloids.

Benzylisoquinolines show a broad range of biological effects and are applied as pharmaceuticals with analgesic, sedative, hypnotic, antihypertensive, tranquilizing, or muscle relaxation activity [50-53]. Furthermore some 1-benzyl-1,2,3,4,-tetrahydroisoquinolines show *in vitro* anti-HIV activity making those compounds

potential lead structures for the treatment of HIV patients [54]. Most berbine alkaloids show a relaxing effect on the central nervous system and hence are applied as potent sedatives [55]. Recently berbine derivatives are being investigated as drugs for the treatment of schizophrenia [56].

So far, there are several alkaloids with potential application as pharmaceuticals. However, the isolation of these alkaloids from their natural source is very time consuming and results in extremely low yields. Moreover, total organic synthesis of those chiral and complex alkaloids is inefficient and can not be accomplished with satisfactory enantiomeric excess [57-59].

Hence the biocatalytic approach of SCHRITTWIESER *et al.* is an important step towards the production of enantiomerically pure (*S*)-berbines and (*R*)-benzylisoquinolines [48]. A broad spectrum of substrates was investigated and it was shown that BBE accepts non-natural benzylisoquinolines in (*S*)-configuration (Fig.9).

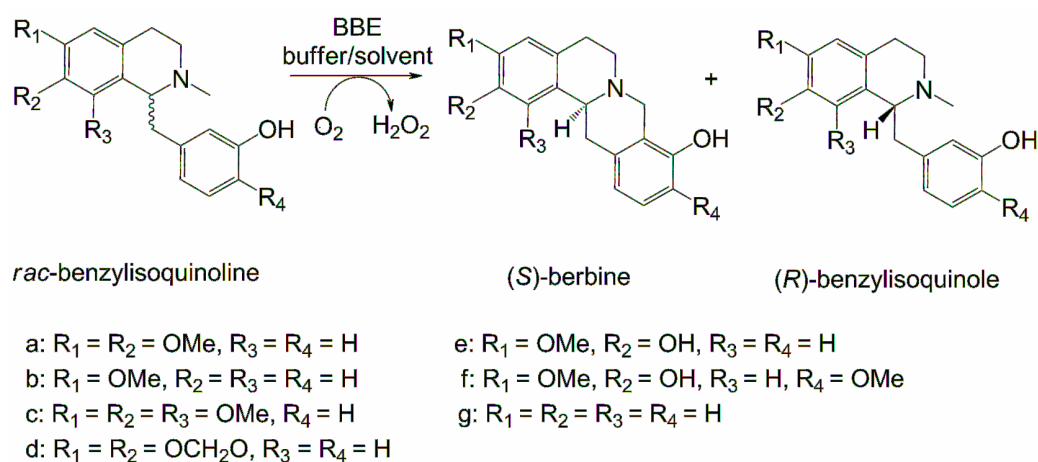


Fig.9: Kinetic resolution of racemic benzylisoquinolines catalysed by BBE.

Furthermore the reaction was optimized regarding pH, temperature and solvent [47, 60]. Due to the low solubility of benzylisoquinolines in aqueous buffer the use of cosolvents is required to allow substrate concentrations of at least 20 g L^{-1} . Interestingly, BBE exhibited an unexpectedly high tolerance towards different organic solvents with $70\% \text{ v v}^{-1}$ toluene being the best solvent concentration for efficient catalysis. High conversion rates can be achieved using pH values between 8 and 11 and a temperature from 30 to $50 \text{ }^\circ\text{C}$. Using optimized reaction conditions the model reaction was performed in 500 mg scale with 50% conversion in 24 h giving enantiopure (*S*)-berbine ($ee > 97\%$) and (*R*)-benzylisoquinole ($ee > 97\%$) [60].

Moreover, the conversion of different racemic benzyloquinolines was studied (Fig.5). In all cases the (*S*)-enantiomer of the respective benzyloquinoline was accepted as substrate resulting in the formation of (*S*)-berbines and (*R*)-benzyloquinolines in optically pure form (ee >97%) and in good to excellent yield (22% - 50%).

It is noteworthy that BBE converts 1,2,3,4-tetrahydrobenzyloquinolines mainly to 9-hydroxy functionalized products and not to the 11-hydroxy functionalized regioisomers. In a further study Resch *et al.* attempted to change regioselectivity of BBE by medium engineering and by blocking the “normal” reaction centre with a fluoro moiety. This proved to be an efficient strategy for completely changing regioselectivity leading to the formation of new 11-hydroxy functionalized products (Resch *et al.* 2012, submitted).

In conclusion, the studies with BBE as a potential industrial biocatalyst show that the enzyme can be successfully applied for the preparation of enantiomerically pure isoquinoline and berbine derivatives.

The family of BBE-like enzymes in the plant kingdom: how many and what for?

The group of BBE-like proteins is steadily increasing and sequence alignments provide strong evidence that a variety of plant proteins possess conserved histidine and cysteine residues for bicovalent attachment of the cofactor. The availability of whole genomes for different plants enabled a targeted search of BBE-homologues in 26 plant species as shown in Tab.2. Using the Blast tool provided on the phytozome website (<http://www.phytozome.net/search.php>) many BBE-homologues could be identified in the available plant genomes. The highest number of BBE homologues was found in the poplar *Populus trichocarpa*, which possesses 57 BBE-like proteins. To our knowledge this plant does not accumulate complex alkaloids and hence BBE-like proteins in poplar seem to fulfil roles apart from alkaloid biosynthesis. Furthermore, our analysis revealed that a high number of BBE-homologues are also present in the orders of Fabales (e.g. soybean), Rutales (e.g. citrus fruits) and Brassicales (e.g. *Arabidopsis*), suggesting a high abundance of bicovalent flavoproteins in the plant kingdom. Poales, such as rice, sorghum or maize, possess

comparatively few BBE-homologues proteins, the same applies for grape. Finally, in mosses and algae BBE-like proteins seem to be rare (Tab.2).

In addition to this bioinformatical analysis, there is also experimental evidence that flavoproteins from different plant sources possess both a covalent histidinyl- and cysteinyl- linkage of the cofactor [20, 61-65]. In plants bicovalent flavoproteins are involved in many different processes. They comprise oxidases in alkaloid biosynthesis (BBE, STOX) [20, 64], cannabinoid metabolism (THCA synthase) [66], or active plant defence (nectarin V, carbohydrate oxidases from *Helianthus annuus* and *Lactuca sativa*) [67, 68]. In the seaweed *Chondrus crispus* a BBE-like enzyme was found to catalyze the oxidation of a variety of hexose sugars [69-72]. A further group of bicovalently linked plant proteins is known to act as pollen allergens and is found in various grasses, such as timothy (Phl p 4) [65] or Bermuda grass (Cyn d 4, earlier referred to as BG60) [73].

Tab.2: BBE-like proteins in various plant species & families.

Plant	Family	Common name	BBE-like homologues
<i>Populus trichocarpa</i>	<i>Salicaceae</i>	Western balsam poplar	57
<i>Glycine max</i>	<i>Fabaceae</i>	soybean	46
<i>Citrus clementina</i>	<i>Rutaceae</i>	clementine	39
<i>Prunus persica</i>	<i>Rosaceae</i>	peach	30
<i>Arabidopsis thaliana</i>	<i>Brassicaceae</i>		28
<i>Eucalyptus grandis</i>	<i>Myrtaceae</i>	eucalyptus	27
<i>Mimulus guttatus</i>	<i>Scrophulariaceae</i>	common monkey-flower	25
<i>Citrus sinensis</i>	<i>Rutaceae</i>	orange	24
<i>Cucumis sativus</i>	<i>Cucurbitaceae</i>	cucumber	23
<i>Aquilegia coerulea</i>	<i>Ranunculaceae</i>	Rocky mountain columbine	18
<i>Medicago truncatula</i>	<i>Fabaceae</i>	barrel medic	18
<i>Manihot esculenta</i>	<i>Euphorbiaceae</i>	cassava (manioc)	17
<i>Zea mays</i>	<i>Poaceae</i>	maize	16
<i>Ricinus communis</i>	<i>Euphorbiaceae</i>	ricinus	15
<i>Setaria italica</i>	<i>Poaceae</i>	foxtail millet	13
<i>Sorghum bicolor</i>	<i>Poaceae</i>	sorghum	13
<i>Carica papaya</i>	<i>Caricaceae</i>	papaya	12
<i>Oryza sativa</i>	<i>Poaceae</i>	rice	11
<i>Brachypodium distachyon</i>	<i>Poaceae</i>	purple false brome	10
<i>Vitis vinifera</i>	<i>Vitaceae</i>	grape	5
<i>Physcomitrella patens</i>	<i>Funariaceae</i>		1
<i>Chlamydomonas reinhardtii</i>	<i>Chlamydomonadaceae</i>		0
<i>Selaginella moellendorffii</i>	<i>Selaginellaceae</i>		0
<i>Volvox carteri</i>	<i>Volvocaceae</i>		0

In *Papaveraceae* bicovalently linked flavoproteins are reported to catalyze crucial oxidations in alkaloid biosynthesis. As discussed before, BBE catalyzes the oxidative formation of the methylene bridge of (*S*)-scoulerine in different poppy species [17, 74]. Moreover, (*S*)-tetrahydroprotoberberine oxidase (STOX) is described as a flavin containing oxidase accepting tetrahydroprotoberberines in (*S*)-configuration [75-77]. Due to the lack of a crystal structure of STOX there is no final evidence that the enzyme belongs to the family of bivalent flavoproteins, however, homology modelling and a phylogenetic analysis strongly suggests that the flavin cofactor in STOX is also bicovalently bound [64]. The substrate specificity of STOX from *Argemone mexicana* and *Berberis wilsoniae* were investigated and both enzymes catalyze the oxidation of (*S*)-tetrahydropalmatine to palmatine (Fig.10) [64]. Additionally, (*S*)-scoulerine and (*S*)-canadine were accepted as substrates for STOX from *B. wilsoniae*, and STOX from *A. mexicana* converted (*S*)-coreximine, respectively [64]. Thus STOX is proposed to catalyze the oxidation of different tetrahydroprotoberberines in benzyloquinoline producing plants.

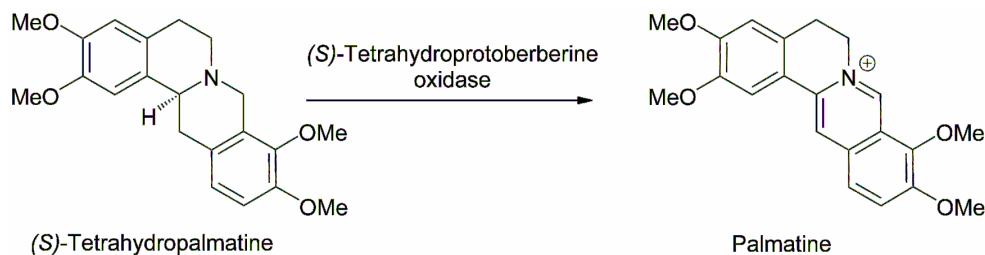


Fig.10: Conversion of (*S*)-tetrahydropalmatine by STOX.

Δ^1 -Tetrahydrocannabinolic acid (THCA) synthase was identified to be an important enzyme in controlling the psychoactivity of *Cannabis sativa* [66]. It catalyzes the oxidative cyclization of the monoterpene moiety of cannabigerolic acid (CBGA) into THCA, which further decarboxylates in a non-enzymatic fashion yielding THC as psychoactive compound (Fig.11) [66, 78]. Cannabinoids are exclusively found in *C. sativa* [79] and the pharmacological importance of these compounds [79-86] boosted investigations on THCA synthase [87]. Successful crystallization of THCA synthase was published in 2005 [61] and the elucidated structure clearly reveals that the enzyme belongs to the PCMH superfamily of flavoproteins with a bivalent tethered cofactor as was already discussed previously for BBE (personal communication, R. KUROKI, Quantum Beam Science Directorate, Japan Atomic

Energy Agency, Tokai, Japan). THCA synthase catalyzes an oxidative ring closure reaction, which is similar to the berberine bridge formation. However, SHOYAMA *et al.* suggest a cationic mechanism for THCA synthase instead of the one-step concerted reaction found for BBE [61].

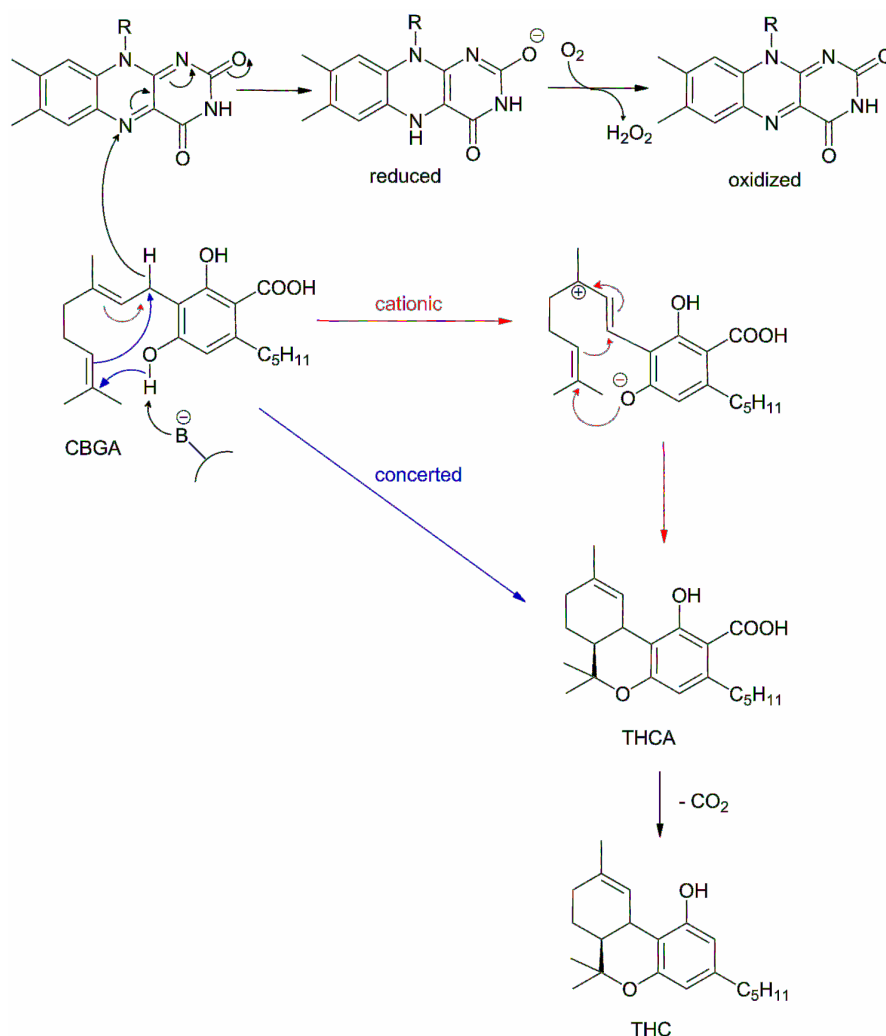


Fig.11: Proposed mechanism for THCA synthase.

Two possible routes for THCA formation, which both are initiated by proton abstraction from CBGA. In the mechanism suggested by SIRIKANTARAMAS *et al.* (red arrows) a cationic intermediate is formed, which further cyclizes yielding THCA, which further undergoes non-enzymatic decarboxylations. We rather suggest a concerted mechanism (blue arrow) as was already reported for BBE. In both cases the reduced flavin is regenerated with molecular oxygen. [66]

According to these authors, catalysis is initiated by a hydride transfer from the C-3 position of CBGA to the N-5 position of the isoalloxazine ring moiety of the FAD cofactor. The resulting carbocation then collapses to the product by nucleophilic attack of the oxyanion previously generated by proton abstraction. The reduced flavin is reoxidized by transferring a hydride to molecular oxygen resulting in the formation of hydrogen peroxide as a side product. (Fig.11) [66] So far, there is no

evidence for the cationic mechanism and we rather suggest that the concerted mechanism of BBE might also be relevant for the C-C bond formation of Δ^1 -tetrahydrocannabinolic acid (THCA) synthase. It is noteworthy that BBE and THCA synthase exhibit substantial sequence similarities and that the crucial catalytic glutamate residue is present in both enzymes suggesting a similar path for catalysis in these two oxidases [14].

Interestingly, not all bivalent flavoproteins are involved in secondary metabolite production in plants. Nectarin V (NEC5) is a BBE-like enzyme and is expressed in the nectary gland of ornamental tobacco [62, 88]. The enzyme shows glucose oxidase activity by oxidizing glucose to gluconolactone and hydrogen peroxide [62]. Hydrogen peroxide in turn seems to play a vital role in defence against microbial attack by preventing microbe contamination of the floral reproductive tract [67, 89-92]. There is also evidence that in contrast to the earlier discussed bivalently flavinylated oxidases, NEC5 does not strictly depend on oxygen as electron acceptor for cofactor reoxidation. According to unpublished data of C. CARTER and R.W. THORNBURG mentioned in [67] dehydroascorbate is accepted instead of molecular oxygen resulting in flavin reoxidation and recycling of ascorbate from dehydroascorbate.

Enzymes involved in plant defence were also identified in other species, such as *H. annuus* (sunflower) or *L. sativa* (lettuce). Both plants express a carbohydrate oxidase with broad substrate specificity for the majority of mono- and disaccharides and with the production of H_2O_2 as a toxic reaction product [68].

Hexoses oxidase (HOX) from the seaweed *C. crispus* is another BBE-like enzyme accepting glucose as substrate [71]. However, this enzyme exhibits a broad substrate range compared to nectarin V. Besides glucose and galactose, HOX accepts various oligomeric sugars such as lactose, maltose, cellobiose and maltotriose as well as glucooligosaccharides with up to seven glucose units [71, 72].

For another group of BBE-like proteins no catalytic function could be identified up to now. These proteins are known to act as pollen allergens and they share the histidine and cysteine motifs for covalent flavinylation [65, 73]. Pollen allergens are generally found in different grasses and types of corn. BG60, later referred to as Cyn d 4, is described as a covalently flavinylated pollen allergen in Bermuda grass [73, 93]. Later, antigens with homology to BG60 were described to be present in celery (Api g 5) and in oilseed rape pollen [94-96]. Moreover, Phl p 4

was discovered in two isoforms in timothy grass [97] and later was identified as BBE-like protein [65]. The crystal structure of Phl p4 from *Phleum pratense* confirms the structural homology to BBE and bivalent attachment of the FAD cofactor (pdb code 3tsh). Blast searches with the two experimentally determined full-length BBE-like pollen allergens BG60 and Phl p 4 resulted in the identification of four additional BBE-like proteins, namely Sec c 4, Hor v 5, Tri a 4 and Lol p 4 from rye, barley, wheat and perennial ryegrass, respectively. Except for Lol p 4 these proteins show almost the same size and show high sequence similarities.

These examples of characterized BBE-like enzymes already suggest that this group of bivalently linked flavoproteins is involved in a variety of chemical reactions and biological functions. Thus it is obvious that specific enzyme functions can not easily be predicted on the sole basis of sequence homology and functional annotations should be performed carefully [98, 99]. This suggestion has been confirmed by various examples, where marginal or even single amino acid exchanges led to a distinct substrate specificity of the respective enzymes [100, 101]. For example, substrate specificity of ChitO from *F. graminearum* was completely changed by a single amino acid replacement in the active site of the enzyme leading to an increased acceptance of glucose and small oligosaccharides such as maltose or lactose [99]. However, we suggest that a comprehensive analysis of sequence homology and available biochemical data of already characterized bivalent flavoproteins can result in reliable predictions of enzyme function, which can further be experimentally proven. One recent example for the practicability of a comprehensive theoretical analysis is the prediction of Gln268 in ChitO as active site residue involved in substrate recognition. Homology modelling of ChitO and a detailed comparison with the elucidated crystal structure of GOOX led to the correct identification of the respective residue [99]. Thus, here we present a detailed analysis of BBE homologues from *Arabidopsis thaliana*, which comprises both sequence homology and analysis of homology models in combination with structural and biochemical data available for BBE and GOOX.

To identify BBE-like enzymes in *A. thaliana* the sequence of BBE from *E. californica* was used for a Blastp search against the whole *Arabidopsis* genome. We found 28 BBE homologues in *A. thaliana*, which are encoded on chromosomes 1, 2, 4, and 5 (Tab.3). As a consequence of the identification of this unexpectedly high number of BBE homologues, the outstanding question has to be addressed

whether *A. thaliana* can produce complex alkaloids or which alternative function these enzymes could adopt *in planta* (for a detailed review on this issue see [98]). It is known that *Arabidopsis* species accumulate simple alkaloids such as camalexin [102]. However, complex alkaloids have not been detected in this plant so far, which does not necessarily imply their absence in *Arabidopsis*. TOGHE *et al.* describe the available chemical information regarding *Arabidopsis* metabolites as insufficient [103] and the recent discovery of volatile terpenoids in *A. thaliana* suggests the presence of a complex secondary metabolism thus lending credibility to the possible occurrence of yet undiscovered alkaloids in the plant [98, 104, 105]. Moreover, the identification of a plant efflux carrier with the ability for berberine transport [106] can be regarded as an indication for the presence of complex alkaloids in *Arabidopsis*.

We analyzed the 28 homologous proteins of *A. thaliana* using the YASARA modelling tool. These BBE homologues all possess a conserved histidine residue on the site corresponding to His104 of BBE, indicating a covalent $\delta\alpha$ -histidinyl linkage of the cofactor. Moreover, 24 out of 28 BBE homologues additionally possess the conserved cysteine residue for 6-*S*-cysteinylation, hence it appears that *A. thaliana* possesses 24 bicovalent flavoenzymes! The remaining four BBE homologous (BBE-like 10, 25, 27, and 28) feature a serine, tyrosine, or histidine residue at the position corresponding to Cys166 of BBE. So far, only 6-*S*-cysteinylation was reported for bicovalently linked flavoproteins; however, other modes of covalent cofactor tethering can not be ruled out. Whether these residues are capable of forming a covalent bond to C6 of the flavin cofactor in the respective protein has to be seen.

Moreover, the homology models were scanned for BBE active site residues, such as Glu417, which is the catalytic base necessary for carbon-carbon bond formation in BBE [14]. Tab.3 shows a compilation of predicted active site residues in the 28 BBE-like *Arabidopsis* proteins.

Tab.3: Predicted active site residues in putative BBE-like proteins of *A. thaliana* through homology modelling.

Locus Name	Working Name	Accession Number	Comparison to Berberine Bridge Enzyme Active Site Residues							
			His104	Cys166	Glu417	Tyr106	His459	His174	Tyr456	Trp165
AT1G01980.1	BBE-like 1	Q9LPC3	His	Cys	Gln	Tyr	Tyr	His	Tyr	Val
AT1G11770.1	BBE-like 2	Q9SA99	His	Cys	Gln	Tyr	--- ^a	His	Tyr	Val
AT1G26380.1	BBE-like 3	Q9FZC4	His	Cys	Gln	Asn	Tyr	His	Phe	Ile
AT1G26390.1	BBE-like 4	Q9FZC5	His	Cys	Gln	Tyr	---	His	---	---
AT1G26400.1	BBE-like 5	Q9FZC6	His	Cys	Gln	Tyr	Phe	His	Leu ^b	Val
AT1G26410.1	BBE-like 6	Q9FZC7	His	Cys	Gln	Asn	---	His	---	Val
AT1G26420.1	BBE-like 7	Q9FZC8	His	Cys	Gln	Leu	---	His	---	Val
AT1G30700.1	BBE-like 8	Q9SA85	His	Cys	Gln	Tyr	Tyr	His	Phe	Ile
AT1G30710.1	BBE-like 9	Q9SA86	His	Cys	Gln	Tyr	---	His	---	Ile
AT1G30720.1	BBE-like 10	Q9SA87	His	Ser	Glu	Phe	---	His	---	Leu
AT1G30730.1	BBE-like 11	Q9SA88	His	Cys	Glu	Phe	---	His	---	Leu
AT1G30740.1	BBE-like 12	Q9SA89	His	Cys	Gln	Tyr	---	His	Tyr	Val
AT1G30760.1	BBE-like 13	Q93ZA3	His	Cys	Gln	Tyr	---	His	Tyr	Leu
AT1G34575.1	BBE-like 14	Q9LNL9	His	Cys	Gln	Tyr	---	His	---	Ile
AT2G34790.1	BBE-like 15	O64743	His	Cys	Gln	Tyr	---	His	---	Leu
AT2G34810.1	BBE-like 16	O64745	His	Cys	Glu	Tyr	Tyr	His	Phe	Val
AT4G20800.1	BBE-like 17	Q9SVG7	His	Cys	Gln	Tyr	Tyr	His	Phe	Val
AT4G20820.1	BBE-like 18	Q9SVG5	His	Cys	Gln	Tyr	Leu	His	Tyr	Val
AT4G20830.1 ^c	BBE-like 19	Q9SVG4	His	Cys	Gln	Tyr	---	His	Tyr	Val
AT4G20830.2 ^c	BBE-like 20	Q9SVG4	His	Cys	Gln	Tyr	---	His	Tyr	Val
AT4G20840.1	BBE-like 21	Q9SVG3	His	Cys	Gln	Tyr	---	His	Tyr	Val
AT4G20860.1	BBE-like 22	Q9SUC6	His	Cys	Gln	Tyr	---	His	---	Ile
AT5G44360.1	BBE-like 23	Q9FKV2	His	Cys	Gln	Tyr	Tyr	His	Tyr	Thr
AT5G44380.1	BBE-like 24	Q9FKV0	His	Cys	Leu	Phe	Tyr	Tyr	Tyr	Leu
AT5G44390.1	BBE-like 25	Q9FKU9	His	Tyr	Gln	Tyr	Tyr	His	Tyr	Val
AT5G44400.1	BBE-like 26	Q9FKU8	His	Cys	Gln	Tyr	Tyr	His	Tyr	Leu
AT5G44410.1	BBE-like 27	Q9FI25	His	Tyr	Gln	Tyr	Phe	Gln	Tyr	Leu
AT5G44440.1	BBE-like 28	Q9FI21	His	His	Gln	Tyr	Phe	Gln	Tyr	Ile

^a prediction of the respective active site residue not feasible due to different secondary structure elements in berberine bridge enzyme and the modelled homologue

^b prediction is not accurate since homology model of BBE-like 5 shows different secondary structure and is rather imprecise in the respective area

^c AT4G20830.1 and AT4G20830.2 represent two isoforms of the respective BBE-like protein in *A. thaliana*

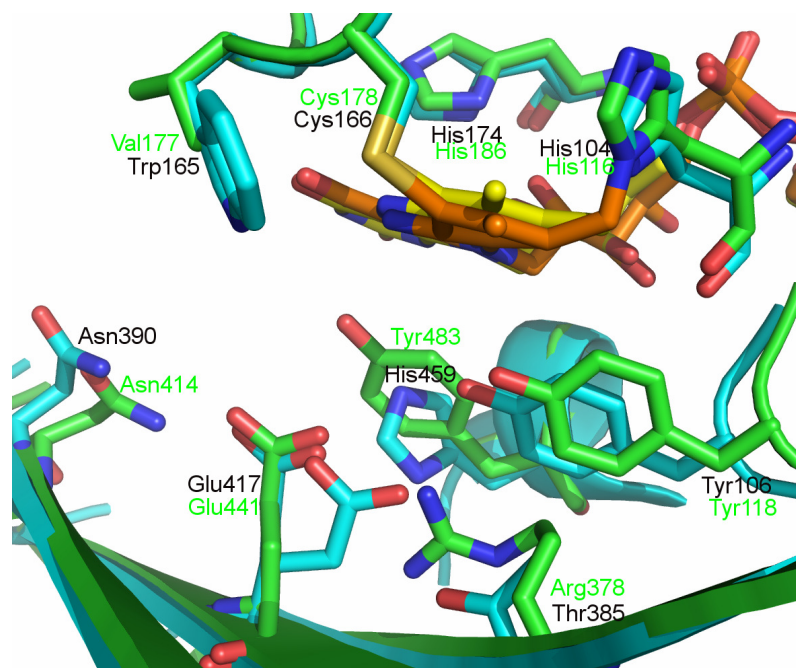


Fig.12: Comparison of BBE-like 16 to the active site of berberine bridge enzyme.

BBE is represented in cyan and BBE-like 16 is shown in green. The bicovalently linked flavin cofactor is shown in yellow and orange for BBE and BBE-like 16, respectively. BBE and BBE-like 16 active site residues are labelled in black and green, respectively. BBE-like 16 possesses the important active site glutamate residue, which has been reported to be the catalytic base in BBE [14].

Interestingly, only three BBE-homologues, BBE-like proteins 10, 11 and 16, possess a glutamate residue at the respective site of Glu417 in BBE. Consequently, these proteins could possibly be involved in ring-closure reactions initiated by proton abstraction from the substrate by the catalytic glutamate residue. BBE-like 11 and BBE-like 16 show overall active site architectures which are highly similar to the structural environment in BBE suggesting that these enzymes could be involved in similar enzymatic reactions (Fig.12). BBE-like 10, however, possesses a serine residue in place of the cysteine required for cofactor attachment. Hence this serine residue could possibly influence the flavin cofactor in BBE-like 10 and modulate the redox potential for efficient catalysis by forming a hitherto uncharacterized novel covalent linkage or by influencing the electronic environment of the cofactor without covalent tethering.

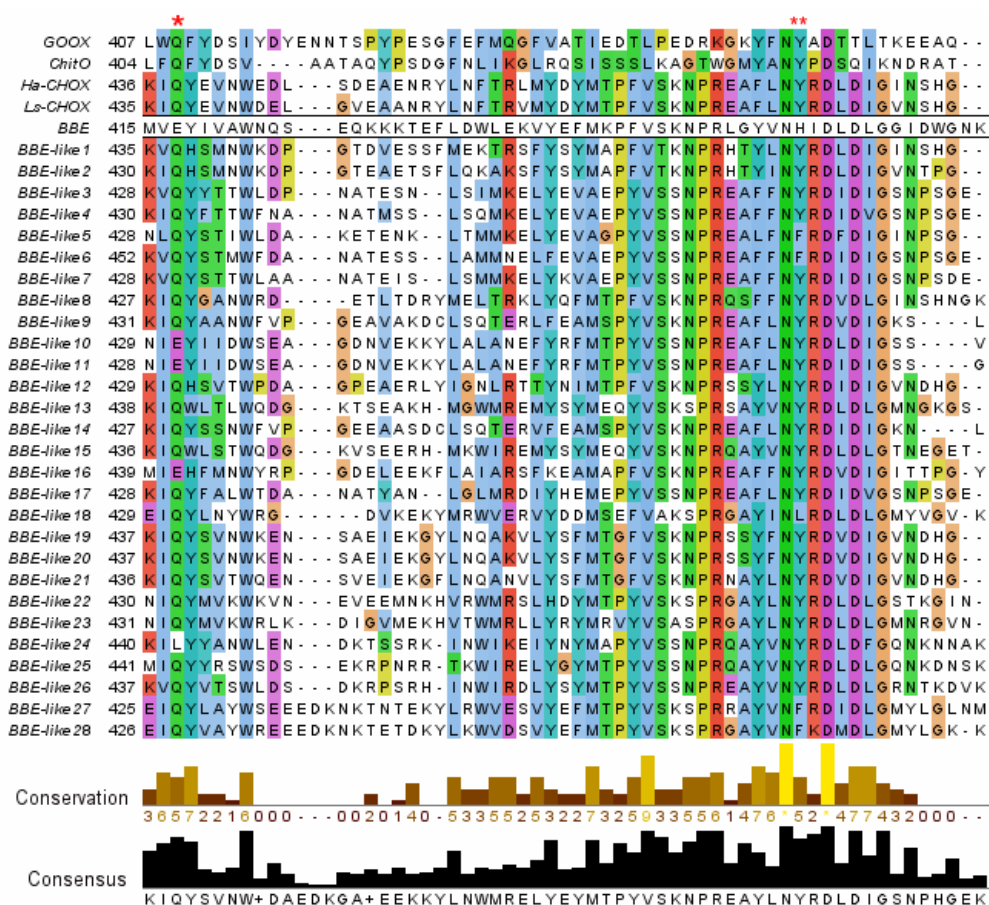


Fig.13 : Multiple sequence alignment of characterized bicovalently flavinylated oxidases and 28 predicted BBE-like proteins from *A. thaliana* using ClustalW.

The sequence of BBE is displayed without colouring and the position of glutamate 417 is indicated (*). The conserved tyrosine residue in carbohydrate oxidases is indicated with **. Conserved amino acid residues are highlighted in coloured boxes. The amino acid sequences of following characterized oxidases were used: GOOX from *A. strictum* (AAS79317), ChitO from *F. graminearum* (XP_391174), carbohydrate oxidases from sunflower (AAL77103) and from lettuce (AAL77102) and BBE from *E. californica* (AC39358).

Except BBE-like 24 the remaining BBE-like proteins exhibit a glutamine residue at the position of Glu417 in BBE (Tab.3, Fig.13). Interestingly, multiple sequence alignments revealed that this active site glutamine residue is also present in characterized carbohydrate oxidases, such as GOOX (AAS79317), ChitO (XP_391174) and the carbohydrate oxidases from sunflower (AAL77103) and lettuce (AAL77102). The proposed mechanism of GOOX suggests an active site tyrosine residue (Tyr429) as general base for catalysis, which initiates substrate conversion by proton abstraction from the OH¹ group of the sugar moiety [7, 107]. Multiple sequence alignments performed with ClustalW [108, 109] and analyzed in Jalview 2.7 [110] resulted in the finding that this tyrosine residue is strictly conserved in carbohydrate oxidases and hence might be a reliable predictor for enzymatic function. 23 out of 28 BBE homologues from *A. thaliana* possess this

conserved tyrosine residue (Fig.13), which supports the idea that some BBE homologues in *A. thaliana* are in fact carbohydrate oxidases. In plants carbohydrate oxidases seem to play a vital role in active plant defence due to their ability to form hydrogen peroxide as product of enzymatic turnover [67, 68]. Thus it is conceivable that a portion of the BBE homologues in *Arabidopsis* acts as carbohydrate oxidases involved, for example in floral defence against pathogen attack (see before).

The occurrence of BBE-like enzymes in fungi

BBE-like enzymes are not restricted to the plant kingdom and are also found in fungi and bacteria. Elucidation of the crystal structure of GOOX from the fungus *Acremonium strictum* provided the first example of a bicovalently flavinylated oxidase [7] and ChitO from *F. graminearum* is a further well-investigated fungal BBE-like enzyme [10].

GOOX was first isolated from wheat bran cultures of *A. strictum* T1 by LIN *et al.* during screening experiments for novel glucooligosaccharide oxidases for application as industrial biocatalysts or diagnostic reagents for alternative carbohydrate assays [111, 112]. The enzyme was described as a flavoprotein catalyzing the oxidation of a variety of carbohydrates like glucose, maltose, lactose, and a variety of oligosaccharides composed of 1,4-linked D-glucofuranosyl residues [107, 111, 113]. The availability of the crystal structure of GOOX led to the discovery of the first bicovalent cofactor attachment. Moreover, it enabled the formulation of a reaction mechanism for GOOX and led to a deeper insight in the mode of substrate binding and substrate specificity [7].

As discussed previously for BBE, GOOX also belongs to the PCMH superfamily of flavoproteins and comprises a flavin- and a substrate-binding domain with an open carbohydrate binding groove allowing bulky oligosaccharide substrates to access the active site. The FAD cofactor is bicovalently attached to His70 and Cys130 of the enzyme and for GOOX this mode of cofactor linkage was reported to tune the redox potential for efficient catalysis, to contribute to flavin and substrate binding, and to increase protein stability [7, 11]. Tyr429 is activated by Asn355 through water-mediated hydrogen bonding and acts as general active site base crucial for catalysis [7, 107]. It initiates oxidation by subtracting a proton from the substrate thereby

causing a direct transfer of a hydride to N(5) of the flavin isoalloxazine ring resulting in the formation of a lactone and reduced flavin [7]. The intermediate lactone spontaneously hydrolyses to the corresponding acid. Stabilization of the negative charge at the N(1)-C(2)=O locus of the isoalloxazine ring could be achieved by His138, Tyr426 and the backbone NH of Tyr144 [7]. The reduced flavin cofactor is reoxidized in a reaction with molecular oxygen (Fig.14).

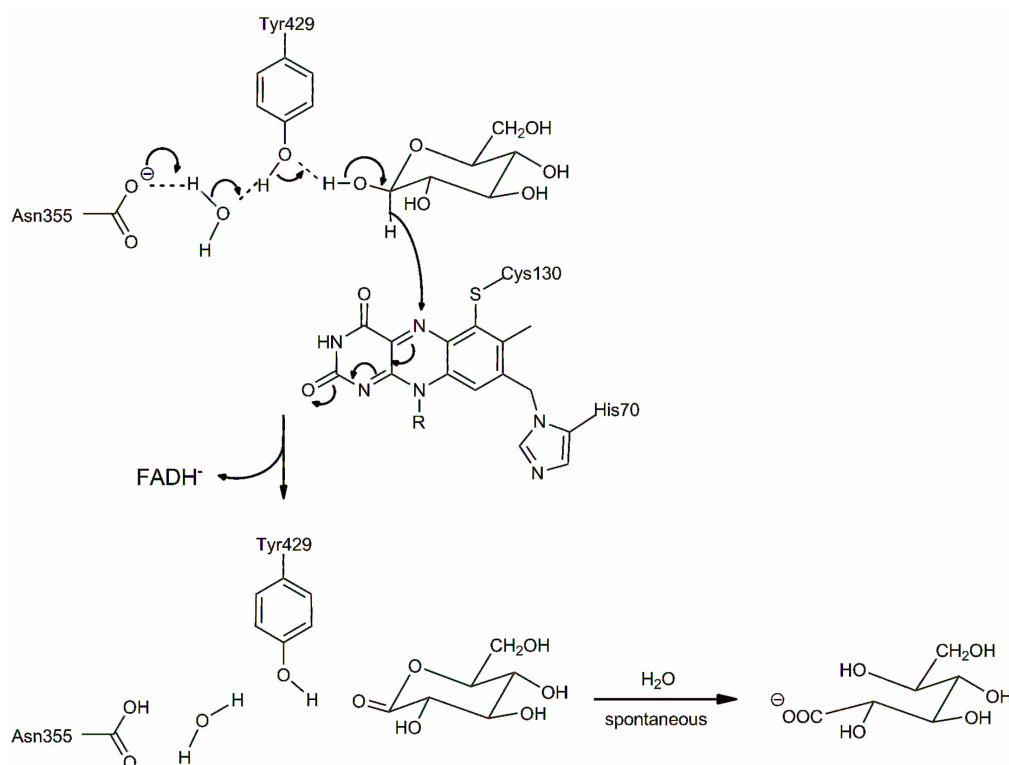


Fig.14: Proposed mechanism for GOOX.

Tyr429, which is activated by Asn355 via water mediated hydrogen bonding, subtracts a proton from the OH¹ group of the substrate thereby causing a direct transfer of a hydride to the N(5) atom of the flavin isoalloxazine ring. The resulting glucono-1,5-lactone spontaneously hydrolyzes to gluconic acid. The reduced flavin cofactor gets reoxidized by molecular oxygen. Fig.14 was modified according to [7].

Recently FOUMANI *et al.* reported the successful expression of a GOOX variant (GOOX-VN) from a different strain of *A. strictum* with altered substrate specificity [114]. This variant comprises fifteen amino acid substitutions compared to GOOX from *A. strictum* T1 leading to an improved substrate acceptance. Additionally to glucose, maltose, lactose, and oligosaccharides composed of 1,4-linked D-glucopyranosyl residues, GOOX-VN accepts galactose, and xylooligosaccharides with similar catalytic efficiency as for cellooligosaccharides. This indicates that

directed evolution on GOOX could lead to improved biocatalysts for oxidative modification of cello- and xylooligosaccharides [114].

Moreover, GOOX is of special interest since many hypothetical bicovalently linked flavoproteins show a tyrosine residue at the position corresponding to the catalytic Tyr429 in GOOX. Hence it is likely that these hypothetical proteins are carbohydrate oxidases with various functions in the respective organism (see discussion in previous section).

Blast searches against the non redundant protein sequence database on NCBI with GOOX or BBE as query resulted in the identification of a great number of putative bicovalently linked flavoprotein oxidases in fungi. Especially moulds and pathogenic fungi which affect plants or insects, were found to possess proteins homologous to BBE and GOOX. Blastp searches clearly revealed the high abundance of putative bicovalently flavinylated proteins among *Ascomycota* and *Basidiomycota*. In Tab.4, we have listed different species possessing one or more hypothetical bicovalently linked flavoproteins.

Different *Aspergillus* species, such as *Aspergillus niger* or *Aspergillus oryzae*, and the basidiomycete *Melampsora laricis* possess with 9, 7, and 10 BBE-homologs the highest number of hypothetical bicovalently linked flavoproteins. HEUTS *et al.* identified 6 new glucooligosaccharide oxidase homologues with altered substrate preference [99, 107]. From these homologues a putative oxidase (XP_391174) from *F. graminearum* was selected for detailed investigations [10, 99]. Surprisingly, the new oxidase displayed a distinct substrate preference as compared to known oligosaccharide oxidases and catalyzed the regioselective oxidation of *N*-acetylated oligosaccharides leading to the name chitooligosaccharide oxidase. ChitO is a bicovalently linked flavoprotein belonging to the same structural class as GOOX or BBE. For ChitO, a glutamine (Gln268) was identified as active site residue responsible for recognition of the *N*-acetyl moiety. Thus, a Q268R mutant protein was prepared with Gln268 replaced with arginine, the amino acid found on the corresponding position in GOOX. Interestingly, this amino acid replacement had a drastic effect on the K_M value for all substrates leading to an increased acceptance of cello-oligosaccharides and a reduced conversion rate for ChitO, which again suggests a possible application of site-directed mutagenesis for the production of improved oligosaccharide oxidases with tailored substrate specificity.

Tab.4: BBE-like proteins in the fungal kingdom.

Phylum	Family	Fungus	BBE/GOOX-homologues	
Ascomycota	<i>Trichocomaceae</i>	<i>Aspergillus niger</i>	9	
	<i>Trichocomaceae</i>	<i>Aspergillus oryzae</i>	7	
	<i>Trichocomaceae</i>	<i>Aspergillus flavus</i>	6	
	<i>Trichocomaceae</i>	<i>Aspergillus kawachii</i>	5	
	<i>Trichocomaceae</i>	<i>Aspergillus terreus</i>	3	
	<i>Trichocomaceae</i>	<i>Aspergillus fumigatus</i>	1	
	<i>Trichocomaceae</i>	<i>Neosartorya fischeri</i>	3	
	<i>Trichocomaceae</i>	<i>Penicillium chrysogenum</i>	3	
	<i>Trichocomaceae</i>	<i>Penicillium marneffei</i>	2	
	<i>Trichocomaceae</i>	<i>Talaromyces stipitatus</i>	1	
	<i>Chaetomiaceae</i>	<i>Chaetomium globosum</i>	6	
	<i>Chaetomiaceae</i>	<i>Chaetomium thermophilum</i>	1	
	<i>Chaetomiaceae</i>	<i>Thielavia heterothallica</i>	2	
	<i>Nectriaceae</i>	<i>Fusarium oxysporum</i>	6	
	<i>Nectriaceae</i>	<i>Fusarium graminearum</i>	4	
	<i>Nectriaceae</i>	<i>Nectria haematococca</i>	4	
	<i>Magnaporthaceae</i>	<i>Magnaporthe oryzae</i>	4	
	<i>Lasiosphaeriaceae</i>	<i>Podospora anserina</i>	4	
	<i>Phaeosphaeriaceae</i>	<i>Phaeosphaeria nodorum</i>	4	
	<i>Sordariaceae</i>	<i>Neurospora tetrasperma</i>	4	
	<i>Sordariaceae</i>	<i>Neurospora crassa</i>	3	
	<i>Sordariaceae</i>	<i>Sordaria macrospora</i>	2	
	<i>Clavicipitaceae</i>	<i>Metarhizium acridum</i>	3	
	<i>Clavicipitaceae</i>	<i>Metarhizium anisopliae</i>	3	
	<i>Clavicipitaceae</i>	<i>Cordyceps militaris</i>	2	
	<i>Leptosphaeriaceae</i>	<i>Leptosphaeria maculans</i>	3	
	<i>Pleurotheciaceae</i>	<i>Pyrenophora tritici-repentis</i>	3	
	<i>Glomerellaceae</i>	<i>Glomerella graminicola</i>	3	
	<i>Chaetomiaceae</i>	<i>Thielavia terrestris</i>	2	
	<i>Orbiliaceae</i>	<i>Arthrotrichum oligospora</i>	2	
	<i>Sclerotiniaceae</i>	<i>Botryotinia fuckeliana</i>	2	
	<i>Sclerotiniaceae</i>	<i>Sclerotinia sclerotiorum</i>	1	
	<i>Tuberaceae</i>	<i>Tuber melanosporum</i>	1	
	<i>Plectosphaerellaceae</i>	<i>Verticillium dahliae</i>	1	
	<i>Arthrodermataceae</i>	<i>Arthroderma gypseum</i>	1	
	<i>Arthrodermataceae</i>	<i>Trichophyton rubrum</i>	1	
	<i>Arthrodermataceae</i>	<i>Trichophyton equinum</i>	1	
	<i>Arthrodermataceae</i>	<i>Arthroderma otae</i>	1	
	<i>Arthrodermataceae</i>	<i>Trichophyton tonsurans</i>	1	
	Basidiomycota	<i>Melampsoraceae</i>	<i>Melampsora laricis</i>	10
		<i>Schizophyllaceae</i>	<i>Schizophyllum commune</i>	5
		<i>Sebacinaceae</i>	<i>Piriformospora indica</i>	3
		<i>Psathyrellaceae</i>	<i>Coprinopsis cinerea</i>	2
<i>Ustilaginaceae</i>		<i>Ustilago maydis</i>	2	
<i>Pucciniaceae</i>		<i>Puccinia graminis</i>	1	
<i>Sporidiobolaceae</i>		<i>Rhodotorula glutinis</i>	1	
<i>Tricholomataceae</i>		<i>Laccaria bicolor</i>	1	

BBE-like enzymes in bacteria: oxidative power for the biosynthesis of antibiotics

In recent years the number of flavoenzymes possessing a bicovalently attached flavin cofactor has steadily risen in bacteria [70, 115-120]. In contrast to plants, none of the bacterial enzymes known so far are involved in cyclization reactions. Instead, the enzymes typically catalyze the oxidation of primary or secondary alcohol groups and the substrates are complex and bulky molecules. Furthermore, the reactions catalyzed by the enzymes are in biosynthetic pathways leading to antibiotics, such as aclacinomycin from *Streptomyces galileus* [115], glycopeptide A40926 (a teicoplanin homologue) from *Nonomuraea* sp. [117], tirandamycin [116, 118] and gilvocarcin V from *Streptomyces* sp. (Fig.15) [119, 121]. The first two reactions comprise a four electron oxidation, *i. e.* the FAD cofactor runs twice through the catalytic cycle of two electron reduction and reoxidation by molecular oxygen in the course of the reaction. Aclacinomycin oxidoreductase (AknOx) first oxidizes the alcohol group at C-4 of the terminal pyranose ring and in the second round of oxidation a C-C double bond is introduced between C-2 and C-3 thus yielding a α,β -unsaturated ketone (Fig.15, a). On the other hand, the reaction catalyzed by the hexose oxidase Dbv29 is a four electron oxidation of a primary alcohol group to a carboxylic acid at C-6 of the sugar moiety (Fig.15, b). In both cases, the enzyme acts on the carbohydrate moiety of the molecule rather than its aglycone. This is in contrast to the reactions in tirandamycin and gilvocarcin V biosynthesis where the oxidation concerns a secondary alcohol group. In the latter case, the oxidation yields a lactone in a complex polyketide molecule whereas the former reaction leads to a ketone group in the bicyclic ketal moiety of the antibiotic (Fig.15, c and d).

It is noteworthy that in all of the reactions considered here, the flavoenzyme catalyzes one of the terminal reactions in the biosynthetic pathways, *i. e.* occurs at a stage where the skeleton of the target molecule is already established. This contrasts to the reactions catalyzed by BBE from *E. californica* and THCA synthase from *C. sativa* where the oxidation reaction is central to the generation of the carbon skeleton of the natural compound produced by these plants (compare Fig.5 and Fig.11).

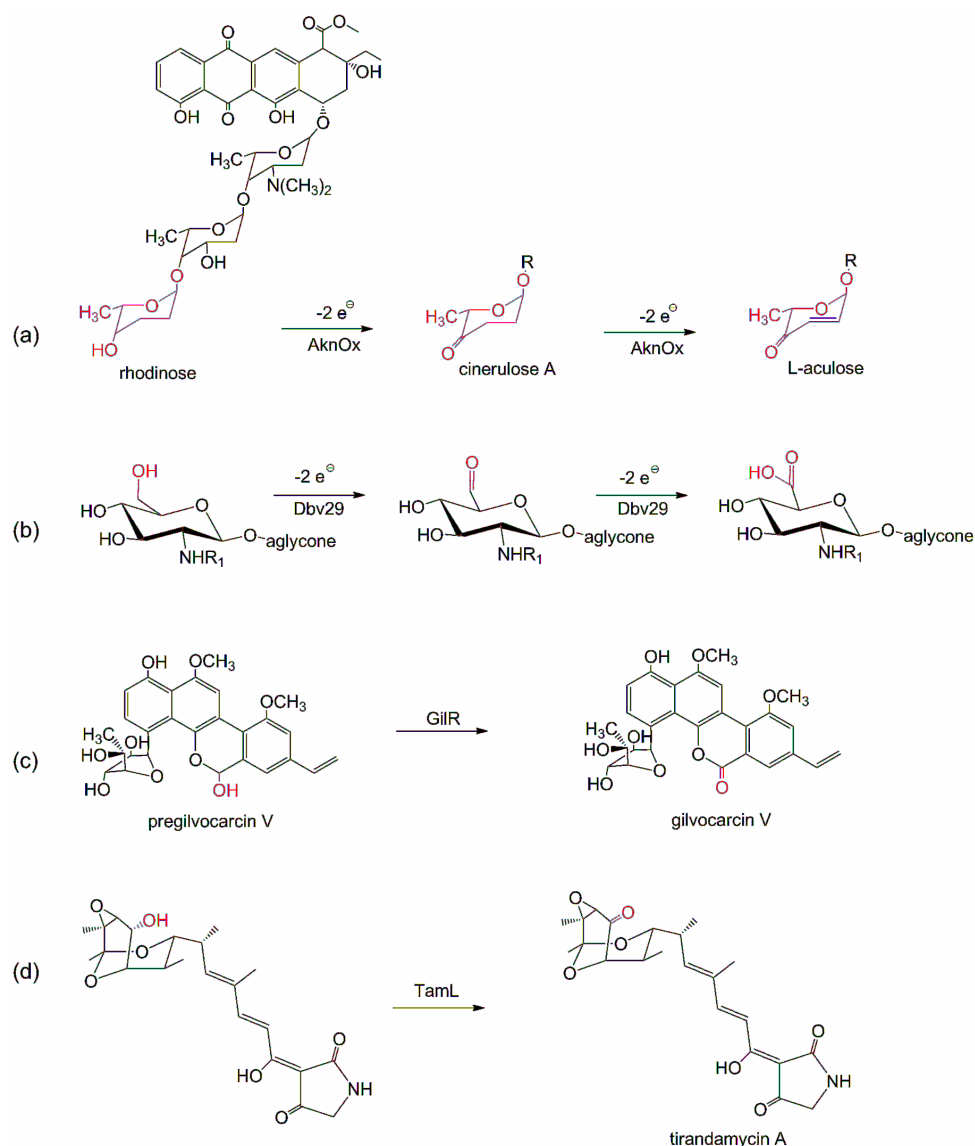


Fig.15: Reactions catalyzed by bicovalent flavoenzymes in the bacterial kingdom.

Reactions catalyzed by (a) AknOx, aclacinomycin reductase from *Streptomyces galileus*, (b) Dbv29 from *Nonomuraea* sp., (c) GilR, pregilvocarcin V dehydrogenase from *Streptomyces*, and (d) TamL, 10-hydroxy-dehydrogenase in tirandamycin biosynthesis from *Streptomyces*.

Similarity searches against the non redundant protein database on NCBI resulted in the discovery of many putative BBE homologues in the bacterial kingdom. In various *Streptomyces* species BBE homologues are found, which according to sequence alignments possess the conserved cysteine and histidine residue for bicovalent flavin attachment. These enzymes are suggested to be potential oxidoreductases, berberine bridge enzymes, FAD binding proteins, twin-arginine translocation pathway signal proteins and interestingly a relatively large number of BBE homologues in *Streptomyces* is defined as lipoproteins. A sequence alignment

of these putative lipoproteins shows high sequence identity of these enzymes in different *Streptomyces* species. A similar search in the genomes of *Pseudomonas* failed to detect BBE homologues. Hence BBE-like enzymes are not uniformly distributed in eubacteria but appear to be present only in distinct genera. Apart from *Streptomyces*, BBE-like proteins were also found in *Bacillus*, *Mycobacterium*, *Ruegeria* and *Frankia* species.

Conclusions

In the last five years, bicovalent flavinylation has emerged as a novel mode of cofactor linkage. Currently, ~25% of covalently linked flavoenzymes feature bicovalent flavinylation, with a large number of bacterial, fungal and plant genes predicted to belong to this family of “BBE-like proteins”. So far, bicovalent flavin attachment is confined to bacteria, fungi, and plants, where some genera seem to be rich in bicovalent flavoproteins and others appear to have only a few members of this family. Bicovalent flavoproteins are totally absent from archaea and the animal kingdom. In nature, these enzymes adopt different roles in the metabolism of plants, fungi, and bacteria. In plants, bicovalent flavoenzymes catalyze complex cyclization reactions in natural product biosynthesis, such as alkaloids and terpenes. Moreover, these enzymes act as sugar and alcohol oxidases and thus fulfil different roles in the respective organism. As sugar oxidases bicovalent flavoproteins are involved in plant or fungal defence against pathogens and as alcohol oxidases they catalyze the final step(s) in antibiotic biosynthesis in bacteria. Hence these enzymes catalyze promising reactions with the potential to produce novel natural products and antibiotics in a biocatalytic setting.

References

- [1] Macheroux, P., Kappes, B., and Ealick, S.E. *FEBS J* **2011**, 278, 2625-2634.
- [2] Singer, T.P., and Kearney, E.B. *Biochem Biophys Acta* **1956**, 15, 151.
- [3] Salach, J., Walker, W.H., Singer, T.P., Ehrenberg, A., Hemmerich, P., Ghisla, S., and Hartmann, U. *Eur J Biochem* **1972**, 26, 267-278.
- [4] Kearney, E.B., Salach, J.I., Walker, W.H., Seng, R.L., Kenney, W., Zeszotek, E., and Singer, T.P. *Eur J Biochem* **1971**, 24, 321-327.
- [5] McIntire, W., Edmondson, D.E., Hopper, D.J., and Singer, T.P. *Biochemistry* **1981**, 20, 3068-3075.
- [6] Mewies, M., McIntire, W.S., and Scrutton, N.S. *Protein Sci* **1998**, 7, 7-20.
- [7] Huang, C.H., Lai, W.L., Lee, M.H., Chen, C.J., Vasella, A., Tsai, Y.C., and Liaw, S.H. *J Biol Chem* **2005**, 280, 38831-38838.
- [8] Heuts, D.P.H.M., Scrutton, N.S., McIntire, W.S., and Fraaije, M.W. *FEBS J* **2009**, 276, 3405-3427.
- [9] Winkler, A., Kutchan, T.M., and Macheroux, P. *J Biol Chem* **2007**, 282, 24437-24443.
- [10] Heuts, D.P.H.M., Winter, R.T., Damsma, G.E., Janssen, D.B., and Fraaije, M.W. *Biochem J* **2008**, 413, 175-183.
- [11] Huang, C.H., Winkler, A., Chen, C.L., Lai, W.L., Tsai, Y.C., Macheroux, P., and Liaw, S.H. *J Biol Chem* **2008**, 283, 30990-30996.
- [12] Winkler, A., Motz, K., Riedl, S., Puhl, M., Macheroux, P., and Gruber, K. *J Biol Chem* **2009**, 284, 19993-20001.
- [13] Kutchan, T.M. Molecular Genetics of Plant Alkaloid Biosynthesis. In: Cordell, G.A., ed. *The Alkaloids*. **1998**, Academic Press, San Diego, CA.
- [14] Winkler, A., Łyskowski, A., Riedl, S., Puhl, M., Kutchan, T.M., Macheroux, P., and Gruber, K. *Nat Chem Biol* **2008**, 4, 739-741.
- [15] Liscombe, D.K., and Facchini, P.J. *Curr Opin Biotechnol* **2008**, 19, 173-180.
- [16] Rink, E., and Bohm, H. *FEBS Lett* **1975**, 49, 396-399.
- [17] Steffens, P., Nagakura, N., and Zenk, M.H. *Phytochemistry* **1985**, 24, 2577-2583.
- [18] Kutchan, T.M., and Dirtrich, H. *J Biol Chem* **1995**, 270, 24475-24481.
- [19] Ghisla, S., Kenney, W.C., Knappe, W.R., McIntire, W., and Singer, T.P. *Biochemistry* **1980**, 19, 2537-2544.
- [20] Winkler, A., Hartner, F., Kutchan, T.M., Glieder, A., and Macheroux, P. *J Biol Chem* **2006**, 281, 21276-21285.
- [21] Massey, V., Ghisla, S., and Moore, E.G. *J Biol Chem* **1979**, 254, 9640-9650.
- [22] Fitzpatrick, P.F., and Massey, V. *J Biol Chem* **1983**, 258, 9700-9705.

- [23] Massey, V., Muller, F., Feldberg, R., Schuman, M., Sullivan, P.A., Howell, L.G., Mayhew, S.G., Matthews, R.G., and Foust, G.P. *J Biol Chem* **1969**, *244*, 3999-4006.
- [24] Massey, V., and Hemmerich, P. *Biochem Soc Trans* **1980**, *8*, 246-257.
- [25] Fraaije, M.W., and Mattevi, A. *Trends Biochem Sci* **2000**, *25*, 126-132.
- [26] Macheroux, P., Kieweg, V., Massey, V., Soderlind, E., Stenberg, K., and Lindqvist, Y. *Eur J Biochem* **1993**, *213*, 1047-1054.
- [27] Wagner, M.A., Trickey, P., Che, Z.W., Mathews, F.S., and Jorns, M.S. *Biochemistry* **2000**, *39*, 8813-8824.
- [28] Ohta-Fukuyama, M., Miyake, Y., Emi, S., and Yamano, T. *J Biochem* **1980**, *88*, 197-203.
- [29] Gomez-Moreno, C., Choy, M., and Edmondson, D.E. *J Biol Chem* **1979**, *254*, 7630-7635.
- [30] Bruhmuller, M., Mohler, H., and Decker, K. *Z Naturforsch B* **1972**, *27*, 1073-1074.
- [31] Gadda, G., Wels, G., Pollegioni, L., Zucchelli, S., Ambrosius, D., Pilone, M.S., and Ghisla, S. *Eur J Biochem* **1997**, *250*, 369-376.
- [32] Muller, F., and Massey, V. *J Biol Chem* **1969**, *244*, 4007-4016.
- [33] Gadda, G., and Fitzpatrick, P.F. *Biochemistry* **1998**, *37*, 6154-6164.
- [34] Ghisla, S., Massey, V., and Yagi, K. *Biochemistry* **1986**, *25*, 3282-3289.
- [35] Ghanem, M., and Gadda, G. *Biochemistry* **2006**, *45*, 3437-3447.
- [36] Hecht, H.J., Kalisz, H.M., Hendle, J., Schmid, R.D., and Schomburg, D. *J Mol Biol* **1993**, *229*, 153-172.
- [37] Wohlfahrt, G., Witt, S., Hendle, J., Schomburg, D., Kalisz, H.M., and Hecht, H.J. *Acta Crystallogr D Biol Crystallogr* **1999**, *55*, 969-977.
- [38] Lindqvist, Y., and Branden, C.I. *J Biol Chem* **1989**, *264*, 3624-3628.
- [39] Trickey, P., Wagner, M.A., Jorns, M.S., and Mathews, F.S. *Structure* **1999**, *7*, 331-345.
- [40] Muh, U., Massey, V., and Williams, C.H. *J Biol Chem* **1994**, *269*, 7982-7988.
- [41] Xia, Z.X., and Mathews, F.S. *J Mol Biol* **1990**, *212*, 837-863.
- [42] Efimov, I., Cronin, C.N., Bergmann, D.J., Kuusk, V., and McIntire, W.S. *Biochemistry* **2004**, *43*, 6138-6148.
- [43] Vrieling, A., Lloyd, L.F., and Blow, D.M. *J Mol Biol* **1991**, *219*, 533-554.
- [44] Hallberg, B.M., Henriksson, G., Pettersson, G., and Divne, C. *J Mol Biol* **2002**, *315*, 421-434.
- [45] Mattevi, A., Vanoni, M.A., Todone, F., Rizzi, M., Teplyakov, A., Coda, A., Bolognesi, M., and Curti, B. *Proc Natl Acad Sci USA* **1996**, *93*, 7496-7501.
- [46] Macheroux, P., Massey, V., Thiele, D.J., and Volokita, M. *Biochemistry* **1991**, *30*, 4612-4619.

- [47] Schrittwieser, J.H., Resch, V., Sattler, J.H., Lienhart, W.D., Durchschein, K., Winkler, A., Gruber, K., Macheroux, P., and Kroutil, W. *Angew Chem Int Ed* **2011**, *50*, 1068-1071.
- [48] Schrittwieser, J.H., Resch, V., Wallner, S., Lienhart, W.D., Sattler, J.H., Resch, J., Macheroux, P., and Kroutil, W. *J Org Chem* **2011**, *76*, 6703-6714.
- [49] Bentley, K.W. *The Isoquinoline Alkaloids*. **1998**, Harwood Academic Publishers, Amsterdam.
- [50] Eisenreich, W.J., Hofner, G., and Bracher, F. *Nat Prod Res* **2003**, *17*, 437-440.
- [51] Gao, J., Liu, W., Li, M., Liu, H., Zhang, X., and Li, Z. *J Mol Struct* **2008**, *892*, 466-469.
- [52] Martin, M.L., Diaz, M.T., Montero, M.J., Prieto, P., San Roman, L., and Cortes, D. *Planta Med* **1993**, *59*, 63-67.
- [53] Chulia, S., Ivorra, M.D., Lugnier, C., Vila, E., Noguera, M.A., and D'Ocon, P. *Br J Pharmacol* **1994**, *113*, 1377-1385.
- [54] Kashiwada, Y., Aoshima, A., Ikeshiro, Y., Chen, Y.P., Furukawa, H., Itoigawa, M., *et al.* *Bioorg Med Chem* **2005**, *13*, 443-448.
- [55] Yamahara, J., Konoshima, T., Sakakibara, Y., Ishiguro, M., and Sawada, T. *Chem Pharm Bull* **1976**, *24*, 1909-1912.
- [56] Li, J., Jin, G., Shen, J., and Ji, R. *Drugs Future* **2006**, *31*, 379-384.
- [57] Barton, D.H., Kirby, G.W., Steglich, W., Thomas, G.M., Battersby, A.R., Dobsan, T.A., and Ramuz, H. *J Chem Soc* **1965**, *65*, 2423-2438.
- [58] Chrzanoska, M., and Rozwadowska, M.D. *Chem Rev* **2004**, *104*, 3341-3370.
- [59] Matulenko, M.A., and Meyers, A.I. *J Org Chem* **1996**, *61*, 573-580.
- [60] Resch, V., Schrittwieser, J.H., Wallner, S., Macheroux, P., and Kroutil, W. *Adv Synth Catal* **2011**, *353*, 2377-2383.
- [61] Shoyama, Y., Takeuchi, A., Taura, F., Tamada, T., Adachi, M., Kuroki, R., Shoyama, Y., and Morimoto, S. *Acta Crystallogr Sect F Struct Biol Cryst Commun* **2005**, *61*, 799-801.
- [62] Carter, C.J., and Thornburg, R.W. *Plant Physiol* **2004**, *134*, 460-469.
- [63] Nandy, A., Petersen, A., Wald, M., Suck, R., Kahlert, H., Weber, B., Becker, W.M., Cromwell, O., and Fiebig, H. *Biochem Biophys Res Commun* **2005**, *337*, 563-570.
- [64] Gesell, A., Chávez, M.L.D., Kramell, R., Piotrowski, M., Macheroux, P., and Kutchan, T.M. *Planta* **2011**, *233*, 1185-1197.
- [65] Dewitt, A.M., Andersson, K., Peltre, G., and Lidholm, J. *Clin Exp Allergy* **2006**, *36*, 77-86.
- [66] Sirikantaramas, S., Morimoto, S., Shoyama, Y., Ishikawa, Y., Wada, Y., Shoyama, Y., and Taura, F. *J Biol Chem* **2004**, *279*, 39767-39774.
- [67] Carter, C., and Thornburg, R.W. *Trends Plant Sci* **2004**, *9*, 320-324.
- [68] Custers, J.H., Harrison, S.J., Sela-Buurlage, M.B., van Deventer, E., Lageweg, W., Howe, P.W., *et al.* *Plant J* **2004**, *39*, 147-160.

- [69] Hansen, O.C., and Stougaard, P. *J Biol Chem* **1997**, *272*, 11581-11587.
- [70] Rand, T., Qvist, K.B., Walter, C.P., and Poulsen, C.H. *FEBS J* **2006**, *273*, 2693-2703.
- [71] Poulsen, C., and Høstrup, P.B. *Cereal Chem* **1998**, *75*, 51-57.
- [72] Van der Lugt, J.P. Evaluation of Methods for Chemical and Biological Carbohydrate Oxidation, In: Technische Universiteit, ed., **1998**, Delft.
- [73] Liaw, S.H., Lee, D.Y., Chow, L.P., Lau, G.X., and Su, S.N. *Biochem Biophys Res Commun* **2001**, *280*, 738-743.
- [74] Steffens, P., Nagakura, N., and Zenk, M.H. *Tetrahedron Lett* **1984**, *25*, 951-952.
- [75] Amann, M., Nagakura, N., and Zenk, M.H. *Tetrahedron Lett* **1984**, *25*, 953-954.
- [76] Amann, M., Nagakura, N., and Zenk, M.H. *Eur J Biochem* **1988**, *175*, 17-25.
- [77] Chou, W.M., and Kutchan, T.M. *Plant J* **1998**, *15*, 289-300.
- [78] Taura, F., Morimoto, S., Shoyama, Y., and Mechoulam, R. *J Am Chem Soc* **1995**, *117*, 9766-9767.
- [79] Turner, C.E., Elsohly, M.A., and Boeren, E.G. *J Nat Prod* **1980**, *43*, 169-234.
- [80] Pertwee, R.G. *Br J Pharmacol* **2006**, *147*, S163-71.
- [81] Pertwee, R.G. *Handb Exp Pharmacol* **2005**, *168*, 1-51.
- [82] Pertwee, R.G. *Int J Obes* **2006**, *30*, S13-8.
- [83] Pertwee, R.G. *Mol Neurobiol* **2007**, *36*, 45-59.
- [84] Grotenhermen, F. *Curr Drug Targets CNS Neurol Disord* **2005**, *4*, 507-530.
- [85] Guzman, M. *Nat Rev Cancer* **2003**, *3*, 745-755.
- [86] Baker, D., Pryce, G., Giovannoni, G., and Thompson, A.J. *Lancet Neurol* **2003**, *2*, 291-298.
- [87] Taura, F., Dono, E., Sirikantaramas, S., Yoshimura, K., Shoyama, Y., and Morimoto, S. *Biochem Biophys Res Commun* **2007**, *361*, 675-680.
- [88] Carter, C., Graham, R.A., and Thornburg, R.W. *Plant Mol Biol* **1999**, *41*, 207-216.
- [89] Chamnongpol, S., Willekens, H., Moeder, W., Langebartels, C., Sandermann, H., Van Montagu, M., Inze, D., and Van Camp, W. *Proc Natl Acad Sci USA* **1998**, *95*, 5818-5823.
- [90] Bolwell, G.P., and Wojtaszek, P. *Physiol Mol Plant Pathol* **1997**, *51*, 347-366.
- [91] Wu, G., Shortt, B.J., Lawrence, E.B., Levine, E.B., Fitzsimmons, K.C., and Shah, D.M. *Plant Cell* **1995**, *7*, 1357-1368.
- [92] Wojtaszek, P. *Biochem J* **1997**, *322*, 681-692.
- [93] Liaw, S.H., Lee, D.Y., Yang, S.Y., and Su, S.N. *J Struct Biol* **1999**, *127*, 83-87.
- [94] Ganglberger, E., Radauer, C., Grimm, R., Hoffmann-Sommergruber, K., Breiteneder, H., Scheiner, O., and Jensen-Jarolim, E. *Clin Exp Allergy* **2000**, *30*, 566-570.

- [95] Bublin, M., Radauer, C., Wilson, I.B., Kraft, D., Scheiner, O., Breiteneder, H., and Hoffmann-Sommergruber, K. *FASEB J* **2003**, *17*, 1697-1699.
- [96] Chardin, H., Mayer, C., Senechal, H., Tepfer, M., Desvaux, F.X., and Peltre, G. *Int Arch Allergy Immunol* **2001**, *125*, 128-134.
- [97] Fischer, S., Grote, M., Fahlbusch, B., Müller, W.D., Kraft, D., and Valenta, R. *J Allergy Clin Immunol* **1996**, *98*, 189-198.
- [98] Facchini, P.J., Bird, D.A., and St-Pierre, B. *Trends Plant Sci* **2004**, *9*, 116-122.
- [99] Heuts, D.P.H.M., Janssen, D.B., and Fraaije, M.W. *FEBS Lett* **2007**, *581*, 4905-4909.
- [100] Frick, S., and Kutchan, T.M. *Plant J* **1999**, *17*, 329-339.
- [101] Frey, M., Chomet, P., Glawischnig, E., Stettner, C., Grün, S., Winklmaier, A., *et al.* *Science* **1997**, *277*, 696-699.
- [102] Tsuji, J., Jackson, E.P., Gage, D.A., Hammerschmidt, R., and Somerville, S.C. *Plant Physiol* **1992**, *98*, 1304-1309.
- [103] Tohge, T., Yonekura-Sakakibara, K., Niida, R., Watanabe-Takahashi, A., and Saito, K. *Pure Appl Chem* **2007**, *79*, 811-823.
- [104] Chen, F., Tholl, D., D'Auria, J. C., Farooq, A., Pichersky, E., and Gershenzon, J. *Plant Cell* **2003**, *15*, 481-494.
- [105] Aharoni, A., Giri, A.P., Deuerlein, S., Griepink, F., de Kogel, W.J., Verstappen, F.W., Verhoeven, H.A., Jongsma, M.A., Schwab, W., and Bouwmeester, H.J. *Plant Cell* **2003**, *15*, 2866-2884.
- [106] Li, L., He, Z., Pandey, G.K., Tsuchiya, T., and Luan, S. *J Biol Chem* **2002**, *277*, 5360-5368.
- [107] Lee, M.H., Lai, W.L., Lin, S.F., Hsu, C.S., Liaw, S.H., and Tsai, Y.C. *Appl Environ Microbiol* **2005**, *71*, 8881-8887.
- [108] Larkin, M.A., Blackshields, G., Brown, N.P., Chenna, R., McGettigan, P.A., McWilliam, H., *et al.* *Bioinformatics* **2007**, *23*, 2947-2948.
- [109] Goujon, M., McWilliam, H., Li, W., Valentin, F., Squizzato, S., Paern, J., and Lopez, R. *Nucleic Acids Res* **2010**, *38*, 695-699.
- [110] Waterhouse, A.M., Procter, J.B., Martin, D.M., Clamp, M., and Barton, G.J. *Bioinformatics* **2009**, *25*, 1189-1191.
- [111] Lin, S.F., Yang, T.Y., Inukai, T., Yamasaki, M., and Tsai, Y.C. *Biochim Biophys Acta* **1991**, *1118*, 41-47.
- [112] Lin, S.F., Hu, H.M., Inukai, T., and Tsai, Y.C. *Biotechnol Adv* **1993**, *11*, 417-427.
- [113] Fan, Z., Oguntimein, G.B., and Reilly, P.J. *Biotechnol Bioeng* **2000**, *68*, 231-237.
- [114] Foumani, M., Vuong, T.V., and Master, E.R. *Biotechnol Bioeng* **2011**, *108*, 2261-2269.
- [115] Alexeev, I., Sultana, A., Mäntsälä, P., Niemi, J., and Schneider, G. *Proc Natl Acad Sci USA* **2007**, *104*, 6170-6175.

-
- [116] Carlson, J.C., Li, S., Gunatilleke, S.S., Anzai, Y., Burr, D.A., Podust, L.M., and Sherman, D.H. *Nature Chem* **2011**, *3*, 628-633.
- [117] Li, Y.S., Ho, J.Y., Huang, C.C., Lyu, S.Y., Lee, C.Y., Huang, Y.T., Wu, C.J., Chan, H.C., Huang, C.J., Huang, C.J., Tsai, M.D., and Li, T.L. *J Am Chem Soc* **2007**, *129*, 13384-13385.
- [118] Mo, X., Huang, H., Ma, J., Wang, Z., Wang, B., Zhang, S., Zhang, C., and Ju, J. *Org Lett* **2011**, *13*, 2212-2215.
- [119] Noinaj, N., Bosserman, M.A., Schickli, M.A., Piszczek, G., Kharel, M.K., Pahari, P., Buchanan, S.K., and Rohr, J. *J Biol Chem* **2011**, *286*, 23533-23543.
- [120] Abad, S., Nahalka, J., Bergler, G., Arnold, S. A., Speight, R., Fotheringham, I., Nidetzky, B., and Glieder, A. *Microb Cell Fact* **2010**, *9*, 24.
- [121] Kharel, M.K., Pahari, P., Lian, H., and Rohr, J. *ChemBioChem* **2009**, *10*, 1305-1308.

CHAPTER 3

3 Aims of the project

Proteins with bicovalently attached flavin cofactors are a novel class of flavoproteins which were found to be present in both prokaryotic and eukaryotic organisms. Recently, bivalent flavoproteins, such as berberine bridge enzyme, were shown to catalyze challenging chemical reactions with no equivalent in organic synthesis [1] which makes these proteins promising candidates for new biotechnological approaches for the production of novel compounds [2]. Thus, a detailed understanding of bivalent flavoproteins is of utmost importance for their application as biocatalysts and so far, many studies were performed to characterize these proteins biochemically and structurally. Today the number of bivalent flavoproteins is steadily increasing and extensive research has been performed to understand this interesting mode of cofactor tethering. However, despite all these efforts, many questions remain unanswered and have to be addressed by further investigations.

A general aim of this thesis project was to perform in-depth studies on bicovalently linked flavoproteins to enlarge the knowledge of this class of proteins. For this reason, several subprojects were defined, which dealt either with the search for new bivalent flavoproteins or with detailed studies on already known members of this protein family.

A central objective of my project was the biochemical and structural characterization of (*S*)-tetrahydroprotoberberine oxidase (STOX), which is a BBE homolog present in different poppy and berberis species. STOX was reported to be involved in benzyloquinoline alkaloid biosynthesis by catalyzing the oxidation of many tetrahydroprotoberberines [3, 4]. At the beginning of my project, DNA sequences of STOX from *Argemone mexicana* and *Berberis wilsoniae* were already available from previous work of KUTCHAN AND COWORKERS [5], making these two enzymes good candidates for my biochemical investigations. Since the access to sufficient protein quantities is a prerequisite for in-depth biochemical and structural characterization, a first aim of my project was to develop an efficient method for heterologous expression of both STOX proteins. Furthermore, the substrate scope of both *Am* and *Bw* STOX had to be elucidated, using available intermediates from benzyloquinoline alkaloid biosynthesis as substrates for activity assays. Unfortunately, the main aim of this project, an in-depth biochemical and structural

characterization, was not successfully reached since the overall protein yield was not high enough for detailed investigations.

A further objective of my project was to perform new studies on berberine bridge enzyme. Today BBE can be regarded as a paradigm for bicovalently linked flavoproteins, as it has been subject to detailed biochemical and structural characterization by ANDREAS WINKLER [1, 6-9]. In his work, ANDREAS WINKLER performed a structure based mutagenic analysis of BBE, which led to a deeper understanding of the role of bicovalent flavinylation for catalysis and to the proposal of a concerted mechanism for BBE. However, the influence of certain amino acid residues on flavin reactivity remained unclear and required further investigations. Thus, in my thesis project I wanted to continue the studies of ANDREAS WINKLER by determining the effect of His174, a highly conserved active site residue, on cofactor binding and catalysis.

Moreover, BBE was identified as promising biocatalyst for the conversion of different non-natural substrates. JÖRG SCHRITTWIESER revealed that some substrates were converted in an unexpectedly slow rate, which could possibly be improved by protein engineering. Therefore, a side project of my thesis dealt with the creation of BBE active site muteins for increased acceptance of non-natural substrates. The availability of protein engineering tools for the design of BBE variants with new substrate preference could open the way to a variety of novel benzyloquinoline alkaloids.

Besides STOX and BBE, investigations were also performed with other bicovalent flavoproteins. In cooperation with the group of SHWU-HUEY LIAW (Faculty of Life Sciences and Institute of Genome Sciences, National Yang-Ming University, Taipei, Taiwan) I tried to investigate the role of bicovalent flavin attachment in Dbv29 from *Nonomuraea* species by measuring the redox potential of wild type and mutant proteins.

All these studies combined with bioinformatical analyses which were performed to get an overview of the quantity and distribution of bicovalent flavoproteins among different genera, were expected to result in new insights into the mode and role of covalent cofactor tethering.

3.1 References

- [1] Winkler, A., Hartner, F., Kutchan, T.M., Glieder, A., and Macheroux, P. *J Biol Chem* **2006**, *281*, 21276-21285.
- [2] Schrittwieser, J.H., Resch, V., Sattler, J.H., Lienhart, W.D., Durchschein, K., Winkler, A., Gruber, K., Macheroux, P., and Kroutil, W. *Angew Chem Int Ed* **2011**, *50*, 1068-1071.
- [3] Amann, M., Nagakura, N., and Zenk, M.H. *Tetrahedron Lett* **1984**, *25*, 953-954.
- [4] Amann, M., Nagakura, N., and Zenk, M.H. *Eur J Biochem* **1988**, *175*, 17-25.
- [5] Gesell, A., Chávez, M.L.D., Kramell, R., Piotrowski, M., Macheroux, P., and Kutchan, T.M. *Planta* **2011**, *233*, 1185-1197.
- [6] Winkler, A., Kutchan, T.M., and Macheroux, P. *J Biol Chem* **2007**, *282*, 24437-24443.
- [7] Winkler, A., Łyskowski, A., Riedl, S., Puhl, M., Kutchan, T.M., Macheroux, P., and Gruber, K. *Nat Chem Biol* **2008**, *4*, 739-741.
- [8] Winkler, A., Puhl, M., Weber, H., Kutchan, T.M., Gruber, K., and Macheroux, P. *Phytochemistry* **2009**, *70*, 1092-1097.
- [9] Winkler, A., Motz, K., Riedl, S., Puhl, M., Macheroux, P., and Gruber, K. *J Biol Chem* **2009**, *284*, 19993-20001.

CHAPTER 4

- 4 (S)-Tetrahydroprotoberberine oxidase
(STOX) - a mysterious enzyme in
alkaloid biosynthesis
-

Author contributions

Investigations on (*S*)-tetrahydroprotoberberine oxidase (STOX) can be regarded as the main objective of this PhD project. Different approaches for heterologous expression of STOX were tested with the aim of getting deeper insights in the properties of this remarkable oxidase. It is noteworthy that several talented students contributed to the progress of this project by helping me with the practical work in the course of their bachelor thesis. BIRGIT LUEF did expression experiments and activity studies for STOX of *Argemone mexicana*. Moreover, as a project student she contributed to the cloning of new constructs of STOX from *Berberis wilsoniae*. Together with HANNAH JARITZ I performed initial fermentation experiments and Hannah additionally made valuable contributions to the manually optimized DNA sequence of *Bw* STOX and she tested the ordered anti-STOX antibody. PHILIPP MARKOLIN cloned and screened the first fusion constructs with citrine as fluorescent tag and last but not least STEFANIE HORVATH and SABRINA TATZL improved this screening method by creating new constructs for facilitated purification using His₈- and StrepII-affinity tags.

4.1 STOX - the early beginnings

Elucidation of biosynthetic routes leading to the formation of various alkaloids in plants has been an early field of biochemical research [1-7]. Due to the pharmacological relevance of many representatives of this group of secondary metabolites [8-16], much effort has been directed towards understanding *de novo* alkaloid biosynthesis [10]. Thus identification of enzymes involved in these complex biosynthetic routes was one major goal of scientists that time. Initial attempts of enzyme characterization encountered many difficulties due to very low levels of enzyme activity in the respective plants, the slow growth of the latter and high inhibitor concentrations, such as phenols or accumulated alkaloids [17]. In the 1980s the availability of plant cell cultures with compressed growth and accelerated alkaloid production facilitated the identification and purification of enzymes in alkaloid biosynthesis [18-20].

(*S*)-Tetrahydroprotoberberine oxidase is an enzyme operating exclusively in alkaloid biosynthesis and was first described by AMANN *et al.* in 1984 [21]. STOX was found to be present in a number of different plant cell cultures capable of producing protoberberines, and in whole plants such as *Papaver somniferum*. The first isolation of STOX is described from cell cultures of *Berberis wilsoniae* var. *subcaulialata*. Already in this early stage of research ZENK and coworkers proposed a flavin-dependence of the enzyme and formulated a reaction mechanism for STOX where it catalyzes the oxidation of (*S*)-tetrahydroprotoberberines to protoberberines in the presence of oxygen (see Figure 16) [21]

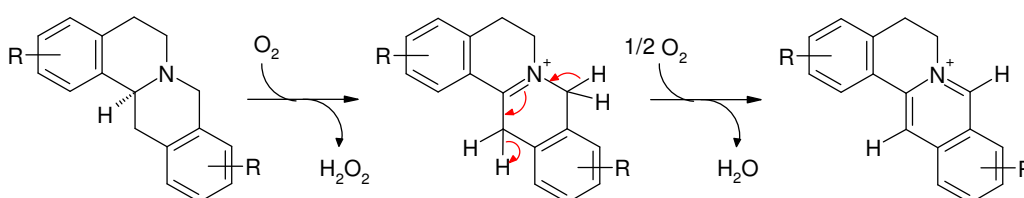


Figure 16: Reaction mechanism of STOX proposed by AMANN *et al.* (1985) [21]

Some years later in 1988 the first purification of STOX from *B. wilsoniae* cell cultures was reported, which in turn enabled a detailed biochemical investigation of this enzyme [22]. It was shown that STOX indeed catalyzes the removal of four

hydrogen atoms from a number of protoberberines at the expense of oxygen and the production of H_2O_2 . Interestingly, the enzyme exhibits a broad substrate specificity by converting the (*S*)-enantiomers of a variety of tetrahydroprotoberberines and 1-benzyl-isoquinolines with (*S*)-scoulerine, (*S*)-canadine, (*S*)-coreximine, (*S*)-tetrahydropalmatine, and (*S*)-norreticuline being the best substrates (see Figure 17) [22, 23]. However, no (*R*)-enantiomers were accepted by STOX leading to the name (*S*)-tetrahydroprotoberberine oxidase. [22, 24]

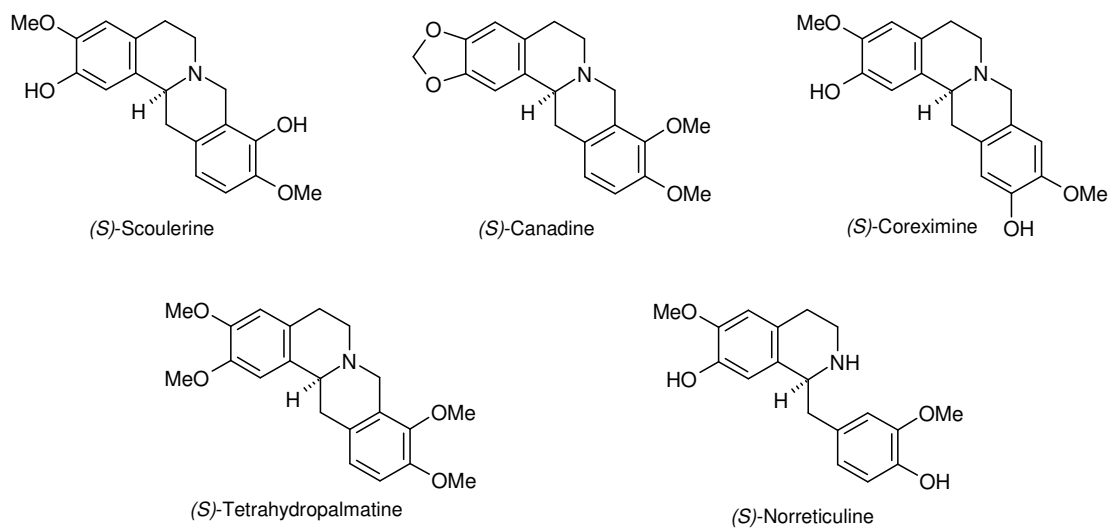


Figure 17: Selected (*S*)-tetrahydroprotoberberines and 1-benzyl-isoquinolines as substrates of STOX

In *planta* STOX was suggested to catalyze the last step in berberine biosynthesis by oxidizing (*S*)-canadine to berberine [10, 22] (see Figure 18).

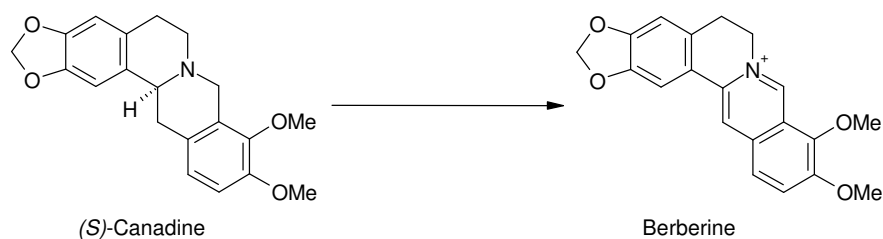


Figure 18: Reaction catalyzed by STOX in *planta*

Biochemical characterization of STOX resulted in the finding that the native protein is a dimer with approximately 105 kDa with a pH optimum for activity of 8.9. Denaturation of the enzyme did not result in release of the flavin cofactor, which is

an indication for covalent flavinylation. Later cofactor linkage was verified by incorporation and detection of D-[2-¹⁴C]riboflavin in the enzyme. [22]

It was shown that in plants STOX is exclusively found in small vesicles that separate from the ER and later fuse with the tonoplast of the cells, thereby releasing the accumulated alkaloids. These vesicles seem to be the exclusive site of benzophenanthridine alkaloid biosynthesis in plants and enzymes involved in this biosynthetic route, such as STOX and BBE, colocalize in these cellular compartments [25].

Besides these biochemical and physiological findings the potential of STOX for industrial applications was realized in the late 1980s and thus STOX was also a prominent enzyme for biotechnological research. Due to the prevalent believe that STOX converts many pharmaceutically active tetrahydroprotoberberines and 1-benzylisoquinolines in enantioselective and stereoselective oxidation reactions, STOX was an ideal candidate as catalyst for kinetic resolution. Racemic substrates could be separated by the conversion of the respective (*S*)-enantiomer in a STOX-catalyzed reaction. Thus, AMANN *et al.* investigated the immobilization of STOX with various techniques and covalent coupling to controlled pore glass was reported as an applicable immobilization method for the enzyme [26, 27]. Interestingly, immobilization seemed to highly increase the lifespan of STOX. Immobilized enzyme showed stable catalytic efficiency for more than a year, whereas purified STOX lost 50 % of its activity in four days [26].

Despite the initial enthusiasm for a possible application of STOX in pharmaceutical industry, research on this oxidase encountered many difficulties and only little progress was made in the last two decades. The lack of a system for heterologous expression of STOX impeded purification of high quantities of the enzyme and thus in-depth investigations were not feasible. Quite recently heterologous expression of STOX was reported for insect cell culture [28]. KUTCHAN and coworkers were able to express the recombinant oxidase from *Argemone mexicana* and *Berberis wilsoniae* in *Spodoptera frugiperda* Sf9 cells. *In-vivo* activity assays led to the suggestion that the two enzymes show different substrate specificities which seem to be narrowed down in comparison to earlier suggestions [22]. Interestingly, both enzymes showed clear oxidase activity with (*S*)-tetrahydropalmatine. STOX from *B. wilsoniae* additionally converted (*S*)-scoulerine and (*S*)-canadine, however, STOX from *A.*

mexicana accepted (*S*)-coreximine as substrate. [28] It is noteworthy that *A. mexicana* STOX did not convert (*S*)-canadine, although it was suggested to be the natural substrate for the enzyme [10, 22]. Different substrate specificities can be ascribed to different active site compositions of the two STOX enzymes as shown by homology modelling [28]. However, this suggestion has to be further confirmed by in-depth characterization of the two oxidases.

These initial investigations clearly showed that STOX is a potent and remarkable oxidase, however, many outstanding questions have to be addressed, which includes an expression system for high protein yields or reconsidering the substrate specificity of the enzyme. With a detailed understanding of STOX, this enzyme might be employed for biotechnological applications.

4.2 Materials and Methods

4.2.1 Reagents

All chemicals were of highest grade commercially available and purchased either from Sigma-Aldrich (St. Louis, MO, USA), Fluka (Buchs, Switzerland), or Merck (Darmstadt, Germany). Restriction enzymes and T4 DNA ligase were obtained from Fermentas (St. Leon-Rot, Germany). Phusion® high fidelity Polymerase was from New England Biolabs (Ipswich, MA, USA). Bacto™ yeast extract and peptone for *Pichia* growth media were from Becton, Dickinson and Company (Franklin, Lakes, NJ, USA). Phenyl-Sepharose 6 FF (high substitution) was purchased from GE Healthcare (Fairfield, CT, USA). Alkaloid standards, as (*S*)-reticuline, (*S*)-norreticuline, (*S*)-scoulerine, (*S*)-canadine, (*S*)-coreximine, (*S*)-tetrahydro-columbamine, and salutaridine were a generous gift from TONI M. KUTCHAN (Donald Danforth Plant Science Center, St. Luis, MO, USA). (*S*)-Tetrahydropalmatine was from CHEMOS GesmbH (Regenstauf, Germany). The anti-flavin antibody was from DALE EDMONDSON (Emory University, Atlanta, GA, USA).

4.2.2 Expression strains

Table 5: *E. coli* and *P. pastoris* strains

Strain	Source	Application
<i>E. coli</i> TOP10	Invitrogen	plasmid storage and isolation
<i>E. coli</i> BL21(DE3)	Novagen	expression strain
<i>E. coli</i> Rosetta™(DE3)	Novagen	enhanced expression of proteins containing rare codons in <i>E. coli</i> codon usage
<i>E. coli</i> BL21(DE3) CodonPlus RIL	Stratagene	enhanced expression of proteins containing rare codons in <i>E. coli</i> codon usage
<i>E. coli</i> Origami B (DE3)	Novagen	expression strain allowing disulfide bond formation in cytoplasm
<i>Pichia pastoris</i> KM71H	Invitrogen	<i>Pichia</i> expression strain

E. coli and *P. pastoris* expression strains were purchased either from Invitrogen (Carlsbad, CA, USA), Novagen (Madison, WI, USA), or Stratagene (La Jolla, CA, USA).

4.2.3 DNA constructs

Table 6 gives a summary of the expression plasmids assembled for testing different strategies of heterologous protein expression in *E. coli* and *P. pastoris*. For expression in *E. coli*, only constructs with the synthetic gene of *A. mexicana* in *E. coli* codon usage were cloned. Expression cassettes for heterologous expression in *P. pastoris* were assembled using genes with different codon usages. (a) denotes the synthetic gene in *E. coli* codon usage, (b) stands for the automatically optimized gene in *P. pastoris* codon usage, (c) for the manually optimized synthetic gene, and (d) stands for native cDNA sequences of *A. mexicana* or *B. wilsoniae*, respectively.

Table 6: Plasmids for heterologous expression of STOX in *E. coli* and *P. pastoris*

Plasmids for expression in *E. coli*

pET21a(+)- <i>Am STOX-His₆</i>	synthetic gene in <i>E. coli</i> codon usage
pMAL- <i>Am STOX-His₆</i>	synthetic gene in <i>E. coli</i> codon usage fused with a N-terminal maltose binding protein
pBAD-MBP- <i>Am STOX-His₆</i>	synthetic gene in <i>E. coli</i> codon usage fused with a N-terminal maltose binding protein under the control of the <i>araBAD</i> promoter

Plasmids for expression in *P. pastoris*

pPICK- <i>PDI</i>	expression cassette containing the auxiliary protein disulfide isomerase (PDI) of <i>P. pastoris</i> under the control of the AOX1 promoter
pPICZalpha- <i>Am STOX-His₆</i> (a)	synthetic <i>Am STOX</i> gene in <i>E. coli</i> codon usage under the control of the AOX1 promoter and the α -factor for secretory expression
pPICZalpha- <i>Am STOX-His₆</i> (b)	synthetic <i>Am STOX</i> gene in <i>P. pastoris</i> codon usage under the control of the AOX1 promoter and the α -factor for secretory expression
pPICZalpha- <i>Am STOX-His₆</i> (d)	native cDNA of <i>Am STOX</i> with the N-terminal signal peptide replaced by the alpha-factor for secreted expression under the control of the AOX1 promoter

pPICZ/B- <i>Am STOX-His₆</i> (d)	native cDNA of <i>Am STOX</i> including the N-terminal signal peptide under the control of the AOX1 promoter
pGAPZalpha- <i>Am STOX-His₆</i> (d)	native cDNA of <i>Am STOX</i> with the N-terminal signal peptide replaced by the alpha-factor for secreted expression under the control of the pGAP promoter
pPpT4-GAP- <i>Am STOX-His₆</i> (d)	native cDNA of <i>Am STOX</i> including the N-terminal signal peptide under the control of the pGAP promoter
pPICZalpha- <i>Bw STOX-His₆</i> (c)	manually optimized <i>Bw STOX</i> gene under the control of the AOX1 promoter and the α -factor
pPICZ/B- <i>Bw STOX-His₆</i> (c)	manually optimized <i>Bw STOX</i> gene including the N-terminal signal sequence under the control of the AOX1 promoter
pGAPZalpha- <i>Bw STOX-His₆</i> (c)	manually optimized <i>Bw STOX</i> gene under the control of the pGAP promoter and the α -factor for secretory expression
pPpT4-GAP- <i>Bw STOX-His₆</i> (c)	manually optimized <i>Bw STOX</i> gene including the N-terminal signal sequence under the control of the pGAP promoter
pPICZ/B- <i>Bw STOX</i> (d)	cDNA of <i>Bw STOX</i> including the N-terminal signal peptide under the control of the AOX1 promoter
pPpT4-GAP- <i>Bw STOX</i> (d)	cDNA of <i>Bw STOX</i> including the N-terminal signal peptide under the control of the pGAP promoter
pPICZalpha- <i>Bw STOX-linker-citrine</i> (c)	manually optimized <i>Bw STOX</i> gene fused to a C-terminal citrine tag with a TEV-polymerase cleavage site as linker
pPICZalpha- <i>HA-Bw STOX-linker-citrine</i> (c)	manually optimized <i>Bw STOX</i> gene fused to a C-terminal citrine tag with a TEV-polymerase cleavage site as linker and a N-terminal HA-tag for immunodetection of the fusion protein
pPICZalpha- <i>Bw STOX-linker-citrine-KDEL</i> (c)	manually optimized <i>Bw STOX</i> gene fused to a C-terminal citrine tag with a TEV-polymerase cleavage site as linker and KDEL as signal peptide for ER retention
pPICZalpha- <i>HA-Bw STOX-linker-citrine-KDEL</i> (c)	manually optimized <i>Bw STOX</i> gene fused to a C-terminal citrine tag with a TEV-polymerase cleavage site as linker, a N-terminal HA-tag for immunodetection, and KDEL as signal peptide for ER retention
pPICZalpha- <i>Bw STOX-linker-citrine-His₈</i> (c)	manually optimized <i>Bw STOX</i> gene fused to a C-terminal citrine tag with a TEV-polymerase cleavage site as linker, and a C-terminal histidine-tag for affinity purification
pPICZalpha- <i>Bw STOX-linker-citrine-StrepII</i> (c)	manually optimized <i>Bw STOX</i> gene fused to a C-terminal citrine tag with a TEV-polymerase cleavage site as linker, and a C-terminal StrepII-tag for affinity purification
pPICZalpha- <i>Bw STOX-linkX-citrine-His₈</i> (c)	manually optimized <i>Bw STOX</i> gene fused to a C-terminal citrine tag with an interrupted TEV-polymerase cleavage site (ANLGFQ) as linker, and a C-terminal histidine-tag for affinity purification

pPICZalpha- <i>Bw</i> <i>STOX-linkX-citrine-StrepII</i> (c)	manually optimized <i>Bw</i> <i>STOX</i> gene fused to a C-terminal citrine tag with an interrupted TEV-polymerase cleavage site (ANLGFQ) as linker, and a C-terminal StrepII-tag
pPICZalpha- <i>Am</i> <i>STOX-linkX-citrine-His₈</i> (b)	automatically optimized <i>Am</i> <i>STOX</i> gene (optimized for expression in <i>Pichia</i>) fused to a C-terminal citrine tag with an interrupted TEV-polymerase cleavage site (ANLGFQ) as linker, and a C-terminal histidine-tag
pPICZalpha- <i>Am</i> <i>STOX-linkX-citrine-StrepII</i> (b)	automatically optimized <i>Am</i> <i>STOX</i> gene (optimized for expression in <i>Pichia</i>) fused to a C-terminal citrine tag with an interrupted TEV-polymerase cleavage site (ANLGFQ) as linker, and a C-terminal StrepII-tag

4.2.4 Cloning and expression in *Escherichia coli*

Standard molecular-biology procedures were performed according to [29].

The cDNA sequence of *A. mexicana* STOX was obtained from previous studies of TONI M. KUTCHAN and coworkers (Accession Number: HQ116698) [28]. A plasmid pJ201 containing a synthetic gene of *Am* STOX lacking the 26 amino acid N-terminal signal peptide and optimized for *E. coli* codon usage [30, 31] was ordered from DNA 2.0 (Menlo Park, CA, USA). The synthetic gene was flanked with *NdeI* and *XhoI* restriction sites for facilitated cloning into the desired expression strains and encoded a C-terminal hexahistidine tag.

The synthetic gene was cloned into pET21a(+) from Novagen using *NdeI* and *XhoI*. The resulting expression plasmid pET21a(+)-*Am* *STOX-His₆* was transformed into various *E. coli* expression strains. *E. coli* BL21(DE3), *E. coli* RosettaTM(DE3), *E. coli* BL21(DE3) CodonPlus RIL and *E. coli* Origami B were used for heterologous expression of *Am* *STOX*. In all cases protein expression was performed according to standard protocols using IPTG for induction (cf. pET system manual, Novagen). Moreover, coexpression of chaperones *dnaK*, *dnaJ*, *grpE*, *groES*, and *groEL* was performed using pG-KJE8 from Takara Bio Inc. (Shiga, Japan).

Furthermore, a fusion of the maltose binding protein (MBP) with *Am* *STOX-His₆* was created which was expected to lead to improved protein expression and folding [32-35]. For assembling the fusion construct, *Am* *STOX* was cloned in frame with the *MBP* gene using the *KpnI* restriction site of the pMAL-c4E vector from New England Biolabs (Ipswich, MA, USA). The resulting expression plasmid pMAL-*Am* *STOX-His₆* coded for a fusion protein, where the maltose binding

protein was fused to the N-terminal part of *Am* STOX. The plasmid sequence was verified by DNA-sequencing (Eurofins DNA, Ebersbach, Germany) and the expression plasmid was transformed into various *E. coli* strains. Protein expression was performed according to standard protocols using the strong tac promoter and IPTG for induction of protein expression (cf. Takara Chaperon Plasmid Set, <http://www.takarabioeurope.com/pdf/3340.pdf>, accessed January 20, 2012). This initial work was performed by MARTIN PUHL (Institute of Biochemistry, Graz, University of Technology).

However, the fusion protein formed insoluble aggregates. Hence a further expression plasmid pBAD-MBP-STOX-His₆ with the slow *araBAD* promoter was cloned. MBP-STOX-His₆ was amplified from pMAL-*Am* STOX-His₆ using the following primers: pBAD_fw: 5'-GCTCTCGAGCAAATAAAAACAGG TGCACG-3' and pBAD_rev: 5'-AATAAGCTT TTAGATAACAATGTTGATTG CTTCC-3' and cloned into pBAD using the *XhoI* and *HindIII* restriction sites. The resulting expression plasmid was verified with DNA sequencing (Eurofins DNA, Ebersbach, Germany). *E. coli* BL21(DE3) and *E. coli* Origami B cells were transformed with pBAD-MBP-STOX-His₆ cells and protein expression was induced with L-arabinose according to standard protocols (cf. pBAD/His A, B, and C pBAD/Myc-His A, B, and C manual, Invitrogen) [36, 37]. Main cultures were grown at 37 °C and 130 rpm. At an OD₆₀₀ of 0.5 protein expression was induced with 0.0002 - 0.2 % L-arabinose. Protein expression was analyzed using SDS-PAGE and MALDI-MS analysis of selected protein bands.

4.2.5 Refolding of inclusion bodies

STOX inclusion bodies expressed in *E. coli* BL21(DE3) were refolded according to the following protocol: Approximately 2 g pellet were resuspended on ice in 13 mL 50 mM Tris/HCl, 25% sucrose, 1 mM Na-EDTA, 0.1% sodium azide, and 10 mM DTT, pH 8.0 and sonicated to obtain cell disruption. 100 µL lysozyme (50mg/mL in H₂O), 250 µL DNase I (1 mg/mL in 50% glycerol, 75 mM NaCl), 50 µL 0.5 M MgCl₂, and 12.5 mL lysis buffer (50 mM Tris/HCl, 1% Triton X-100, 1% sodium deoxycholate, 100 mM NaCl, 0.1% sodium azide, and 10 mM DTT, pH 8.0) were added and incubated for 60 min at room temperature. Subsequently, 350 µL 0.5 M

Na-EDTA in 50 mM Tris/HCl, pH 8.0 were added and the suspension was frozen in liquid nitrogen. After thawing to room temperature, 200 μ L 0.5 M MgCl₂ was added and the resulting mixture was stored at room temperature for 60 min or until the viscosity decreased. After the addition of 350 μ L 0.5 M Na-EDTA in 50 mM Tris/HCl, pH 8.0, the suspension was pelleted at 11,000 x g for 20 min. The supernatant was discarded and the pellet was resuspended under cooling on ice in 10 mL washing buffer (50 mM Tris/HCl, 100 mM NaCl, 1 mM Na-EDTA, 0.1% sodium azide, and 1 mM DTT, pH 8.0), sonicated continuously for 5 min and pelleted by centrifugation. The resulting pellet after centrifugation was used for refolding. It was dissolved in 9 mL 8 M guanidinium hydrochloride solution supplemented with FAD. 1 mL dissolved protein was added dropwise to 200 mL refolding buffer (100 mM Tris-HCl, 200 mM L-arginine, 2 mM Na-EDTA, 0.5 mM oxidized glutathione, 5 mM reduced glutathione, and 50 μ L protease inhibitor cocktail, pH 8.0) and stirred slowly at 4 °C. Addition of dissolved protein solution was repeated after 14 h and 22 h. After 30 hours the resulting solution was filtered through a 0.45 μ m filter and concentrated using Amicon filter devices (Millipore, Billerica, MA, USA). [38-41]

4.2.6 Assembling and transformation of expression cassettes for *P. pastoris*

A detailed analysis of the sequences of both STOX enzymes from *A. mexicana* and *B. wilsoniae* led to the selection of *P. pastoris* as applicable host organism for heterologous protein expression [42, 43]. Thus, several expression cassettes were assembled for *Am* STOX and *Bw* STOX using synthetic genes with different codon usages or native cDNA sequences.

cDNA constructs of STOX from *A. mexicana* (Accession Number: HQ116698) and *B. wilsoniae* (Accession Number: HQ116697) cloned into a pGEM-T vector for expression in insect cell culture were a generous gift from TONI M. KUTCHAN (Donald Danforth Plant Science Center, St. Louis, MO, USA).

For the STOX protein of *A. mexicana*, a synthetic gene in *P. pastoris* codon usage was ordered from GeneArt (Regensburg, Germany) using the GeneOptimizer ®

algorithm provided by the company [44]. The synthetic gene was designed with a C-terminal hexahistidine tag, the 26 amino acid signal peptide was replaced with a small nucleotide sequence (3'-CTCGAGAAAAGAGAGGCTGAAGCT-5') and flanked with *XhoI* and *NotI* restriction sites for in-frame cloning into pPICZ α .

The DNA sequence of *Bw* STOX was optimized manually for expression in *P. pastoris* by comparing the codon usage bias of *Berberis* with the bias of the host organism *P. pastoris*. Rare triplet codons in the cDNA sequence of *Bw* STOX were intentionally replaced with rare codons in the manually optimized sequence. The resulting synthetic gene was ordered from GeneArt (Regensburg, Germany), which comprised the coding sequence including the 24 amino acids signal peptide flanked with *XhoI* and *NotI* restriction sites.

Several strategies for heterologous protein expression in *P. pastoris* KM71H cells were employed including various intracellular expression methods or the application of *Pichia's* secretory machinery. All above mentioned genes were cloned into vectors under the control of the strong AOX1 (pPICZ α and pPICZ/B from Invitrogen) or the constitutive pGAP promoter (pGAPZ α from Invitrogen; pPpT4-GAP from A. GLIEDER, Institute of Molecular Biotechnology, TU Graz) with or without the alpha-factor of *S. cerevisiae*, respectively [45, 46]. For all constructs the respective genes were amplified with PCR technique using specific primers with overhangs comprising restriction sites for subsequent cloning. Cloning into pPICZ α , pPICZ/B, and pGAPZ α was performed using the *XhoI* and *NotI* restriction sites; for pPpT4-GAP *EcoRI*, *AscI*, or *SpeI* were combined with *NotI*, respectively. All constructs were provided with a C-terminal hexahistidine tag for affinity purification which was rendered excisable by flanking *PstI* restriction sites on both ends of the tag (antisense primer: 5'-TTACTGCAGGTGATGATGGTGATGATGCTGCAG-3'). The PCR products were purified, double-digested with the respective restriction enzymes and ligated into the expression plasmids according to standard protocols. All assembled expression plasmids were verified by DNA sequencing (Eurofins DNA, Ebersbach, Germany).

Transformation of the expression cassettes into *P. pastoris* was performed according to a condensed electroporation manual [47]. The constructs were linearized by digestion with *SacI* or *AvrII*, respectively, and desalted using MF-Millipore

membranes (0.0025 μM ; Millipore, Billerica, MA, USA). 5 - 10 μg linearized plasmid DNA were transformed into competent *P. pastoris* KM71H cells or cells (*P. pastoris* KM71H pPICK-PDI) coexpressing the auxiliary protein disulfide isomerase (PDI) of *P. pastoris* using a Bio-Rad MicroPulser Electroporator (Bio-Rad, Hercules, CA, USA) with default settings for *Pichia* (1500 V, 200 Ω , 25 μF). After electroporation the cells were recovered in YPD medium supplemented with a final concentration of 0.5 M sorbitol for 2 - 3 h and aliquots were plated on YPD plates with different concentrations of zeocin as selective pressure (100 $\mu\text{g}/\text{mL}$, 200 $\mu\text{g}/\text{mL}$, 300 $\mu\text{g}/\text{mL}$, 400 $\mu\text{g}/\text{mL}$, 500 $\mu\text{g}/\text{mL}$, 1000 $\mu\text{g}/\text{mL}$ final concentration). After 3 days incubation at 30 $^{\circ}\text{C}$ a random selection of colonies showing zeocin-resistance was singularized by streaking on fresh YPDZ plates. Colonies grown on plates with high selective pressure were preferred since they were more likely to possess multiple copies of the desired expression cassette. The presence of the expression cassette in the genome of *P. pastoris* was confirmed by colony PCR or by performing small scale expression experiments.

4.2.7 Small scale expression in *P. pastoris*

Unless stated otherwise, all culture media for heterologous expression in *Pichia* were prepared according to standard protocols from the *Pichia* protein expression Kit (Invitrogen, Carlsbad, CA, USA). Either YPD medium (1% w/v yeast extract, 2% w/v peptone and 2% glucose) or buffered minimal dextrose (BMD) medium (400 mM potassium phosphate buffer, pH 6.0, 1.34% Yeast Nitrogen Base (YNB), $4 \times 10^{-5}\%$ biotin, and 1% glucose) were used for growing *Pichia* cultures containing expression cassettes with the constitutive pGAP or the strong inducible AOX1 promoter, respectively. For protein expression under the control of the AOX1 promoter buffered minimal methanol (BMM) medium (400 mM potassium phosphate buffer, pH 6.0, 1.34% Yeast Nitrogen Base YNB, $4 \times 10^{-5}\%$ biotin, and 0.5% methanol) or buffered MM with doubled (BMM2 containing 1% methanol) or tenfold (BMM10 containing 5% methanol) concentration of methanol compared to BMM were prepared.

In the course of this thesis conditions for heterologous protein expression were optimized by changing various critical parameters as temperature during induction, pH of the culture media, concentration of methanol, or concentration of glucose,

respectively. Cultures with modified parameters were assessed for viability of the eukaryotic host and for protein expression in selected marker strains (e.g. expression of BBE from *P. pastoris* KM71H pPICZalpha-BBE-ER from previous work of ANDREAS WINKLER [48]). In the following section only optimized conditions for heterologous protein expression in *P. pastoris* are described.

4.2.7.1 Micro scale experiments in 96-deep-well plates

Micro scale experiments were performed according to the optimized protocol published by WEIS *et al.* [49]. Strains transformed with either pGAPZalpha or pPpT4-GAP were grown in YPD medium. Thus, deep-well plates were filled with 250 μ L YPD medium and inoculated with positive clones. The cultures were grown under standard conditions (28 °C, 340 rpm, 80% humidity) for 60 hours and then again 250 μ L YPD were added to each position of the deep-well plate. After additional 12, 24, and 48 h 50 μ L of YPD were added to compensate for volume loss. The cells were harvested by centrifugation after a total cultivation time of 132 h.

Protein expression under the control of the AOX1 promoter was performed in BMD medium with methanol induction. Deep-well plates were filled with 250 μ L BMD and inoculated with positive clones after singularizing on YPDZ plates. The cultures were grown at 28 °C, 340 rpm, and 80% humidity for 60 hours. Protein expression was induced by the addition of 250 μ L BMM2, and after additional 12, 24, and 48 h 50 μ L BMM10 were added. The cells were harvested 24 h after the last induction by centrifugation (4000 x g, 4 °C, 10 min).

In all cases replica plates were prepared from new expression colonies 60 h after inoculation.

4.2.7.2 Expression in shake flasks

Shake flask experiments were carried out in wide-necked 300 mL shake flasks with 50 mL medium and covered with two layers of cotton cloth. Again, strains transformed with either pGAPZalpha or pPpT4-GAP were grown in YPD medium for 132 h. Shake flasks were filled with medium, inoculated with single expression

colonies, and grown at 28 °C and 150-180 rpm. Fresh YPD medium was added regularly to compensate for volume loss.

Strains transformed with pPICZalpha or pPICZ/B vector constructs were grown in BMD medium and protein expression was induced by the addition of methanol. Shake flasks were filled with 50 mL freshly prepared BMD medium and inoculated with single expression colonies. The colonies were grown at 28 °C and 150 rpm for 60 h. Then 5 mL BMM10 medium were added to each flask and shaking was increased to 180 rpm for sufficient oxygen supply. 12, 24, and 48 h after the first induction 50 µL methanol were supplemented to each flask. Expression was stopped by centrifugation 24 h after the last induction (4000 x g, 4 °C, 15 min).

4.2.8 Large scale expression and purification

General protocols for *Pichia* fermentation are described in the EasySelect Pichia Expression Kit manual (Invitrogen, Carlsbad, CA, USA) or in [50]. A modified protocol for expression of STOX was available from previous work of ANDREAS WINKLER. This manual was further optimized and was published in detail in [51]. Large scale expression was performed in a 7 L Biostat CT fermenter (Sartorius Stedim Biotech GmbH, Goettingen, Germany) with an initial batch phase using basal salt medium with glycerol as carbon source, a subsequent glycerol fed-batch for biomass production and an expression phase with continuous methanol feed. Process parameters were automatically controlled to $\geq 30\%$ oxygen and 30 °C. pH was adjusted to pH 5.0 during biomass production and was increased to 6.0 during methanol adaptation. This pH adjustment was proven to be crucial for heterologous expression of BBE and was hence also implemented in case of STOX fermentation. For media composition and detailed operation procedures see [51].

After 96 h induction with methanol, $(\text{NH}_4)_2\text{SO}_4$ was added to the fermentation broth to a final concentration of 1 M and cells were harvested by centrifugation. Subsequently, the supernatant, which contained the secreted protein fraction, was subjected to a two-step purification protocol comprising hydrophobic interaction chromatography and gel filtration as described in [51].

4.2.9 Design of a fluorescence-based screening system for heterologous protein expression in *P. pastoris*

A new screening system for the identification of applicable *Pichia* expression strains was established using a fluorescence-based strategy with citrine as fluorescent marker. Fusion constructs with citrine attached to the C-terminus of *Am* or *Bw* STOX, respectively, via a TEV-polymerase linker sequence ENLYFQ [52] were generated using overlap-extension-PCR (OE-PCR). The fusion was designed to facilitate screening by using the fluorescence of citrine as a marker for protein expression.

4.2.9.1 Assembly of expression cassettes using OE-PCR

A pPICZ/*B-citrine* vector as template for the citrine moiety and the protocol for assembling linear expression cassettes with OE-PCR were obtained from the Institute of Molecular Biotechnology (TU Graz).

Different tags or signal sequences were attached at the N- or the C-terminal end of various fusion constructs. These tags include a HA-tag for facilitated antibody detection, a C-terminal KDEL signal sequence for retention in the ER [53-56], a SKL signal sequence for peroxisome targeting [57-59], or His₈- or StrepII- tags for affinity purification. The before described tags, signal and linker sequences were attached using respective oligonucleotide primers with overhangs encoding for the desired sequences. All fusion constructs were assembled as linear cassettes with flanking *XhoI* and *NotI* restriction sites for cloning into pPICZalpha or pPICZ/B.

In a first step the fragments, which should be further assembled to fusion constructs, were amplified separately using primers with overlapping extensions. Primers were ordered from VBC Biotech (Vienna, Austria) and were designed individually for each construct. In all cases the required overlapping region was added as 5'-extension of the oligonucleotide and the melting temperature of the initially binding 3'-region was at least 60 °C. A 50 µL reaction contained 0.2 mM dNTPs, 1x HF reaction buffer (New England Biolabs, Ipswich, MA, USA), 1 U Phusion DNA polymerase (New England Biolabs), 20 pmol each of forward and reverse primer, and 20 - 100 ng template DNA. The following program was used for the initial PCR:

30 sec at 98 °C, 35 cycles with 10 sec at 98 °C, 30 sec at 60 °C, and 1 min 30 sec or 45 sec at 72 °C (for STOX fragments or citrine fragments, respectively), followed by a final extension step of 10 min at 72 °C. PCR products were purified from agarose gels and consequently subjected to OE-PCR.

The STOX and citrine fragments were linked in a primerless amplification reaction by recognition of the overlapping linker region. In all cases the linker comprised a TEV-polymerase recognition site (ENLYFQ) for facilitated cleavage of the fusion protein. A typical 50 µL reaction mixture consisted of 0.2 mM dNTPs, 1x HF reaction buffer (New England Biolabs), 1 U Phusion DNA polymerase (New England Biolabs), and 5 ng and 2.5 ng purified STOX and citrine DNA fragment, respectively. The following cycling parameters were used for this first step of OE-PCR: 30 sec at 98 °C, 15 cycles with 10 sec at 98 °C, 20 sec at 58 °C, and 1 min 45 sec at 72 °C, followed by a final extension step of 7 min at 72 °C. In a second step of OE-PCR the assembled expression cassettes were amplified by the addition of the two terminal primers by pipetting a new reaction mixture directly on the PCR reaction mixture from the first step. 20 µL consisting of 1x HF reaction buffer (New England Biolabs), 0.2 mM dNTPs, 1 U Phusion DNA polymerase (New England Biolabs), and 10 pmol each of forward and reverse primer, were added to 50 µL of initial PCR reactions. The following program was used for this final step: initial denaturation for 30 sec at 98 °C, 25 cycles of 20 sec at 98 °C, 20 sec at 58 °C, and 1 min 45 sec at 72 °C, followed by a final extension step of 7 min at 72 °C. All PCR products were purified from agarose gels and subcloned into the pJET 1.2 vector using the CloneJET™ PCR Cloning Kit (Fermentas Inc., Glen Burnie MA, USA). The assembled expression cassettes were verified by plasmid sequencing (Eurofins DNA, Ebersbach, Germany) and correct cassettes were cloned into pPICZalpha or pPICZ/B, respectively, using the *XhoI* and *NotI* restriction sites.

Again the resulting expression plasmids were verified by sequencing (Eurofins DNA, Ebersbach, Germany) and were subjected to linearization and desalting. The prepared linear cassettes were transformed into competent *P. pastoris* expression strains as described in 4.2.6.

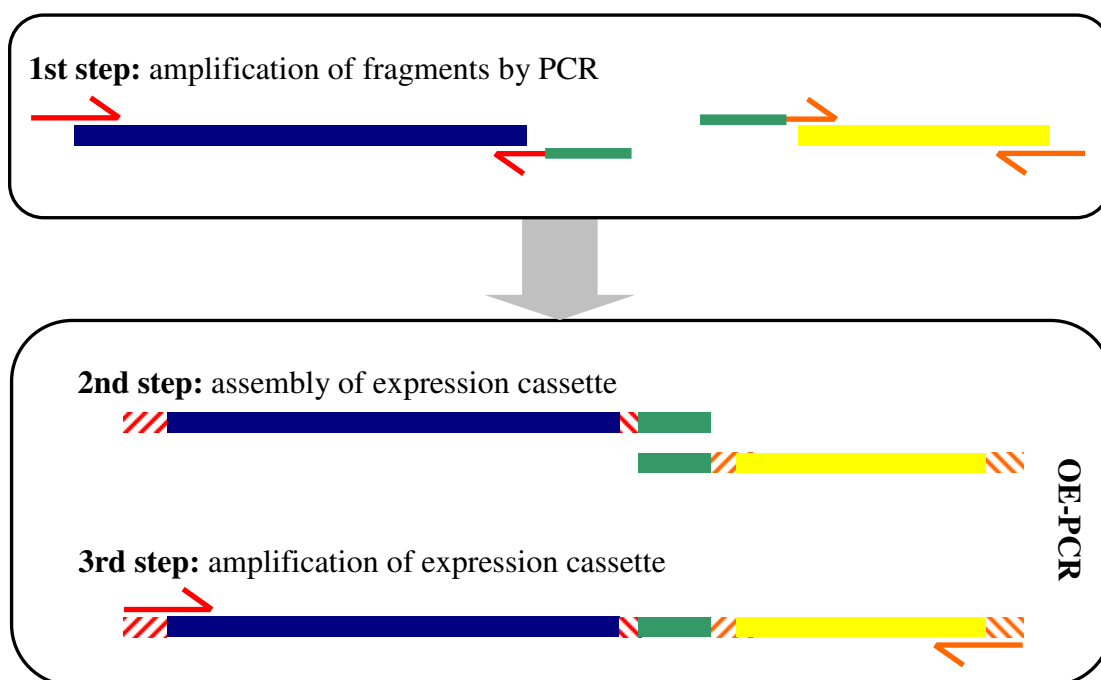


Figure 19: Assembly of linear expression cassettes using OE-PCR.

The gene of interest (*Am* or *Bw* STOX) is shown in blue, citrine in yellow, and the linking TEV polymerase site in green. Primers (represented in red and orange) with 5'-extensions are used to generate the overlapping ends on the two fragments, which are required for OE-PCR. Subsequently, the fragments are connected and further amplified using the outer primers.

4.2.9.2 Fluorescence-based screening procedure

Initial screening was performed in micro scale using deep-well plates. For each plate 80 positive transformants were picked and used for inoculating a single well each. Additionally, *P. pastoris* KM71H pPICZ/B-citrine, which expresses citrine intracellularly and *P. pastoris* KM71H pPICZalpha-BBE-ER for secreted expression of BBE were used as positive expression controls. *P. pastoris* KM71H without integration of any expression cassette or transformed with the pPICK-PDI vector were used as negative controls, respectively. At least two deep-well plates were prepared for each construct, which implies a screening of at least 160 transformants. The plates were grown as described in 4.2.7.1 with the exception that all plates were protected from light during the induction phase. Since citrine fluorescence was quenched with light, this step turned out to be crucial for a reproducible screening.

After a total cultivation time of 132 h the cells were harvested by centrifugation or were subjected directly to fluorescence measurements with a SPECTRAMax

GEMINI XS microplate spectrofluorometer (Molecular Devices, Sunnyvale, CA, USA). In case of direct measurement 50 μ L cell suspension were transferred to a new 98-well plate and mixed with 150 μ L distilled water each. These dilutions were analyzed in the SPECTRAmax GEMINI XS plate reader using 500 and 550 nm as excitation and emission wavelengths and a cut-off of 530 nm. For fluorescence analysis of the secreted protein fraction in the medium and the in-cell fluorescence the supernatant was carefully transferred to a new 96-well plate using a multichannel transfer pipette. Again for each position 50 μ L of supernatant were mixed with 150 μ L distilled water and subjected to fluorescence scanning. The remaining pellets were resuspended in 400 μ L distilled water and for each position 50 μ L of suspension were diluted to 200 μ L and fluorescence was determined.

Consequently, the eight colonies exhibiting the highest citrine fluorescence were singularized and subjected to a second round of screening, where each colony was used for inoculating ten wells thus enabling investigation of the stability of citrine expression. At least two consecutive rescreen experiments were performed to identify the most promising strains with high and stable expression of the fluorescent marker.

Usually four candidates were selected for expression experiments in shake flasks. Expression was performed according to the protocol described in 4.2.7.2 with the exception that all colonies had to be protected from light during protein expression. After 72 h of induction all cells were harvested and citrine fluorescence was used for detecting the fusion protein in the following purification steps or analyses.

4.2.9.3 Fluorescence microscopy

A *Pichia* strain transformed with the expression plasmid pPICZalpha-Bw *STOX-linker-citrine* showing high citrine fluorescence in micro scale experiments was cultivated in shake flasks as described in 4.2.7.2. After 24 h of induction with methanol the cell suspensions were subjected to fluorescence microscopy. Fluorescence microscopy was performed using either a Zeiss Axiovert 35 microscope with a 100-fold oil immersion objective and a UV lamp, or measurements were performed on a Leica TCS 4d confocal microscope with appropriate laser and filter settings for optimized GFP fluorescence and transmitted

light (differential interference contrast) detection [60]. Vital staining with MitoTracker® Mitochondrion Selective Probes (Invitrogen, Carlsbad, CA, USA) was used to assign the localization of the fluorescent citrine marker.

4.2.9.4 Native PAGE for fluorescent fusion proteins

Intracellular STOX-citrine fusion proteins were analyzed using native PAGE. Strains expressing the fluorescent fusion protein were compared to control strains expressing the citrine label without fusion to a target protein.

Cells were harvested at 4000 x g and 4 °C for 15 min and resuspended in an equal volume of breaking buffer (100 mM Tris/HCl, 150 mM NaCl, 5% glycerol, supplemented with protease inhibitor cocktail, pH 8.0). Cell disruption was done with glass bead lysis in a MSK homogenizer (B. Braun Biotech International GmbH, Melsungen, Germany). Samples were mixed with an equal volume of glass beads and subjected to homogenization for 3 min with CO₂ cooling. Glass beads and cell debris were removed by centrifugation at 18000 x g and 4 °C for 20 min. The supernatant contained the soluble protein fraction and was subjected to native PAGE analysis.

Gels and buffers were prepared according to standard protocols, however, without the use of sodium dodecyl sulphate, β-mercaptoethanol, and dithiothreitol [61, 62]. Samples were carefully mixed with loading dye and loaded onto an acrylamide gel (5% stacking gel, 12.5% separating gel, both pH 8.8). Native PAGE was performed in a running buffer containing 3 g/L Tris base, 14.2 g/L glycine, and 0.34 g/L EDTA at 4 °C and 45 V for 15 h. Then in-gel fluorescence of the citrine marker was determined using a Molecular Imager FXTM Pro Plus laser scanner (BioRad, Hercules, CA, USA). After fluorescence imaging proteins were stained using SYPRO® Ruby Protein Gel Stain (Invitrogen, Carlsbad, CA, USA). Protein bands, which showed in-gel fluorescence, were excised and extracted from the gel for MALDI-MS analysis.

4.2.10 Isolation of periplasmic proteins

In order to determine if secreted STOX is retained in the periplasm, spheroblasting was performed to isolate the periplasmic protein fraction. All isolation steps were performed as described in [63]. After a total cultivation time of 132 hours, the fermentation broth was harvested and cells were pelleted by centrifugation at 4000 x g and 4 °C for 10 min. Cells were washed with freshly prepared SED-buffer (1 M sorbitol, 25 mM EDTA, 50 mM DTT, pH 8.0) and subsequently with 1 M sorbitol. Then the cells were resuspended in STE-buffer containing 1 M sorbitol, 1 mM EDTA, and 20 mM Tris/HCl, pH 7.0. Spheroblasting was performed by adding zymolyase to a final concentration of 0.5 µg/mL and incubation for 30 min at 37 °C. Then zymolyase concentration was increased to a final concentration of 2.5 µg/mL and spheroblasting was continued for additional 60 min at 37 °C. Subsequently, spheroblasts and intact cells were pelleted at 1000 x g and 4 °C for 60 min. The supernatant, which contained the periplasmic protein fraction, was sterile filtered through 0.20 µm filters (Sarstedt, Nümbrecht, Germany) and stored at 4 °C.

4.2.11 Protein purification

Protein purification was performed either with a two-step protocol comprising a hydrophobic interaction chromatography and a consecutive gel filtration, or with affinity columns using the attached His₆-, His₈-, or StrepII-tag for facilitated purification. Extracellular proteins were purified directly from the fermentation medium. Proteins, which were accumulated inside the cells, were released by glass bead lysis as already described in 4.2.9.4.

Proteins, which were not equipped with affinity-tags were purified according to the two-step procedure described in [48]. A final concentration of 1 M ammonium sulphate was added to the fermentation medium containing the extracellular protein fraction or to the supernatant after cell lysis and centrifugation. The resulting solution was loaded onto a XK16/20 phenylsepharose 6 FF (high substitution) column with a 20 mL bed volume or a XK 50/20 phenylsepharose 6 FF (high substitution) column (200 mL bed volume) equilibrated with 100 mM Tris/HCl, 150 mM NaCl, 1 M ammonium sulphate, pH 8.0 (buffer A). After complete loading of the supernatant the column was washed with 4 column volumes of buffer A. Elution was performed

by decreasing the salt concentration using a linear gradient of buffer A against water. Elution fractions were collected and fractions containing STOX were identified using SDS-PAGE, activity assays, or citrine fluorescence. These fractions were pooled and concentrated for gel filtration using the Centriprep system from Amicon (Cleveland, OH, USA). Aliquots of 2 mL from the concentrated samples were loaded onto a XK16/75 Superdex™ 75 prep grade (Amersham Biosciences, Piscataway, NJ, USA) gel-filtration column equilibrated with 50 mM Tris/HCl, 150 mM NaCl, pH 9.0 and eluted using a flow rate of 1 mL/min. Fractions containing the desired protein were concentrated and analyzed using SDS-PAGE and MALDI-TOF analysis.

Proteins equipped with a His₆- or His₈-tag were purified according to standard protocols using HisTrap™ HP affinity columns (GE Healthcare, Fairfield, CT, USA). Proteins possessing a StrepII-tag for facilitated purification were loaded onto a XK16/20 StrepTactin Sepharose High Performance column (GE Healthcare) preequilibrated with 100 mM Tris/HCl, 150 mM NaCl, 1 mM EDTA, pH 8.0, and were eluted with 2.5 mM D-desthiobiotin in 100 mM Tris/HCl, 150 mM NaCl, 1 mM EDTA, pH 8.0.

4.2.12 Activity assays

Activity assays were performed with various substrates in order to determine substrate specificity of STOX. (*S*)-reticuline, (*S*)-norreticuline, (*S*)-scoulerine, (*S*)-canadine, (*S*)-coreximine, (*S*)-tetrahydrocolumbamine, (*S*)-tetrahydropalmatine, and salutaridine were available from the natural products collection from TONI M. KUTCHAN (Donald Danforth Plant Science Center, St. Louis, MO, USA) and were therefore used as potential substrates for STOX.

A typical reaction mixture consisted of 8 µL of sample (supernatant of fermentation), 8 µL of 100 mM Tris/HCl, pH 9.0, and 2 µL of 1 mM substrate in methanol and was incubated at 37 °C for 24 hours. For visualization the reaction mixtures were separated using thin layer chromatography with CH₂Cl₂/MeOH/25% NH₄OH (90/9/1) as mobile phase. After separation the resulting spots were visualized by irradiation with UV-light.

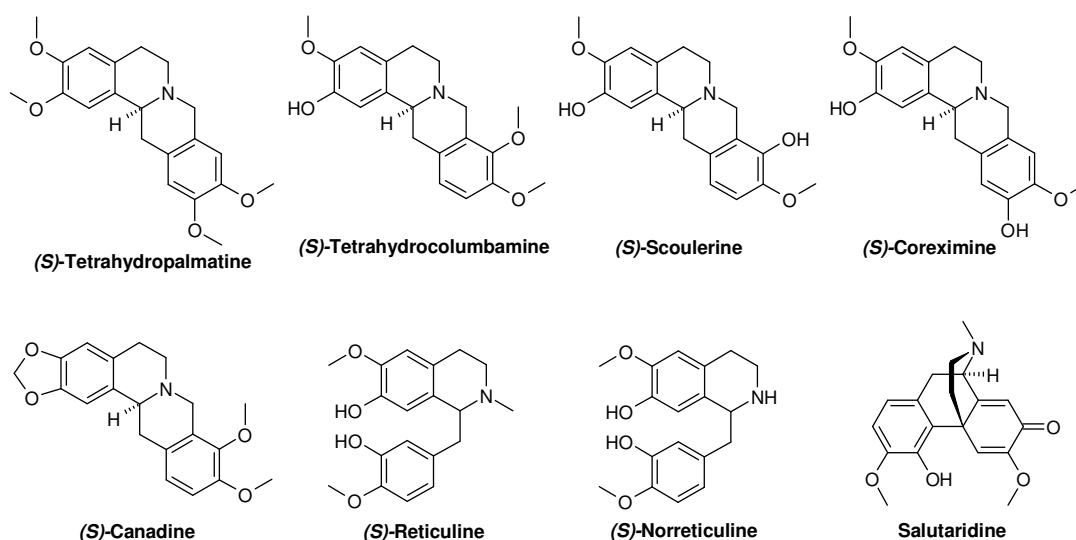


Figure 20: Potential substrates for *Am* and *Bw* STOX

Furthermore, activity assays with (*S*)-tetrahydropalmatine were scaled up and were analyzed using HPLC. 50 μL of sample (supernatant after fermentation) were incubated with 150 μL of 1 mM (*S*)-tetrahydropalmatine in 150 mM NaCl, 50 mM Tris/HCl, pH 9.0, at 37 $^{\circ}\text{C}$ for 24 h. The reaction mixture was centrifuged at 17,000 $\times g$ for 5 min and the clear supernatant was used for further analysis. 10 μL of the reaction mixture were loaded onto an Atlantis[®] dC₁₈ column (5 μm , 4.6 \times 250 mm, Waters, Milford, MA, USA). Substrate and product were separated during an isocratic elution at 60% MeOH / 40% 10 mM (NH₄)HCO₃, pH 7.0, for 30 min. A photodiode array detector was used for following the elution profile.

4.2.13 Immunoblotting

Western blot and Dot blot assays were performed using different antibodies. An antibody produced in rabbit and raised against STOX (expressed as inclusion bodies in *E. coli* and purified using SDS-PAGE) was ordered from Eurogentec (Seraing, Belgium) and was tested for reactivity with the enzyme.

Affinity tags, as His- or StrepII-tag, were detected using available standard antibodies (GE Healthcare Fairfield, CT, USA). Moreover, an anti-flavin antibody, which recognizes covalently bound flavins, was a gift from D. EDMONDSON (Emory University, Atlanta, GA, USA) and was used for the detection of covalently bound flavins. Western blots were performed according to standard protocols and Dot blots were performed as described in [48].

4.3 Results

4.3.1 Computational analysis

Due to initial difficulties in expressing both STOX from *A. mexicana* and *B. wilsoniae* detailed sequence analyses were performed to predict special structural features, which could hamper heterologous expression in a given host system and to get important information for the design of new expression constructs. Signal peptides for targeting the respective protein to the secretory pathway were predicted using the SignalP 4.0 server offered at CBS (Center for Biological Sequence Analysis, Technical University of Denmark) [64-68]. Further predictions on protein localization were made using the pSORT server <http://psort.hgc.jp/form.html> [69-75], and the TargetP server offered at CBS [65, 76]. *N*-glycosylation was analyzed using the NetNGlyc 1.0 Server at CBS [77], or MitoProt II v1.101 offered from the Institute of Human Genetics (Helmholtz Center Munich) [78]. For both *Am* and *Bw* STOX, homology models were generated with the structure of BBE (3D2H) as template using the SWISS-MODEL server developed by the structure bioinformatics group at the Swiss Institute of Bioinformatics & the Biozentrum University of Basel [79-81].

4.3.1.1 Prediction of signal peptides and protein localization

Information regarding the subcellular localization of proteins can be very helpful for selecting applicable strategies for heterologous protein expression in various host organisms [82-84].

Both *Am* and *Bw* STOX proteins were clearly predicted to possess a cleavable leader peptide at the N-terminus of the protein. This signal peptide targets the proteins to the secretory pathway and is typically cleaved off after translocation through the ER [69, 73]. For STOX from *A. mexicana* and *B. wilsoniae* a sequence of 26 and 24 amino acids, respectively, was predicted as cleavable leader peptide (see Figure 21). Predictions of protein localization performed with TargetP or pSORT confirmed sorting of *Am* and *Bw* STOX to the secretory route. However, results were not unambiguous in both cases. *Am* STOX was suggested for secretion or for transport to peroxisomes or chloroplasts and hence the probability for complete passing through

the secretory system is decreased. In case of *Bw* STOX a clear extracellular localization was predicted using TargetP. However, pSORT analysis suggested either a complete secretion to the medium or vacuolar targeting. Moreover, analysis with MitoProt II v1.101 resulted in proposed export of *Bw* STOX to mitochondria.

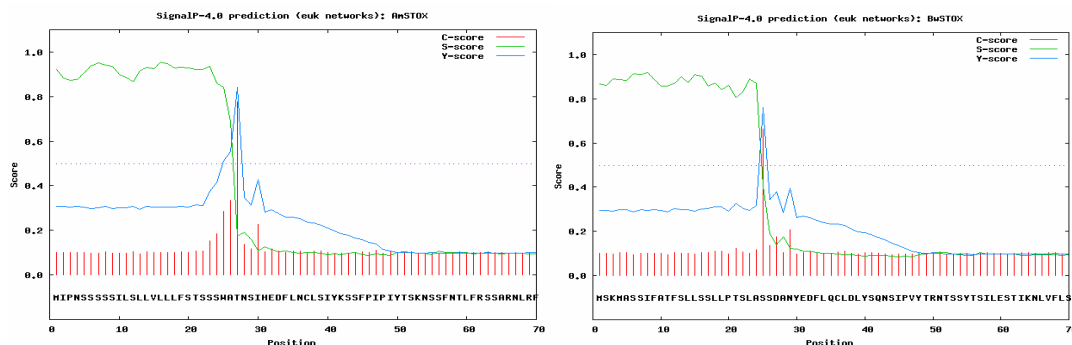


Figure 21: Prediction of N-terminal target sequences using SignalP

The left panel shows the signal peptide prediction for *Am* STOX. Results for *Bw* STOX are shown in the right panel. Red lines represent the C-score (cleavage score), which is significantly high at the cleavage site. Green lines represent the S-score (signal score) and denote the probability for amino acids for being part of a signal peptide. The Y-score (blue line) is a merge of cleavage and signal prediction. A significant peak in the Y-score gives the cleavage site. *Am* STOX and *Bw* STOX both possess cleavage sites after 26 and 24 amino acid residues, respectively.

4.3.1.2 Prediction of N-glycosylation sites

N-glycosylation can be regarded as one of the most frequent posttranslational modifications in eukaryotic proteins, which was reported to have a strong influence on protein stability [85, 86]. Thus, potential N-glycosylation sites were predicted for *Am* and *Bw* STOX.

Table 7: N-glycosylation sites in *Am* and *Bw* STOX

Predictions were performed using NetNGlyc 1.0 with a threshold of 0.5. Asparagines predicted to be potential N-glycosylation sites feature the Asn-Xaa-Ser/Thr motif.

<i>Am</i> STOX			<i>Bw</i> STOX		
position	sequon	potential	position	sequon	potential
4	NSSS	0.6937	51	NTSS	0.5192
74	NSTQ	0.6503	483	NGTA	0.5203
135	NITV	0.6458			
162	NESK	0.7041			
440	NESE	0.5064			

Am STOX was suggested to be highly glycosylated by featuring five potential *N*-glycosylation sites, four of them being present in the mature protein after signal peptide cleavage. All potential asparagines (Asn74, Asn135, Asn162, and Asn440) are located within an Asn-Xaa-Ser/Thr sequon (Xaa is any amino acid except proline) and were predicted to be exposed to the surface of the protein as evident from analysis of the homology model.

Prediction of *N*-glycosylation sites in *Bw* STOX resulted in the identification of two asparagines, Asn51 and Asn483, which showed potentials above the default threshold and which were positioned at the surface of the protein.

4.3.2 *E. coli* expression experiments

Expression experiments in *E. coli* were performed solely with STOX from *A. mexicana*, thus, STOX in this chapter always denotes the protein from *Argemone*. Different strains, chaperone coexpression, and a protein fusion with the maltose binding protein were tested but unfortunately no soluble and active protein was expressed in any of the experiments. Inclusion bodies were formed using *E. coli* ORIGAMI B pET21a(+)-*Am* STOX-*His*₆ (see Figure 22) or a ORIGAMI B strain coexpressing chaperones *dnaK*, *dnaJ*, *grpE*, *groES*, and *groEL*. Variation of IPTG concentrations or temperature during induction did not lead to improved expression of soluble protein. Analysis of the supernatant after cell disruption resulted in the identification of marginal amounts of soluble protein using MALDI-MS technique. However, the protein did not show any activity with (*S*)-reticuline and (*S*)-scoulerine. Furthermore, purification of the his-tagged protein with Ni-NTA affinity columns was not successful, which implied a very low abundance of STOX.

Later a STOX fusion protein was generated, where STOX was fused to the C-terminal end of the maltose binding protein. It is suggested that MBP promotes the solubility of its binding partners and leads to high expression of soluble fusion protein in the cytoplasm of *E. coli* [87]. Unfortunately, this did not apply for the STOX fusion, which was expressed as insoluble inclusion bodies. Again varying conditions and the presence of chaperones did not improve expression of soluble protein.

Due to the expression of insoluble inclusion bodies, protein refolding attempts were made to obtain correctly folded and active protein. Generally, refolding of STOX-inclusion bodies resulted in the formation of solubilized protein, which was identified as STOX by MALDI-MS. However, this protein lacked the required cofactor and all attempts to supply FAD for reconstitution were unsuccessful. Thus, no further investigations could be performed with this enzyme.

In spite of these problems, STOX inclusion bodies could be employed as ideal antigen for antibody production. An anti-STOX antibody was ordered from Eurogentec (Searing, Belgium), which was raised against inclusion bodies of STOX expressed in *E. coli* ORIGAMI B and purified using SDS-PAGE. Unfortunately, the immunization process was unsuccessful leading to an antibody with unspecific reactions. Analyses of all bleeds showed that the resulting anti-STOX antibody reacts with a large number of *E. coli* proteins, but does not show any preference for STOX. Isolation of total IgG with protein A sepharose columns did not improve the quality of the anti-STOX antibody.

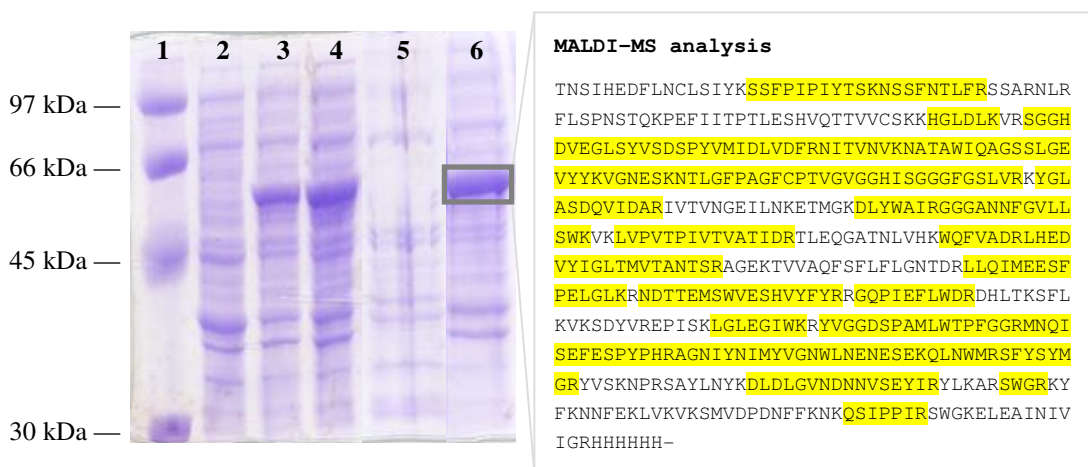


Figure 22: Expression of STOX in *E. coli* ORIGAMI B

Expression was performed with *E. coli* ORIGAMI B pET21a(+)-*Am STOX-His₆*. Main cultures were grown at 37 °C to an OD₆₀₀ of 0.75, then IPTG was added to a final concentration of 0.1 mM and protein expression was performed at 20 °C for 14 h. The SDS-gel shows the result of heterologous protein expression. Lane 1: LMW standard; lane 2: cells before induction with IPTG; lane 3 and 4: cells after 4 h and 14 h of induction, respectively; lane 5: soluble protein after cell disruption; lane 6: insoluble protein fraction after cell disruption. The panel at the right site shows the identification of *Am* STOX using MALDI-MS. The amino acid sequence of *Am* STOX is displayed in the box and peptides, which were identified using MALDI-MS analysis, are highlighted in yellow.

4.3.3 Expression of *Am* and *Bw* STOX in *P. pastoris*

Expression experiments in *P. pastoris* were performed with various constructs of *Am* and *Bw* STOX using different promoters and the alpha-factor or a native signal peptide for secreted protein expression (cf. Table 6). Initial experiments were performed in small or micro scale to obtain a throughput fast enough to screen at least 100 - 200 *Pichia* colonies transformed with the expression plasmid in a reasonable time. Since linear expression cassettes were integrated into the genome of *P. pastoris*, the resulting transformants showed different expression efficiencies depending on the number and location of integrated sequences.

Expression experiments were performed as described in 4.2.7. After 72 hours of induction with methanol, fermentation medium as well as cells were tested for intracellular and secreted protein expression.

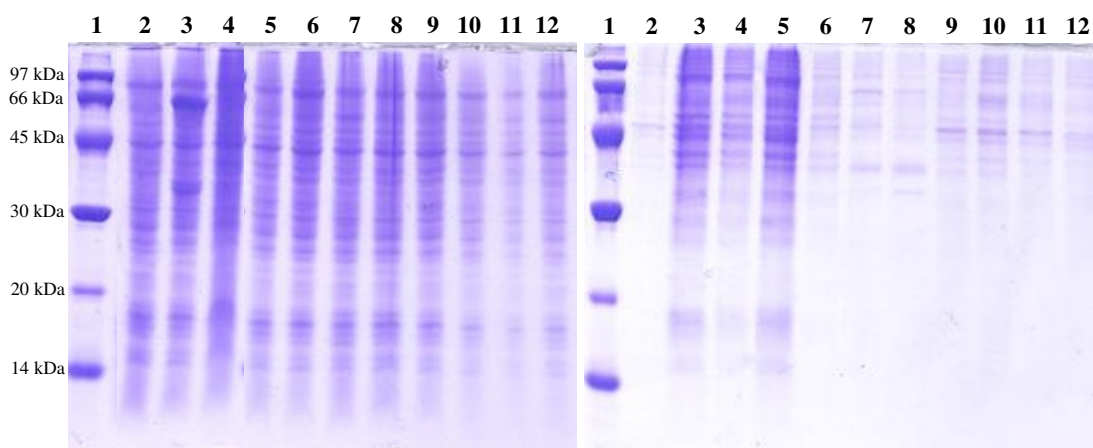


Figure 23: Intracellular and secreted protein fractions from *Pichia* expression

LMW marker was used as protein standard (lane 1). The gel on the left shows cell pellets containing the intracellular protein fraction after cell harvest. The gel on the right shows secreted proteins accumulated in the fermentation medium, which were concentrated using TCA precipitation. On both gels samples were applied in the following order: lane 2, *P. pastoris* KM71H (negative control); lane 3, *P. pastoris* KM71H coexpression PDI; lane 4, BBE expressing strain *P. pastoris* KM71H pPICZalpha-BBE-ER; lanes 5 and 6, *P. pastoris* KM71H pPICZalpha-*Am* STOX-*His*₆; lanes 7 and 8; *P. pastoris* KM71H pPICZ/B-*Am* STOX-*His*₆; lanes 9 and 10, *P. pastoris* KM71H pPICZalpha-*Bw* STOX-*His*₆; lanes 11 and 12, *P. pastoris* KM71H pPICZalpha-*Bw* STOX-*His*₆. All strains showed similar expression patterns of intracellular and secreted proteins. Solely coexpression of PDI in lane 2 resulted in the formation of a new protein band of approximately 60 kDa.

Both *Am* and *Bw* STOX should be directed to the secretory machinery and should concentrate in the medium. Unfortunately, none of the employed constructs led to the

formation of satisfactory amounts of secreted protein. Some expression experiments seemed to result in the expression of marginal amounts of STOX as observable through in-gel fluorescence, SDS-PAGE, immunoblotting, or enzyme activity. However, these experiments could not be reproduced since protein expression turned out to be very unstable.

Generally, the lack of an applicable detection system for *Am* and *Bw* STOX hampered identification of heterologously expressed protein. SDS-PAGE, immunoblotting, and MALDI-MS analysis of excised protein bands were applied to identify expressed STOX in the fermentation supernatant, in periplasmic fractions, or inside host cells. Unfortunately, no differences were observed in the expression pattern of strains transformed with *Am* or *Bw* STOX expression cassettes and the respective negative controls (*P. pastoris* KM71H) as obvious from Figure 23. All available antibodies showed cross-reactivity with various *Pichia* proteins and did not specifically react with *Am* or *Bw* STOX.

Moreover, alteration of fermentation parameters as the pH value, temperature, or methanol concentration did not lead to improved expression of *Am* or *Bw* STOX.

Considering the interminable problems of expressing detectable amounts of STOX in small scale and micro scale experiments, fermentation was scaled up to improve heterologous protein expression. The most promising colonies from small scale experiments were selected for fermentation in 7 L Biostat CT fermenters (Sartorius Stedim Biotech GmbH, Goettingen, Germany). Large scale fermentation enables tight and automatic process control with accurate pH adjustment and oxygen supply [42, 43, 45, 50]. Additionally, definite media for optimal biomass production and consecutive heterologous protein expression were used in large scale fermentation.

Fermentation was performed according to the manual described in 4.2.8 and in [51] with different pH-values from pH 5.0 to 7.0. Biomass was produced in a batch reactor followed by a fed-batch phase with glycerol as carbon source and after reaching cell densities of approximately 200 mg/mL heterologous protein expression was induced by the addition of methanol (cf. Figure 24).

After 72 h or 96 h of induction, cells were harvested by centrifugation. The supernatant was supplied with 1 M ammonium sulphate, loaded onto a XK 50/20 phenylsepharose 6 FF (high substitution) column and purified as described in 4.2.8.

For BBE, large scale expression resulted in the formation of large quantities of secreted protein, which could be purified with the optimized two-step protocol [48, 51]. Although STOX was believed to exhibit a similar expression pattern, neither *Am* nor *Bw* STOX could be detected or purified from supernatants of large scale fermentation. Even immunoblotting, activity assays, and MALDI-MS analysis did not result in the identification of at least marginal amounts of heterologously expressed protein. Whether protein expression was hampered under the given conditions or whether protein was expressed and immediately degraded, could not be determined.

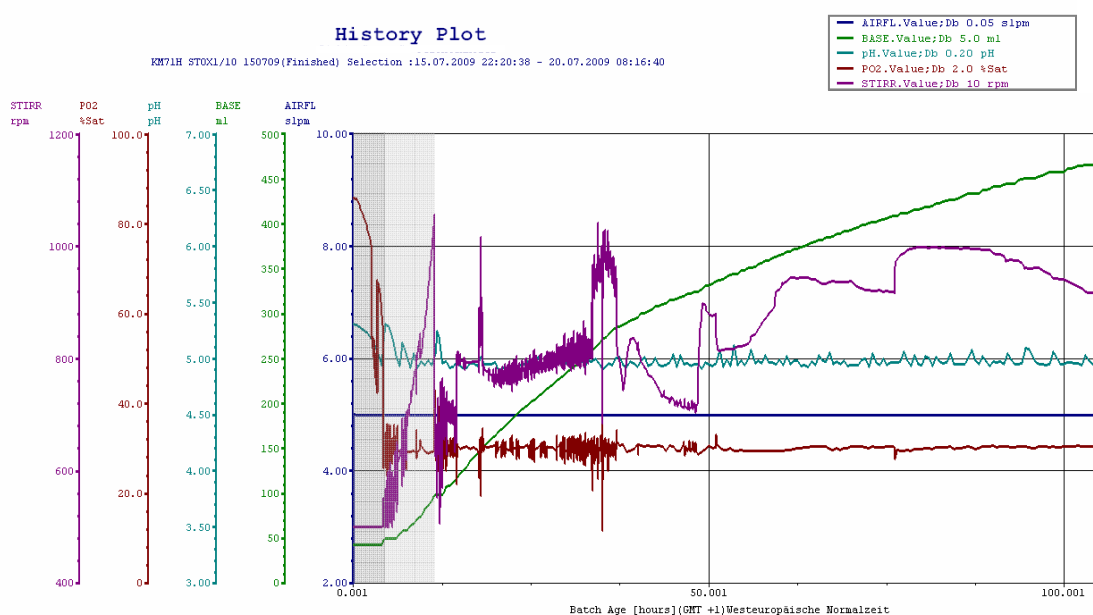


Figure 24: History plot of a typical *Pichia* fermentation

Fermentation of *P. pastoris* KM71H pPICZalpha-*Am* STOX-*His*₆. Important process parameters as pH value, oxygen saturation (pO₂), stir speed, addition of base, and oxygenation (airflow) are shown in the diagram. During the whole process the pH value was automatically adjusted to 6.0. The consumption of base was indicative for viability of the *Pichia* culture. Dark grey and light grey shades represent initial batch and fed-batch phase for biomass production, respectively. The rest of the diagram shows the prolonged expression phase with methanol feeding. Rapid alterations of stir speed were caused by changes in methanol feed.

4.3.3.1 Substrate specificity of *Am* STOX

Besides the search for an applicable *Pichia* strain for heterologous expression of STOX, investigations on substrate specificity were a major objective of this project. Initial experiments were performed with STOX from *A. mexicana* since only expression cassettes with this STOX protein were available at the beginning of my work.

Due to the fact that expression of *Am* STOX could not be optimized, supernatants from *Pichia* fermentations containing secreted protein served as samples for determining STOX activity. Therefore, substrate specificity as suggested in literature [22, 23, 28] was revised using all available alkaloid standards. In-depth investigations were performed with (*S*)-scoulerine, (*S*)-reticuline, (*S*)-norreticuline, (*S*)-coreximine, (*S*)-canadine, and (*S*)-tetrahydropalmatine. Available amounts of (*S*)-tetrahydrocolumbamine and salutaridine allowed initial screening experiments, but no further analysis.

Interestingly, the fermentation supernatant of one transformant of *P. pastoris* KM71H pPICZ/B-*Am* STOX-*His*₆ (namely colony 10) showed clear oxidase activity with (*S*)-tetrahydropalmatine as substrate. Thin layer chromatograms with reaction mixtures of colony 10 from *P. pastoris* KM71H pPICZ/B-*Am* STOX-*His*₆ and (*S*)-tetrahydropalmatine displayed the formation of a new product spot. This observation proved to be reproducible with supernatants from new expression experiments containing the secreted protein fraction of the before mentioned colony 10. Furthermore, HPLC analysis of the reaction mixtures confirmed (*S*)-tetrahydropalmatine as substrate for *Am* STOX. Time dependent HPLC analysis of reaction mixtures clearly showed substrate conversion and a concomitant formation of a new product peak. Comparison of the UV-vis spectrum of this new product with the known spectrum of palmatine (the spectrum was available from unpublished work of TONI M. KUTCHAN, Donald Danforth Plant Science Center, St. Louis, MO, USA) allowed the conclusion that *Am* STOX catalyzes the oxidation of (*S*)-tetrahydropalmatine to palmatine. Negative controls performed with fermentation supernatants containing the secreted protein fraction of wild type *P. pastoris* KM71H did not result in any conversion of the substrate.

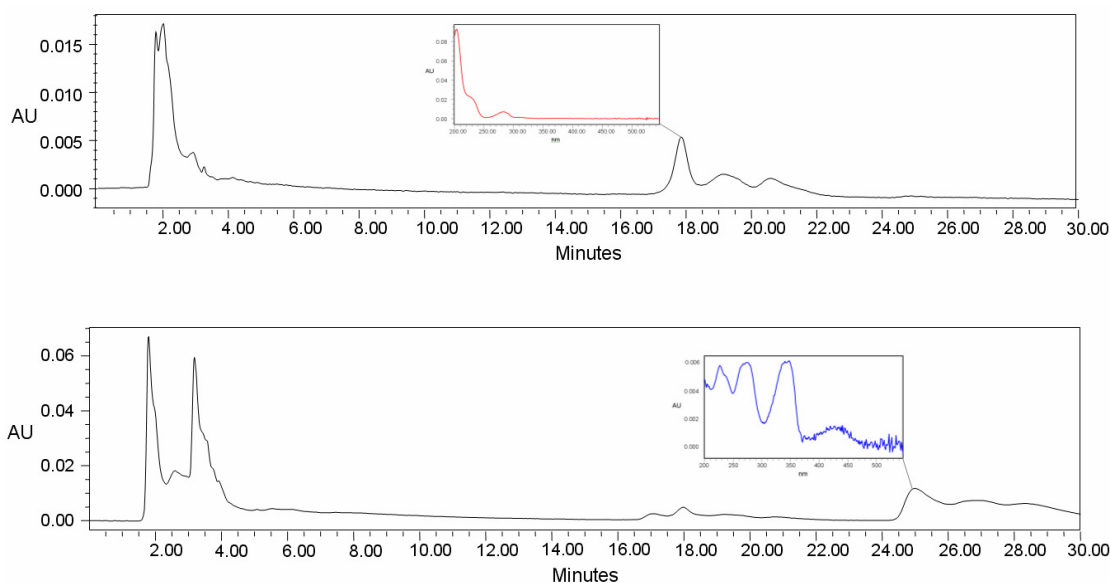


Figure 25: HPLC analysis of conversion of (*S*)-tetrahydropalmatine with *Am* STOX

The upper chromatogram shows the negative control, where (*S*)-tetrahydropalmatine was incubated with *P. pastoris* KM71H. The lower chromatogram shows the oxidation of (*S*)-tetrahydropalmatine yielding palmatine catalyzed by *Am* STOX from the fermentation supernatant from *P. pastoris* KM71H pPICZ/B-*Am* STOX-*His*₆ colony 10. Both assays were performed under the same conditions. 1 mM substrate was incubated with fermentation supernatants at 37 °C for 24 h; pH was adjusted to pH 9.0. The inlays show the UV-vis spectra of (*S*)-tetrahydropalmatine and palmatine, respectively.

Although most tested alkaloid standards shared the (*S*)-tetrahydroprotoberberine structure and differed solely in the substitution pattern of rings A and D, STOX seemed to be specific for (*S*)-tetrahydropalmatine. No product formation was detectable in activity assays performed with (*S*)-scoulerine, (*S*)-reticuline, (*S*)-norreticuline, (*S*)-coreximine, (*S*)-salutaridine, and (*S*)-tetrahydrocolumbamine. For (*S*)-canadine, results were contradictory. Formation of a presumably new product was observed in initial screening assays; however, this turnover could never be reproduced.

4.3.4 Design of a fluorescence-based screening system

In the course of this thesis project the identification of applicable expression strains was recognized as a central issue in establishing heterologous protein expression with *P. pastoris* as host organism. The lack of a specific antibody or a quick and easy activity assay impeded a high-throughput screening of *Pichia* transformants, which would have increased the possibility of finding applicable expression strains. Thus, a

new screening system based on the use of a fluorescent label was implemented for both *Am* and *Bw* STOX.

Initial constructs comprised a fusion of the respective STOX protein with a C-terminal citrine-tag as fluorescent marker and a linking TEV protease cleavage site for facilitated removal of the tag. OE-PCR was applied to generate the new expression cassettes and this method proved to be very convenient for fast shuffling of DNA sequences. A multitude of constructs could be assembled simultaneously by using different primers for the PCR reactions.

The fluorescence-based screening system was first tested with colonies of *P. pastoris* KM71H pPICZalpha-*Bw* STOX-linker-citrine. Initial screening steps were performed in micro scale with methanol induction. The best transformants were identified by measuring the fluorescence of the citrine marker. Subsequently, selected colonies were singularized and at least two rescreen experiments were performed to identify colonies with the most stable fluorescence. Thus, this new method enabled easy and fast identification of *Pichia* transformants with a strong expression of the fluorescent marker. Interestingly, citrine fluorescence could not be observed in the supernatant after cell harvest. All heterologously expressed fusion protein seemed to be retained inside the cells as was evident from fluorescence measurements. Therefore, whole cells were analyzed in all further experiments.

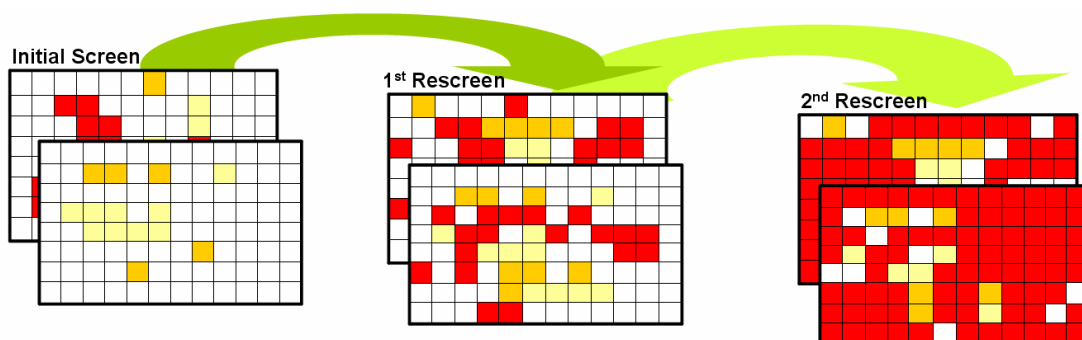


Figure 26: Schematic representation of the fluorescence-based screening

The figure shows the fluorescence pattern as observed in a fluorescence-based screening. Different colours represent the intensity of fluorescence at each position of the deep-well plate. White implies no, yellow a weak and red a strong fluorescence signal, respectively.

Implementation of the fluorescence based screening system also helped to get new insights in the heterologous expression of STOX. Since citrine was fused to the C-terminus of *Bw* STOX, it became obvious that the fusion was efficiently

transcribed and translated. Hence mRNA instability, unfavourable mRNA secondary structures or inadequate codon usage could be ruled out as cause of poor heterologous expression of *Bw* STOX.

Due to the easy traceability of fluorescent tags, protein purification was performed by exploiting citrine fluorescence. The best colony from screening (*P. pastoris* KM71H pPICZalpha-*Bw* STOX-linker-citrine colony 60) was cultivated in 40 300-mL shake flasks with 50 mL culture volume and purification was performed with consecutive hydrophobic interaction and gel filtration chromatography as described in 4.2.11. Cells were disrupted mechanically by glass bead lysis and intracellular proteins were purified from the resulting supernatant. Throughout all purification steps, fractions containing the citrine marker were identified by fluorescence measurements.

In the end a yellow fluorescing protein solution was obtained, however, to our surprise the fluorescent marker did not exist as fusion with the protein of interest. SDS-PAGE and MALDI-MS analysis clearly revealed that the purified citrine was an approximately 30 kDa protein which was not linked to *Bw* STOX.

Further analysis led to the identification of marginal amounts of the *Bw* STOX fusion protein using MALDI-MS analysis, namely in the insoluble fraction after Merckenschlager homogenization and in the fraction containing 90 - 120 kDa proteins after gel filtration (cf. Figure 27). These results were further confirmed with immunoblotting using the ant flavin antibody directed against covalently linked flavins. The antibody showed reactivity with those protein bands, which were previously identified as STOX-fusion by MALDI-MS.

However, the STOX-fusion seemed to be highly unstable after gel filtration and precipitation was observed. Hence it was concluded that stability problems seem to contribute to the difficulties in heterologous expression of STOX from *B. wilsoniae*.

Activity assays performed with the fraction containing the *Bw* STOX-citrine fusion protein after the two-step purification procedure did not result in determinable conversion of any tested substrate.

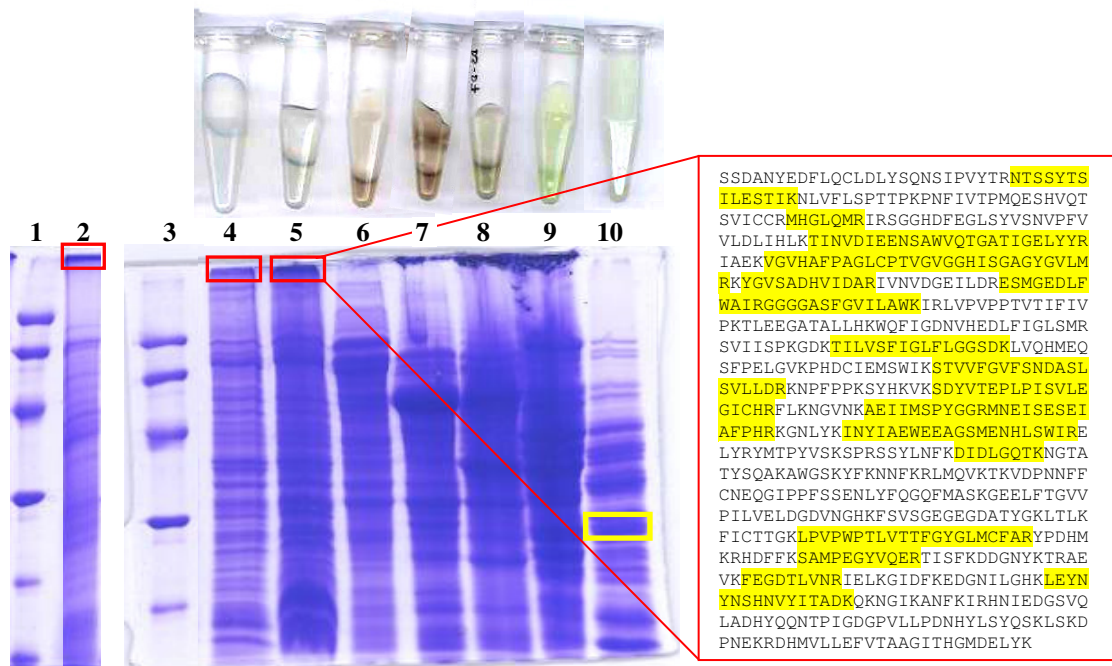


Figure 27: Identification of the STOX-fusion after a two-step purification procedure

SDS-gels from different fractions of the purification of *Bw* STOX-citrine from *P. pastoris* KM71H pPICZalpha-*Bw* STOX-linker-citrine colony 60. Lanes 1 and 3: LMW standard with bands of 97, 66, 45, 30, 20 and 14 kDa; lane 2: pellet with insoluble proteins after glass bead lysis; lane 4 to lane 10: fractions collected from gel filtration. Lane 4 contains proteins bigger than 120 kDa, lane 5 proteins with a size between 90 and 120 kDa, lane 6 proteins with 70 - 90 kDa, lane 7 proteins with 60 - 70 kDa, lane 8 proteins with 50 - 60 kDa, lane 9 proteins with 40 - 50 kDa, and lane 10 proteins with a size up to 30 kDa.

Red and yellow boxes on the SDS-gels display protein bands which were identified as STOX-fusion and citrine by MALDI-MS analysis, respectively. The protein sequence of *Bw* STOX-citrine is shown on the right side and peptide fragments from a tryptic digest, which were identified by MALDI-MS, are highlighted in yellow.

Fractions collected from gel filtration showed different colours after concentrating as evident from the samples depicted above the SDS-gel. The samples correspond to the subjacent protein fractions. Especially protein fractions from lane 9 and 10 showed a yellow fluorescence, which is characteristic for citrine.

4.3.4.1 Native PAGE analysis

Native PAGE experiments were performed with the best fluorescing transformant of the first screening (*P. pastoris* KM71H pPICZalpha-*Bw* STOX-linker-citrine colony 60) and with different reference strains as wild type *P. pastoris* KM71H, a strain expressing BBE and a strain expressing the citrine marker. Cells were disrupted using a Merckenschlager device and supernatants containing soluble proteins were

applied to the gels. Using a fluorescence scanner, the fluorescence signal of citrine was recorded from native gels after electrophoresis. It is noteworthy that the strain expressing the STOX fusion protein and the reference strain expressing the citrine marker showed different fluorescence patterns. The control strain showed one fluorescent band, whereas colony 60 of *P. pastoris* KM71H pPICZalpha-Bw *STOX-linker-citrine* exhibited two fluorescent bands with different mobility. As expected wild type *Pichia pastoris* KM71H and the BBE expression strain did not show any fluorescence.

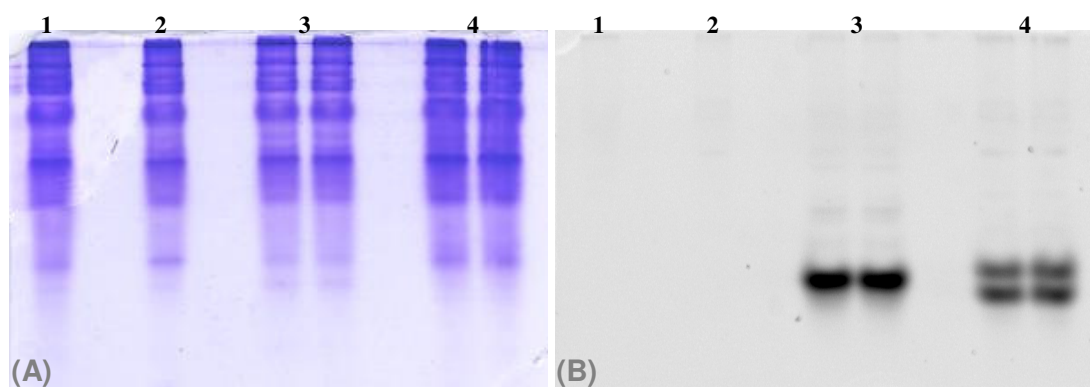


Figure 28: Native PAGE analysis of strains expressing the fluorescent fusion

Native PAGE analysis of *P. pastoris* KM71H pPICZalpha-Bw *STOX-linker-citrine*

(A) shows the Coomassie stain of the gel after native PAGE analysis of supernatants after cell disruption. (B) shows fluorescence signals when scanning for citrine fluorescence. Lane 1: *Pichia pastoris* wild type strain; lane 2: BBE expressing strain without a citrine tag; lane 3: reference strain expressing citrine; lane 4: best clone from screening (colony 60), which expresses the citrine-tagged STOX protein.

4.3.4.2 Fluorescence microscopy

Since pPICZalpha was used for assembling the first expression cassettes of the fluorescent labelled fusion constructs, the resulting fusion protein was supposed to be under the control of the alpha-factor for secretion. Hence it was assumed that the STOX-citrine fusion would pass through the secretory machinery and would be released into the medium. However, all fluorescent measurements resulted in the finding that the citrine marker is retained in the cells and no fluorescence was observed in the medium.

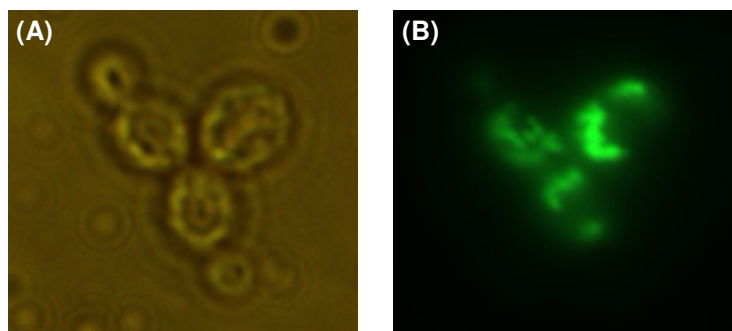


Figure 29: Fluorescence microscopy of *Pichia* cells expressing the STOX fusion

Fluorescence microscopy was performed with the strain showing the best fluorescence after 72 hours of induction with methanol. (A) shows a microscopy image of the cells and (B) represents the corresponding image from fluorescence microscopy.

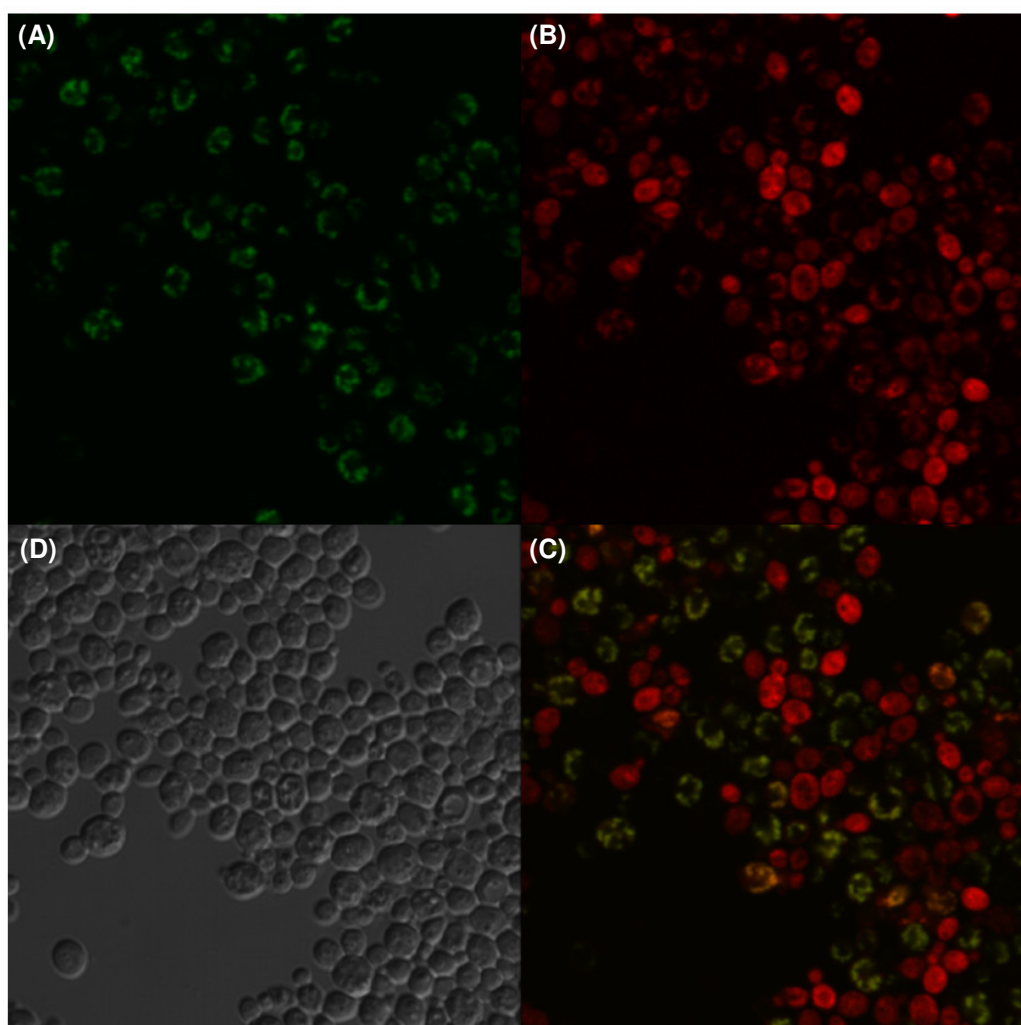


Figure 30: Confocal fluorescence microscopy for determining protein localization

(A) shows a fluorescence microscopy image of *P. pastoris* KM71H pPICZalpha-Bw STOX-linker-citrine colony 60 with 500 nm excitation and 550 nm emission wavelength for the citrine marker. (B) shows a mitochondrial stain. (C) represents an overlay of citrine-signal and stained mitochondria. Colocalization is represented in orange. (D) shows a microscopy image of the fixed cells.

Figure 29 confirms the intracellular localization of the fluorescent marker since citrine fluorescence is exclusively found inside the cells.

In-depth analyses were performed with confocal fluorescence microscopy in order to determine the localization of the fluorescent marker. Here, the fluorescence pattern of newly formed daughter cells suggested a special heredity of the examined compartment, which is characteristic for mitochondria (see Figure 30). Staining of the mitochondrial compartment using the MitoTracker® Mitochondrion Selective Probes (Invitrogen, Carlsbad, CA, USA) partially corroborated this suggestion. However, these results have to be considered with caution since citrine fluorescence of the cells was very strong and hence led to fluorescence channel crosstalk.

4.3.4.3 The use of affinity tags for facilitated purification

To optimize protein purification, new expression cassettes with STOX-fusion proteins comprising a C-terminal His₈- or StrepII-tag were assembled for both *Am* and *Bw* STOX. Expression cassettes were assembled using OE-PCR as described in 4.3.4 and colonies with strong citrine fluorescence were identified in three consecutive screening experiments.

After fermentation in shake flasks, cells were disrupted with glass bead lysis and the resulting supernatants containing the soluble protein fractions were loaded onto the respective affinity columns.

Interestingly, purification with His₈- and StrepII-tag did not lead to comparable results. Fusion proteins equipped with a C-terminal His₈-tag were purified with Ni-NTA columns. Here only the citrine marker without fusion to the protein of interest was eluted from the column. Marginal amounts of fusion protein were detected in the pellet after cell disruption. However, when StrepTactin columns and the constructs with the C-terminal StrepII-tag were used, no 30 kDa band was monitored in any elution fraction and hence citrine was apparently not cleaved off. Instead, marginal amounts of a 100 kDa protein were eluted from the column and were identified as *Am* or *Bw* STOX-fusion, respectively.

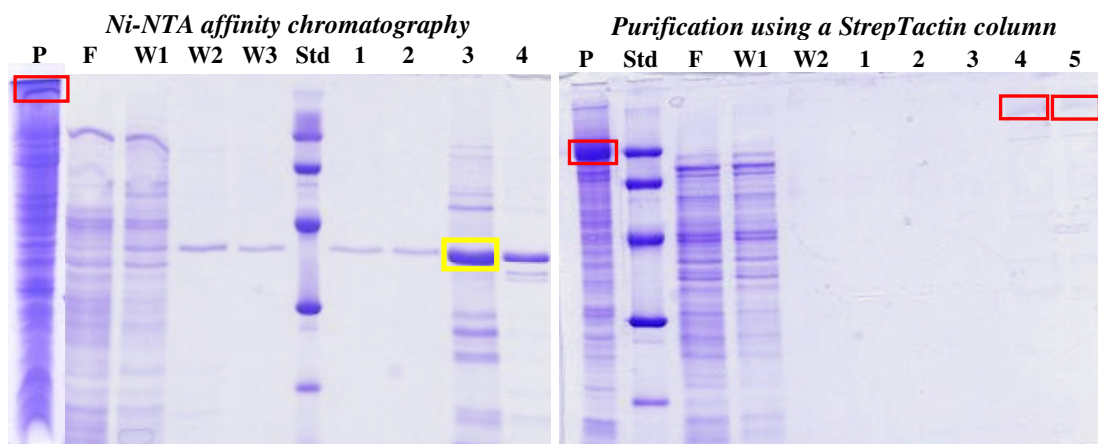


Figure 31: Affinity purification of tagged STOX-citrine fusion proteins

The SDS-gels show affinity purifications of *Bw* STOX-linker-citrine-His₆/StrepII using Ni-NTA or StrepTactin columns, respectively. Abbreviations denote: Std, LMW-standard (97, 66, 45, 30, 20 kDa); P, pellet after cell disruption; F, flow through; W1, W2, W3, wash fractions 1, 2, and 3; 1, 2, 3, 4, 5: elution fractions 1, 2, 3, 4, and 5. Identified proteins are marked with red and yellow boxes for the STOX-citrine fusion protein and the unfused citrine marker, respectively.

The purification of unfused citrine using Ni-NTA chromatography indicated that the fusion protein is cleaved under certain circumstances. The linker region, which connects STOX and citrine moieties, comprises a TEV-protease cleavage site that could be recognized by intracellular proteases of *P. pastoris*. Therefore, the linking TEV-polymerase recognition site Glu-X-X-Tyr-X-Gln was mutated to Ala-X-X-Gly-X-Gln, which should prevent unfavourable proteolytic cleavage. Identification of potential expression strains was performed as described above and the best transformants were applied for expression in shake flasks and for affinity purification. To our surprise the new constructs without a cleavable linking region led to the same results as the respective constructs with the intact TEV-protease recognition site. Citrine without fusion to STOX was purified using Ni-NTA affinity chromatography, and purification with StrepTactin columns resulted in the identification of marginal amounts of soluble STOX-fusion protein. Hence it was concluded that the linker region did not play a decisive role for proteolytic cleavage and that removal of the TEV-protease recognition site did not positively effect protein purification.

4.3.4.4 Targeted protein expression

Deliberate subcellular targeting of heterologously expressed proteins has repeatedly been shown to be a crucial factor for protein expression [88-91]. Under methanol induction peroxisomes account for a large percentage of total cell volume of *P. pastoris* and hence are ideal for protein storage. Various investigations demonstrated that certain heterologously expressed proteins show increased stability when transported to peroxisomes [88, 90]. Peroxisomes shield proteins against proteolytic degradation and prevent undesired modifications, which could be introduced by the secretory machinery [88]. However, other proteins were shown to depend on posttranslational modifications, which are introduced in the ER or when passing the secretory route [91]. Generally, there is no unique solution for optimal subcellular targeting of heterologously expressed proteins and sorting has to be addressed individually for every protein.

For *Am* and *Bw* STOX new expression cassettes comprising the respective fusion constructs with C-terminal ER- and peroxisomal- targeting sequences were generated. Identification of promising expression strains was performed using citrine fluorescence. Unfortunately, ER-targeting did not improve heterologous expression of *Am* or *Bw* STOX and did not result in *P. pastoris* expression strains capable of producing sufficient amounts of STOX. Hence, this method of subcellular targeting was ruled out as possible expression strategy.

Peroxisome targeting, however, is described in literature as an applicable method for increased protein expression since it offers an ideal environment for oxidases and can contribute to reduce toxic effects of heterologous protein expression [90, 92]. Hence it would be possible that peroxisome targeting leads to increased accumulation of heterologously expressed *Am* and *Bw* STOX. In the course of this thesis initial experiments were performed with *Am* and *Bw* STOX fusion proteins comprising a C-terminal peroxisome sorting sequence. In these experiments no increased heterologous protein expression was observable; however, further in-depth analyses would be necessary to confirm these results.

4.4 Discussion

4.4.1 General aspects

(*S*)-Tetrahydroprotoberberine oxidase is a remarkable enzyme, which is of special interest for many biochemists and pharmacologists. It is suggested to be involved in benzyloquinoline alkaloid biosynthesis [21, 22], a biosynthetic route leading to the formation of many pharmacological active compounds [9, 10, 27]. Moreover, STOX is exceptional in a biochemical and structural aspect since it shows high sequence similarity to BBE from *E. californica*. Sequence alignments revealed that STOX from *A. mexicana* and from *B. wilsoniae* share 38.3 and 38.2% sequence identity with the latter mentioned BBE. It is noteworthy that these similarities are found over the entire protein length and that special regions, as the cofactor binding sites in BBE, are completely conserved in both *Am* and *Bw* STOX (see Figure 33). For BBE, bicovalent cofactor tethering to the imidazole ring of His104 and to the thiolate moiety of Cys166 has been experimentally proven [93-95]. These residues are also strictly conserved in *Am* and *Bw* STOX and hence both proteins are expected to possess a bicovalently attached flavin as shown in Figure 32.

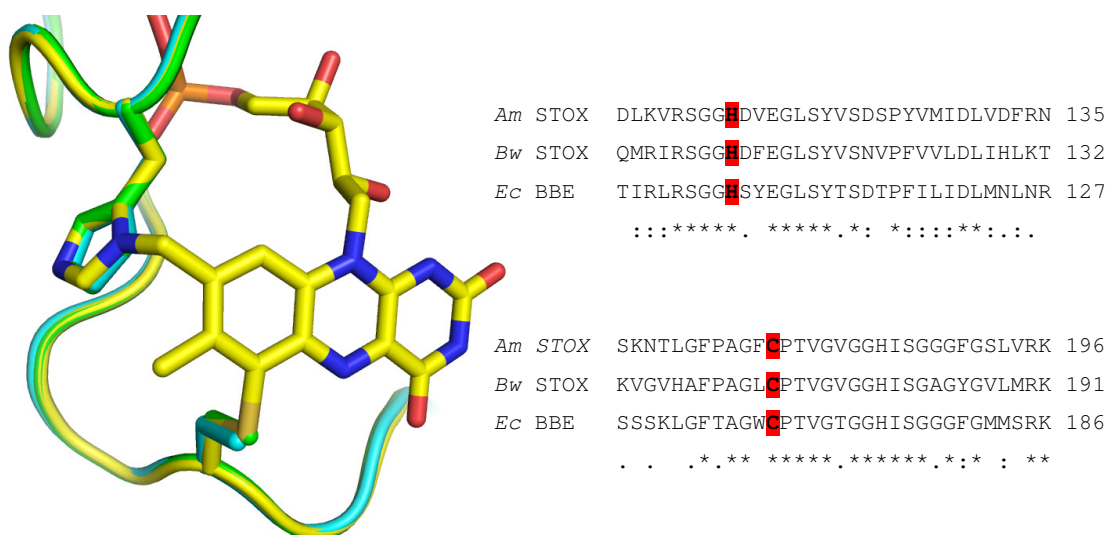


Figure 32: Bicovalent flavinylation of BBE and STOX

The graphical representation shows an alignment of the flavin binding site of BBE with comparative models of *Am* and *Bw* STOX generated with the SWISS-MODEL server [79-81]. BBE is coloured yellow, whereas *Am* and *Bw* STOX are shown in cyan and green, respectively. The FAD-cofactor and linking amino acid residues are shown in stick representation. The sequence alignment on the right shows the sites of covalent flavin attachment as highlighted with red boxes.

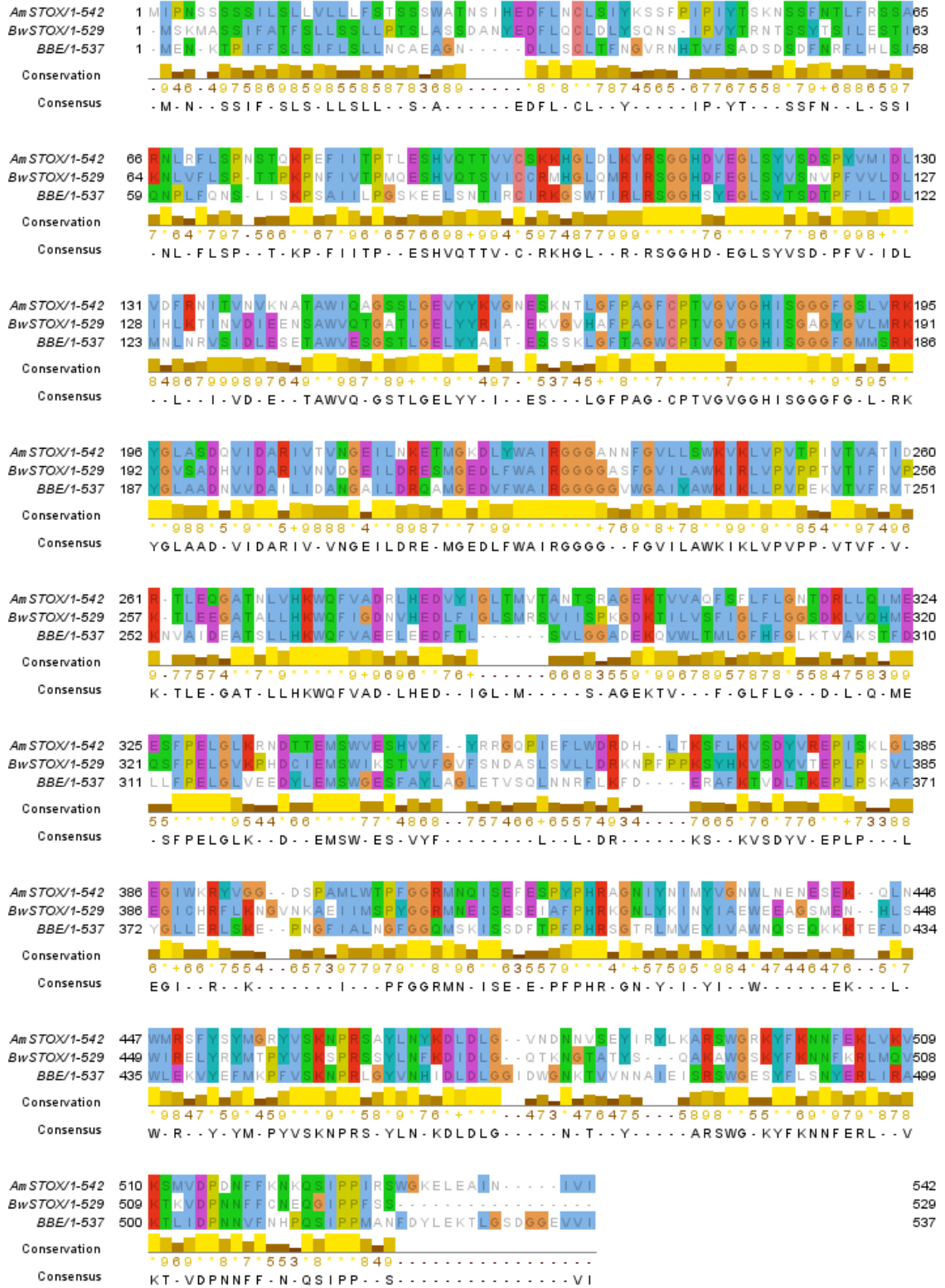


Figure 33: Sequence alignment of BBE from *E. californica* with *Am* and *Bw* STOX

The alignment was performed using ClustalW at EBI [96, 97] and Jalview 2.7 [98] for visualization of the results. The default ClustalX colour scheme was applied to colour different amino acids.

Unfortunately, covalent linkage of *Am* and *Bw* STOX could not be verified in the course of this thesis since the amounts of heterologously expressed protein were not sufficient for in-depth characterization. However, since all sequence analyses suggested a bicovalent flavin tethering to a histidine and a cysteine residue, both STOX enzymes were treated as bicovalently flavinylated oxidases.

4.4.2 Substrate specificity of *Am* and *Bw* STOX

Enzymes with bicovalent cofactor linkage are capable of catalyzing challenging enzymatic reactions as the berberine bridge formation of BBE [48], the cyclization of cannabigerolic acid yielding THCA catalyzed by THCA synthase [99, 100], or various other C-C bond formation and oxidation reactions [101-104].

Since both *Am* and *Bw* STOX were predicted to belong to the class of bicovalently flavinylated oxidoreductases, these proteins are presumably involved in catalyzing challenging oxidation reactions. A comparison of the active site of BBE with homology models of *Am* and *Bw* STOX indicated different amino acid compositions of the catalytic region as shown in Figure 34.

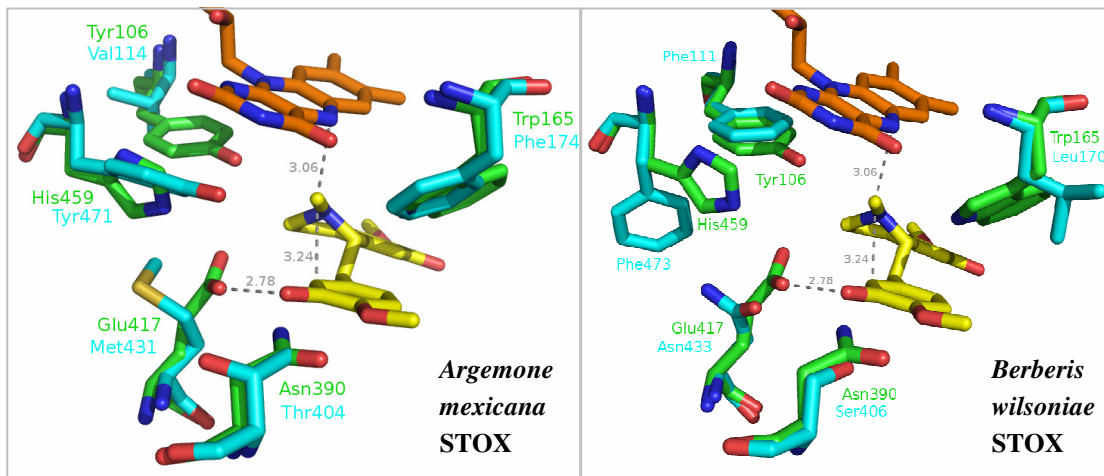


Figure 34: Active site comparison of BBE with *Am* and *Bw* STOX, respectively

The illustration on the left shows the comparison of BBE with *Am* STOX; on the right the BBE active site is compared to *Bw* STOX. In both representations the substrate (*S*)-reticuline is shown in yellow and the flavin cofactor is coloured orange. Active site residues of BBE are shown in green, whereas respective residues of the homology models of *Am* and *Bw* STOX are shown in cyan.

In the models of *Am* and *Bw* STOX a methionine or an asparagine residue is present on the position corresponding to Glu417 of BBE (cf. also Table 8). These amino acid

residues can not act as catalytic base for deprotonating the substrate and hence BBE, *Am* and *Bw* STOX seem to have different functions *in planta*.

Table 8: Active site comparison of BBE with *Am* and *Bw* STOX

BBE	<i>Bw</i> STOX	<i>Am</i> STOX
Glu417	Asn	Met
Trp165	Leu	Phe
His459	Phe	Tyr
Tyr106	Val	Phe

Previous studies resulted in the suggestion of many potential substrates for STOX of *B. wilsoniae* [21-23]. AMANN and coworkers suggested that STOX catalyzes the stereospecific oxidation of many tetrahydroprotoberberines and 1-benzyl isoquinoline alkaloids [22] as shown in Figure 35.

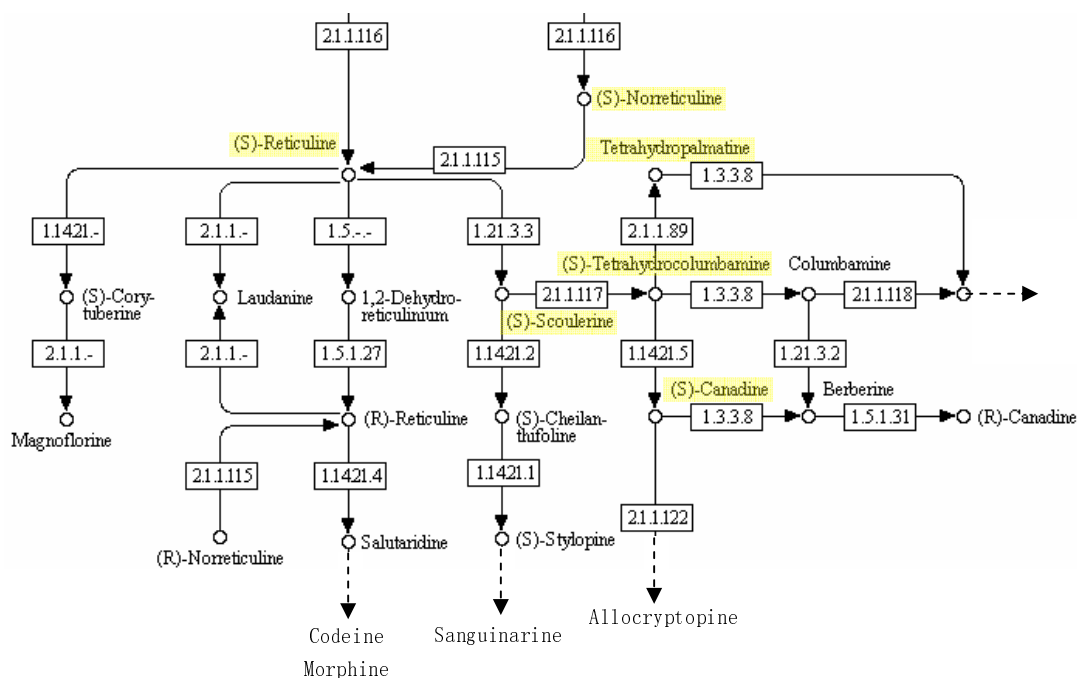


Figure 35: Partial scheme of benzyloquinoline alkaloid biosynthesis

Substances, which were suggested as potential substrates of STOX by Amann *et al.* [22], are highlighted in yellow boxes. The detailed scheme of relevant parts of the benzyloquinoline alkaloid pathway was taken from the KEGG database [105, 106].

However, it is questionable whether STOX can actually catalyze the oxidation of this multitude of different substrates with reasonable efficiency. Recently, substrate specificity of *Am* and *Bw* STOX was reinvestigated by KUTCHAN and coworkers. Here *Am* STOX was proposed to accept (*S*)-tetrahydropalmatine and (*S*)-coreximine,

whereas *Bw* STOX showed activity with (*S*)-tetrahydropalmatine, (*S*)-scoulerine, and (*S*)-canadine [28].

Activity assays performed in our lab with STOX from *A. mexicana* clearly confirmed its oxidase activity on (*S*)-tetrahydropalmatine as evident from Figure 25. Since purification of the oxidase was not feasible due to marginal protein production, fermentation supernatants containing the secreted protein fractions were investigated using activity assays. Interestingly, in contrast to previous suggestions of KUTCHAN and coworkers (*S*)-coreximine could not be confirmed as substrate for *Am* STOX. However, (*S*)-canadine could be a possible substrate for enzymatic oxidation. In this case results from our experiments were contradictory, which can possibly be attributed to poor protein expression and impurities of the used substrate. Hence activity assays have to be repeated with purified (*S*)-canadine, however, the available amount of substrate did not suffice for this purification.

In case of *Bw* STOX, activity assays performed in our lab did not result in any conversion of potential substrates. This is contrary to the findings of KUTCHAN and coworkers [28], who proposed the conversion of (*S*)-tetrahydropalmatine, (*S*)-scoulerine, and (*S*)-canadine. Hence, the availability of purified *Bw* STOX would be required to accurately assess substrate specificity of this oxidase.

4.4.3 Heterologous expression of STOX - a mystery

In-depth studies on low abundance proteins are often confounded by the lack of an applicable heterologous expression system for generating sufficient amounts of soluble protein. The necessity for posttranslational modifications, transport to certain cellular compartments, the processing of prepeptides, or the requirement for catalytically essential cofactors impede heterologous protein expression in many cases [48].

In case of STOX from *B. wilsoniae*, expression of marginal amounts of the enzyme in plant or insect cell culture enabled initial experiments on substrate specificity [26, 28]. However, mechanistic and structural studies were not feasible due to insufficient protein amounts. Thus, we attempted to heterologously express *Am* and *Bw* STOX in new host organisms in order to obtain high protein yields.

Initially, *E. coli* was chosen as host for the heterologous expression of *Am* STOX. Today it is generally accepted that differences in codon bias of native source and host organism can negatively effect heterologous protein expression [107-109]. Hence, a synthetic gene in *E. coli* codon usage was ordered for heterologous expression of *Am* STOX to prevent a high number of rare codons during translation. However, heterologous expression attempts performed with various *E. coli* strains solely resulted in the formation of insoluble inclusion bodies, which could not be refolded into active protein. Upon refolding, the supplied FAD cofactor was not incorporated into the protein, which implied that the resulting *Am* STOX did not show any catalytic activity. Hence, the generation of a protein fusion with the maltose binding domain was a new approach for heterologous expression of *Am* STOX. The maltose binding protein is known to increase the stability and solubility of its fusion partners [87]; however, fusion to the MBP did not improve the expression behaviour of *Am* STOX and insoluble inclusion bodies were formed. Additionally, the use of chaperones and the variation of conditions for heterologous expression did not result in the formation of soluble and active protein.

Hence, it was concluded that *E. coli* seems to be unsuitable as host organism for the heterologous expression of *Am* or *Bw* STOX. As plant proteins, *Am* and *Bw* STOX require posttranslational modifications, protein translocation after heterologous expression, covalent attachment of the flavin cofactor, and possibly an applicable environment for disulfide bond formation.

Disulfide connectivity predictions performed with DiANNA 1.0 web server [110-112] suggested the formation of disulfide bridges in both *Am* and *Bw* STOX, whereas the probability is higher for *Bw* STOX with 7 cysteines in the protein sequence. Moreover, both proteins were predicted to be secretory proteins as shown in 4.3.1.1. Particularly proteins which pass through the secretory machinery in eukaryotes, in many cases can not efficiently be expressed in *E. coli* [113]. Possible reasons are the necessity of signal peptide cleavage or posttranslational modifications, such as glycosylation, which can affect function, structure, and stability of glycoproteins [113-116].

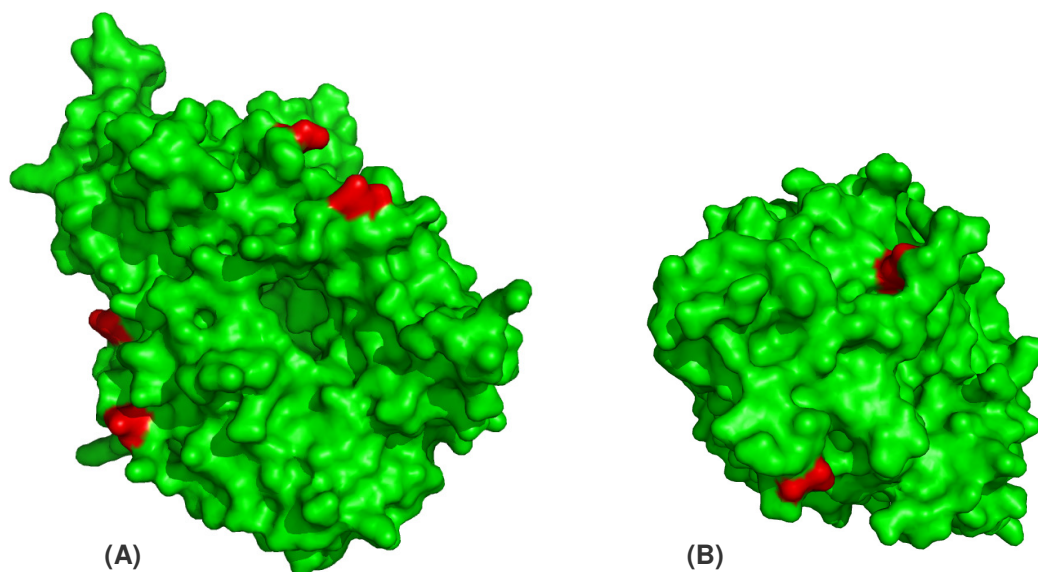


Figure 36: Localization of potentially glycosylated asparagines in *Am* and *Bw* STOX

(A) shows a surface representation of the model of *Am* STOX whereas (B) shows a model of *Bw* STOX. In both representations the protein is coloured green and potentially glycosylated asparagines are highlighted in red.

Analysis of *Am* and *Bw* STOX revealed that both proteins seem to be glycosylated. For *Am* STOX and *Bw* STOX four and two potential asparagines were identified, respectively, which are part of an Asn-Xaa-Ser/Thr sequon and which are located on the protein surface (see Figure 36).

For both *Am* and *Bw* STOX, *P. pastoris* was expected to be an applicable host for heterologous protein expression. This organism possesses many eukaryotic features including a secretory pathway and the ability to introduce many posttranslational modifications to proteins [45, 46, 82, 113]. Although *N*-glycosylation differs between *Pichia* and higher eukaryotes [42, 43, 117, 118], the methylotrophic yeast seemed to be an ideal organism for heterologous expression of secretory plant enzymes as was previously shown for BBE [48]. Solely large scale fermentation performed with *Pichia* resulted in sufficient protein yields for in-depth mechanistic and structural characterization [48, 94, 95]

Heterologous expression of *Am* and *Bw* STOX was initially performed according to the protocols optimized for BBE expression using the pPICZalpha vector with the tightly controlled and strong AOX promoter and the *S. cerevisiae* alpha-factor prepropeptide for secretion into the fermentation medium. Unfortunately, no transformants with high yield of heterologously expressed proteins were detected and modified

protocols with various pH-values, temperature, and expression vectors with different promoters and signal peptides did not lead to improved protein expression. Additionally, the use of a synthetic gene which was manually optimized to circumvent transcriptional and translational bottlenecks in the expression of *Bw* STOX did not result in higher protein yields.

One major problem was the lack of an applicable screening system to identify transformants which produce sufficient amounts of heterologously expressed protein. It is noteworthy that for most proteins, which were successfully expressed in *Pichia*, activity based screening or immunoblotting with specific antibodies were available for identifying applicable expression strains. E.g. BBE from *Eschscholzia californica* was detected using activity assays with (*S*)-reticuline or by immunoblotting [48], an antflavin antibody was used to detect human, rat and zebrafish monoamine oxidases [119-122], and presence of hydroxy nitril lyase HNL from *Hevea brasiliensis* or of alternative pig liver esterase APLE was determined using specific activity assays [63, 123]. For both *Am* and *Bw* STOX no such methods existed, which complicated the initial selection of *Pichia* transformants for further expression experiments, thus reducing the probability of identifying a good expressing colony.

Since heterologous expression of *Am* and *Bw* STOX was not successful, possible reasons for the marginal protein yield had to be identified. Transcriptional or translational barriers, as mRNA instability and stagnant translation due to excessive use of rare codons, protein instability in the given environment, or failed secretion leading to protein accumulation and protein degradation instead of release to the medium, could be the reasons for unsuccessful expression experiments. However, none of the latter could be ruled out as possible reason for insufficient protein production.

Thus, a new screening system using a C-terminal citrine marker for fluorescence analysis of protein expression was applied. For both *Am* and *Bw* STOX various fusion constructs with the fluorescent citrine tag were cloned as listed in Table 6. Generally, citrine is a variant of the yellow fluorescing protein YFP, which is described as a highly sensitive fluorescence marker and which was already successfully used for visualizing proteins inside cells [124].

Using the fluorescent marker, transcriptional and translational barriers could be ruled out as cause of insufficient protein expression. Screening experiments performed with different fusion constructs led to the identification of strains with strong expression of the fluorescent citrine marker and hence also the respective STOX protein was formed in the *Pichia* cells. However, a thorough analysis of cultures after protein expression revealed that the heterologously expressed STOX-citrine fusion was retained inside the cells and was not released into the medium even when a signal peptide for targeting to the secretory machinery was used. All citrine fluorescence was monitored inside the host organism, which was in contrast to initial expectations. Possible explanations for this observation would be erroneous targeting of the fusion to certain intracellular compartments or protein accumulation in the secretory route, e.g. in the plasma membrane. Both *Am* and *Bw* STOX-citrine fusion proteins should possess a high molecular weight of at least 90 kDa, depending on the extent of glycosylation, and due to this size the fusion proteins might get stuck in the secretion apparatus.

Fluorescence microscopy was used to determine the intracellular localization of the *Bw* STOX fusion protein. However, even with vital staining methods protein localization could not be assigned accurately. Microscopy images did not show the citrine marker stuck in the inner or outer plasma membrane or inside the periplasm. Moreover, the nucleus was excluded as potential site of citrine localization. Thus, cytoplasm, vacuoles, peroxisomes, ER or mitochondria remained possible localization sites for the fluorescent citrine marker. For peroxisomes it was reported that the green fluorescent protein GFP, which is highly homologous to the YFP variant citrine, is able to spontaneously enter into peroxisomes and hence can cause unexpected results [125]. Peroxisomal targeting of the citrine marker could not completely be excluded; however, it was assessed as unlikely. Heritage of fluorescent compartments to daughter cells was rather indicative for a mitochondrial localization of the fusion protein, which was not expected. Predictions done with MitoProt II v1.101 resulted in the suggestion that *Bw* STOX could probably be targeted to mitochondria, for *Am* STOX mitochondrial localization was not predicted. It remains unclear if both *Am* and *Bw* STOX-fusion proteins are transported to and stored inside mitochondria of the host cells. Further in-depth analyses with confocal fluorescent microscopy and comparison of different fusion

proteins with targeting sequences for ER or peroxisomes, respectively, could help in elucidating this mystery.

A further unexpected observation was made, when affinity chromatography was performed to purify expressed fusion proteins. Experiments carried out with fusion constructs that were provided with a C-terminal His₈-tag yielded in the purification of citrine that lost its fusion partner *Am* or *Bw* STOX. The same applied for a two-step purification of the untagged *Bw* STOX-fusion protein. In both cases, marginal amounts of the fusion protein were detected in the insoluble protein fraction after cell disruption using MALDI-MS. For fusion constructs equipped with a C-terminal StrepII-tag, results from affinity purification were different compared to the latter experiments. Here only marginal amounts of intact *Am* or *Bw* STOX-citrine-StrepII fusion protein were obtained and no cleaved citrine was detected. An explanation for these different results from purification of His₈- and StrepII-tagged fusion proteins was not found up to now.

Initially, it was assumed that proteolytic cleavage of the TEV-protease recognition site in the linking region between *Am* or *Bw* STOX and citrine could be the cause for obtaining the unfused fluorescent tag. Thus, new constructs were generated with a mutated linker region which does not comprise a protease recognition site any more and hence should not undergo proteolytic cleavage. Interestingly, attempts to purify the new fusion proteins resulted in the same findings as before. Fusion constructs equipped with a C-terminal His₈-tag seemed to be cleaved resulting in the purification of a 30 kDa citrine fragment. When a StrepII-tag was used marginal amounts of STOX-citrine fusion protein were purified, which were not sufficient for further experiments.

Generally, heterologous expression attempts of *Am* and *Bw* STOX remained unsuccessful albeit different expression systems and strategies were tested. Since both *Am* and *Bw* STOX were originally cloned from poppy plants, host organisms for heterologous expression need to possess an eukaryotic machinery for posttranslational protein modification and protein secretion. Thus, *P. pastoris* seemed to be an ideal candidate for establishing a new system for high yield expression of the two STOX proteins. Many strategies, which were supposed to be well suited for heterologous protein expression, were tested and did only result in marginal protein amounts. Unfortunately, these yields were not sufficient for any

structural or mechanistic study. Although *P. pastoris* today is a well investigated model organism for heterologous protein expression, a lot of questions concerning protein expression, folding, translocation and degradation remain unsolved and have to be addressed in further studies. *Am* and *Bw* STOX could be such candidates for developing new expression strategies; however, it is not possible to predict whether heterologous expression of the two proteins in *P. pastoris* can be successful at all. Apart from method development with *P. pastoris*, other host organisms could be used for heterologous protein expression, such as *Schizosaccharomyces pombe* or *Yarrowia lipoytica* [126-128].

4.4.4 Fluorescence-based screening system

An applicable screening system for identifying transformants with high expression levels of the desired protein is a prerequisite for heterologous protein expression in *Pichia pastoris*. Due to the lack of such a screening possibility for the heterologous expression of *Am* and *Bw* STOX, a fluorescence-based screening protocol was established using a C-terminal citrine tag as fluorescent marker.

OE-PCR was applied to assemble all expression cassettes for the new fusion constructs and this method proved to be very time-saving, cost-effective and well applicable for simultaneous assembly of many different expression cassettes.

The expression cassettes were transformed into *P. pastoris* expression strains and screening for citrine-fluorescence enabled a high-throughput selection of good candidates for heterologous protein expression. It is noteworthy that this fluorescence-based screening system allowed the identification of transformants which showed strong citrine fluorescence in relatively short time periods. Thus for all new constructs promising colonies could be selected. Albeit purification of the fusion proteins was not successful in the end, new findings were made in these experiments. Hence, the use of fluorescent labelling of proteins, which are difficult to express and to detect, can be regarded as a promising way of establishing a system for heterologous expression of these enzymes.

4.5 References

- [1] Bhakuni, D.S., Jain, S., and Gupta, S. *Tetrahedron* **1980**, *36*, 2491-2495.
- [2] Robinson, R. *The Structural Relation of Natural Products*. **1955**, Clarendon Press, Oxford.
- [3] Kirby, G.W. *Science* **1967**, *155*, 170-173.
- [4] Barton, D.H., Hesse, R.H., and Kirby, G.W. *J Chem Soc Perkin 1*. **1965**, 6379-6389.
- [5] Gear, J.R., and Spenser, I.D. *Nature* **1961**, *191*, 1393-1395.
- [6] Money, T., Wright, I.G., McCapra, F., and Scott, A.I. *Proc Natl Acad Sci USA* **1965**, *53*, 901-903.
- [7] Battersby, A.R. *Biochem Soc Symp* **1970**, *29*, 157-168.
- [8] Bhakuni, D.S., and Jain, S. In: Brossi, A., ed. *The Alkaloids Vol. 28*, **1986**, Academic Press, New York, 95-181.
- [9] Facchini, P.J., and St-Pierre, B. *Curr Opin Plant Biol* **2005**, *8*, 657-666.
- [10] Liscombe, D.K., and Facchini, P.J. *Curr Opin Biotechnol* **2008**, *19*, 173-180.
- [11] Martin, M.L., Diaz, M.T., Montero, M. J., Prieto, P., San Roman, L., and Cortes, D. *Planta Med* **1993**, *59*, 63-67.
- [12] Morais, L.C., Barbosa-Filho, J.M., and Almeida, R.N. *J Ethnopharmacol* **1998**, *62*, 57-61.
- [13] Jow, G.M., Wu, Y.C., Guh, J.H., and Teng, C.M. *Life Sci* **2004**, *75*, 549-557.
- [14] Yamahara, J., Konoshima, T., Sakakibara, Y., Ishiguro, M., and Sawada, T. *Chem Pharm Bull* **1976**, *24*, 1909-1912.
- [15] Jang, S.I., Kim, B.H., Lee, W.Y., An, S.J., Choi, H.G., Jeon, B.H., Chung, H.T., Rho, J.R., Kim, Y.J., and Chai, K.Y. *Arch Pharm Res* **2004**, *27*, 923-929.
- [16] Mo, J., Guo, Y., Yang, Y.S., Shen, J.S., Jin, G.Z., and Zhen, X. *Curr Med Chem* **2007**, *14*, 2996-3002.
- [17] Chou, W.M., and Kutchan, T.M. *Plant J* **1998**, *15*, 289-300.
- [18] Zenk, M.H. *Phytochemistry* **1991**, *30*, 3861-3863.
- [19] Eilert, U., and Constabel, F. *Protoplasma* **1985**, *128*, 38-42.
- [20] Gundlach, H., Muller, M.J., Kutchan, T.M., and Zenk, M.H. *Proc Natl Acad Sci USA* **1992**, *89*, 2389-2393.
- [21] Amann, M., Nagakura, N., and Zenk, M.H. *Tetrahedron Lett* **1984**, *25*, 953-954.
- [22] Amann, M., Nagakura, N., and Zenk, M.H. *Eur J Biochem* **1988**, *175*, 17-25.
- [23] Beecher, C.W.W., and Kelleher, W.J. *Tetrahedron Lett* **1984**, *25*, 4595-4598.
- [24] Bjorklund, J.A., Frenzel, T., Rueffer, M., Kobayashi, M., Mocek, U., Fox, C., Beale, J.M., Groeger, S., Zenk, M.H., and Floss, H.G. *J Am Chem Soc* **1995**, *117*, 1533-1545.

- [25] Bock, A., Wanner, G., and Zenk, M.H. *Planta* **2002**, *216*, 57-63.
- [26] Amann, M., and Zenk, M.H. *Phytochemistry* **1987**, *26*, 3235-3240.
- [27] Zenk, M.H., Rueffer, M., Amann, M., Deus-Neumann, B., and Nagakura, N. *J Nat Prod* **1985**, *48*, 725-738.
- [28] Gesell, A., Chávez, M.L.D., Kramell, R., Piotrowski, M., Macheroux, P., and Kutchan, T.M. *Planta* **2011**, *233*, 1185-1197.
- [29] Ausubel, F.M., Brent, R., Kingston, R.E., Moore, D.D., Seidmann, J.G., Smith, J.A., and Struhl, K. *Curr Prot Mol Biol* **2003**, Wiley, New York.
- [30] Villalobos, A., Ness, J.E., Gustafsson, C., Minshull, J., and Govindarajan, S. *BMC Bioinformatics* **2006**, *7*, 285.
- [31] Welch, M., Govindarajan, S., Ness, J.E., Villalobos, A., Gurney, A., Minshull, J., and Gustafsson, C. *PLoS One* **2009**, *4*, e7002.
- [32] Heuts, D.P.H.M., Janssen, D.B., and Fraaije, M.W. *FEBS Lett* **2007**, *581*, 4905-4909.
- [33] Nishihara, K., Kanemori, M., Yanagi, H., and Yura, T. *Appl Environ Microbiol* **2000**, *66*, 884-889.
- [34] Nishihara, K., Kanemori, M., Kitagawa, M., Yanagi, H., and Yura, T. *Appl Environ Microbiol* **1998**, *64*, 1694-1699.
- [35] Thomas, J.G., Ayling, A., and Baneyx, F. *Appl Biochem Biotechnol* **1997**, *66*, 197-238.
- [36] Guzman, L.M., Belin, D., Carson, M.J., and Beckwith, J. *J Bacteriol* **1995**, *177*, 4121-4130.
- [37] Miyada, C.G., Stoltzfus, L., and Wilcox, G. *Proc Natl Acad Sci USA* **1984**, *81*, 4120-4124.
- [38] Basu, A., Li, X., and Leong, S.S. *Appl Microbiol Biotechnol* **2011**, *92*, 241-251.
- [39] Su, Z., Lu, D., and Liu, Z. *Methods Biochem Anal* **2011**, *54*, 319-338.
- [40] Mayer, M., and Buchner, J. *Methods Mol Med* **2004**, *94*, 239-254.
- [41] Singh, S.M., and Panda, A.K. *J Biosci Bioeng* **2005**, *99*, 303-310.
- [42] Cregg, J.M., Cereghino, J.L., Shi, J., and Higgins, D.R. *Mol Biotechnol* **2000**, *16*, 23-52.
- [43] Cereghino, J.L., and Cregg, J.M. *FEMS Microbiol Rev* **2000**, *24*, 45-66.
- [44] Fath, S., Bauer, A.P., Liss, M., Spriestersbach, A., Maertens, B., Hahn, P., Ludwig, C., Schafer, F., Graf, M., and Wagner, R. *PLoS One* **2011**, *6*, e17596.
- [45] Weidner, M., Taupp, M., and Hallam, S.J. *J Vis Exp* **2010**, *36*. pii: 1862. doi, 10.3791/1862.
- [46] Mattanovich, D., Branduardi, P., Dato, L., Gasser, B., Sauer, M., and Porro, D. *Methods Mol Biol* **2012**, *824*, 329-358.
- [47] Lin-Cereghino, J., Wong, W. ., Xiong, S., Giang, W., Luong, L. ., Vu, J., Johnson, S.D., and Lin-Cereghino, G. . *BioTechniques* **2005**, *38*, 44, 46, 48.

- [48] Winkler, A., Hartner, F., Kutchan, T.M., Glieder, A., and Macheroux, P. *J Biol Chem* **2006**, *281*, 21276-21285.
- [49] Weis, R., Luiten, R., Skranc, W., Schwab, H., Wubbolts, M., and Glieder, A. *FEMS Yeast Res* **2004**, *5*, 179-189.
- [50] Cino, J. High Yield Protein Production from *Pichia Pastoris* yeast: A Protocol for Benchtop Fermentation. In: Edison, N.J., ed. *New Brunswick Scientific*.
- [51] Schrittwieser, J.H., Resch, V., Wallner, S., Lienhart, W.D., Sattler, J.H., Resch, J., Macheroux, P., and Kroutil, W. *J Org Chem* **2011**, *76*, 6703-6714.
- [52] Tözsér, J., Tropea, J.E., Cherry, S., Bagossi, P., Copeland, T.D., Wlodawer, A., and Waugh, D.S. *FEBS J* **2005**, *272*, 514-523.
- [53] Vitale, A., and Denecke, J. *Plant Cell* **1999**, *11*, 615-628.
- [54] Lee, H.I., Gal, S., Newman, T.C., and Raikhel, N.V. *Proc Natl Acad Sci USA* **1993**, *90*, 11433-11437.
- [55] Denecke, J., De Rycke, R., and Botterman, J. *EMBO J* **1992**, *11*, 2345-2355.
- [56] Napier, R.M., Fowke, L.C., Hawes, C., Lewis, M., and Pelham, H.R.B. *J Cell Sci* **1992**, *102*, 261-271.
- [57] Gould, S.J., Keller, G.A., Hosken, N., Wilkinson, J., and Subramani, S. *J Cell Biol* **1989**, *108*, 1657-1664.
- [58] Keller, G.A., Krisans, S., Gould, S.J., Sommer, J.M., Wang, C.C., Schliebs, W., Kunau, W., Brody, S., and Subramani, S. *J Cell Biol* **1991**, *114*, 893-904.
- [59] Wolins, N.E., and Donaldson, R.P. *J Biol Chem* **1994**, *269*, 1149-1153.
- [60] Kohlwein, S.D. *Microsc Res Tech* **2000**, *51*, 511-529.
- [61] Da Cunha, E.S., Domingues, C.C., and De Paula, E. *Anal Biochem* **2011**, *418*, 158-160.
- [62] Wittig, I., and Schagger, H. *Proteomics* **2005**, *5*, 4338-4346.
- [63] Hermann, M., Kietzmann, M.U., Ivancic, M., Zenzmaier, C., Luiten, R.G., Skranc, W., et al. *J Biotechnol* **2008**, *133*, 301-310.
- [64] Petersen, T.N., Brunak, S., Von Heijne, G., and Nielsen, H. *Nat Methods* **2011**, *8*, 785-786.
- [65] Nielsen, H., Engelbrecht, J., Brunak, S., and Von Heijne, G. *Protein Eng* **1997**, *10*, 1-6.
- [66] Nielsen, H., and Krogh, A. *Proceedings - International Conference on Intelligent Systems for Molecular Biology* **1998**, *6*, 122-130.
- [67] Bendtsen, J.D., Nielsen, H., Von Heijne, G., and Brunak, S. *J Mol Biol* **2004**, *340*, 783-795.
- [68] Emanuelsson, O., Brunak, S., von Heijne, G., and Nielsen, H. *Nat Protoc* **2007**, *2*, 953-971.
- [69] Nakai, K., and Kanehisa, M. *Proteins Struct Funct Genet* **1991**, *11*, 95-110.
- [70] von Heijne, G. *Nucleic Acids Res* **1986**, *14*, 4683-4690.

- [71] Klein, P., Kanehisa, M., and DeLisi, C. *Biochim Biophys Acta Biomembr* **1985**, *815*, 468-476.
- [72] Hartmann, E., Rapoport, T.A., and Lodish, H.F. *Proc Natl Acad Sci USA* **1989**, *86*, 5786-5790.
- [73] Nakai, K., and Kanehisa, M. *Genomics* **1992**, *14*, 897-911.
- [74] Howe, C.J., and Wallace, T.P. *Nucleic Acids Res* **1990**, *18*, 3417.
- [75] Bendiak, B. *Biochem Biophys Res Commun* **1990**, *170*, 879-882.
- [76] Emanuelsson, O., Nielsen, H., Brunak, S., and Von Heijne, G. *J Mol Biol* **2000**, *300*, 1005-1016.
- [77] Gupta, R., Jung, E., and Brunak, S. *in preparation* **2004**.
- [78] Claros, M. G., and Vincens, P. *Eur J Biochem* **1996**, *241*, 779-786.
- [79] Arnold, K., Bordoli, L., Kopp, J., and Schwede, T. *Bioinformatics* **2006**, *22*, 195-201.
- [80] Kiefer, F., Arnold, K., Künzli, M., Bordoli, L., and Schwede, T. *Nucleic Acids Res* **2009**, *37*, D387-D392.
- [81] Peitsch, M.C. *Bio/Technology* **1995**, *13*, 658-660.
- [82] Mokdad-Gargouri, R., Abdelmoula-Soussi, S., Hadiji-Abbes, N., Amor, I.Y., Borchani-Chabchoub, I., and Gargouri, A. *Methods Mol Biol* **2012**, *824*, 359-370.
- [83] Byrne, L.J., O'Callaghan, K.J., and Tuite, M.F. *Methods Mol Biol* **2005**, *308*, 51-64.
- [84] Freigassner, M., Pichler, H., and Glieder, A. *Microb Cell Fact* **2009**, *8*.
- [85] Shental-Bechor, D., and Levy, Y. *Proc Natl Acad Sci USA* **2008**, *105*, 8256-8261.
- [86] Wormald, M.R., and Dwek, R.A. *Structure* **1999**, *7*, R155-60.
- [87] Fox, J.D., and Waugh, D.S. *Methods Mol Biol* **2003**, *205*, 99-117.
- [88] van Dijk, R., Faber, K.N., Kiel, J.A., Veenhuis, M., and van der Klei, I. *Enzyme Microb Technol* **2000**, *26*, 793-800.
- [89] Schnell, J.A., Han, S., Miki, B.L., and Johnson, D.A. *Plant Cell Rep* **2010**, *29*, 987-996.
- [90] Abad, S., Nahalka, J., Bergler, G., Arnold, S.A., Speight, R., Fotheringham, I., Nidetzky, B., and Glieder, A. *Microb Cell Fact* **2010**, *9*, 24.
- [91] Medina-Godoy, S., Valdez-Ortiz, A., Valverde, M.E., and Paredes-Lopez, O. *Biotechnol J* **2006**, *1*, 1085-1092.
- [92] Wang, Y., Xuan, Y., Zhang, P., Jiang, X., Ni, Z., Tong, L., Zhou, X., Lin, L., Ding, J., and Zhang, Y. *FEMS Yeast Res* **2009**, *9*, 732-741.
- [93] Winkler, A., Kutchan, T.M., and Macheroux, P. *J Biol Chem* **2007**, *282*, 24437-24443.
- [94] Winkler, A., Łyskowski, A., Riedl, S., Puhl, M., Kutchan, T.M., Macheroux, P., and Gruber, K. *Nat Chem Biol* **2008**, *4*, 739-741.

- [95] Winkler, A., Motz, K., Riedl, S., Puhl, M., Macheroux, P., and Gruber, K. *J Biol Chem* **2009**, *284*, 19993-20001.
- [96] Larkin, M.A., Blackshields, G., Brown, N.P., Chenna, R., McGettigan, P.A., McWilliam, H., *et al.* *Bioinformatics* **2007**, *23*, 2947-2948.
- [97] Goujon, M., McWilliam, H., Li, W., Valentin, F., Squizzato, S., Paern, J., and Lopez, R. *Nucleic Acids Res* **2010**, *38*, 695-699.
- [98] Waterhouse, A.M., Procter, J.B., Martin, D.M., Clamp, M., and Barton, G.J. *Bioinformatics* **2009**, *25*, 1189-1191.
- [99] Taura, F., Morimoto, S., Shoyama, Y., and Mechoulam, R. *J Am Chem Soc* **1995**, *117*, 9766-9767.
- [100] Sirikantaramas, S., Morimoto, S., Shoyama, Y., Ishikawa, Y., Wada, Y., Shoyama, Y., and Taura, F. *J Biol Chem* **2004**, *279*, 39767-39774.
- [101] Huang, C.H., Lai, W.L., Lee, M.H., Chen, C.J., Vasella, A., Tsai, Y.C., and Liaw, S.H. *J Biol Chem* **2005**, *280*, 38831-38838.
- [102] Li, Y.S., Ho, J.Y., Huang, C.C., Lyu, S.Y., Lee, C.Y., Huang, Y.T., *et al.* *J Am Chem Soc* **2007**, *129*, 13384-13385.
- [103] Noinaj, N., Bosserman, M.A., Schickli, M.A., Piszczek, G., Kharel, M.K., Pahari, P., Buchanan, S.K., and Rohr, J. *J Biol Chem* **2011**, *286*, 23533-23543.
- [104] Alexeev, I., Sultana, A., Mäntsälä, P., Niemi, J., and Schneider, G. *Proc Natl Acad Sci U. S. A.* **2007**, *104*, 6170-6175.
- [105] Kanehisa, M., Goto, S., Sato, Y., Furumichi, M., and Tanabe, M. *Nucleic Acids Res* **2012**, *40*, D109-D114.
- [106] Kanehisa, M., and Goto, S. *Nucleic Acids Res* **2000**, *28*, 27-30.
- [107] Gustafsson, C., Govindarajan, S., and Minshull, J. *Trends Biotechnol* **2004**, *22*, 346-353.
- [108] Gouy, M., and Gautier, C. *Nucleic Acids Res* **1982**, *10*, 7055-7074.
- [109] Kane, J. F. *Curr Opin Biotechnol* **1995**, *6*, 494-500.
- [110] Ferrè, F., and Clote, P. *Nucleic Acids Res* **2006**, *34*, 182-185.
- [111] Ferrè, F., and Clote, P. *Nucleic Acids Res* **2005**, *33*, 230-232.
- [112] Ferrè, F., and Clote, P. *Bioinformatics* **2005**, *21*, 2336-2346.
- [113] Yin, J., Li, G., Ren, X., and Herrler, G. *J Biotechnol* **2007**, *127*, 335-347.
- [114] Jung, E., and Williams, K.L. *Biotechnol Appl Biochem* **1997**, *25*, 3-8.
- [115] Linskens, M.H.K., Grootenhuis, P.D.J., Blaauw, M., Winkel, B.H.D., Van Ravestein, A., Van Haastert, P.J.M., and Heikoop, J.C. *FASEB J* **1999**, *13*, 639-645.
- [116] Weis, R., Gaisberger, R., Gruber, K., and Glieder, A. *J Biotechnol* **2007**, *129*, 50-61.
- [117] Cregg, J.M., Expression in the Methylotrophic Yeast *Pichia Pastoris*. In: Fernandez, J.M. and Hoeffler, J.P., eds. *Gene Expression Systems: Using Nature for the Art of Expression* **1999**, Academic Press, San Diego, CA, 157-191.

- [118] Higgins, D.R., and Cregg, J.M. *Pichia* protocols, *Methods in Molecular Biology* vol. 103, **1998**, Humana Press, Totowa, NJ.
- [119] Wang, J., and Edmondson, D.E. *Protein Expr Purif* **2010**, *70*, 211-217.
- [120] Upadhyay, A.K., and Edmondson, D.E. *Protein Expr Purif* **2008**, *59*, 349-356.
- [121] Li, M., Hubalek, F., Newton-Vinson, P., and Edmondson, D.E. *Protein Expr Purif* **2002**, *24*, 152-162.
- [122] Newton-Vinson, P., Hubalek, F., and Edmondson, D.E. *Protein Expr Purif* **2000**, *20*, 334-345.
- [123] Hasslacher, M., Schall, M., Hayn, M., Bona, R., Rumbold, K., Luckl, J., Griengl, H., Kohlwein, S.D., and Schwab, H. *Protein Expr Purif* **1997**, *11*, 61-71.
- [124] Nyfeler, B., and Hauri, H.P. *Biochem Soc Trans* **2007**, *35*, 970-973.
- [125] Lenassi Zupan, A., Trobec, S., Gaberc-Porekar, V., and Menart, V. *J Biotechnol* **2004**, *109*, 115-122.
- [126] Giga-Hama, Y., and Kumagai, H. *Biotechnol Appl Biochem* **1999**, *30*, 235-244.
- [127] Madzak, C., Gaillardin, C., and Beckerich, J.M. *J Biotechnol* **2004**, *109*, 63-81.
- [128] Dominguez, A., Ferminan, E., Sanchez, M., Gonzalez, F.J., Perez-Campo, F.M., Garcia, S., *et al.* *Int Microbiol* **1998**, *1*, 131-142.

CHAPTER 5

- 5 Catalytic and structural role of a conserved active site histidine in berberine bridge enzyme

Author contributions

Information and results regarding the BBE H174A variant protein are summarized in the following manuscript, which was prepared for submission to *Biochemistry*. The project was started by ANDREAS WINKLER in the course of his Phd thesis when he designed and expressed the BBE H174A variant protein. ANDREAS WINKLER determined the crystal structure of the variant protein and did most of the biochemical characterization. Later I continued the studies on the H174A variant protein and I contributed to this work by repeating stopped flow measurements and by performing experiments for trapping the “overreduced” state of this variant protein. Moreover, I wrote parts of the manuscript including the introduction and all biochemical parts. The crystal structure of BBE H174A was described by ANDREAS WINKLER. In the course of this project STEFANIE HORVATH assisted me as project student by doing parts of the kinetic experiments.

Catalytic and structural role of a conserved active site histidine in berberine bridge enzyme

Silvia Wallner^{1‡}, Andreas Winkler^{2‡}, Sabrina Riedl^{1†}, Corinna Dully¹, Stefanie Horvath¹, Karl Gruber^{4*}, and Peter Macheroux^{1*}

¹ Institute of Biochemistry, Graz University of Technology, Petersgasse 12/2, A-8010 Graz, Austria

² Department for Biomolecular Mechanisms, Max Planck Institute for Medical Research, Jahnstraße 29, D-69120 Heidelberg, Germany

⁴ Institute of Molecular Biosciences, University of Graz, Humboldtstraße 50/3, A-8010 Graz, Austria

ABSTRACT: Berberine bridge enzyme (BBE) is a paradigm for the class of bicovalently flavinylated oxidases, which catalyzes the oxidative cyclization of (*S*)-reticuline to (*S*)-scoulerine. His174 was identified as a potentially important active site residue because its putative role for the stabilization of the reduced state of the flavin cofactor. It is also strictly conserved in the family of BBE-like oxidases. Here, we present a detailed biochemical and structural characterization of the BBE His174Ala variant supporting its role for catalysis as well as structural organization of the active site. Substantial changes in all kinetic parameters and a decrease in midpoint potential were observed for the BBE His174Ala variant protein. Moreover, the crystal structure of the BBE His174Ala showed significant structural rearrangements compared to wild type enzyme. Based on our findings, we propose that His174 is part of a hydrogen bonding network that stabilizes the negative charge at the N(1)-C(2)=O locus via interaction with the hydroxyl group at the C2' of the ribityl side chain. Hence replacement of this residue with alanine abolishes the stabilizing effect and results in drastically decreased kinetic parameters as well as a lower midpoint redox potential.

Enzymes with bicovalently linked flavin cofactors have repeatedly been demonstrated to catalyze challenging chemical reactions in both eukaryotic and prokaryotic systems (1, 2, 3, 4, 5, 6, 7, 8, 9, 10). Today, the number of enzymes known to possess both covalent cysteinyl and histidinyl groups on the flavin is increasing and extensive research is performed to identify new members of this class of flavoproteins. However, despite these ongoing studies the mode of bicovalent tethering of the flavin cofactor and the influence of certain amino acid residues on flavin reactivity are not fully understood and require further investigation. Here we present a new mutagenic analysis of berberine bridge enzyme (BBE, (*S*)-reticuline oxidase, EC 1.2.1.3.3), which addresses the role of His174

for flavin reactivity and bicovalent cofactor linkage.

BBE is a well characterized flavin-dependent oxidase, which catalyzes the unique oxidative cyclization of the *N*-methyl moiety of (*S*)-reticuline into the berberine bridge atom of (*S*)-scoulerine (1, 11). It was shown before that BBE belongs to a recently discovered protein family with bicovalent cofactor binding (1). A structure based mutagenic analysis led to a deeper understanding of the role of bicovalent flavinylation for catalysis and to the proposal of a concerted mechanism for BBE (12). It was demonstrated that bicovalent flavinylation shifts the redox potential of the cofactor to a remarkably high value of + 132 mV and hence facilitates the oxidative ring closure in (*S*)-reticuline yielding (*S*)-scoulerine as product (13). Replacement of either Cys166 or His104 with Ala resulted in a decrease in midpoint potential of the flavin and in lower rates of substrate turnover (2, 13).

Recent studies on various oxidases revealed that catalysis requires stabilization of the transiently formed negative charge at the N(1)-C(2)=O locus of the flavin cofactor (14, 15). Thus, positively charged amino acids such as lysine (16, 17, 18, 19, 20) or arginine (21) are frequently positioned in close vicinity to the N1 position of the isoalloxazine ring to stabilize the uptake of the negative charge in the flavin ring system. Moreover, a histidine residue (22, 23, 24) or a helix dipole (14, 25, 26, 27) can supply the positive charge for stabilization. In BBE no such functionality can be found near the N(1)-C(2)=O locus indicating that stabilization of the negative charge is achieved by a different mechanism. Although this positive charge is missing in BBE, a tyrosine and a histidine residue are positioned near the N(1)-C(2)=O locus and can interact directly or via a C2' hydroxyl group of the ribityl side chain of the flavin. Interestingly, the respective histidine residue (His174) is conserved among related bicovalently flavinylated proteins with oxidase activity, whereas no strict conservation is found for the corresponding

tyrosine residue. Hence, here we addressed the potential role of His174 for stabilizing the negative charge in the course of catalysis.

The mechanism of covalent flavinylation has been studied for representative proteins with monocovalently tethered flavins (28, 29, 30, 31). In all cases flavinylation was reported to occur autocatalytically and for most investigated proteins similar mechanisms for covalent flavin coupling at the C8 α were suggested (14). The proposed mechanism starts with proton abstraction from the C8 methyl group of the flavin with subsequent stabilization of the negative charge at the N(1)-C(2)=O locus of the isoalloxazine ring (14). Again some examples have shown that this stabilization can be attributed to a positive amino acid residue such as a lysine in monomeric sarcosine oxidase (18) or an arginine in *p*-cresol methylhydroxylase (21) and vanillyl-alcohol oxidase (14). Up to now no bicovalently flavinylated protein has been investigated with regard to mechanistic aspects of bicovalent flavin attachment. Former mutagenesis studies showed that both covalent linkages seem to form independent of each other, because both histidinylated and cysteinylated single variant proteins could be expressed and isolated (2, 3, 13, 14, 32). However, amino acid residues involved in the process of covalent flavin attachment were not addressed yet. Again, the earlier identified amino acid residue His174 could also be relevant for covalent flavinylation.

Thus, in this study a BBE variant was created, where the conserved histidine residue His174 was replaced with alanine and the influence of this amino acid residue on spectral and kinetic parameters as well as on the midpoint potential of the flavin cofactor was determined. Moreover, the crystal structure of the His174Ala variant protein was solved to a resolution of 2.65 Å. Here we demonstrate that His174 plays a role for stabilizing the negative charge in the isoalloxazine ring system during catalysis, since the respective variant protein features a reduced midpoint potential of the cofactor and significantly decreased overall enzyme efficiency. Also covalent flavinylation seems to be affected by the removal of His174 since artificially reduced protein reversibly breaks and reforms 6-*S*-cysteinylated in an oxygen dependent manner.

Experimental Procedures

Reagents. All chemicals were purchased from Sigma-Aldrich and were of the highest quality available. QuikChange® XL kit for site-directed mutagenesis was from Stratagene and oligonucleotide primers were ordered from VBC-Biotech. (*S*)-reticuline was

obtained from the natural product collection at the Donald Danforth Plant Science Center (St. Louis, US).

Site-directed Mutagenesis. Mutagenesis was performed following the instructions of the QuikChange® XL Site-directed Mutagenesis kit (Stratagene) using the expression vector pPICZ α BBE-ER as described in (1) as template for the polymerase chain reaction. Replacement of His174 with Ala was accomplished by using 5'-CGTTGGTACTGGGGGTGCTATTAGTGGT-3' as sense and the complementary antisense primer. The underlined nucleotides represent the mutated codon. Introduction of the desired mutation was verified by plasmid sequencing.

Transformation, Expression and Protein Purification. The newly generated expression plasmid pPICZ α BBE H174A was transformed into *Pichia pastoris* KM71H using electroporation. Integration of the expression cassettes into the *Pichia* genome was verified using colony polymerase chain reaction. Applicable expression strains were identified in small scale in 300mL shake flasks with 50 mL buffered minimal dextrose medium. Induction was started with 0.1 % methanol with consecutive methanol addition as described in (33). Large scale expression of the BBE variant protein was carried out in a BBI CT5-2 fermenter (Sartorius). Fermentation was performed following the *Pichia* Fermentation Process Guidelines from Invitrogen with a modified basal salt medium. After 96 h methanol induction the fermentation was stopped and purification was performed as described in (1, 34). Expression of the correct variant protein was verified by MALDI time-of-flight mass spectrometry as described previously (1).

Steady-state Kinetic Analysis. Steady-state turnover rates were determined by following the conversion of (*S*)-reticuline to (*S*)-scoulerine by HPLC analysis of the reaction mixture as described previously (1).

Transient Kinetics. Reductive half-reactions were analyzed with a stopped-flow device (SF-61DX2, Hi-Tech) in an anaerobic atmosphere of approx. 0.8 ppm oxygen in a glove box from Belle technology. All samples were rendered oxygen-free by flushing with nitrogen and subsequent incubation in the glove box. Changes in flavin absorbance were followed using a PM-61s photomultiplier or a KinetaScanT diode array detector (MG-6560). Apparent rate constants for the reductive half reaction were determined at six different substrate concentrations from 30 to 300 μ M (*S*)-reticuline with a protein concentration of 15 μ M in 150 mM NaCl, 50 mM Tris-HCl, pH 9.0 and 37 °C. Fitting of the obtained transients at 446 nm was performed with

SpecFit 32 (Spectrum Software Associates) using a function of two exponentials. Rates for the oxidative half-reaction were determined by mixing air-saturated buffer (21% oxygen) with a substrate-reduced enzyme solution. Reduction of the flavin-cofactor was performed with substoichiometric amounts of (*S*)-reticuline in order to prevent lag-phases in the reoxidation process.

Anaerobic Photoreduction. Anaerobic photoreduction was carried out as described in (35). The reaction mixture consisted of 1 mM EDTA, 1 μ M 5-deazariboflavin, and 15 μ M enzyme solution in 150 mM NaCl, 50 mM Tris-HCl at different pH-values (pH 5.0 - 9.0). Prior to photoreduction the reaction mixtures were rendered anaerobic by repeated cycles of evacuation and flushing with nitrogen in a special glass cuvette. Photoillumination was carried out with a conventional slide projector. All spectra were recorded with a Specord205 spectrophotometer (Analytic Jena) at 25 °C. 7.5 M urea in 50 mM Tris/HCl, pH 8.0 or acetonitrile were used for the denaturation of completely reduced protein samples. For denaturation the anaerobic samples were mixed in equal amounts with denaturation reagent (urea or acetonitrile) and were kept at 60 °C for 45 min. Afterwards spectra of the denatured protein samples were recorded.

Redox Potential Determination. Redox potentials were determined using the dye-equilibration method with the xanthine/xanthine oxidase electron delivering system as described by Massey (36). All experiments were performed in 50 mM potassium phosphate buffer, pH 7.0, at 25 °C containing benzyl viologen (5 μ M) as mediator, 250 μ M xanthine, and xanthine oxidase in catalytic amounts (approximately 1 nM). For maintaining anaerobic conditions, all experiments were carried out with a stopped flow device (SF-61DX2, Hi-Tech) positioned in a glove box from Belle Technology. Spectra were recorded with a KinetaScanT diode array detector (MG-6560). Toluylene blue ($E_M = + 115$ mV), thionine acetate ($E_M = + 64$ mV), toluidine blue ($E_M = + 34$ mV) and indigotrisulfonic acid potassium salt ($E_M = - 81$ mV) were used as dyes for redox potential determination. The potentials were calculated from plots of $\log([\text{ox}]/[\text{red}])$ of the respective BBE variant protein versus $\log([\text{ox}]/[\text{red}])$ of the dye according to Minnaert (37).

Crystallization and Data Collection. Crystallization of the BBE His174Ala variant was essentially performed as described previously for the BBE variants His104Ala and Cys166Ala (12). Briefly, crushed crystals of wild type BBE grown using the sitting drop vapor diffusion method (12) were used for

micro seeding crystallization setups of the BBE His174Ala variant. These were prepared by mixing 0.8 μ L of protein at 120 mg/mL with 1.2 μ L reservoir solution (0.2 M MgCl_2 and 30% (w/v) polyethylene glycol 4,000 in 0.1 M Tris/HCl, pH 8.5) and equilibrated for 16 hours prior to seeding. Monoclinic crystals appeared after 1 week and continued to grow for 3 weeks prior to reaching final dimensions. Substrate soaked crystals were then obtained by 5 min incubation in the presence of 20 mM (*S*)-reticuline in the reservoir solution prior to flash freezing upon plunging into liquid nitrogen.

A dataset for a substrate soaked His174Ala crystal was collected at beamline X11, DESY (Hamburg, Germany). Processing of the data was performed using XDS (38) and due to isomorphism with monoclinic wild type BBE crystals (PDB code 3D2H) the structure could be solved by rigid body fitting using the program package PHENIX (39). The obtained model was further refined using the same software starting with simulated annealing followed by several rounds of maximum likelihood least squares refinement of models modified using the graphics program Coot (40) employing σ_A -weighted $2F_o - F_c$ and $F_o - F_c$ electron density maps. A summary of data collection, processing and refinement statistics is presented in Supplementary Table S1. R_{free} values (41) were computed from 5% randomly chosen reflections not used throughout the refinement. (*S*)-reticuline was excluded from the initial refinement process and inserted only in later rounds when clear electron density was visible.

Results

General Properties. BBE His174Ala was expressed in *P. pastoris* KM71H cells using the fermentation protocol established for wild type BBE (1). The protein could be detected in the fermentation supernatant in similar amounts as wild type BBE and purification was performed using a two-step purification protocol with consecutive hydrophobic interaction and gel filtration chromatography. To test for covalent attachment of the FAD cofactor, protein samples were precipitated with 13% (w/v) trichloroacetic acid and no free flavin could be detected in the supernatant after centrifugation. Thus it was assumed that in BBE His174Ala the flavin cofactor is bound in a covalent manner. This finding was later confirmed by elucidation of the three-dimensional X-ray structure of the variant protein. The observed electron density demonstrates a clear bicovalent linkage of the

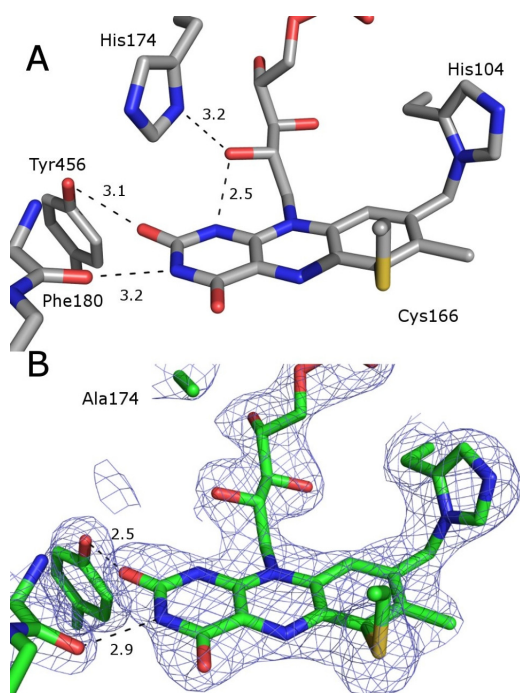


Figure 1. Amino acids in close proximity to the N(1)-C(2)=O region of the isoalloxazine ring system of wild type BBE (A). For comparison the same region is shown for the His174Ala variant protein structure (B) showing the sideways movement of the flavin ring as indicated by the strengthened hydrogen bond to Tyr456 and the Phe180 main chain carbonyl. The electron density shown in panel B represents the $2F_o - F_c$ map contoured at 1.5σ . Distances for hydrogen bonds are given in Å.

FAD to His104 and Cys166 in position 8a and 6, respectively (Figure 1).

Spectral Properties. UV-visible absorbance spectra were recorded for native and denatured variant protein, respectively, and are shown in Figure 2. The spectral characteristics of His174Ala reflect the covalent flavinylation as observed for wild type BBE (1). The spectrum after denaturation shows only one absorption maximum at ~ 440 nm and thus indicates a modification of the flavin in its C6 position (13, 42).

Photoreduction. Photoreduction was performed in the presence of EDTA and 5-deazariboflavin by exposing the anaerobic sample to light. His174Ala showed a different reduction pattern compared to wild type BBE and spectra recorded during the reduction of this variant are shown in Figure 3.

Light illumination of the His174Ala variant leads to a marginal formation of a red anionic semiquinone, which was already shown for both wild type BBE and the Cys166Ala variant (13). After apparent complete reduction of the His174Ala variant a non-isosbestic hypsochromic shift of the absorption maximum to ~ 357 nm was observed, which was not detected in wild type BBE

(Supplementary Figure S1). However, more significant differences between wild type BBE and the His174Ala variant were observed upon reoxidation of the flavin cofactor after complete photoreduction. Reoxidation of wild type BBE resulted in an absorption spectrum with a long wavelength absorbance between 550 and 900 nm, which is indicative for the generation of 6-thio FAD (1). However, reoxidation of the His174Ala variant protein resulted in an absorption spectrum with characteristics of the Cys166Ala variant and no 6-thio FAD was observed (13). In case of the His174Ala variant the resulting spectrum of the reoxidized FAD cofactor showed a broad maximum ranging from 350–370 nm, which suggests a cleavage of the 6-S-cysteinyl bond. Interestingly, when exposed to oxygen this spectrum slowly loses its broad maximum and after some hours virtually the same spectrum as at the beginning of the experiment was obtained. Thus, it is suggested that the covalent cysteinyl bond is reversibly cleaved upon complete photoreduction and that reoxidation of the cofactor induces an autocatalytic process for reforming the covalent linkage.

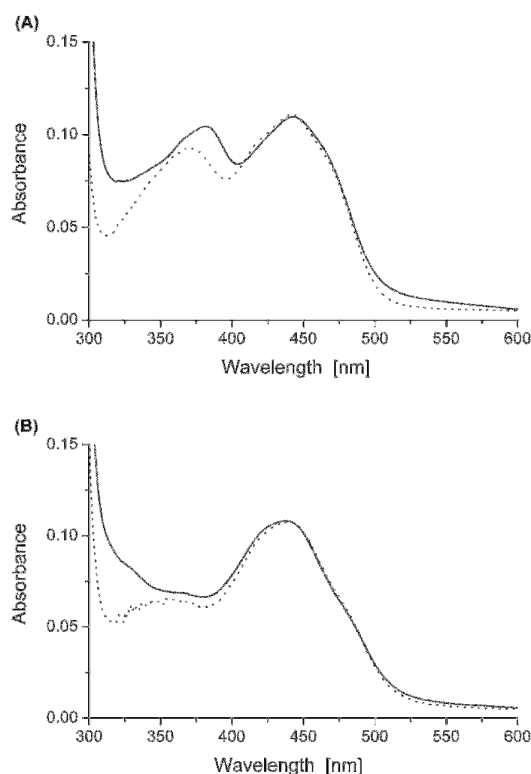


Figure 2. Absorption spectra of the His174Ala variant in comparison to the wild type enzyme. (A) Absorption spectra of the native enzymes and (B) after heat denaturation. *Solid lines* represent the wild type enzyme in its native and denatured form, respectively. *Dashed lines* represent the His174Ala variant. All spectra are normalized to a protein concentration of ~ 10 μ M.

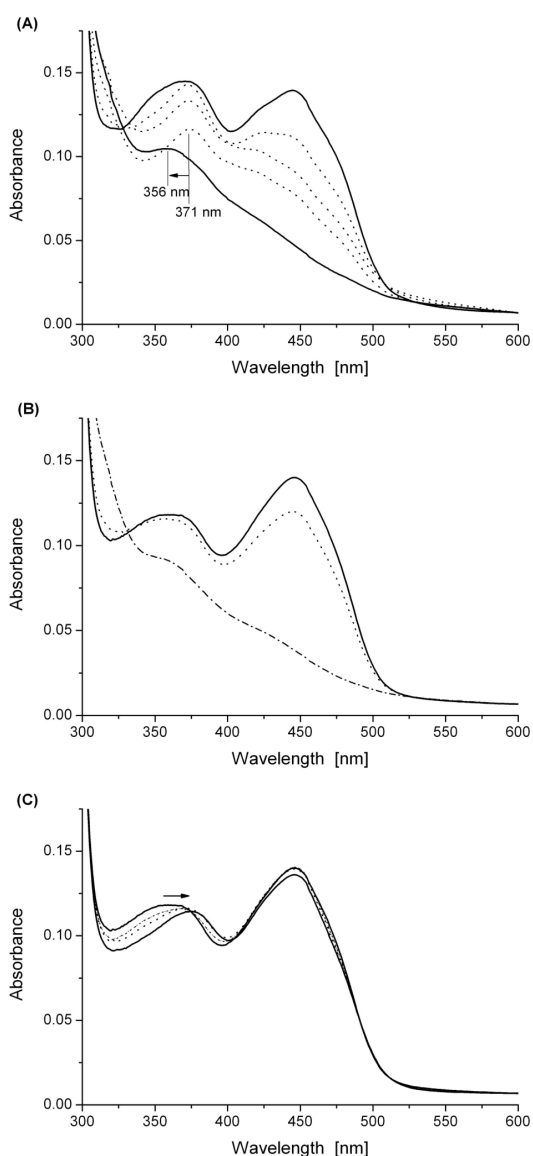


Figure 3. Anaerobic photoreduction and reoxidation of BBE His174Ala. (A) Selected spectra of the complete photoreduction. *Solid lines*, spectrum prior to illumination and spectrum of the fully reduced flavin cofactor. *Dotted lines*, selected spectra recorded during the course of photoreduction. The hypsochromic shift in the maximum of the fully reduced species to 350 nm is indicated by a black arrow. (B) Selected spectra recorded upon admission of oxygen. *Dash-dotted line*, fully reduced flavin cofactor after photoillumination. *Dotted line*, spectrum after 5 seconds of exposure to oxygen. *Solid line*, characteristic spectrum of BBE His174Ala after reoxidation. (C) Slow regeneration of the initial absorption spectrum. *Solid lines*, flavin cofactor 5 min and 5 hours after admission of oxygen. *Dashed lines*, spectral changes that indicate a slow regeneration of the flavin cofactor.

To test this hypothesis the completely reduced species was denatured by the addition of urea from a side arm of the anaerobic cuvette. The

absorption spectrum of fully reduced and subsequently denatured His174Ala variant are shown in Figure 4. Strikingly, the resulting spectrum has similar spectral properties as the Cys166Ala variant by exhibiting two absorption maxima at ~350 and 450 nm (42). Again this is indicative for a cleavage of the 6-*S*-cysteinyl linkage in His174Ala, which seems to occur in the last phase of photoreduction. Thus, it appears that the covalent flavinylation is affected by the removal of His174 since wild type and variant enzyme exhibit different behaviour upon photoirradiation.

Redox Potential Determination. To better understand the influence of His174 on covalent flavinylation and kinetic properties of the His174Ala variant, the redox potential of the FAD cofactor was determined. A xanthine/xanthine oxidase system in the presence of suitable redox indicators was used and a plot of $\log(\text{BBE}_{\text{ox}}/\text{BBE}_{\text{red}})$ versus $\log(\text{dye}_{\text{ox}}/\text{dye}_{\text{red}})$ as described by Minnaert (37) allowed the estimation of the respective redox potential. Interestingly, for the His174Ala variant protein we observed a midpoint potential of +44 mV, which rather resembles the potentials of the Cys166Ala and His104Ala variants with only one covalent cofactor linkage. The crystal structure of BBE His174Ala shows clear electron density for an 8 α -histidyl and a 6-*S*-cysteinyl bond and hence did not suggest a decreased midpoint potential, due to incomplete formation of the bicovalent linkage.

Kinetic Characterization. Kinetic properties of BBE His174Ala were determined to address the role of His174 for catalysis. High performance liquid chromatography was used to analyze the reaction mixture after various time points of (*S*)-reticuline conversion as reported for wild type BBE (1). Table 1 shows a compilation of kinetic parameters determined for the His174Ala variant protein, BBE wild type and the single variant proteins with one missing covalent linkage (Cys166Ala and His104Ala). Substantial changes in all kinetic parameters were observed for BBE His174Ala. A k_{cat} value of $0.07 \pm 0.01 \text{ s}^{-1}$ was determined, which amounts to a ~120-fold decrease in catalytic activity compared to wild type enzyme ($k_{\text{cat}} = 8.0 \pm 0.2 \text{ s}^{-1}$). Thus BBE His174Ala is less active than the monocovalently linked Cys166Ala and His104Ala variant proteins (2, 13).

For the BBE His174Ala variant an eight-fold increase in the K_{M} value was observed compared to the wild type enzyme ($K_{\text{M}} = 68 \pm 30 \mu\text{M}$ and 8.7 ± 0.8 for BBE His174Ala and wild type, respectively), which implies that replacement of His174 affects substrate binding.

Table 1: Summary of kinetic parameters^a

	k_{red} [s ⁻¹]	k_{ox} [M ⁻¹ s ⁻¹]	k_{cat} [s ⁻¹]	E_0 [mV]	K_d [μM]
BBE H174A	0.08 ± 0.01	(7.0 ± 0.3)·10 ³	0.07 ± 0.01	44 ± 3	68 ± 30
BBE wild type	103 ± 4	(0.5 ± 0.1)·10 ⁵	8.0 ± 0.2	132 ± 4	8.7 ± 0.8
BBE C166A	0.28 ± 0.02	(1.0 ± 0.1)·10 ⁵	0.48 ± 0.05	53 ± 2	17 ± 3
BBE H104A	3.4 ± 0.3	(0.8 ± 0.1)·10 ⁵	0.54 ± 0.02	28 ± 4	4 ± 2

^a Kinetic data for wild-type BBE, C166A and H104A variant proteins are taken from (1) and (2).

To address the influence of the introduced amino acid exchange on specific reaction steps, reductive and oxidative half-reactions of (*S*)-reticuline conversion were determined for the His174Ala variant. Again, all experiments were performed under identical reaction conditions as published for wild type BBE (1). Interestingly, the His174Ala variant protein showed a very pronounced effect on the reductive half-reaction. For BBE His174Ala a limiting reductive rate of 0.08 ± 0.01 s⁻¹ was determined, which is a ~1300-fold decrease in k_{red} compared to wild type enzyme ($k_{\text{red}} = 103 \pm 4 \text{ s}^{-1}$). The oxidative rate was also influenced by the His to Ala replacement yielding a k_{ox} of (7.0 ± 0.3)·10³ M⁻¹ s⁻¹ compared to (0.5 ± 0.1)·10⁵ M⁻¹ s⁻¹ for wild type enzyme (12).

It was shown before that for the wild type enzyme the oxidative step is the rate-limiting step in substrate turnover (13). However, the kinetic parameters of BBE His174Ala suggest that the substantially decreased reductive rate can be regarded as the rate-limiting step in enzymatic turnover of the variant protein.

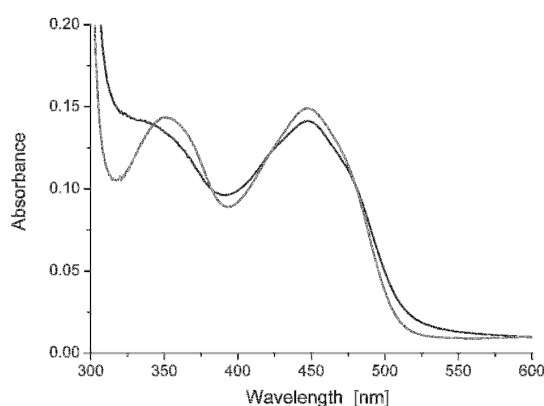


Figure 4. Absorption spectrum of “overreduced” and consecutively denatured His174Ala. The black line represents BBE His174Ala after reoxidation of a protein sample when denatured in its completely reduced form, whereas the grey line shows the absorption spectrum of denatured Cys166Ala.

Similar properties were observed for BBE Glu417Gln, where the catalytic glutamate residue was replaced with glutamine. For Glu417Gln a limiting reductive rate of 0.067 ± 0.007 s⁻¹ was observed (12), which is similar to the rate determined for BBE His174Ala.

Structural characterization. In order to rationalize the observed significant changes on the rate constants for both reductive and oxidative reaction steps we determined the crystal structure of BBE His174Ala. Due to the pronounced reduction in the reductive rate the crystal was soaked with (*S*)-reticuline to allow a better characterization of the mode of substrate binding. However, only slow-growing monoclinic crystals of the His174Ala variant could be obtained, which due to their comparatively small size did not diffract as well as the native wild type protein or the His104Ala and Cys166Ala variants described previously (2, 12). With respect to the substrate soaked wild type crystals the resolution of 2.65 Å is, however, slightly better than the 2.8 Å obtained previously with wild type BBE. Initial electron density maps confirmed the presence of the bicovalent cofactor attachment and replacement of His174 with Ala (Figure 1 B). While the overall structural change compared to both the monoclinic and tetragonal crystal forms is relatively small (RMSD for C α atoms 0.28 and 0.39 for 3D2D and 3D2J (12)), there are some significant structural rearrangements extending from the site of the amino acid substitution to the substrate binding site. As shown in Figure 5, removal of the histidine side chain leads to a peptide flip of the neighboring Ala163 residue with its carbonyl oxygen now forming a hydrogen bond to an ordered water molecule present on the re side of the isoalloxazine ring close to the C4a position, not observed in the substrate soaked monoclinic wild type structure (12).

Interestingly, also the amide proton of the same peptide bond interacts with a ligand not seen in any of the previously described structures.

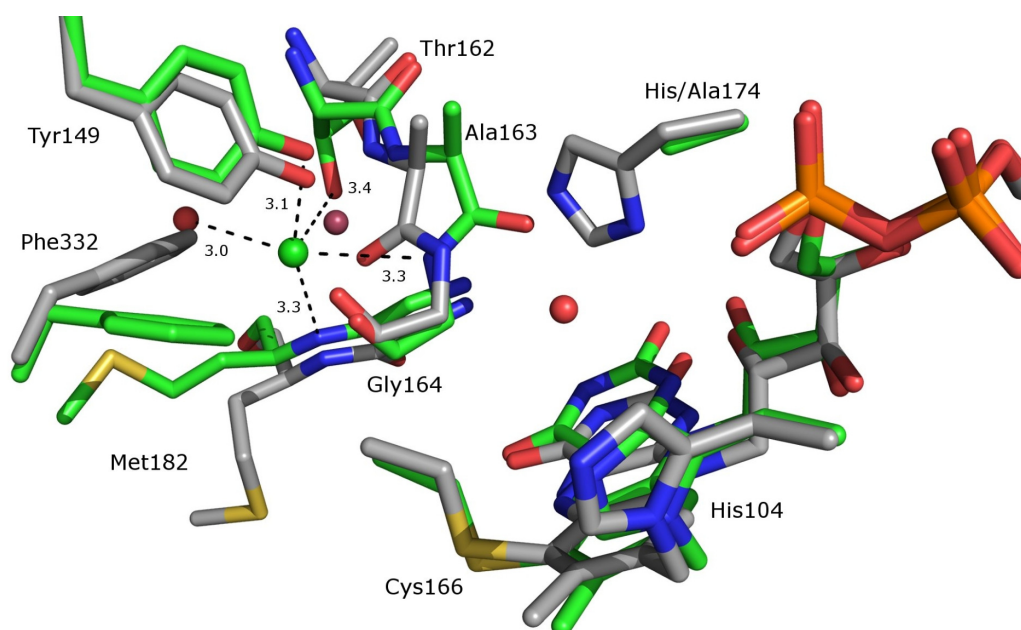


Figure 5. Structural changes due to His174Ala substitution observed in close proximity to the isoalloxazine ring system. Wild type carbon atoms are shown in gray and the corresponding elements of the His174Ala structure in green. Due to the missing imidazole ring of His174 a flipped peptide bond is observed between Ala163 and Gly164. The corresponding amide proton then provides one ligand for a newly formed chloride binding site. Distances for the partial octahedral coordination of the anion are given in Å. Water molecules shown in red belong to His174Ala and one colored in violet to the wild type protein.

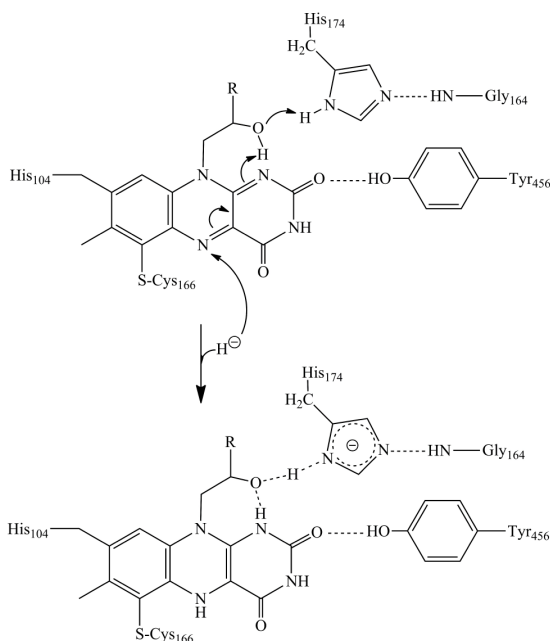
The chloride ion positioned into the electron density for this ligand is supported by its refined B factor, which is close to that of surrounding water molecules, and its well defined octahedral coordination with average distances of 3.2 Å to its hydrogen bond donors (Figure 5). As a consequence of the formed chloride coordination shell, the side chain of Phe332 repositions and via Met182 also induces rearrangements of Trp165, which is an important residue in the substrate binding site of BBE (Supplementary Figure S2). Last but not least, also the isoalloxazine of the flavin cofactor itself is shifted by ~1 Å into the back of the substrate binding pocket due to the missing hydrogen bond between His174 and the C2' hydroxyl group of the ribityl chain. This in turn opens space for a different rotamer of Phe351 which renders the whole active site entrance loop more ordered when compared to wild type structures. Observing all these changes at the active site of the protein it is also interesting to note that the mode of (*S*)-reticuline binding itself is only marginally affected by the His174Ala mutation. However, the distance for backwards movement of the isoalloxazine ring system is partially followed by the substrate increasing the hydrogen bond distance to the catalytic base Glu417 from 2.8 Å in the wild type structure (12) to 3.2 Å.

Another important feature of the electron density shown in Figure 1 is its intactness

with respect to the isoalloxazine ring system although the crystal was incubated for four weeks under identical conditions as wild type BBE crystallized in the same crystal form. For the latter protein degradation to the 4a-spirohydantoin was already observed after five days (3D2D) (12), suggesting a reduced reactivity of the flavin cofactor with respect to potential degradation pathways in the His174Ala variant.

Discussion

The major objective of this study was to investigate the role of His174, a conserved active site amino acid among bicovalent flavoproteins, for substrate turnover and bicovalent flavinylation of BBE. Sequence alignments of all known bicovalently linked flavoproteins resulted in the finding that all bicovalent oxidases feature this histidine residue which interacts with the C2' hydroxyl group of the ribityl side chain of the flavin cofactor (Figure 1 A). Interestingly, GilR from *Streptomyces* sp. and most pollen allergens from different grasses possess a leucine or an asparagine residue instead of the conserved histidine (see Supplementary Figure S3). Recently, GilR was reported as the first bicovalently linked dehydrogenase (4) and for most pollen allergens no catalytic function was shown up to now. However, initial studies on Phl p 4 from timothy grass also showed

Scheme 1.

dehydrogenase activity of the enzyme (W. Keller and D. Zafred, University of Graz, personal communication). These findings suggest that the conserved histidine residue is especially important for oxidases but not for dehydrogenases within this family of bicovalent flavoenzymes.

A pronounced influence of the amino acid replacement in the His174Ala variant protein was observed for all kinetic parameters. A ~120 fold decrease in catalytic activity compared to the wild type enzyme was determined for the His174Ala variant protein. This influence is much stronger compared to the monocovalently linked BBE variants (Cys166Ala and His104Ala) and is in the range of the Glu417Gln variant protein, where the catalytic glutamate residue was exchanged (12). Strikingly, the same effect was obtained for the reductive rate of BBE His174Ala. A drastic 1300-fold decrease in k_{red} was determined compared to the wild type enzyme. Hence the reduced k_{red} and k_{cat} -values of the His174Ala variant suggest that His174 is required for efficient catalysis. It is obvious from the wild type crystal structure that His174 can not directly interact with the flavin isoalloxazine ring, however, it is involved in a hydrogen bonding network by interacting with the C2' hydroxyl group of the ribityl side chain of the flavin which again interacts with the N(1)-C(2)=O locus of the isoalloxazine ring system.

Hence this hydrogen bonding network might form a proton transfer relay, which stabilizes the intermediate negative charge during substrate turnover (Scheme 1). This lack in stabilization of the reduced form of the cofactor could also explain the decreased

redox potential of the His174Ala variant protein. Although this variant features a bicovalent cofactor linkage its redox potential (44 ± 3 mV) is lowered comparable to the wild type enzyme (132 ± 4 mV) but is in the range of the monocovalent Cys166Ala and His104Ala variant proteins (53 ± 2 mV and 28 ± 4 mV).

Moreover, the substantially decreased substrate turnover is not solely attributed to the lack in stabilization of the negatively charged intermediate but is also a result of structural alterations. In the crystal structure of the His174Ala mutant protein the flavin cofactor and the substrate (*S*)-reticuline are slightly shifted in the active site leading to an increased distance between the catalytically essential Glu417 and the 3' hydroxyl residue of the substrate. In a previous study, we have shown that Glu417 initiates substrate oxidation by deprotonation of the 3' hydroxyl residue of (*S*)-reticuline (12). This deprotonation increases the nucleophilicity of the C2' atom which now attacks the *N*-methyl group of the substrate resulting in methylene bridge formation and concomitant hydride transfer to the flavin cofactor. Hence an increased hydrogen bonding distance between Glu417 and the C3' hydroxyl residue could hamper proton abstraction and hence slow down the initiation of the concerted reaction.

Besides this strong influence on k_{cat} and k_{red} , we also observed a seven-fold decrease in the oxidative rate when histidine 174 was replaced with alanine. Interestingly, His174Ala was the first BBE variant protein with a significant effect on the rate of cofactor reoxidation. In the crystal structure of the His174Ala variant protein a peptide flip of Ala163 is observed which forms a hydrogen bond to a structured water molecule in the substrate soaked crystal. Possibly this water molecule influences reoxidation of the reduced cofactor by blocking the site for dioxygen binding.

Moreover, interesting observations were made upon photoreduction of the BBE His174Ala variant protein. When the wild type enzyme is completely reduced by photoirradiation, 6-thio FAD is formed, which can effectively be stabilized by histidine 174 (1). In case of the His174Ala variant no 6-thio FAD was observed which might be attributed to a lack of stabilization of this modified flavin. In the His174Ala variant full reduction of the flavin cofactor resulted in the cleavage of the C(6)-carbon to sulfur bond, i.e. the cysteinyl linkage (Figure 4). Here the resulting spectrum rather resembled the denatured Cys166Ala variant with only one covalent linkage.

In conclusion, our results have shown that His174 is an essential active site residue in

BBE which participates in the stabilization of the reduced form of the flavin by maintaining a hydrogen bond network via the ribityl C2' hydroxyl residue. Moreover, His174 engages in a hydrogen bond interaction to the main chain amide group of Gly164, which is apparently beneficial for the proper alignment of other residues involved in the enzymatic reaction, such as Trp165. Hence, the replacement of His174 destabilizes the reduced state of FAD by disrupting the hydrogen bond network leading to a less favorable redox potential of the cofactor and a disordering of other amino acid residues in and near the active site of the enzyme.

ASSOCIATED CONTENT

Supporting Information. Supporting information available including data statistics of X-ray chromatography, supplementary figures to the results section, and a sequence alignment of bivalent flavoproteins. This material is available free of charge via the Internet at <http://pubs.acs.org>.

AUTHOR INFORMATION

Corresponding Author

* Prof. Dr. Karl Gruber, Institute of Molecular Biosciences, University of Graz, Humboldtstraße 50/3, A-8010 Graz, Austria, Tel.: +43-316-380 5483, email: karl.gruber@uni-graz.at

* Prof. Dr. Peter Macheroux, Graz University of Technology, Institute of Biochemistry, Petersgasse 12/II, A-8010 Graz, Austria, Tel.: +43-316-873 6450, email: peter.macheroux@tugraz.at

Present Addresses

† Institute of Biophysics and Nanosystems Research, Austrian Academy of Sciences, Schmiedlstraße 6, A-8042 Graz, Austria

Author Contributions

‡The first two authors have contributed equally to this work.

ABBREVIATIONS

BBE, berberine bridge enzyme; FAD, flavin adenine dinucleotide; GilR, pregilvocarcin V dehydrogenase; PDB, protein databank; RMSD, root mean square deviation; XDS, X-ray detector software.

REFERENCES

- Winkler, A., Hartner, F., Kutchan, T. M., Glieder, A., and Macheroux, P. (2006) Biochemical evidence that berberine bridge enzyme belongs to a novel family of flavoproteins containing a bi-covalently attached FAD Cofactor. *J. Biol. Chem.* **281**, 21276-21285.
- Winkler, A., Motz, K., Riedl, S., Puhl, M., Macheroux, P., and Gruber, K. (2009) Structural and mechanistic studies reveal the functional role of bivalent flavinylation in berberine bridge enzyme. *J. Biol. Chem.* **284**, 19993-20001.
- Heuts, D. P. H. M., Winter, R. T., Damsma, G. E., Janssen, D. B., and Fraaije, M. W. (2008) The Role of double covalent flavin binding in chito-oligosaccharide oxidase from *Fusarium graminearum*. *Biochem. J.* **413**, 175-183.
- Kharel, M. K., Pahari, P., Lian, H., and Rohr, J. (2009) GilR, an unusual lactone-forming enzyme involved in gilvocarcin biosynthesis. *ChemBioChem.* **10**, 1305-1308.
- Mo, X., Huang, H., Ma, J., Wang, Z., Wang, B., Zhang, S., Zhang, C., and Ju, J. (2011) Characterization of TrdL as a 10-hydroxy dehydrogenase and generation of new analogues from a tirandamycin biosynthetic pathway. *Org. Lett.* **13**, 2212-2215.
- Carlson, J. C., Li, S., Gunatilleke, S. S., Anzai, Y., Burr, D. A., Podust, L. M., and Sherman, D. H. (2011) Tirandamycin biosynthesis is mediated by co-dependent oxidative enzymes. *Nat. Chem.* **3**, 628-633.
- Rand, T., Qvist, K. B., Walter, C. P., and Poulsen, C. H. (2006) Characterization of the flavin association in hexose oxidase from *Chondrus crispus*. *FEBS J.* **273**, 2693-2703.
- Huang, C. H., Lai, W. L., Lee, M. H., Chen, C. J., Vasella, A., Tsai, Y. C., and Liaw, S. H. (2005) Crystal structure of glucooligosaccharide oxidase from *Acremonium Strictum*: A novel flavinylation of 6-S-cysteinyl, 8 α -N1-histidyl FAD. *J. Biol. Chem.* **280**, 38831-38838.
- Alexeev, I., Sultana, A., Mäntsälä, P., Niemi, J., and Schneider, G. (2007) Aclacinomycin oxidoreductase (AknOx) from the biosynthetic pathway of the antibiotic aclacinomycin is an unusual flavoenzyme with a dual active site. *Proc. Natl. Acad. Sci. U. S. A.* **104**, 6170-6175.
- Sosio, M., Stinchi, S., Beltrametti, F., Lazzarini, A., and Donadio, S. (2003) The gene cluster for the biosynthesis of the glycopeptide antibiotic A40926 by *Nonomuraea* species. *Chem. Biol.* **10**, 541-549.
- Dittrich, H., and Kutchan, T. M. (1991) Molecular cloning, expression, and induction of berberine bridge enzyme, an enzyme essential to the formation of benzophenanthridine alkaloids in the response of plants to pathogen attack. *Proc. Natl. Acad. Sci. U. S. A.* **88**, 9969-9973.
- Winkler, A., Łyskowski, A., Riedl, S., Puhl, M., Kutchan, T. M., Macheroux, P., and Gruber, K. (2008) A concerted mechanism for berberine bridge enzyme. *Nat Chem Biol.* **4**, 739-741.
- Winkler, A., Kutchan, T. M., and Macheroux, P. (2007) 6-S-Cysteinylation of bi-covalently attached FAD in berberine bridge enzyme tunes the redox potential for optimal activity. *J. Biol. Chem.* **282**, 24437-24443.

14. Heuts, D. P. H. M., Scrutton, N. S., McIntire, W. S., and Fraaije, M. W. (2009) What's in a covalent bond?: On the role and formation of covalently bound flavin cofactors. *FEBS J.* *276*, 3405-3427.
15. Fraaije, M. W., and Mattevi, A. (2000) Flavoenzymes: diverse catalysts with recurrent features. *Trends Biochem. Sci.* *25*, 126-132.
16. Wagner, M. A., Trickey, P., Che, Z. W., Mathews, F. S., and Jorns, M. S. (2000) Monomeric sarcosine oxidase: 1. Flavin reactivity and active site binding determinants. *Biochemistry* *39*, 8813-8824.
17. Lindqvist, Y., and Branden, C. I. (1989) The active site of spinach glycolate oxidase. *J. Biol. Chem.* *264*, 3624-3628.
18. Trickey, P., Wagner, M. A., Jorns, M. S., and Mathews, F. S. (1999) Monomeric sarcosine oxidase: structure of a covalently flavinylated amine oxidizing enzyme. *Structure* *7*, 331-345.
19. Muh, U., Massey, V., and Williams Jr., C. H. (1994) Lactate monooxygenase. I. Expression of the mycobacterial gene in *Escherichia coli* and site-directed mutagenesis of lysine 266. *J. Biol. Chem.* *269*, 7982-7988.
20. Xia, Z. X., and Mathews, F. S. (1990) Molecular structure of flavocytochrome b₂ at 2.4 Å resolution. *J. Mol. Biol.* *212*, 837-863.
21. Efimov, I., Cronin, C. N., Bergmann, D. J., Kuusk, V., and McIntire, W. S. (2004) Insight into covalent flavinylation and catalysis from redox, spectral, and kinetic analyses of the R474K mutant of the flavoprotein subunit of *p*-cresol methylhydroxylase. *Biochemistry* *43*, 6138-6148.
22. Ghanem, M., and Gadda, G. (2006) Effects of reversing the protein positive charge in the proximity of the flavin N(1) locus of choline oxidase. *Biochemistry* *45*, 3437-3447.
23. Hecht, H. J., Kalisz, H. M., Hendle, J., Schmid, R. D., and Schomburg, D. (1993) Crystal structure of glucose oxidase from *Aspergillus niger* refined at 2.3 Å resolution. *J. Mol. Biol.* *229*, 153-172.
24. Wohlfahrt, G., Witt, S., Hendle, J., Schomburg, D., Kalisz, H. M., and Hecht, H. J. (1999) 1.8 and 1.9 Å resolution structures of the *Penicillium amagasakiense* and *Aspergillus niger* glucose oxidases as a basis for modelling substrate complexes. *Acta Crystallogr. D Biol. Crystallogr.* *55*, 969-977.
25. Vrielink, A., Lloyd, L. F., and Blow, D. M. (1991) Crystal structure of cholesterol oxidase from *Brevibacterium sterolicum* refined at 1.8 Å resolution. *J. Mol. Biol.* *219*, 533-554.
26. Hallberg, B. M., Henriksson, G., Pettersson, G., and Divne, C. (2002) Crystal structure of the flavoprotein domain of the extracellular flavocytochrome cellobiose dehydrogenase. *J. Mol. Biol.* *315*, 421-434.
27. Mattevi, A., Vanoni, M. A., Todone, F., Rizzi, M., Teplyakov, A., Coda, A., Bolognesi, M., and Curti, B. (1996) Crystal structure of D-amino acid oxidase: a case of active site mirror-image convergent evolution with flavocytochrome b₂. *Proc. Natl. Acad. Sci. U. S. A.* *93*, 7496-7501.
28. Jin, J., Mazon, H., Van Den Heuvel, R. H. T., Heck, A. J., Janssen, D. B., and Fraaije, M. W. (2008) Covalent flavinylation of vanillyl-alcohol oxidase is an autocatalytic process. *FEBS J.* *275*, 5191-5200.
29. Kim, J., Fullert, J. H., Kuusk, V., Cunane, L., Chen, Z. W., Mathews, F. S., and McIntire, W. S. (1995) The cytochrome subunit is necessary for covalent FAD attachment to the flavoprotein subunit of *p*-cresol methylhydroxylase. *J. Biol. Chem.* *270*, 31202-31209.
30. Hassan-Abdallah, A., Bruckner, R. C., Zhao, G., and Jorns, M. S. (2005) Biosynthesis of covalently bound flavin: isolation and *in vitro* flavinylation of the monomeric sarcosine oxidase apoprotein. *Biochemistry* *44*, 6452-6462.
31. Brandsch, R., and Bichler, V. (1991) Autoflavinylation of apo6-hydroxy-D-nicotine oxidase. *J. Biol. Chem.* *266*, 19056-19062.
32. Huang, C. H., Winkler, A., Chen, C. L., Lai, W. L., Tsai, Y. C., Macheroux, P., and Liaw, S. H. (2008) Functional roles of the 6-S-cysteinyl, 8α-N1-histidyl FAD in glucooligosaccharide oxidase from *Acremonium strictum*. *J. Biol. Chem.* *283*, 30990-30996.
33. Weis, R., Luiten, R., Skranc, W., Schwab, H., Wubbolts, M., and Glieder, A. (2004) Reliable high-throughput screening with *Pichia pastoris* by limiting yeast cell death phenomena. *FEMS Yeast Res.* *5*, 179-189.
34. Schrittwieser, J. H., Resch, V., Wallner, S., Lienhart, W. D., Sattler, J. H., Resch, J., Macheroux, P., and Kroutil, W. (2011) Biocatalytic organic synthesis of optically pure (S)-p-coulerine and berberine and benzyloisoquinoline alkaloids. *J. Org. Chem.* *76*, 6703-6714.
35. Massey, V., and Hemmerich, P. (1978) Photoreduction of flavoproteins and other biological compounds catalyzed by deazaflavins. *Biochemistry* *17*, 9-17.
36. Massey, V. (1991) In: Curti, B., Zanetti, G., and Ronchi, S., eds. *Flavins and Flavoproteins*, Walter de Gruyter, Como, Italy, 59-66.
37. Minnaert, K. (1965) Measurement of the equilibrium constant of the reaction between cytochrome c and cytochrome a. *Biochim. Biophys. Acta.* *110*, 42-56.
38. Kabsch, W. (1993) Automatic processing of rotation diffraction data from crystals of initially unknown dymmetry land cell constants. *J. Appl. Crystallogr.* *26*, 795-800.
39. Adams, P. D., Grosse-Kunstleve, R. W., Hung, L. -, Ioerger, T. R., McCoy, A. J., Moriarty, N. W., Read, R. J., Sacchettini, J. C., Sauter, N. K., and Terwilliger, T. C. (2002) PHENIX: building new software for automated crystallographic structure determination. *Acta Crystallogr. Sect. D Biol. Crystallogr.* *58*, 1948-1954.
40. Emsley, P., and Cowtan, K. (2004) Coot: model-building tools for molecular graphics. *Acta Crystallogr. Sect. D Biol. Crystallogr.* *60*, 2126-2132.
41. Kleywegt, G. J., and Brunger, A. T. (1996) Checking your imagination: applications of the free R value. *Structure* *4*, 897-904.
42. Singer, T. P., and Edmondson, D. E. (1980) Structure, Properties, and Determination of Covalently Bound Flavins. *Methods Enzymol.* *66*, 353-264.

Supplementary Information

Table S1. Data collection and refinement statistics.

	BBE H174A
Space group	<i>C2</i>
Cell dimensions	
a,b,c (Å)	98.76, 92.94, 63.58
α,β,γ (°)	90, 100.3, 90
Wavelength (Å)	0.8104
Resolution (Å)	45-2.65 (2.75-2.65)*
No. of unique reflections	16,229
Completeness (%)	98.2 (97.9)
Redundancy	3.7 (3.6)
R_{sym}	0.123 (0.531)
$I / \sigma I$	9.7 (2.7)
Refinement range (Å)	43.19-2.65
$R_{\text{work}} / R_{\text{free}}$	0.1779/0.2348
<u>No. atoms</u>	
Protein	3940
Cofactor/sugars/substrate	53/86/24
Solvent	109
<u>B-factors (average)</u>	
Protein	28.8
Cofactor/sugars/substrate	21.3/52.8/37.2
Solvent	25.6
<u>R.m.s. deviations</u>	
Bond lengths (Å)	0.005
Bond angles (°)	1.0

* Values in parentheses are for the highest-resolution shell.

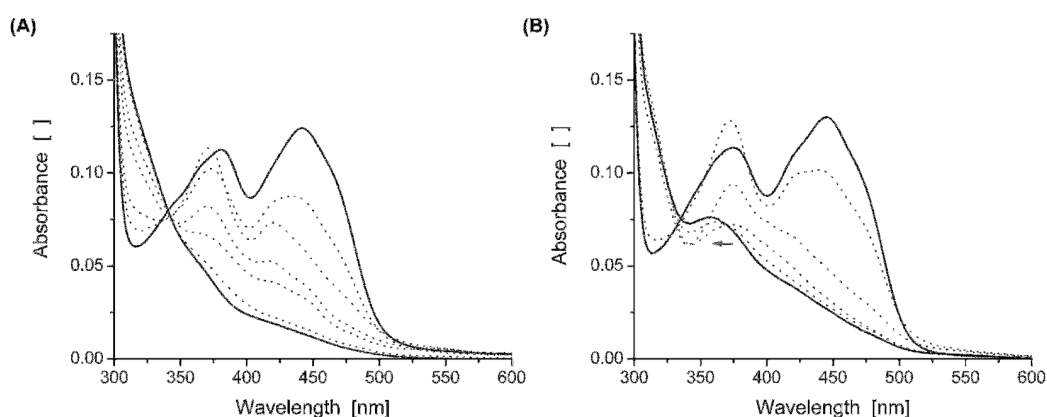
Figure S1.

Figure S1: Anaerobic photoreduction of BBE wild type and His174Ala variant protein: (A) shows the anaerobic photoreduction of wild type BBE, and (B) shows BBE His174Ala, respectively. Absorption spectra prior to photoradiation with the two characteristic flavin peaks and spectra of the fully reduced proteins are shown as *solid lines*. Spectra recorded during the course of photoreduction are shown as *dotted lines*. The grey arrow indicates the hypsochromic shift of the peak maximum in the reduced species of the His174Ala variant protein.

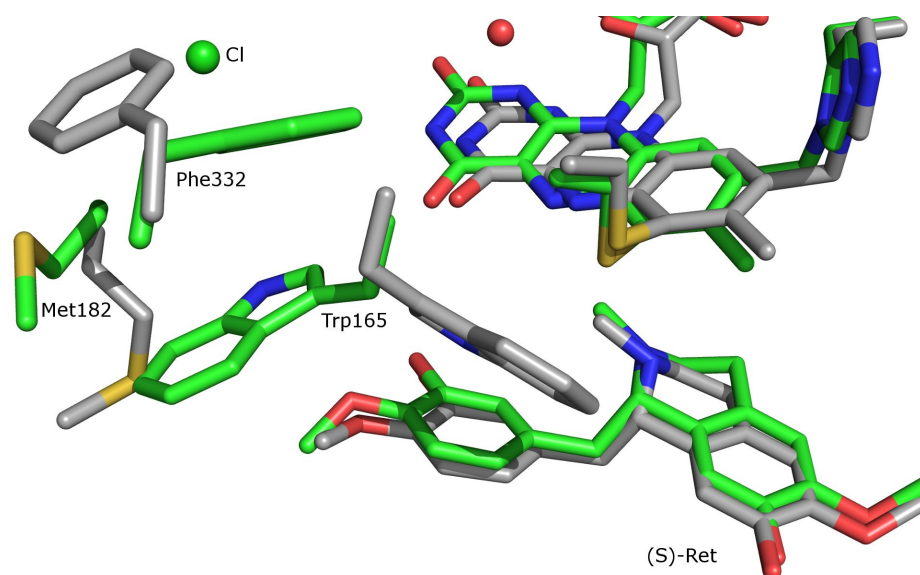
Figure S2.

Figure S2: Additional structural changes due to altered amino acid side chains involved in the formation of the chloride ion coordination shell. Starting from Phe332 these changes extend via Met182 all the way to the active site amino acid Trp165, which is in direct contact with (*S*)-reticuline.

Figure S3.

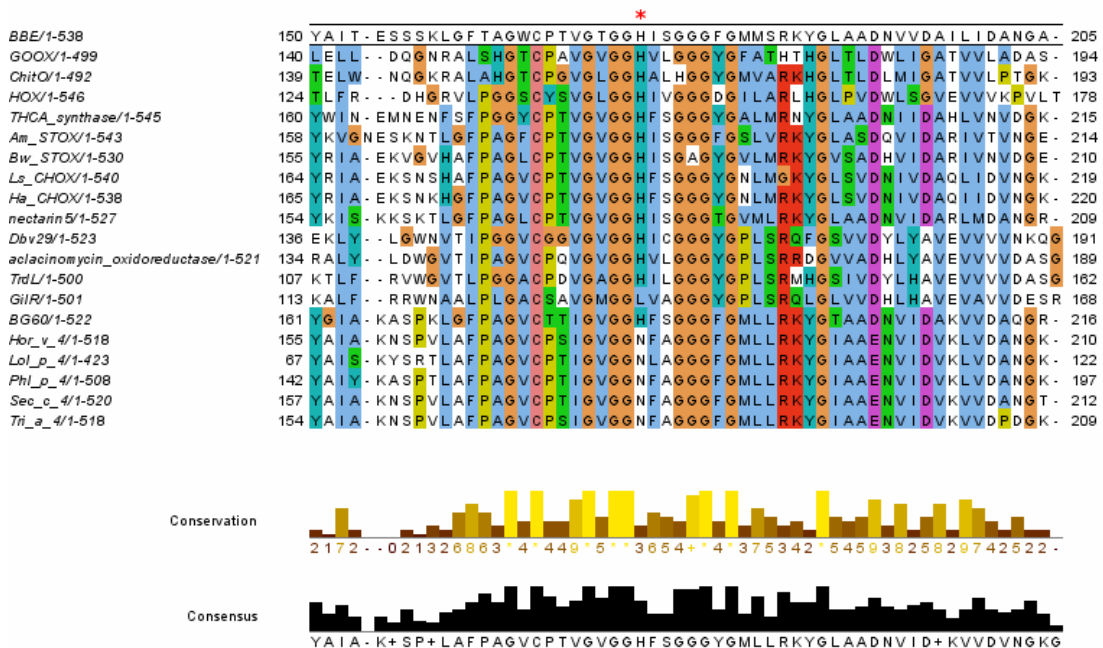


Figure S3: Sequence alignment of known bicovalently linked flavoproteins. The position of His174 of BBE is marked with an asterisk. GOOX, glucooligosaccharide oxidase from *Acremonium strictum* (AAS79317.1); ChitO, chitooligosaccharide oxidase from *Fusarium graminearum* (XP_391174.1); HOX, hexose oxidase from *Chondrus crispus* (AAB49376.1); THCA_synthase, tetrahydrocannabinolic acid synthase from *Cannabis sativa* (BAE48253.1); Am_STOX, (*S*)-tetrahydroprotoberberine oxidase from *Argemone mexicana* (HQ116698); Bw_STOX from *Berberis wilsoniae* (HQ116697); Ls_CHOX, carbohydrate oxidase from *Lactuca sativa* (AAL77102.1); Ha_CHOX, carbohydrate oxidase from *Helianthus annuus* (AAL77103.1); nectarin 5 from *Nicotiana langsdorffii* (AAP30841.1); Dbv29 from *Nonomuraea* sp. (2WDW); aclacinomycin oxidoreductase from *Streptomyces galilaeus* (2IPI); TrdL, 10-hydroxy-dehydrogenase in tirandamycin biosynthesis from *Streptomyces* sp. (ADY38530.1); GilR, pregilvocarcin V dehydrogenase from *Streptomyces griseoflavus* (3POP); BG60, FAD-linked oxidoreductase from Bermuda grass (AAS02108); Hor v 4, pollen allergen from *Hordeum vulgare* (CAH92635); Lol p 4, pollen allergen from *Lolium perenne* (CAH92637); Phl p 4, pollen allergen from timothy grass (CAD54671); Sec c 4, pollen allergen from rye (CAH92630); Tri a 4, pollen allergen from *Triticum aestivum* (CAH92633).

CHAPTER 6

- 6** Tuning BBE for new biocatalytic applications - active site redesign of berberine bridge enzyme
-

Author contributions

New active site muteins of BBE were designed to obtain biocatalysts with improved activity in the conversion of non-natural substrates. Rational active site redesign was performed in cooperation with JÖRG SCHRITTWIESER in the course of his PhD project. I contributed to this project by performing site-directed mutagenesis together with JÖRG SCHRITTWIESER and by assisting in screening for applicable expression strains and in large-scale protein expression. Selection of active site amino acids for site-directed mutagenesis and kinetic characterization of the mutant proteins was performed by JÖRG SCHRITTWIESER at the Department of Chemistry, Organic & Bioorganic Chemistry at the University of Graz.

Active site redesign of BBE is described in detail in the PhD thesis of JÖRG SCHRITTWIESER entitled “Chemo-enzymatic asymmetric approaches to benzyl-isoquinoline and berbine alkaloids“, hence only a brief summary of the project is presented in this chapter.

6.1 Biocatalytic synthesis of berbine and benzyloquinoline alkaloids

Berbine and benzyloquinoline alkaloids are two related classes of natural products [1], which are reported to exhibit a broad spectrum of pharmacological activities including antispasmodic, analgesic, sedative, hypnotic, muscle relaxant, or anti-inflammatory effects [2-5]. Moreover, some 1-benzyl-1,2,3,4-tetrahydroisoquinolines were described to exhibit anti-HIV activity and berbine derivatives are now being investigated as potent drugs for the treatment of schizophrenia [6, 7]. Berbine and benzyloquinoline alkaloids are produced by a variety of plants belonging to the families of *Papaveraceae* and *Berberidaceae*. Isolation of these natural products is time-consuming and does result in very low yields of the respective natural product [8]. So far, many efforts were made to synthesize these alkaloids; however, total organic synthesis usually resulted in low overall yields and unsatisfactory *ee* values [9, 10]. Recently a biocatalytic approach was published by SCHRITTWIESER *et al.* [11], where BBE was used for the production of enantiomerically pure (*S*)-berbines and (*R*)-benzyloquinolines. Racemic 1-benzyl-1,2,3,4-tetrahydroisoquinolines as substrates for enzymatic deracemization were synthesized using different chemical approaches as described in [11, 12]. These substrates were further converted in a biocatalytic step using heterologously expressed BBE, which exclusively accepts the (*S*)-enantiomer of benzyloquinolines leading to the formation of the corresponding (*S*)-berbines. Hence this biocatalytic organic synthesis can be regarded as a source of enantiopure (*R*)-benzyloquinolines and (*S*)-berbines [11-13] and thus can be exploited for the synthesis of new biological active compounds. Albeit BBE was demonstrated to accept non-natural substrates [11], initial kinetic studies revealed that not all benzyloquinoline derivatives can be converted by the enzyme, which might be attributed to sterical hindrance or interference with the enzyme mechanism [14]. Thus, protein engineering could lead to improved biocatalysts accepting a broad range of non-natural substrates and giving access to a variety of new pharmaceutically active compounds.

6.2 Objectives

The aim of this project was the implementation of a protein engineering approach to modify the active site of BBE for improved acceptance of two model substrates, which were converted with unexpectedly low rates in initial experiments performed with wild type BBE. These two non-natural substrates feature an anilic amino group instead of the phenolic moiety at C2' (model substrate **a**), or an *N*-ethyl instead of an *N*-methyl substituent (model substrate **b**).

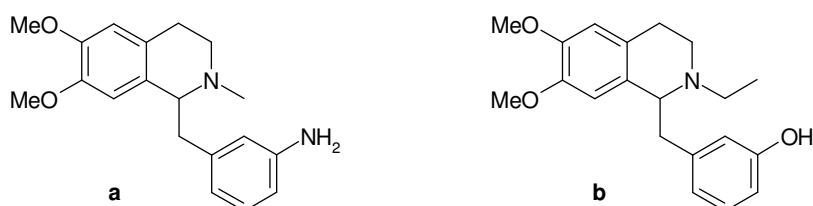


Figure 37: Model substrates for protein engineering of BBE

Rational active site redesign of BBE was planned by identifying possibly beneficial mutations in the crystal structure of the substrate-bound enzyme (see Figure 38). In case of model substrate **a**, a stronger activation of the -NH_2 group might be required for the initial deprotonation step and might hence facilitate C-C bond formation. Asn390 and Ser280 were identified as possible targets for site-directed mutagenesis. Replacing either of these amino acid residues with aspartic acid by creating a BBE N390D or S280D variant would result in a more basic active site environment and hence could facilitate proton abstraction from the anilic amino group.

In case of model substrate **b** the larger *N*-ethyl substituent might cause sterical hindrance and thus result in low conversion rates. Sterical problems might be overcome by replacing bulky active site amino acids with smaller residues, which should result in more space for accommodating substrates with larger *N*-alkyl chains. Trp165 and His459 were identified as possible targets and were replaced with phenylalanine and leucine or valine, respectively, by generating BBE W165F, H459L and H459V variants.

Figure 38 shows a comparison of wild type BBE and all described mutant proteins, which could possibly facilitate conversion of model substrates **a** or **b**.

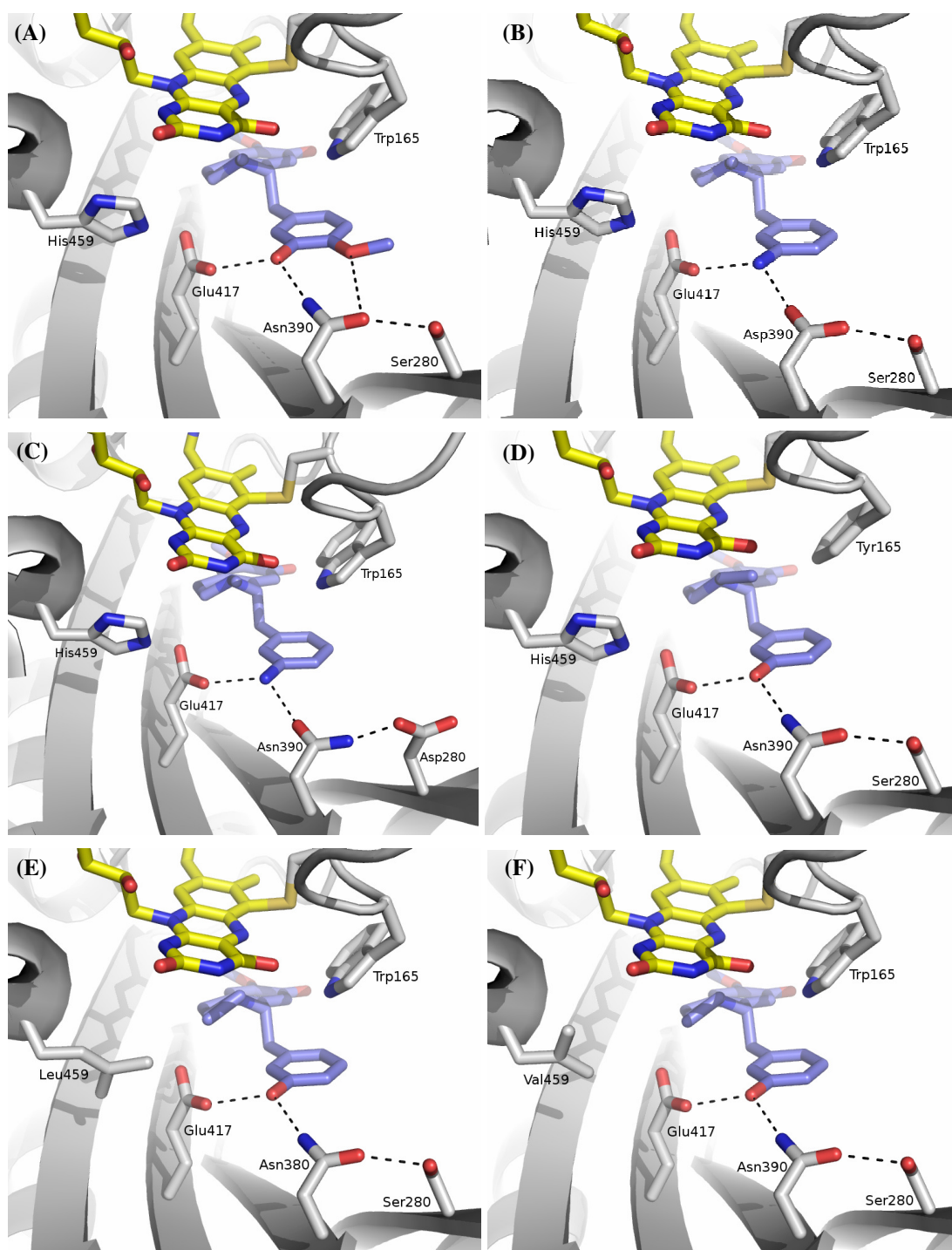


Figure 38: Active site representation of BBE wild type and new mutant proteins

(A) shows the active site of wild type BBE with bound (*S*)-reticuline drawn in blue. (B) and (C) show the hypothetical active site of BBE N390D and S290D, respectively. Model substrate **a** comprising an anilic amino moiety instead of the 3'-hydroxyl group is represented in blue. (D), (E), and (F) show active site representations of BBE W165F, H459L, and H159V, respectively. Model substrate **b** featuring an *N*-ethyl instead of an *N*-methyl moiety, is drawn in blue.

The flavin cofactor is coloured yellow in all illustrations. Important active site amino acids are labelled and shown as stick representation. Figure 38 was modified according to [14].

A further aim of the mutagenic approach was to change regioselectivity of BBE. Conversion of (*S*)-reticuline with wild type BBE was demonstrated to exclusively lead to ring closure at C2' and to formation of (*S*)-scoulerine as sole product [15]. However, studies performed with the E417Q variant of BBE resulted in drastically reduced turnover rates and in the identification of the regioisomer (*S*)-coreximine as second product of enzymatic conversion [16]. Hence the idea came up to create an improved mutein which favours ring closure at C6' with high catalytic activity. The low conversion rate of BBE E417Q can at least partly be attributed to the impeded deprotonation of the C3' hydroxyl group [16]. This suggests that a new amino acid residue needs to be introduced in the active site of BBE, which is able to form a hydrogen bond to the C5' moiety of the substrate after a 180° rotation. The latter requirements seem to be best fulfilled, when Leu295 is replaced by glutamate resulting in a BBE E417Q/L295E double mutant protein.

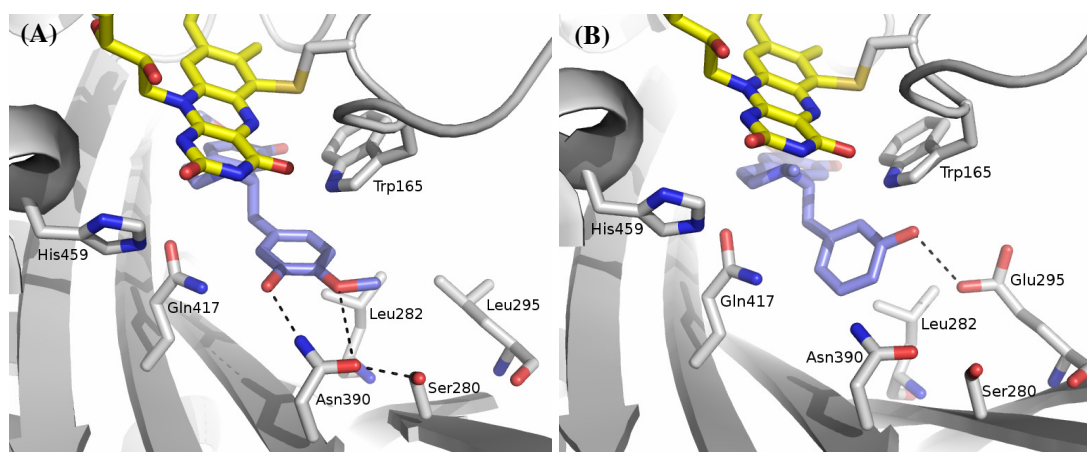


Figure 39: Active site representations of BBE E417Q and L295E E417Q

(A) shows an active site representation of BBE E417Q with the substrate (*S*)-reticuline drawn in blue. (B) shows an active site representation of the double mutant BBE E417Q/L295E with model substrate **a** in blue and possible hydrogen bonding to glutamate 295.

Figure 39 was modified according to [14].

Hence the objective of this project was the generation of all new active site mutant proteins and the characterization of these variants in regard to conversion of model substrates **a** and **b**.

6.3 Materials and Methods

6.3.1 Reagents

Unless stated otherwise all chemicals were of highest grade commercially available and were purchased either from Sigma-Aldrich (St. Louis, MO, USA), Fluka (Buchs, Switzerland), or Merck (Darmstadt, Germany). Polyacrylamide gel electrophoresis purified mutagenesis primers were obtained from VBC-Biotech (Vienna, Austria), and QuikChange® XL Site-Directed Mutagenesis Kit was from Stratagene (La Jolla, CA, USA). The anti-BBE antibody was a generous gift from Toni M. Kutchan (Donald Danforth Plant Science Center, St. Luis, MO, USA).

6.3.2 Site-directed mutagenesis

Site directed mutagenesis was performed with the expression vector pPICZalpha-*BBE-ER* as described in [15] to generate the N390D, S280D, H459L, H459V, and W165F variants and with pPICZalpha-*BBE-ER E417Q* for creation of the E417Q/L295E double mutetin. All desired mutations were introduced according to the QuikChange® XL Site-directed Mutagenesis kit (Stratagene) using a two-step protocol. In a first step, forward and reverse strand were synthesized in independent PRC reactions by adding solely sense or antisense primer. A typical 50 µL reaction contained 0.2 mM dNTPs, 1x Reaction buffer (Stratagene), 1 U Pfu Turbo DNA polymerase, 20 pmol of sense or antisense primer, and 100 ng template DNA. The following program was used for the initial PCR: 1 min at 95 °C, 4 cycles with 50 sec at 95 °C, 50 sec at 60 °C, and 6 min at 68 °C, followed by a final extension step of 7 min at 68 °C. In the second step 25 µL of forward and reverse reaction were mixed in a new reaction tube and polymerase chain reaction was performed using the following program: 1 min at 95 °C, 18 cycles with 50 sec at 95 °C, 50 sec at 60 °C, and 6 min at 68 °C, followed by a final extension step of 7 min at 68 °C.

The following sense and corresponding antisense primer were used for introducing the desired mutations. The underlined nucleotides represent the replaced codons. Replacement of Asn390 with aspartate was accomplished using 5'-GGGTTTATTGC TTTGGATGGATTTGGAGGCC-3' as sense and the corresponding antisense primer. For creating the S280D variant, the primer pair 5'-GAAGATTTTACTTTA

GACGTCCTCGGTGGTGCGG-3' (sense) and its complementary were used. The H459L, H459V, and W165F variants were created using the following oligonucleotides: 5'-GACTTGGGTATGTTAATCTTATTGATCTTGATCTTGGA GGG-3' (H459L, sense), 5'-GACTTGGGTATGTTAATGTTATTGATCTTGATCT TGGAGGG-3' (H459V, sense), 5'-GATTTACGGCTGGTTTCGTCCAACCGT TGG-3' (Y165F, sense) and the corresponding antisense primers.

Replacement of Leu295 with glutamate for generating the double mutant protein was accomplished using 5'-GTGTGGTTGACAATGGAAGGGTTTCATTTCCGGAC-3' (sense) and its complementary.

The introduction of the correct mutations was verified by plasmid sequencing.

6.3.3 Transformation, expression, and purification

All mutated vectors were transformed into *P. pastoris* KM71H or a strain coexpressing protein disulfide isomerase (PDI). Positive transformants were identified on YPD plates containing different concentrations of zeocin (100, 200, 300, 400 and 500 µg/mL) and initial screening experiments were performed in deep-well plates according to the optimized protocol of WEIS *et al.* [17]. Promising colonies for application in rescreen experiments were identified using Dot Blot analysis with an anti-BBE antibody for immunodetection of the respective BBE variant protein. At least two rescreen experiments were performed to identify colonies with consistently high expression of the heterologous protein.

All further experiments, which were performed with the best colonies from the screening procedure, were carried out as described in [11, 12]. Expression was first scaled up from micro scale to experiments in shake flasks, which yielded sufficient amounts of heterologous protein for initial activity assays with non-natural model substrates. Furthermore, final protein production was carried out in a 7 L Biostat CT fermenter (Sartorius Stedim Biotech GmbH, Goettingen, Germany) and protein purification was performed according to a two-step purification procedure using a hydrophobic interaction chromatography step followed by gel filtration as described in [15].

6.4 Results and discussion

Introduction of the desired mutations using mutagenesis PCR was successful in all cases. Moreover, the enhanced screening procedure performed with deep-well plates in micro scale with subsequent immunoblotting for identifying promising expression strains proved to be very efficient. Initial experiments led to the identification of applicable expression strains for all six BBE variants, which actually seemed to be superior to the best strain for production of the wild type enzyme. Generally, heterologous protein expression in *P. pastoris* depends on the site and number of integration of the respective expression cassette into the genome of the organism, which leads to transformants with varying efficiency in heterologous protein expression [18-20]. Hence a reliable screening procedure for the identification of transformants with high expression yields is of utmost importance and the screening procedure, which was applied for initial experiments, proved to be a fast and reliable system for identifying promising expression strains.

Whereas micro scale experiments were performed for all new mutants, only strains expressing BBE W165F and E417Q/L295E were selected for scale up and shake flask experiments. BBE W165F was selected to study the effect of an enlarged active site space on acceptance of bulky non-natural substrates and the double mutant E417Q/L295E was selected to investigate regioselectivity of the enzyme (see chapter 6.2). Both mutant proteins could be expressed in satisfactory amounts according to the protocol described in [12]. Small amounts of BBE W165F and E417Q/L295E were purified in a two-step protocol using hydrophobic interaction and gel filtration chromatography and were used for initial activity assays with the new model substrates. In these trial experiments the double mutant E417Q/L295E did not show any activity with the tested model substrates or with (*S*)-reticuline implying that the introduced glutamate residue at position 295 could not restore BBE activity. Unexpected conformational changes as a result of the amino acid replacement or a modification of the flavin's redox potential due to changes in the environment of the cofactor could have led to complete loss of activity. Since the aim of the project was the investigation of improved BBE variants and since BBE E417Q/L195E did not show any detectable catalytic activity no further experiments were performed with this mutant protein.

However, initial activity assays revealed that BBE W165F is able to convert different model substrates. In a further step, scale up to fermentation was performed to obtain enough protein for a complete kinetic characterization of the W165F mutant. It is noteworthy that fermentation according to the protocol described in [12] was very successful yielding in the purification of approximately 1.5 g of pure enzyme from one batch. This is approximately the eightfold yield compared to a normal batch for the production of wild type BBE and is an evidence for the excellent performance of the new screening system.

So far, only initial experiments were performed for BBE W165F. Kinetic parameters as k_{cat} , K_{M} or $k_{\text{cat}}/K_{\text{M}}$ have to be determined for the conversion of various model substrates and have to be compared to the kinetic profile of the wild type enzyme. All kinetic experiments were performed by JÖRG SCHRITTWIESER at the Department of Chemistry, Organic & Bioorganic Chemistry at the University of Graz and thus preliminary results of this work are summarized in his PhD thesis entitled “Chemo-Enzymatic Asymmetric Approaches to Benzyloquinoline and Berberine Alkaloids” [14].

6.5 References

- [1] Bentley, K.W. *The Isoquinoline Alkaloids* **1998**, Harwood Academic Publishers, Amsterdam.
- [2] Martin, M.L., Diaz, M.T., Montero, M.J., Prieto, P., San Roman, L., and Cortes, D. *Planta Med* **1993**, *59*, 63-67.
- [3] Chulia, S., Ivorra, M.D., Lugnier, C., Vila, E., Noguera, M.A., and D'Ocon, P. *Br J Pharmacol* **1994**, *113*, 1377-1385.
- [4] Yamahara, J., Konoshima, T., Sakakibara, Y., Ishiguro, M., and Sawada, T. *Chem Pharm Bull* **1976**, *24*, 1909-1912.
- [5] Eisenreich, W.J., Hofner, G., and Bracher, F. *Nat Prod Res* **2003**, *17*, 437-440.
- [6] Kashiwada, Y., Aoshima, A., Ikeshiro, Y., Chen, Y.P., Furukawa, H., Itoigawa, M., *et al.* *Bioorg Med Chem* **2005**, *13*, 443-448.
- [7] Li, J., Jin, G., Shen, J., and Ji, R. *Drugs Future* **2006**, *31*, 379-384.
- [8] Barton, D.H., Kirby, G.W., Steglich, W., Thomas, G.M., Battersby, A.R., Dobsan, T.A., and Ramuz, H. *J Chem Soc* **1965**, *65*, 2423-2438.
- [9] Chrzanowska, M., and Rozwadowska, M.D. *Chem Rev* **2004**, *104*, 3341-3370.
- [10] Matulenko, M.A., and Meyers, A.I. *J Org Chem* **1996**, *61*, 573-580.
- [11] Schrittwieser, J.H., Resch, V., Sattler, J.H., Lienhart, W.D., Durchschein, K., Winkler, A., Gruber, K., Macheroux, P., and Kroutil, W. *Angew Chem Int Ed* **2011**, *50*, 1068-1071.
- [12] Schrittwieser, J.H., Resch, V., Wallner, S., Lienhart, W.D., Sattler, J.H., Resch, J., Macheroux, P., and Kroutil, W. *J Org Chem* **2011**, *76*, 6703-6714.
- [13] Resch, V., Schrittwieser, J.H., Wallner, S., Macheroux, P., and Kroutil, W. *Adv Synth Catal* **2011**, *353*, 2377-2383.
- [14] Schrittwieser, J. Chemo-enzymatic asymmetric approaches to benzyloisoquinoline and berbine alkaloids **2011**, Department of Chemistry, Organic and Bioorganic Chemistry, University of Graz, Graz.
- [15] Winkler, A., Hartner, F., Kutchan, T.M., Glieder, A., and Macheroux, P. *J Biol Chem* **2006**, *281*, 21276-21285.
- [16] Winkler, A., Łyskowski, A., Riedl, S., Puhl, M., Kutchan, T.M., Macheroux, P., and Gruber, K. *Nat Chem Biol* **2008**, *4*, 739-741.
- [17] Weis, R., Luiten, R., Skranc, W., Schwab, H., Wubbolts, M., and Glieder, A. *FEMS Yeast Res* **2004**, *5*, 179-189.
- [18] Daly, R., and Hearn, M.T. *J Mol Recognit* **2005**, *18*, 119-138.
- [19] Macauley-Patrick, S., Fazenda, M.L., McNeil, B., and Harvey, L.M. *Yeast* **2005**, *22*, 249-270.
- [20] Cereghino, J.L., and Cregg, J.M. *FEMS Microbiol Rev* **2000**, *24*, 45-66.

CHAPTER 7

- 7 Redox potential determinations for Dbv29 -
a bicovalently flavinylated oxidase
-

Author contributions

Investigations on Dbv29 were performed in cooperation with the group of SHWU-HUEY LIAW (Faculty of Life Sciences and Institute of Genome Sciences, National Yang-Ming University, Taipei, Taiwan).

I contributed to this project by doing redox potential measurements for Dbv29 wild type and mutant proteins. In the course of this study BIRGIT LUEF assisted me as project student by doing parts of the practical work.

7.1 Dbv29 - oxidative power for A40926 maturation

Dbv29 is a recently discovered hexose oxidase, which was reported to be the last enzyme in the biosynthesis of A40926, an important glycopeptide antibiotic of *Nonomuraea* species [1-3]. Glycopeptide antibiotics are produced by a large number of actinomycetes [4], and are widely used for the treatment of life-threatening infections caused by gram-positive bacteria as enterococci or staphylococci [5-7]. However, the emergence of multidrug-resistant *Enterococcus* and *Staphylococcus aureus* strains, which can not be treated with the clinically approved glycopeptide antibiotics vancomycin or teicoplanin, clearly reveals the need for second-generation antibiotics with improved antimicrobial efficacy and pharmacokinetics [8-13]. Today new semi-synthetic antibiotics, such as dalbavancin, an A40926 derivative, are in advanced clinical development and show promising results [14-17]. However, the array of semi-synthetic drugs is limited and the manipulation of biosynthetic pathways for glycopeptide antibiotic production could lead to a now inconceivable variety of new antibacterial compounds [18]. Thus, understanding biosynthetic pathways and enzymes involved therein, is a major objective in the indispensable search for new pharmaceuticals [19].

7.1.1 A40926 and the *dbv* gene cluster for A40926 biosynthesis

A40926 belongs to the teicoplanin family of glycopeptides and was found to be a secondary metabolite of the filamentous actinomycete *Nonomuraea* sp. strain ATCC 39727 [3]. This antibiotic compound inhibits cell wall synthesis of gram-positive bacteria by binding to the D-alanyl-D-alanine termini of growing peptidoglycan chains, thereby terminating transpeptidation and transglycosylation reactions in peptidoglycan synthesis [5-7, 20].

In chemical terms, A40926 (see Figure 40) consists of a heptapeptide core made of the proteinogenic and non-proteinogenic amino acids tyrosine, β -hydroxytyrosine, 4-hydroxyphenylglycine, and 3,5-dihydroxyphenylglycine, with extensive cross-linking of the aromatic side chains. This molecule is decorated with two chlorine atoms and two sugar moieties, one of them being an amino sugar residue attached to

an acyl chain via an amide bond [18]. The acyl moiety was reported to be relevant for the antimicrobial activity of A40926 since it anchors the compound to the bacterial cell membrane, thereby causing an increased concentration of the compound near the target peptidoglycans [21, 22]. Another characteristic of A40926 is the oxidation of the *N*-acyl glucosaminy C-6 hydroxy substituent to a carboxy group (highlighted in red in Figure 40) [1].

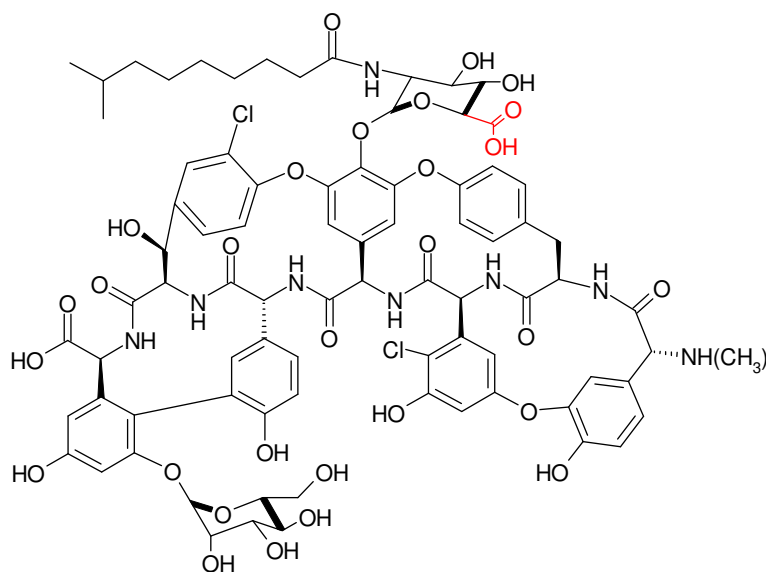


Figure 40: Structure of the glycopeptide antibiotic A40926

DONADIO and coworkers [2] characterized the gene cluster which is responsible for A40926 biosynthesis in *Nonomuraea* species. It consists of 37 open reading frames (ORFs) with gene products required for synthesis of the non-proteinogenic amino acids, generation of the hexapeptide, crosslinking and chlorination of the aromatic residues, addition and modification of sugar moieties, regulation of biosynthesis, transport of the antibiotic, and which serve as resistance factors. 10 ORFs were identified to be unique to the *dbv* biosynthetic cluster, among them being *dbv29*, which codes for a putative hexose oxidase with typical motifs for bicovalent linkage of the flavin cofactor. In A40926, the glucosamine moiety needs to be oxidized to the corresponding acid, and hence Dbv29 was suggested to be responsible for this modification step [2].

7.1.2 What is known about Dbv29?

Dbv29 is a primary alcohol glycopeptide hexose oxidase, which catalyzes the four-electron oxidation of the C-6 hydroxyl residue of an *N*-acylglucosamine moiety as last step of A40926 biosynthesis [1].

Initially, Dbv29 was described as the first FMN-dependent oxidase; however, the currently available crystal structure clearly reveals that the enzyme possesses an FAD cofactor [19].

Dbv29 is a member of the *p*-cresol methylhydroxylase (PCMH) superfamily of flavoproteins and thus comprises a flavin binding and a substrate binding domain [23]. Today, two crystal structures are available for Dbv29 (pdb codes 2WDW and 2WDX), which show the protein in its native form and in complex with a reaction intermediate. Interestingly, native Dbv29 exists as homodimer with large interface regions, whereas no considerable protein-protein interactions were found in the complexed form suggesting that monomers are formed upon complex formation (see Figure 41) [19].

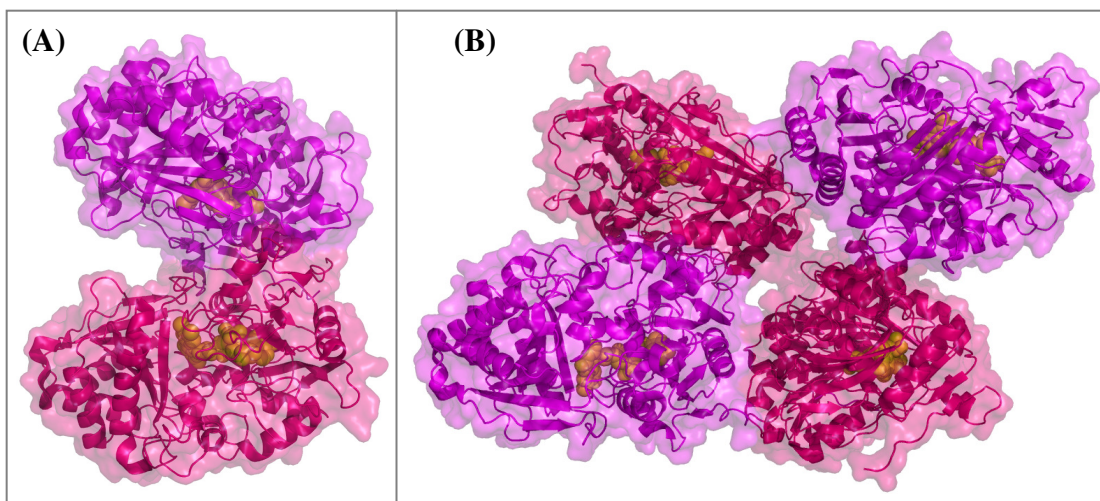


Figure 41: Crystal structure of Dbv29

(A) Dbv29 in its native form (pdb accession number 2WDW). The protein forms homodimers with large interface regions. (B) An asymmetric unit from crystallization of Dbv29 in complex with its reaction intermediate (pdb accession number 2WDX). No considerable subunit-subunit interaction was detected suggesting that complexed Dbv29 exists in a monomeric form. In both representations Dbv29 monomers are shown in magenta and pink, respectively. Bicovalently linked FAD cofactors are drawn in yellow. The representations were drawn using Pymol Molecular Graphics Systems, Version 1.3, Schrödinger, LLC.

Sequence alignments with other bicovalently linked oxidoreductases, such as BBE, GOOX, HOX, and ChitO, revealed that Dbv29 possesses the required histidine and cysteine residue for bicovalent flavin tethering. Surprisingly, a close examination of the crystal structure of both native and complexed Dbv29 exhibited that not all flavins show bicovalent linkages. For the dimer (pdb code 2WDW) the FAD cofactor in chain A seems to be trapped in the protein scaffold without covalent linkage, whereas histidinylation and cysteinylolation are present in chain B. The same applies for Dbv29 in complex with the reaction intermediate (pdb code 2WDX). The asymmetric unit comprises four molecules of Dbv29, of which three seem to be bicovalently flavinylated (chain B, C, and D), whereas a noncovalent cofactor is shown in chain A. However, most likely this concomitant occurrence of noncovalently and covalently linked FAD-cofactors seem to be a misinterpretation of electron density and hence an error in the crystal structures, and Dbv29 can be regarded as bicovalently flavinylated oxidase.

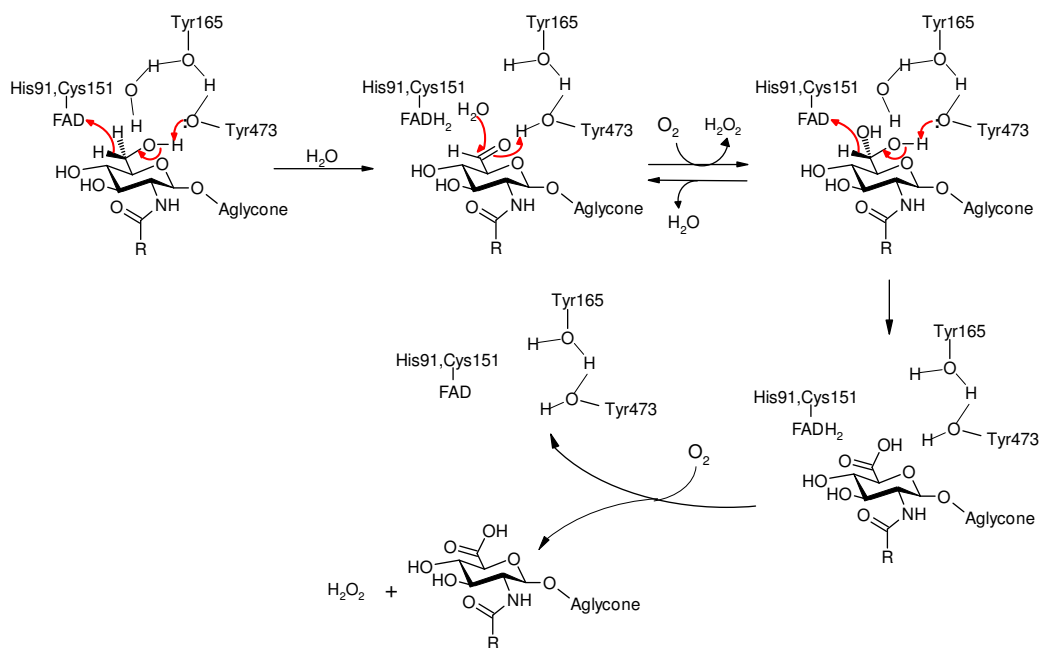


Figure 42: Proposed mechanism for Dbv29

Tyr165 and Tyr473 seem to be the catalytic bases in Dbv29. Tyr473, which is activated by Tyr165, initiates oxidation by deprotonating the C6 hydroxyl group of the aminosugar moiety consequently leading to a hydride transfer to N5 of the flavin isoalloxazine ring. An aldehyde intermediate is formed, which can hydrate to the diol found in the crystal structure. Besides the flavin cofactor is reoxidized with molecular oxygen resulting in the formation of hydrogen peroxide. A second hydride transfer to the flavin cofactor is again initiated by Tyr473 by deprotonation of the diol intermediate. This second oxidation step leads to the formation of the oxidized aminosugar moiety and hydrogen peroxide. Figure 42 was modified according to [19].

Dbv29 is remarkable in many aspects. LIU *et al.* reported the serendipitous crystallization of the enzyme in complex with a reaction intermediate, which led to the suggestion of a mechanism for Dbv29 and to unexpected opportunities for creating new teicoplanin analogs with enhanced antimicrobial properties [19]. This reaction intermediate was interpreted as diol and led to the suggestion of the reaction mechanism shown in Figure 42.

These new insights enabled LIU *et al.* to create new teicoplanin analogs with novel antimicrobial effects by intercepting the enzyme mechanism through modification of the reaction intermediates [19].

Furthermore, Dbv29 is a very interesting paradigm for studying the bicovalent mode of cofactor attachment. Dbv29 is the first bicovalently flavinylated enzyme, where the double mutant protein H91A/C151A could be expressed heterologously without losing the noncovalently bound flavin cofactor. The double mutant H91A/C151A retained its yellow colour indicating that the flavin cofactor is trapped in the protein. However, a further double mutant protein, where tyrosine 165 and tyrosine 473 were both replaced with alanine, led to the loss of the covalent FAD and of total catalytic activity. Hence this is a further evidence for the catalytic mechanism presented in Figure 42 [19].

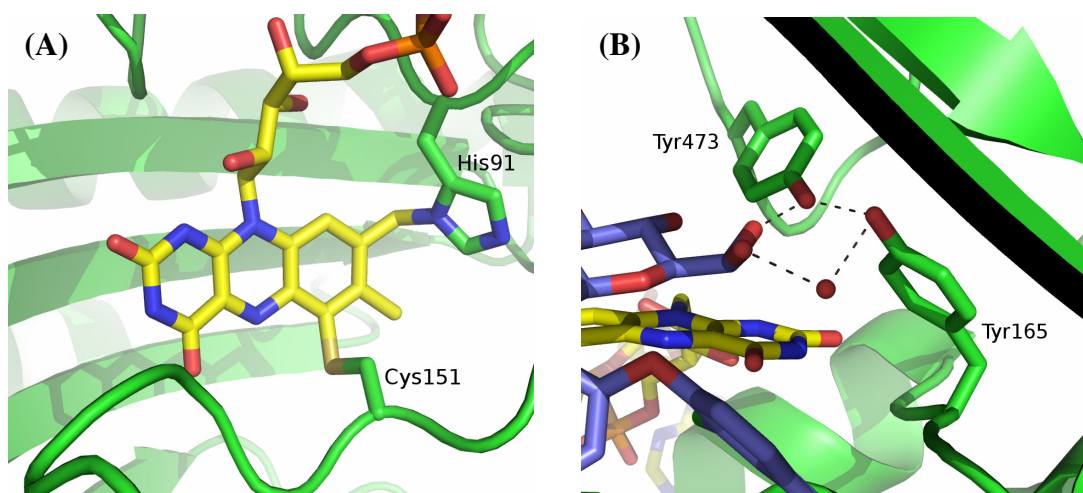


Figure 43: The active site architecture of Dbv29

(A) site of bicovalent flavinylation: The flavin cofactor, which is attached to histidine 91 and cysteine 151 of Dbv29, is shown in yellow. His91 and Cys151 are drawn in stick representation. (B) view of the catalytic centre of Dbv29. The catalytic residues tyrosine 165 and tyrosine 473 interact with the water-coordinated diol intermediate. The diol intermediate is shown in blue. Figure B was modified according to [19].

Initial activity studies performed with Dbv29 H91A, C151A, and the double mutein H91A/C151A resulted in the finding that all muteins retained some catalytic activity (11%, 23%, and 5% compared to wild type Dbv29, respectively). However, redox potentials of the mutant proteins were not determined so far [19]. Since H91A, C151A, and the double mutein H91A/C151A are available for in-depth characterization, determination of the redox potentials of the bicovalently, monocovalently, and noncovalently linked flavin could lead to new insights in the mode and roles of covalent cofactor tethering.

7.2 Materials and Methods

7.2.1 Reagents

Unless stated otherwise all chemicals were of highest grade commercially available and were purchased either from Sigma-Aldrich (St. Louis, MO, USA), Fluka (Buchs, Switzerland), or Merck (Darmstadt, Germany). Dbv29 wild type and mutant proteins were from the group of SHWU-HUEY LIAW (Faculty of Life Sciences and Institute of Genome Sciences, National Yang-Ming University, Taipei, Taiwan).

7.2.2 Dbv29 wild type and mutants

The following proteins were received for performing redox potential determinations. All samples were purified to near homogeneity and concentrated to approximately 25 - 30 mg/mL in 50 mM HEPES, 100 mM NaCl, 10% glycerol, pH 7.0.

Table 9: Dbv29 wild type and mutant proteins for redox potential determination

Dbv29	wild type strain with bicovalent flavinylation
Dbv29 H91A	mutant with covalent linkage to Cys151; His91 was replaced with alanine
Dbv29 H91C	mutant with covalent linkage to Cys151; His91 was replaced with cysteine
Dbv29 C151A	mutant with covalent linkage to His91; Cys151 was replaced with alanine
Dbv29 H151A/C151A	mutant protein, where both His91 and Cys151 were replaced with alanine
Dbv29 H151C/C151A	mutant protein, where His91 and Cys151 were replaced with cysteine and alanine, respectively

7.2.3 Redox potential determination

All redox potentials were determined using the dye-equilibration method with the xanthine/xanthine oxidase electron delivering system and appropriate redox indicators as described by MASSEY [24]. Unless stated otherwise, all experiments were performed in 50 mM HEPES, 100 mM NaCl, 10% glycerol, pH 7.0, at 25 °C.

Reaction mixtures contained either benzyl or methyl viologen as mediator (5 or 10 μ M, respectively), 300 μ M xanthine, and xanthine oxidase from bovine milk (Grade III) in catalytic amounts (approximately 2 nM). Solutions of 30 μ M enzyme, mediator and xanthine were rapidly mixed with solutions of redox indicator and catalytic amounts of xanthine oxidase. Concentrations of the respective redox dyes were chosen in a way that the absorbance changes at the wavelength employed for redox potential calculation were roughly in the same range as for the enzyme.

For maintaining anoxic conditions, all solutions were flushed with nitrogen and all experiments were carried out with a SF-61DX2 stopped flow device (TgK Scientific, Bradford-On-Avon, UK) positioned in a glove box from Belle Technology (Weymouth, UK). Spectra were recorded with a KinetaScanT diode array detector MG-6560 (TgK Scientific) equipped with an auto-shutter device to reduce photochemical effects during the course of the experiment. A typical reduction experiment lasted for approx. 75 min, and 300 scans were recorded during that time.

Used redox dyes and their corresponding redox potentials were 2,6-dichloroindophenol ($E_M = +217$ mV), toluylene blue ($E_M = +115$ mV), thionine acetate ($E_M = +64$ mV), toluidine blue ($E_M = +34$ mV), indigotrisulfonic acid potassium salt ($E_M = -81$ mV), indigodisulfonic acid dipotassium salt ($E_M = -125$ mV; 30 °C), and phenosafranin ($E_M = -252$ mV).

The potentials of Dbv29 wild type and mutant proteins were calculated from plots of $\log([\text{ox}]/[\text{red}])$ of the respective protein *versus* $\log([\text{ox}]/[\text{red}])$ of the dye according to MINNAERT [25].

7.3 Results

7.3.1 Spectral characteristics of Dbv29 wild type and muteins

Albeit spectral characteristics of Dbv29 were already published in [1], UV-vis spectra of all received protein samples were recorded to confirm protein concentrations and to test for precipitated protein as shown in Figure 44.

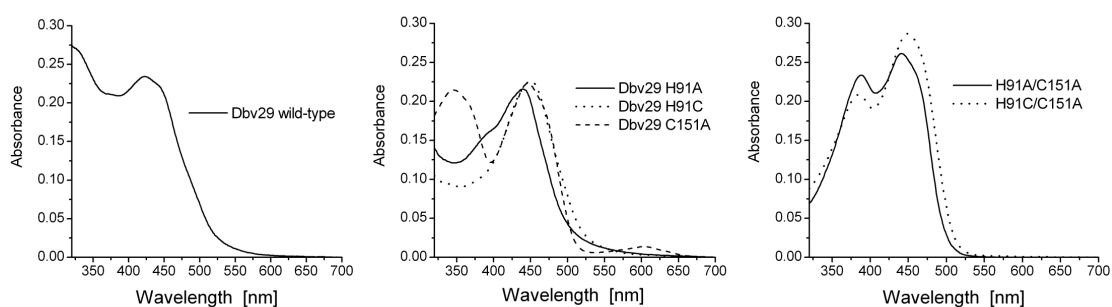


Figure 44: UV-vis spectra of Dbv29 wild type and mutant proteins

All measurements were carried out at a concentration of approximately 30 μM of the respective protein. The first graph shows the spectral characteristics of wild type Dbv29 with bicovalent flavinylation. The second graph shows UV-vis spectra of all mutant proteins, which possess one remaining covalent linkage of the flavin cofactor, whereas the last graph represents muteins, where both covalent linkages were removed.

Interestingly, wild type Dbv29 showed an absorption spectrum with a peak maximum at 425 nm and a less pronounced shoulder between 320 and 350 nm, which did not match with results from other bicovalently flavinylated proteins [26-29]. Moreover, the spectra of all mutant proteins showed substantial differences compared with the wild type. Dbv29 C151A exhibited two defined absorption maxima at 345 and 445 nm, whereas the strong hypsochromic shift of the second absorption band (345 nm) was indicative of an 8α -modification of the flavin cofactor [30].

Dbv29 H91A and H91C, where the covalent histidinylation was removed by amino acid replacement with alanine and cysteine, showed UV-vis absorbance spectra with one pronounced maximum at 440 and 450 nm, respectively. For Dbv29 H91A an additional shoulder between 365 and 400 nm was monitored, which was completely absent in the H91C mutant protein.

The double mutant proteins, Dbv29 H91A/C151A and H91C/C151A exhibited two distinct absorbance maxima at 390 and 440 nm, or at 385 and 450 nm, respectively, which resemble spectra of noncovalently bound flavin cofactors.

7.3.2 Redox potentials of Dbv29 wild type and muteins

Redox potentials were determined for Dbv29 wild type and all available mutant proteins using redox dyes, which led to a fairly parallel reduction of the flavin cofactor and the respective dye. At least three independent experiments were performed for determining the potential of the FAD cofactor in Dbv29 wild type and muteins. To confirm results from the experiments, higher and lower limits for the potentials were measured with redox dyes that were reduced before and after the flavin cofactor. All determined potentials are listed in Table 10.

Table 10: Redox potential determination for Dbv29 wild type and mutant proteins

	midpoint potential [mV]	average slope	number of measurements
Dbv29 wild type	114.5 ± 2.0	0.9030	4
Dbv29 H91A	35.3 ± 2.0	0.5257	4
Dbv29 H91C	64.8 ± 2.5	0.5359	5
Dbv29 C151A	59.0 ± 0.9	0.8811	5
Dbv29 H91A/C151A	-81.4 ± 2.7	1.1539	5
Dbv29 H91C/C151A	-80.2 ± 2.0	1.0694	3

For wild type Dbv29 a high midpoint potential of 114.5 ± 2.0 mV was calculated from experiments with toluylene blue ($E_M = +115$ mV) as appropriate redox dye (see Figure 45).

The average slope of 0.90 indicated a simultaneous two electron reduction of bicovalently tethered flavin cofactor and redox dye, as was already observed for wild type BBE or GOOX [27, 29]. Additional experiments were performed in the presence of 2,6-dichloroindophenol ($E_M = +217$ mV) or thionine acetate ($E_M = +64$ mV) to verify the calculated redox potential of wild type Dbv29. The two redox reporters were reduced before and after the flavin cofactor, respectively, giving the higher and lower limit for the midpoint potential of the enzyme-bound flavin.

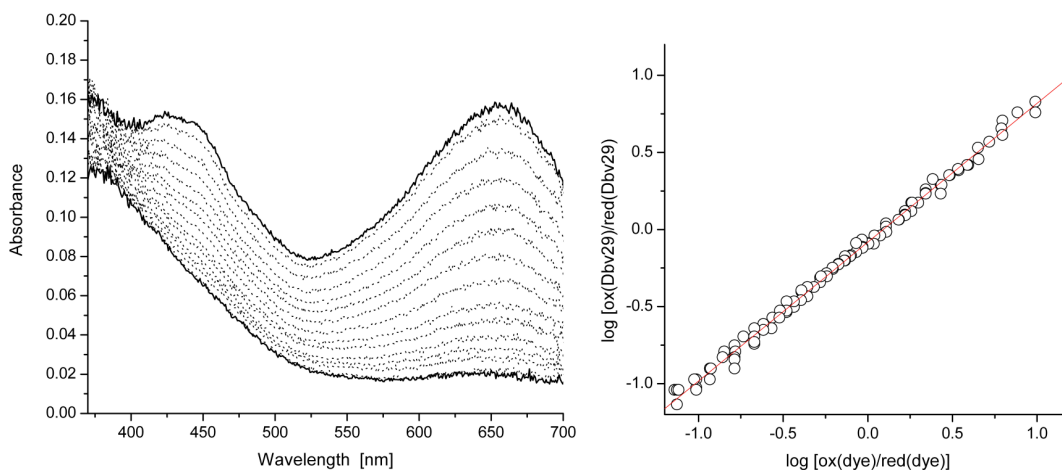


Figure 45: Redox potential determination of wild type Dbv29

Simultaneous reduction of wild type Dbv29 and toluylene blue using the xanthine/xanthine oxidase system. Selected spectra of the course of reduction are shown at the left. The diagram at the right shows the Nernst plot, which was used for calculating the redox potential of the enzyme-bound flavin cofactor. In the given example, data points for analysis were extracted at 450 and 663 nm for flavin and dye, respectively, where no significant influence of the other chromophore could be observed.

All mutant proteins exhibited a decreased redox potential compared to the wild type enzyme, with a more pronounced effect for mutants that lost both covalent linkages. For the single mutant proteins H91A, H91C, and C151A, redox potentials were determined to be 35.3 ± 2.0 , 64.8 ± 2.5 , and 59.0 ± 0.9 mV, respectively. These measurements were performed in the presence of toluidine blue ($E_M = +34$ mV) or thionine acetate ($E_M = +64$ mV) as reporter dye. Evaluation of the data by plotting $\log[\text{ox}(\text{flavin})/\text{red}(\text{flavin})]$ versus $\log[\text{ox}(\text{dye})/\text{red}(\text{dye})]$ resulted in an average slope of 0.88 for the C151A mutant and in a decreased value of 0.53 - 0.54 for H91A and H91C. This deviation from unity was monitored in measurements performed with both toluidine blue and thionine acetate and is indicative for a transfer of only one electron to the enzyme-bound flavin cofactor with simultaneous transfer of two electrons to the redox dye. Similar observations were made for GOOX H70A and were interpreted as a result from kinetic inhibition of a two-electron transfer to the flavin [27].

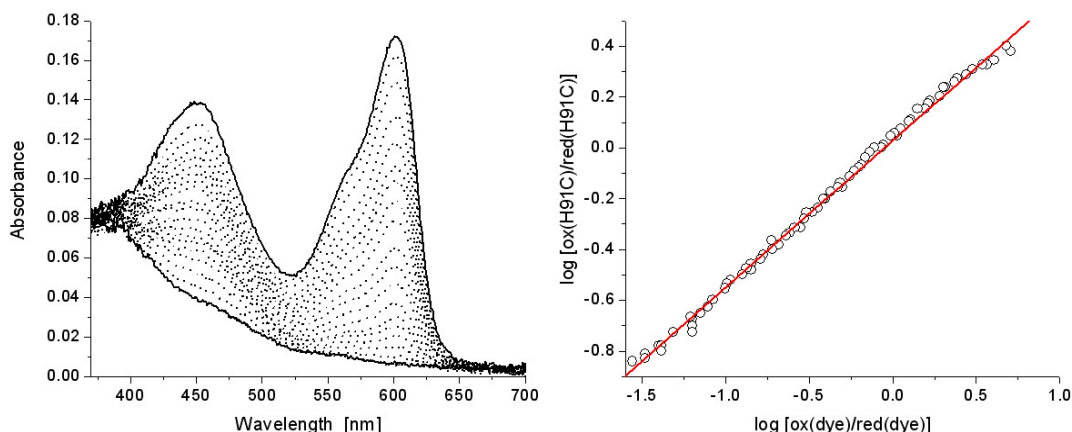


Figure 46: Redox potential determination of Dbv29 H91C

Simultaneous reduction of Dbv29 H91C and thionine acetate using the xanthine/xanthine oxidase system. Selected spectra of the course of reduction are shown at the left. The diagram at the right shows the Nernst plot, which was used for calculating the redox potential of the enzyme-bound flavin cofactor. In the given example, data points for analysis were extracted at 450 and 600 nm for flavin and dye, respectively, where no significant influence of the other chromophore could be observed.

No flavin radical was observed in the course of the experiments performed with H91A and H91C (see Figure 46); hence the reduced slope can not be attributed to a thermodynamic stabilization of the flavin radical over the hydroquinone form. Additionally, the deviation from unity could possibly be explained by a lack in equilibrium between cofactor and reporter dye reduction. However, this was ruled out by performing experiments with different concentrations of xanthine oxidase resulting in time courses of 1 to 12 h for complete cofactor and reporter dye reduction. Evaluation of these experiments did not show any significant alterations in the slope of the Nernst plot, suggesting that equilibrium was reached in all cases. In order to confirm the calculated redox potentials of Dbv29 H91A and H91C, higher and lower limits for the potential of the mutant proteins were determined using toluylene blue ($E_M = +115$ mV) and indigotrisulfonic acid potassium salt ($E_M = -81$ mV) as reporter dyes. Hence these control experiments show that the redox potential calculations of Dbv29 H91A and H91C are reproducible, however, should be interpreted with care.

For the double mutant proteins Dbv29 H91A/C151A and H91C/C151A redox potentials were calculated to be -81.4 ± 2.7 and -80.2 ± 2.0 mV and hence are the first experimental evidence that removal of both covalent linkages in a bicovalently flavinylated enzyme has a very pronounced effect on the midpoint potential of the

flavin cofactor. In both cases indigo-trisulfonic acid potassium salt ($E_M = -81$ mV) was used as reporter dye and higher and lower limits were determined using toluidine blue ($E_M = +34$ mV) and phenosafranin ($E_M = -252$ mV). The average slopes from the Nernst plot were close to unity and hence suggest simultaneous two-electron reduction of the flavin cofactor and the redox dye.

7.4 Discussion

Dbv29 is a member of the group of bicovalently flavinylated oxidases, which shows cofactor tethering to histidine 91 and cysteines 151 of the protein. Sequence alignments to well-characterized representatives of this group and an alignment of the elucidated crystal structures of BBE and Dbv29 showed that these proteins are highly homologous and adopt the same fold and mode of cofactor linkage (see Figure 47).

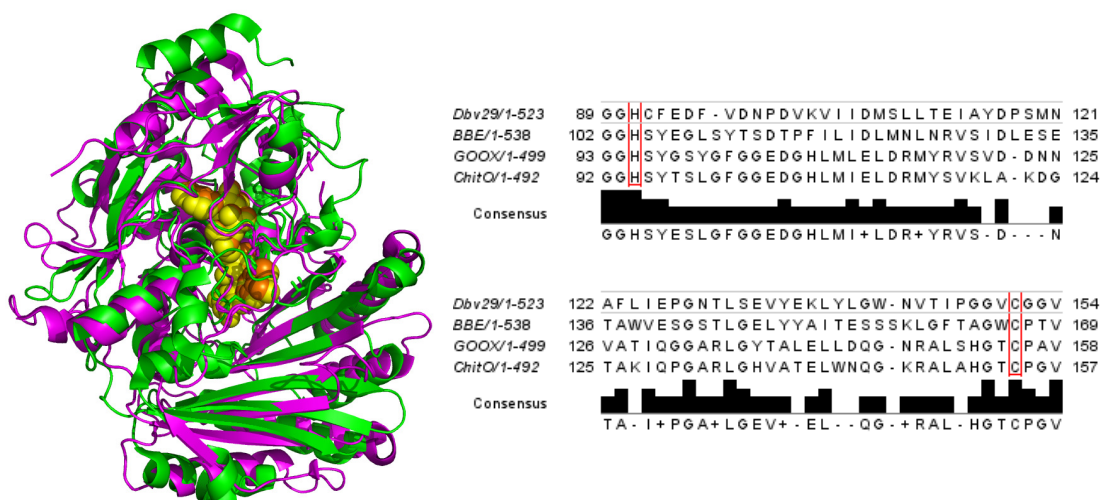


Figure 47: Bicovalent flavinylation of Dbv29

The graphical representation shows an alignment of Dbv29 (magenta) and BBE (green) drawn with Pymol Molecular Graphics Systems, Version 1.3, Schrödinger, LLC. The bicovalently linked FAD cofactors are shown as yellow and orange spheres, respectively.

The part of a multiple sequence alignment of Dbv29, BBE, GOOX, and ChitO shows the motifs for bicovalent flavin attachment. Linking cysteine and histidine residues are highlighted in red boxes. The multiple sequence alignment was performed with ClustalW on EBI [31, 32] and analyzed in Jalview 2.7 [33].

So far, Dbv29 is the only bicovalently flavinylated enzyme, where a mutation of both linking histidine and cysteine residues did not lead to the loss of the flavin cofactor. Both double mutant proteins exhibit a clear yellow colour which indicates a non-covalent incorporation of the FAD. To gain further insights in the role of covalent modification of the flavin, redox potentials were determined for Dbv29 wild type and mutant proteins.

Generally, properties of the FAD cofactor for wild type and mutant proteins addressing covalent flavinylation are in good agreement between Dbv29 and the

well-characterized enzymes GOOX, BBE, and ChitO [27-29, 34]. Except for wild type Dbv29, absorbance spectra of the flavin cofactors are comparable to the respective muteins of other enzymes. Wild type Dbv29 shows a hypsochromic shift to a broad absorption maximum at 420 nm and another strong absorbance at 320 nm. To the best of my knowledge these spectral characteristics do not correlate with the absorbance spectra of other bicovalently flavinylated enzymes and hence might be attributed to differences in the electronic environment of the cofactor as a result of active site amino acid composition. An effect of surrounding active site residues on absorbance spectra was also monitored for Dbv29 H91A and H91C. When His91 was replaced with alanine, a single absorbance maximum at 450 nm was observed, whereas replacement of His91 with cysteine resulted in a slightly hypsochromic shift of the maximum and in the formation of an absorbance shoulder from 360 to 400 nm. These spectral characteristics correlate with the characteristic absorbance spectrum of 6-*S*-cysteinylation as reported for trimethylamine dehydrogenase [35]. It is noteworthy that replacement of the linking histidine residue with a cysteine in Dbv29 H91C could possibly lead to the formation of a new mode of covalent flavinylation, where two cysteines tether the FAD cofactor. However, absorbance spectra of the monomeric sarcosine oxidase (MSOX), which possesses an 8 α -(*S*-cysteinyl)FAD cofactor, and Dbv29 H91C show substantial differences in their spectral characteristics and hence do not support this hypothesis [36].

Dbv29 C151A exhibits two absorbance maxima at 450 and 350 nm, whereas the hypsochromic shift of the second absorbance band to 350 nm is indicative for an 8 α -modification of the flavin cofactor [29, 30]. The expression of both single mutant proteins with replaced histidinylation and cysteinylation provides a further evidence for the independent formation of both types of covalent linkages.

Interestingly, Dbv29 was the first bicovalent flavoprotein, where both covalent linkages could be removed simultaneously without loss of the FAD cofactor and both Dbv29 H91A/C151A and H91C/C151A show spectral characteristics which resemble free FAD. So far, GOOX H70A/C130A was isolated as apo form without any flavin cofactor and double mutant proteins addressing the bicovalent flavin attachment could not be expressed in case of BBE or ChitO [27-29, 34, 37].

Similar to the spectral properties, redox potentials determined for Dbv29 wild type and mutant proteins correlate to potentials obtained for the bicovalent flavoproteins mentioned above. A high redox potential of 114.5 ± 2.0 mV was determined for wild

type Dbv29, which confirms the strong influence of covalent tethering on the midpoint potential. Moreover, potentials obtained for all single and double mutant proteins suggest that both covalent linkages contribute to an additive increase of the redox potential and that the nature of amino acid replacement in the muteins is decisive for redox properties. Elimination of one covalent linkage in C151A, H91A and H91C led to a significant drop of redox potential, to +59, +35, and +65 mV, respectively. This decrease in redox potential of approximately 50 to 80 mV is in agreement with flavin derivative studies which demonstrated a strong effect of 6-*S*-cysteinyl and 8 α -histidinyl linkages on the redox potential of the cofactor (increase in midpoint potential by ~ 50 mV) [38, 39].

Interestingly, replacement of histidine 91 with alanine showed a more pronounced effect on the redox potential than the amino acid exchange with cysteine (decrease of ~80 and 50 mV, respectively). Hence the nature of the surrounding amino acid residues seems to influence the redox potential of the cofactor, albeit no covalent linkages are formed in most cases. For H91C, there is a remaining probability that cysteine covalently attaches to the flavin cofactor instead of histidine. However, spectral analyses of H91C could not confirm an 8 α -*S*-cysteinylation and a crystal structure would be required for determining the mode of covalent flavinylation in H91C.

Redox potential determinations performed with both Dbv29 H91A and H91C mutant proteins led to Nernst slopes of ~0.5, which was also reported for the respective muteins of GOOX and ChitO [27, 28]. No flavin radical was observed during redox potential determinations and a lack in equilibrium was ruled out by performing experiments under varying conditions which led to complete reduction of cofactor and reporter dye in different time periods. As already suggested for GOOX H70A, kinetic inhibition of the electron transfer to the flavin cofactor could cause the deviation in Nernst slope. Interestingly, in case of BBE H104A no kinetic effect was observed and a slope close to unity was obtained suggesting a simultaneous 2-electron reduction [34].

Redox potentials of Dbv29 H91A/C151A and H91C/C151A were determined to be -81 and -80 mV, respectively, which implies a decrease in redox potential of about 195 mV compared to the wild type protein. This substantial decrease unequivocally demonstrates the importance of covalent cofactor tethering for the flavin redox potential and it is the first experimental evidence that removal of both covalent

linkages results in more pronounced effects compared to the single mutant proteins. The decrease in redox potential for the double mutant proteins is even higher than the cumulative effects of the H91A and C151A mutants, which might be attributed to a strong impact of the amino acid composition of the flavin binding site. It was already reported that the surrounding of the cofactor significantly influences the redox potential of noncovalent flavoproteins [40] leading to potentials between -367 and -1 mV [41-51]. Hence, the potentials of Dbv29 H91A/C151A and H91C/C151A are in the given range of noncovalent redox potentials.

Taken together, Dbv29 is the first bicovalent flavoprotein, where the effect of both 6-S-cysteinylation and 8 α -histidinylolation could be studied in detail since single and double mutant proteins comprising a monocovalent or noncovalent flavin were available. Redox potentials determined for Dbv29 wild type and mutant proteins corroborated the influence of covalent flavin coupling on the redox potential. Wild type Dbv29 exhibits a remarkably high potential which turns the enzyme into a potent oxidase and midpoint potentials of all mutant proteins were decreased in comparison to the wild type. However, a further biochemical characterization of all Dbv29 mutant proteins has to be performed to correlate changes in redox potential with kinetic properties, which could help revealing the precise function of bicovalent flavinylation.

7.5 References

- [1] Li, Y.S., Ho, J.Y., Huang, C.C., Lyu, S.Y., Lee, C.Y., Huang, Y.T., *et al.* *J Am Chem Soc* **2007**, *129*, 13384-13385.
- [2] Sosio, M., Stinchi, S., Beltrametti, F., Lazzarini, A., and Donadio, S. *Chem Biol* **2003**, *10*, 541-549.
- [3] Goldstein, B.P., Selva, E., Gastaldo, L., Berti, M., Pallanza, R., Ripamonti, F., Ferrari, P., Denaro, M., Arioli, V., and Cassani, G. *Antimicrob Agents Chemother* **1987**, *31*, 1961-1966.
- [4] Donadio, S., Sosio, M., Stegmann, E., Weber, T., and Wohlleben, W. *Mol Genet Genomics* **2005**, *274*, 40-50.
- [5] Lancini, G.C., and Cavalleri, B. **1997**, Glycopeptide Antibiotics (Dalbaheptides), in *Biotechnology Volume 7*, VCH, Weinheim, Germany, 369-396.
- [6] Kahne, D., Leimkuhler, C., Lu, W., and Walsh, C. *Chem Rev* **2005**, *105*, 425-448.
- [7] Nicolaou, K.C., Boddy, C.N., Brase, S., and Winssinger, N. *Angew Chem Int Ed Engl* **1999**, *38*, 2096-2152.
- [8] Murray, B.E. *N Engl J Med* **2000**, *342*, 710-721.
- [9] Rice, L.B. *Am J Infect Control* **2006**, *34*, 11-19.
- [10] Fischbach, M.A., and Walsh, C.T. *Science* **2009**, *325*, 1089-1093.
- [11] Payne, D.J., Gwynn, M.N., Holmes, D.J., and Pompliano, D.L. *Nat Rev Drug Discov* **2007**, *6*, 29-40.
- [12] Anstead, G.M., and Owens, A.D. *Curr Opin Infect Dis* **2004**, *17*, 549-555.
- [13] Arias, C.A., and Murray, B.E.N. *Engl J Med* **2009**, *360*, 439-443.
- [14] Pope, S.D., and Roecker, A.M. *Pharmacotherapy* **2006**, *26*, 908-918.
- [15] Roecker, A.M., and Pope, S.D. *Expert Opin Pharmacother* **2008**, *9*, 1745-1754.
- [16] Dorr, M.B., Jabes, D., Cavaleri, M., Dowell, J., Mosconi, G., Malabarba, A., White, R.J., and Henkel, T.J. *J. Antimicrob Chemother* **2005**, *55*, 25-30.
- [17] Malabarba, A., and Ciabatti, R. *Curr Med Chem* **2001**, *8*, 1759-1773.
- [18] Sosio, M., and Donadio, S. *J Ind Microbiol Biotechnol* **2006**, *33*, 569-576.
- [19] Liu, Y.C., Li, Y.S., Lyu, S.Y., Hsu, L.J., Chen, Y.H., Huang, Y.T., *et al.* *Nat Chem Biol* **2011**, *7*, 304-309.
- [20] Chan, H.C., Huang, Y.T., Lyu, S.Y., Huang, C.J., Li, Y.S., Liu, Y.C., Chou, C.C., Tsai, M.D., and Li, T.L. *Mol Biosyst* **2011**, *7*, 1224-1231.
- [21] Beauregard, D.A., Williams, D.H., Gwynn, M.N., and Knowles, D.J. *Antimicrob Agents Chemother* **1995**, *39*, 781-785.
- [22] Truman, A.W., Robinson, L., and Spencer, J.B. *ChemBioChem* **2006**, *7*, 1670-1675.
- [23] Dym, O., and Eisenberg, D. *Protein Sci* **2001**, *10*, 1712-1728.

- [24] Massey, V. **1991**, In: Curti, B., Zanetti, G., and Ronchi, S., eds. *Flavins and Flavoproteins*, Walter de Gryter, Como, Italy, 59-66.
- [25] Minnaert, K. *Biochim Biophys Acta* **1965**, *110*, 42-56.
- [26] Winkler, A., Hartner, F., Kutchan, T.M., Glieder, A., and Macheroux, P. *J Biol Chem* **2006**, *281*, 21276-21285.
- [27] Huang, C.H., Winkler, A., Chen, C.L., Lai, W.L., Tsai, Y.C., Macheroux, P., and Liaw, S.H. *J Biol Chem* **2008**, *283*, 30990-30996.
- [28] Heuts, D.P.H.M., Winter, R.T., Damsma, G.E., Janssen, D.B., and Fraaije, M.W. *Biochem J* **2008**, *413*, 175-183.
- [29] Winkler, A., Kutchan, T.M., and Macheroux, P. *J Biol Chem* **2007**, *282*, 24437-24443.
- [30] Singer, T.P., and Edmondson, D.E. *Structure, Properties, and Determination of Covalently Bound Flavins*, **1980**.
- [31] Larkin, M.A., Blackshields, G., Brown, N.P., Chenna, R., McGettigan, P.A., McWilliam, H., et al. *Bioinformatics* **2007**, *23*, 2947-2948.
- [32] Goujon, M., McWilliam, H., Li, W., Valentin, F., Squizzato, S., Paern, J., and Lopez, R. *Nucleic Acids Res* **2010**, *38*, W695-9.
- [33] Waterhouse, A.M., Procter, J.B., Martin, D.M., Clamp, M., and Barton, G.J. *Bioinformatics* **2009**, *25*, 1189-1191.
- [34] Winkler, A., Motz, K., Riedl, S., Puhl, M., Macheroux, P., and Gruber, K. *J Biol Chem* **2009**, *284*, 19993-20001.
- [35] Steenkamp, D.J., McIntire, W., and Kenney, W.C. *J Biol Chem* **1978**, *253*, 2818-2824.
- [36] Hassan-Abdallah, A., Zhao, G., and Jorns, M.S. *Biochemistry* **2006**, *45*, 9454-9462.
- [37] Winkler, A., Łyskowski, A., Riedl, S., Puhl, M., Kutchan, T. M., Macheroux, P., and Gruber, K. *Nat Chem Biol* **2008**, *4*, 739-741.
- [38] Ghisla, S., Kenney, W.C., Knappe, W.R., McIntire, W., and Singer, T.P. *Biochemistry* **1980**, *19*, 2537-2544.
- [39] Williamson, G., and Edmondson, D.E. *Biochemistry* **1985**, *24*, 7790-7797.
- [40] Heuts, D.P.H.M., Scrutton, N.S., McIntire, W.S., and Fraaije, M.W. *FEBS J* **2009**, *276*, 3405-3427.
- [41] Byron, C.M., Stankovich, M.T., Husain, M., and Davidson, V.L. *Biochemistry* **1989**, *28*, 8582-8587.
- [42] Husain, M., Stankovich, M.T., and Fox, B.G. *Biochem J* **1984**, *219*, 1043-1047.
- [43] Vinod, M.P., Bellur, P., and Becker, D.F. *Biochemistry* **2002**, *41*, 6525-6532.
- [44] Chaiyen, P., Brissette, P., Ballou, D.P., and Massey, V. *Biochemistry* **1997**, *36*, 2612-2621.
- [45] Negri, A., Tedeschi, G., Cecilian, F., and Ronchi, S. *Biochim Biophys Acta* **1999**, *1431*, 212-222.

- [46] Williamson, G., Edmondson, D.E., and Muller, F. *Biochim Biophys Acta* **1988**, 953, 258-262.
- [47] Stankovich, M.T., and Fox, B.G. *Biochim Biophys Acta* **1984**, 786, 49-56.
- [48] Tedeschi, G., Zetta, L., Negri, A., Mortarino, M., Ceciliani, F., and Ronchi, S. *Biochemistry* **1997**, 36, 16221-16230.
- [49] Stewart, R.C., and Massey, V. *J Biol Chem* **1985**, 260, 13639-13647.
- [50] Hunt, J., Massey, V., Dunham, W.R., and Sands, R.H. *J Biol Chem* **1993**, 268, 18685-18691.
- [51] Gadda, G., and Fitzpatrick, P.F. *Biochemistry* **1998**, 37, 6154-6164.

CHAPTER 8

8 Appendix

List of Abbreviations

4'OMT	3'-hydroxy- <i>N</i> -methylcoclaurine 4'- <i>O</i> -methyltransferase
6OMT	corcoclaurine 6- <i>O</i> -methyltransferase
7OMT	reticuline 7- <i>O</i> -methyltransferase
<i>A. mexicana</i> (<i>Am</i>)	<i>Argemone mexicana</i>
<i>A. strictum</i>	<i>Acremonium strictum</i>
<i>A. thaliana</i>	<i>Arabidopsis thaliana</i>
AknOx	aclacinomycin oxidoreductase
AOX	alcohol oxidase
APLE	alternative pig liver esterase
<i>B. wilsoniae</i> (<i>Bw</i>)	<i>Berberis wilsoniae</i>
BBE	berberine bridge enzyme
BMD	buffered minimal medium with dextrose
BMM	buffered minimal medium with methanol
<i>C. crispus</i>	<i>Chondrus crispus</i>
<i>C. japonica</i>	<i>Coptis japonica</i>
<i>C. sativa</i>	<i>Cannabis sativa</i>
CBGA	cannabigerolic acid
CBS	Center for Biological Sequence Analysis
CAS	canadine synthase
ChitO	chitooligosaccharide oxidase
CHS	cheilanthifoline synthase
CNMT	coclaurine <i>N</i> -methyltransferase
COR	codeinone reductase
CTS	corytuberine synthase
DBOX	dihydrobenzophenanthridine oxidase
DNA	deoxyribonucleic acid
dNTP	deoxynucleoside triphosphate
DRR	1,2-dehydroreticuline reductase
DRS	1,2-dehydroreticuline synthase
DTT	dithiothreitol
<i>E. californica</i> (<i>Ec</i>)	<i>Eschscholzia californica</i>
<i>E. coli</i>	<i>Escherichia coli</i>
EDTA	ethylenediaminetetraacetic acid
ER	endoplasmic reticulum
<i>F. graminearum</i>	<i>Fusarium graminearum</i>
FAD	flavin adenine dinucleotide
FMN	flavin mononucleotide
GFP	green fluorescing protein
GilR	pregilvocarcin V dehydrogenase
GOOX	glucooligosaccharide oxidase
<i>H. annuus</i>	<i>Helianthus annuus</i>
HA	hemagglutinin
HNL	hydroxyl nitril lyase

HOX	hexose oxidase
HPLC	high pressure liquid chromatography
IPTG	isopropyl- β -D-thiogalactopyranoside
K_M	Michaelis constant
<i>L. sativa</i>	<i>Lactuca sativa</i>
MALDI-MS	matrix-assisted laser desorption/ionization mass spectrometry
MBP	maltose binding protein
MeOH	methanol
MSH	<i>N</i> -methyl-stylophine 14-hydroxylase
NaCl	sodium chloride
NCBI	National Center for Biotechnology Information
NCS	norcochlorine synthase
NEC5	nectarin V
NMCH	<i>N</i> -methylcochlorine 4'- <i>O</i> -methyltransferase
OD	optical density
OE-PCR	overlap-extension polymerase chain reaction
<i>P. pastoris</i>	<i>Pichia pastoris</i>
<i>P. somniferum</i>	<i>Papaver somniferum</i>
PAGE	polyacrylamide gel electrophoresis
PCMH	<i>p</i> -cresolmethylhydroxylase
PCR	polymerase chain reaction
PDI	protein disulfide isomerase
PRH	protopine 6-hydroxylase
<i>S. cerevisiae</i>	<i>Saccharomyces cerevisiae</i>
SalAT	salutaridinol-7- <i>O</i> -acetyltransferase
SalR	salutaridine:NADPH 7-oxidoreductase
SalSyn	salutaridine synthase
SanR	sanguinarine reductase
SDS	sodium dodecylsulphate
SOMT	scoulerine-9- <i>O</i> -methyltransferase
STOX	(<i>S</i>)-tetrahydroprotoberberine oxidase
STS	stylophine synthase
<i>T. flavum</i>	<i>Thalictrum flavum</i>
TamL	10-hydroxy dehydrogenase in tirandamycin biosynthesis
TCA	trichloroacetic acid
TEV	Tobacco Etch Virus
THC	tetrahydrocannabinol
THCA	tetrahydrocannabinolic acid
THS	thebaine synthase
TNMT	(<i>S</i>)-tetrahydroprotoberberine <i>cis-N</i> -methyltransferase
Tris	tris(hydroxymethyl)aminomethane
YFP	yellow fluorescing protein
YNB	Yeast Nitrogen Base
YPD	yeast extract/peptone/dextrose

List of Publications

PAPERS IN REVIEWED JOURNALS

Catalytic and structural role of a conserved active site histidine in berberine bridge enzyme.

Wallner, S., Winkler, A., Riedl, S., Dully, C., Horvath, S., Gruber, K., and Macheroux, P. **2012**, manuscript in preparation.

Inverting the regioselectivity of BBE to access 11-hydroxy-functionalized tetrahydroprotoberberines applying a positional blocking strategy.

Resch, V., Lechner, H., Schrittwieser, J. H., Wallner, S., Gruber, K., Macheroux, P., and Kroutil, W. **2012**, manuscript in preparation.

Biocatalytic organic synthesis of optically pure (S)-scoulerine and berbine and benzyloquinoline alkaloids.

Schrittwieser, J. H., Resch, V., Wallner, S., Lienhart, W.-D., Sattler, J. H., Resch, J., Macheroux, P. and Kroutil, W., *J. Org. Chem.* **2011**, *76*, 6703-6714.

Biocatalytic oxidative C-C bond formation catalyzed by berberine bridge enzyme: optimal reaction conditions.

Resch, V., Schrittwieser, J. H., Wallner, S., Macheroux, P., and Kroutil, W. *Adv. Synth. Catal.* **2011**, *353*, 2377-2383.

The flavoprotein-catalyzed reduction of aliphatic nitro-compounds represents a biocatalytic equivalent to the Nef-reaction.

Durchschein, K., Ferreira-da Silva, B., Wallner, S., Macheroux, P., Kroutil, W., Glueck, S. M., and Faber, K. *Green Chem.* **2010**, *12*, 616-619.

Structure of glycerol trinitrate reductase (GTNR) from *Agrobacterium radiobacter* – an enzyme belonging to the family of enoate reductases.

Oberdorfer, G., Wallner, S., Durchschein, K., Faber, K., Macheroux, P., and Gruber, K. manuscript in preparation

REVIEW ARTICLE**Berberine bridge enzyme and the family of bicovalent flavoenzymes.**

Wallner, S., Dully, C., Daniel, B., and Macheroux, P. *Flavoproteins* **2012** in press

POSTER PRESENTATIONS ON INTERNATIONAL CONFERENCES**STOX, a bi-covalently flavinylated oxidase with unknown function in alkaloid biosynthesis.**

Wallner, S., Luef, B., and Macheroux, P. *Trends in Enzymology*, Ascona, **2010**.

Further insights into the bicovalent flavinylation of berberine bridge enzyme.

Wallner, S., Winkler, A., Dully, C., Trenker, R., and Macheroux, P. *17th International Symposium on Flavins and Flavoproteins*, Berkeley, **2011**.

CONFERENCE PROCEEDINGS**Further insights into the bicovalent flavinylation of berberine bridge enzyme.**

Wallner, S., Winkler, A., Dully, C., Horvath, S., Trenker, R., Gruber, K., and Macheroux, P. *17th International Symposium on Flavins and Flavoproteins*, Berkeley, **2011**.

Curriculum vitae

Contact Information and Personal Information

Name	Silvia WALLNER
Address	Hinterwölch 19, 9413 St. Gertraud
Mobil	0699/12332340
Email	silvia.wallner@tugraz.at
Date and place of birth	17 th May 1984 in Graz, Austria
Citizenship	Austrian



Education

1990 - 1994	Elementary School in Hengsberg, Austria
1994 - 2002	Grammar School in Leibnitz, Austria
2002 - 2005	Studies of Technical Chemistry (F800) at Graz University of Technology
08/2005	First section of the diploma completed
2005 - 2008	Studies of Biochemistry, Biotechnology and Food Chemistry (F809) at Graz University of Technology
06/2007 - 08/2007	Summer School at Syracuse University, Syracuse, NY
02/2007 - 04/2008	Diploma thesis project at the Institute of Biochemistry, TU Graz (Supervisor: Prof. Peter Macheroux)
8. 4. 2008	Defense of diploma thesis, diploma completed
10/2008 - 04/2012	PhD project at the Institute of Biochemistry, TU Graz (Supervisor: Prof. Peter Macheroux)

Research Activities

1.7.2004 - 30.7.2004 and 1.7.2005 - 30.7.2005	Internship at JOANNEUM RESEARCH Forschungsgesellschaft mbH (Graz) at the Institute of Chemical Process Development and Control with Ing. Constanze Dolezal: <i>“Development of optical sensors for monitoring the CO₂ concentration in the stomach of intensive care patients”</i> and <i>“Optical Sensors for monitoring the oxygen concentration in packaged goods for quality control”</i>
07/2006	Project at the Department of Biochemistry, TU Graz, with Prof. Peter Macheroux: <i>“Cloning, Expression and Purification of E. coli AroH”</i>

06/2007 - 08/2007	Project at the Faculty of Bioinorganic Chemistry and Biophysics, at the Department of Chemistry, Syracuse University, NY, with Prof. James Dabrowiak: <i>“Adsorption of Carboplatin by mesoporous MCM-41”</i>
02/2007 - 04/2008	Diploma thesis project entitled <i>“Thermodynamic Interaction Studies on the Pdx1/Pdx2 Interface of Bacillus subtilis”</i> at the Institute of Biochemistry, TU Graz (Supervisor: Prof. Peter Macheroux)
10/2008 - 04/2012	Work on PhD-project entitled <i>“Flavoproteins with Bicovalent Cofactor Tethering”</i> at the Institute of Biochemistry, TU Graz (Supervisor: Prof. Peter Macheroux)

Further Occupational Activities

10.7.2006 - 14.7.2006 and 28.2.2011 - 4.3.2011	Teaching assignment at the University college of Teacher Education in Styria (course instructor at a teacher training program for additional qualifications in chemistry)
10/2002 - 07/2003	Occupation as flute teacher in Lieboch and Hengsberg
10/2003 - 07/2008	Employment as music teacher in Dobl
10/2004 - 07/2008	Employment as music teacher in Dobl and Graz-Don Bosco

Other Qualifications

Language Skills	German as mother tongue fluent in English and Italian, basics in Spanish and French
Computer Skills	Microsoft Office, skills in Bioinformatics (databases, sequence alignments, Pymol, ect.), Origin 7.0 for ITC data analysis
